# UNIVERSIDAD COMPLUTENSE DE MADRID

## FACULTAD DE CIENCIAS QUÍMICAS
## DEPARTAMENTO DE QUÍMICA ORGÁNICA I



# TESIS DOCTORAL

## Blockade of tumoral processes by inhibition of angiogenesis and RAS protein activity

Bloqueo de procesos tumorales mediante la inhibición de angiogénesis y de la actividad de la proteína RAS

MEMORIA PARA OPTAR AL GRADO DE DOCTORA

PRESENTADA POR


**Nagore Isabel Marín Ramos**

DIRECTORES

**María Luz López Rodríguez**
**Jesús Jiménez Barbero**


**Madrid, 2017**

UNIVERSIDAD COMPLUTENSE DE MADRID
FACULTAD DE CIENCIAS QUÍMICAS
Departamento de Química Orgánica I


# BLOCKADE OF TUMORAL PROCESSES BY INHIBITION OF ANGIOGENESIS AND RAS PROTEIN ACTIVITY

BLOQUEO DE PROCESOS TUMORALES MEDIANTE LA INHIBICIÓN DE ANGIOGÉNESIS Y DE LA ACTIVIDAD DE LA PROTEÍNA RAS

PhD Candidate

**Nagore Isabel Marín Ramos**

Advisors:
Dra. Mª Luz López Rodríguez
Dr. Jesús Jiménez Barbero

MADRID, 2015

*A mis padres, que me dieron las alas para volar.*
*A Javi, que me ha acompañado en este vuelo,*
*incluso en las peores tormentas.*

*El presente trabajo ha sido realizado en el laboratorio de Química Médica en el Departamento de Química Orgánica I de la Facultad de Ciencias Químicas de la Universidad Complutense de Madrid (UCM), dirigido por la Catedrática* ***Dra. Mª Luz López Rodríguez*** *y el Profesor de Investigación* ***Dr. Jesús Jiménez Barbero****, y bajo la supervisión la* ***Dra. Silvia Ortega Gutiérrez*** *y la* ***Dra. Mª del Mar Martín-Fontecha Corrales****, a quienes deseo expresar mi afecto y mi más profundo agradecimiento por su acogida en este grupo de investigación, por sus continuas enseñanzas a lo largo de todo este tiempo, y por todo el ánimo, apoyo y confianza depositados en mí para la realización de este proyecto.*

*Asimismo, quiero expresar mi agradecimiento:*

*Al personal del Campus de Excelencia Internacional Moncloa, por haber confiado en mí y por su apoyo constante durante la realización de esta tesis doctoral.*

*Al Profesor Mark R. Philips del New York University Langone Medical Center y a todo su grupo de investigación, por su cálida acogida durante mi estancia predoctoral y su inestimable asesoramiento, en especial a la Dra. Helen Court por guiarme en la investigación.*

*A la Dra. Cristina Sánchez y la Dra. Clara Andradas, del Dpto. de Bioquímica y Biología Molecular I de la UCM, y al Dr. Faustino Mollinedo y a la Dra. Consuelo Gajate, del Centro de Investigación del Cáncer (CSIC-Universidad de Salamanca), por la realización de los modelos in vivo.*

*Al personal del CAI de Resonancia Magnética Nuclear y del CAI de Microscopía de Fluorescencia de la UCM por su ayuda y asesoramiento.*

*A todos los compañeros de laboratorio que he tenido la suerte de conocer a lo largo de estos años, porque de cada uno de ellos he adquirido conocimientos valiosísimos tanto para la ciencia como para la vida, y por los maravillosos momentos que hemos compartido.*

*A mi familia y amigos de Bilbao, Santa Coloma, Vitoria, Granada, Madrid… y a los que, como yo, os habéis convertido en electrones deslocalizados, porque quizás el lugar donde te lleve el camino sea lo menos importante cuando en el bagaje llevas los recuerdos y amistades de tan buenas personas. Gracias a todos, porque por muy grande que sea la distancia que nos separa siempre estáis ahí, y porque sin vuestro apoyo incondicional jamás habría logrado llegar hasta aquí.*

# TABLE OF CONTENTS

## ABBREVIATIONS AND ACRONYMS

Throughout this manuscript, abbreviations and acronyms recommended by the American Chemical Society in the Organic Chemistry and Medicinal Chemistry areas have been employed (revised in the *Journal of Organic Chemistry* and *Journal of Medicinal Chemistry* on May 2015; http://pubs.acs.org/paragonplus/submission/joceah/joceah_abbreviations.pdf and http://pubs.acs.org/paragonplus/submission/jmcmar/jmcmar_abbreviations.pdf). In addition, those indicated below have also been used.

| | |
|---|---|
| Ang2 | angiopoietin 2 |
| ATCC | American type culture collection |
| ATR | attenuated total reflectance |
| BFC | biotinyl-*S*-farnesylcysteine |
| bFGF | basic FGF |
| BNip3 | BCL2/adenovirus E1B 19 kDa protein-interacting protein 3 |
| c-KIT | tyrosine-protein kinase KIT (CD117) |
| CAI | centro de asistencia a la investigación |
| cPARP | cleaved PARP |
| CSI | chlorosulfonylisocyanate |
| DIAD | diisopropylazodicarboxylate |
| DIEA | *N,N*-diisopropylethylamine |
| EDC | ethyl-3-(3-(dimethylamino)-propyl)carbodiimide |
| EGF | epidermal growth factor |
| FBS | fetal bovine serum |
| FGFR | FGF receptor |
| Ftase | farnesyl transferase |
| GAP | GTPase activating protein |
| GEF | guanine nucleotide exchange factor |
| GGTase I | geranylgeranyltransferase type I |
| HIF-1$\alpha$ | hypoxia-inducible factor-1$\alpha$ |
| [$^3$H]-SAM | [$^3$H]-*S*-adenosylmethionine |
| HTS | high-throughput screening |
| HUVECs | human umbilical vein endothelial cells |
| ICMT | isoprenylcysteine carboxyl methyltransferase |
| iNOS | inducible nitric oxide synthase |
| LC-3 | microtubule-associated protein light chain 3 |

| | |
|---|---|
| mTOR | mammalian target of rapamycin |
| NGS | normal goat serum |
| o/n | overnight |
| PARP | poly(ADP-ribose) polymerase |
| PDGF | platelet derived growth factor |
| p-NA | *p*-nitroaniline |
| qPCR | quantitive polymerase chain reaction |
| RAF | rapidly accelerated fibrosarcoma |
| RBD | Ras binding domain |
| Rce1 | Ras-converting enzyme 1 |
| SEM | standard error media |
| siRNA | small interfering RNA |
| TBTU | *O*-(benzotriazol-1-yl)-*N,N,N′,N′*-tetramethyluronium tetrafluoroborate |
| TKI | tyrosine kinase inhibitor |
| tPSA | topological polar surface area |
| UCM | Universidad Complutense de Madrid |
| VEGF | vascular endothelial growth factor |

## RESUMEN

### CAPÍTULO I: NUEVOS INHIBIDORES DE ANGIOGÉNESIS CON ACTIVIDAD ANTITUMORAL *IN VIVO*

La angiogénesis, el proceso de formación de nuevos vasos sanguíneos, es un requerimiento esencial para la supervivencia y proliferación de los tumores sólidos.[1] Por consiguiente, la búsqueda de inhibidores de la angiogénesis se ha convertido en una importante línea de investigación en el área de cáncer, y se ha traducido en la presencia de múltiples fármacos en el mercado que han mejorado claramente los resultados en pacientes con distintos tipos de tumores y metástasis. Sin embargo, todavía existen limitaciones, como la falta de eficacia en algunos pacientes, y la aparición de efectos adversos o de resistencia al tratamiento.[2-4] Se considera que cuando se bloquea farmacológicamente la señalización del factor de crecimiento vascular endotelial (VEGF), otros factores proangiogénicos -especialmente el factor de crecimiento de fibroblastos (FGF)- cumplen su función, favoreciendo la angiogénesis tumoral.[2,5,6] Además, se ha descrito que el aumento de la hipoxia tumoral causado por la terapia antiangiogénica potencia la supervivencia celular al estimular varios factores, particularmente el factor inducible por hipoxia-1$\alpha$ (HIF-1$\alpha$).[7]

En este contexto, el principal objetivo del presente trabajo es la identificación de nuevas estructuras químicas capaces de bloquear la angiogénesis afectando varios factores proangiogénicos (especialmente VEGF y FGF), así como de inducir una inhibición sostenida de la señalización proangiogénica generada por la hipoxia. Este objetivo general supone llevar a cabo los siguientes pasos:

1. Identificación de un *hit* y proceso *hit to lead*.
2. Caracterización biológica de los compuesto(s) seleccionado(s) en relación a su capacidad para bloquear la señalización proangiogénica ante la hipoxia.
3. Estudio del efecto antitumoral de los compuesto(s) seleccionado(s).

Por tanto, en este capítulo describimos una nueva serie de compuestos antiangiogénicos.[8] Entre ellos, el compuesto óptimo **22** (UCM-2711) inhibe la señalización proangiogénica en hipoxia en

células de cáncer de mama. Más concretamente, la administración de **22** disminuye los niveles de las moléculas proangiogénicas VEGF, FGF, y óxido nítrico (NO). Además, este compuesto inhibe las formas activas de los receptores correspondientes a los mencionados factores (las formas fosforiladas de VEGFR y FGFR) y baja los niveles de la enzima óxido nítrico sintasa inducible (iNOS). Dichos efectos se correlacionan con un bloqueo en las vías de señalización MEK/ERK y PI3K/AKT, así como de la migración celular; y están mediados por HIF-1*α*, puesto que los efectos del compuesto **22** prácticamente desaparecen cuando su expresión se reduce mediante un *knock-down* genético. Adicionalmente, la evaluación del perfil genético ha permitido identificar un conjunto de genes relacionados con la angiogénesis cuya expresión se altera con el compuesto **22**. Finalmente, la administración del compuesto **22** a un modelo *xenograft* produjo reducciones en el crecimiento tumoral entre el 46 y el 55% en un 38% de los animales tratados. Cabe destacar que en los tumores que respondieron al tratamiento, se observó además una reducción significativa del número de vasos sanguíneos y de los niveles de VEGF, apoyando así el mecanismo de acción del compuesto. Aunque sería deseable una mayor eficacia, el hecho de que el compuesto **22** no indujese toxicidad alguna *in vivo*, y que fuese capaz de bloquear de forma efectiva la angiogénesis en los tumores que respondieron al tratamiento, refuerza el potencial del compuesto como un *lead* para el desarrollo de nuevos agentes antiangiogénicos aptos para el tratamiento del cáncer, ya sea solos o en combinación con otros fármacos de referencia.

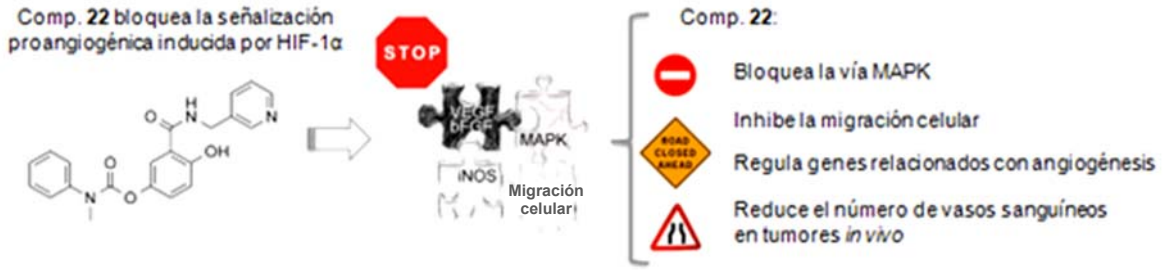


## CAPÍTULO II: PROCESO DE OPTIMIZACIÓN Y CARACTERIZACIÓN BIOLÓGICA DE UN NUEVO INHIBIDOR DE ICMT CON ACTIVIDAD ANTITUMORAL

Las mutaciones puntuales del gen *ras* llevan a la producción de una proteína Ras constitutivamente activa, resultando así en una estimulación constante de la proliferación celular y la inhibición de la señalización intracelular que conduce a la apoptosis. Sin embargo, pese a más de tres décadas de intenso esfuerzo, ningún fármaco que inhiba eficazmente las oncoproteínas Ras ha llegado a fase clínica, lo cual ha motivado la amplia creencia de que las proteínas Ras son '*undruggable*'.[9,10] Por ello, la posibilidad de bloquear la actividad de Ras interfiriendo con las

modificaciones post-traduccionales responsables de su activación ha ganado atención en los últimos años.

Ras es un miembro de una gran clase de proteínas conocidas como las proteínas CAAX, donde C es cisteína, A es normalmente un aminoácido alifático, y X es cualquier aminoácido. Su producto primario tras la traducción contiene una secuencia CAAX, que sirve como sustrato de tres enzimas que la modifican de manera secuencial para crear un dominio lipídico e hidrofóbico que media la asociación con membranas celulares. Primero, la secuencia CAAX intacta sirve de sustrato para su prenilación por la geranilgeranilasa tipo I (GGTase I) o la farnesiltransferasa (FTasa).[11] A continuación, se da la proteólisis de los tres últimos aminoácidos AAX, gracias a la enzima convertidora de Ras (Rce1).[12,13] Y por último, la nueva prenilcistína C-terminal sirve como sustrato para una enzima metiltransferasa específica, la isoprenilcisteína carboximetiltransferasa (ICMT), que metila el grupo carboxilo libre, neutralizando la carga negativa de la prenilcisteína y aumentando así su afinidad por la membrana.[14]

En ausencia de cualquiera de estas modificaciones post-traducccionales, Ras pierde su habilidad para inducir transformación tumoral. Sin embargo, hasta el momento los intentos de bloquear los primeros dos pasos de estas modificaciones post-traduccionales han fracasado.[15-18] Además, el hecho de que los genomas de mamíferos codifiquen únicamente para un miembro de la clase ICMT de las metiltransferasas, y que ésta no presente homología con ninguna otra metiltransferasa, convierte la inhibición de ICMT en una prometedora alternativa para las terapias antitumorales. En este contexto, en nuestro grupo de trabajo hemos iniciado un proyecto orientado al diseño, síntesis y desarrollo de nuevos inhibidores de ICMT. Esto nos ha llevado al nuevo *lead* UCM-1325, que mostró el mejor perfil en términos de capacidad inhibitoria de ICMT. Así pues, los principales objetivos del presente trabajo son:

1. Optimización del *lead* UCM-1325.
2. Estudio del mecanismo de acción de los compuesto(s) seleccionado(s).

Por consiguiente, en este capítulo describimos el proceso de optimización del *lead* UCM-1325 hasta llegar al *lead* optimizado UCM-1336 (**3**), que mostró una inhibición de ICMT del 93% a 50 $\mu$M ($CI_{50}$ = 2 $\mu$M), siendo por tanto seleccionado para su estudio biológico y caracterización del mecanismo de acción. Este nuevo compuesto potencia la muerte celular programada, afectando especialmente a aquellas líneas celulares que expresan K-Ras mutante oncogénica; e induce una deslocalización de todas las isoformas de Ras. Además, UCM-1336 (**3**) reduce significativamente la actividad de Ras, bloquea la activación de las vías de señalización MEK/ERK y PI3K/AKT, y afecta la capacidad de migración de las células tumorales. Cabe destacar que UCM-1336 (**3**) ha mostrado una mayor potencia que el ya validado inhibidor de ICMT *cysmethynil* en todos los ensayos

realizados, sugiriendo que podría funcionar como un nuevo inhibidor de ICMT que contribuiría a la definitiva validación de dicha enzima desde un punto de vista mecanístico, como una diana de interés terapéutico para el tratamiento de cánceres caracterizados por una elevada activación de Ras. Todos estos prometedores resultados nos han llevado a estudiar la eficacia *in vivo* del compuesto UCM-1336 (**3**) en un modelo *xenograft* de cáncer de páncreas en ratón, experimentos que se están realizando actualmente.

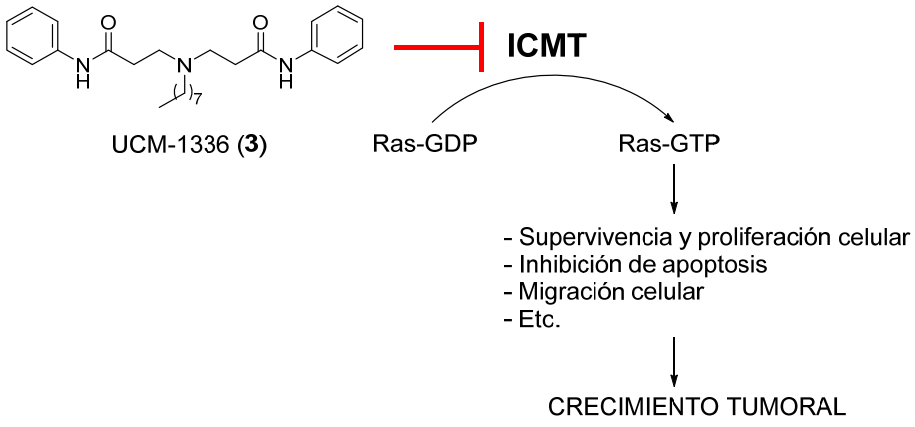


**Bibliografía:**

1. Folkman, J. Tumor angiogenesis: therapeutic implications. *New Eng. J. Med.* **1971**, *285*, 1182-1186.

2. Gacche, R. N.; Meshram, R. J. Angiogenic factors as potential drug target: efficacy and limitations of anti-angiogenic therapy. *Biochim. Biophys. Acta* **2014**, *1846*, 161-179.

3. Wu, J. M.; Staton, C. A. Anti-angiogenic drug discovery: lessons from the past and thoughts for the future. *Expert Opin. Drug Discov.* **2012**, *7*, 723-743.

4. Bellou, S.; Pentheroudakis, G.; Murphy, C.; Fotsis, T. Anti-angiogenesis in cancer therapy: Hercules and hydra. *Cancer Lett.* **2013**, *338*, 219-228.

5. Helfrich, I.; Scheffrahn, I.; Bartling, S.; Weis, J.; von Felbert, V.; Middleton, M.; Kato, M.; Ergun, S.; Augustin, H. G.; Schadendorf, D. Resistance to antiangiogenic therapy is directed by vascular phenotype, vessel stabilization, and maturation in malignant melanoma. *J. Exp. Med.* **2010**, *207*, 491-503.

6. Petrillo, M.; Scambia, G.; Ferrandina, G. Novel targets for VEGF-independent anti-angiogenic drugs. *Expert Opin. Investig. Drugs* **2012**, *21*, 451-472.

7. Semenza, G. L. Hypoxia-inducible factors: mediators of cancer progression and targets for cancer therapy. *Trends Pharmacol. Sci.* **2012**, *33*, 207-214.

8. Marín-Ramos, N. I.; Alonso, D.; Ortega-Gutiérrez, S.; Ortega-Nogales, F. J.; Balabasquer, M.; Vázquez-Villa, H.; Andradas, C.; Blasco-Benito, S.; Pérez-Gómez, E.; Canales, Á.; Jiménez-Barbero, J.; Marquina, A.; del Prado, J. M.; Sánchez, C.; Martín-Fontecha, M.; López-Rodríguez, M. L. New inhibitors of angiogenesis with antitumor activity in vivo. *J. Med. Chem.* **2015**, *58*, 3757-3766.

9. Vogelstein, B.; Papadopoulos, N.; Velculescu, V. E.; Zhou, S.; Diaz, L. A.; Kinzler, K. W. Cancer genome landscapes. *Science* **2013**, *339*, 1546-1558.

10. Cox, A. D.; Fesik, S. W.; Kimmelman, A. C.; Luo, J.; Der, C. J. Drugging the undruggable Ras: mission possible? *Nat. Rev. Drug Discov.* **2014**, *13*, 828-851.

11. Wright, L. P.; Philips, M. R. CAAX modification and membrane targeting of Ras. *J. Lipid. Res.* **2006**, *47*, 883-891.

12. Boyartchuk, V. L.; Ashby, M. N.; Rine, J. Modulation of Ras and a-factor function by carboxyl-terminal proteolysis. *Science* **1997**, *275*, 1796-1800.

13. Schmidt, W. K.; Tam, A.; Fujimura-Kamada, K.; Michaelis, S. Endoplasmic reticulum membrane localization of Rce1p and Ste24p, yeast proteases involved in carboxyl-terminal CAAX protein processing and amino-terminal a-factor cleavage. *Proc. Natl. Acad. Sci. U.S.A.* **1998**, *95*, 11175-11180.

14. Dai, Q.; Choy, E.; Chiu, V.; Romano, J.; Slivka, S. R.; Steitz, S. A.; Michaelis, S.; Philips, M. R. Mammalian prenylcysteine carboxyl methyltransferase is in the endoplasmic reticulum. *J. Biol. Chem.* **1998**, *273*, 15030-15034.

15. DeGraw, A. J.; Keiser, M. J.; Ochocki, J. D.; Shoichet, B. K.; Distefano, M. D. Prediction and evaluation of protein farnesyltransferase inhibition by commercial drugs. *J. Med. Chem.* **2010**, *53*, 2464-2471.

16. Niessner, H.; Beck, D.; Sinnberg, T.; Lasithiotakis, K.; Maczey, E.; Gogel, J.; Venturelli, S.; Berger, A.; Mauthe, M.; Toulany, M.; Flaherty, K.; Schaller, M.; Schadendorf, D.; Proikas-Cezanne, T.; Schittek, B.; Garbe, C.; Kulms, D.; Meier, F. The farnesyl transferase inhibitor lonafarnib inhibits

mTOR signaling and enforces sorafenib-induced apoptosis in melanoma cells. *J. Invest. Dermatol.* **2011**, *131*, 468-479.

17. Bergo, M. O.; Lieu, H. D.; Gavino, B. J.; Ambroziak, P.; Otto, J. C.; Casey, P. J.; Walker, Q. M.; Young, S. G. On the physiological importance of endoproteolysis of CAAX proteins: heart-specific Rce1 knockout mice develop a lethal cardiomyopathy. *J. Biol. Chem.* **2004**, *279*, 4729-4736.

18. Bhadoriya, K. S.; Sharma, M. C.; Jain, S. V. Pharmacophore modeling and atom-based 3D-QSAR studies on amino derivatives of indole as potent isoprenylcysteine carboxyl methyltransferase (Icmt) inhibitors. *J. Mol. Struct.* **2015**, *1081*, 466-476.

## SUMMARY

## SUMMARY

### CHAPTER I: NEW INHIBITORS OF ANGIOGENESIS WITH ANTITUMOR ACTIVITY IN VIVO

Angiogenesis, the process of new blood vessel formation, is an essential requirement for the survival and proliferation of solid tumors.[1] Accordingly, the search for angiogenesis inhibitors has become a leading line of investigation in anticancer research, and it has translated into several drugs in the market that have clearly improved outcomes in patients with different tumor types and metastatic disease. However, several limitations still exist, such as the lack of efficacy in some patients, the appearance of adverse effects, and drug resistance.[2-4] It has been suggested that when the vascular endothelial growth factor (VEGF) signaling is pharmacologically blocked, other proangiogenic factors -especially the fibroblast growth factor (FGF)- take over its signaling, thereby supporting tumor angiogenesis.[2,5,6] Besides, it has been described that increasing tumor hypoxia during antiangiogenic therapy enhances cell survival through the stimulation of several factors, particularly the hypoxia-inducible factor-1$\alpha$ (HIF-1$\alpha$).[7]

In this context, the main objective of the present work is the identification of new small molecules able to block angiogenesis affecting various proangiogenic factors (especially VEGF and FGF signaling pathways), and to induce a sustained inhibition of the proangiogenic signaling generated by hypoxia. This overall objective involves the following steps:

1. Hit identification and hit to lead process.
2. Biological characterization of selected compound(s) in terms of impairment of proangiogenic signaling under hypoxia.
3. Antitumor effect of selected compound(s).

Hence, in this chapter we describe a new series of antiangiogenic compounds.[8] Among them, the optimal compound **22** (UCM-2711) inhibits the proangiogenic signaling under hypoxic conditions in breast cancer cells. Specifically, administration of **22** decreases the levels of the proangiogenic molecules VEGF, FGF, and nitric oxide (NO). Moreover, this compound inhibits the active forms of the corresponding receptors of these factors (phosphorylated forms of VEGFR and FGFR) and the levels of the inducible nitric oxide

synthase (iNOS) enzyme. These effects correlate with a blockade of the MEK/ERK and PI3K/AKT pathways and the inhibition of cellular migration; and they are mediated by HIF-1*α*, since the effects of compound **22** mostly disappear when its expression is knocked-down. Additionally, gene profiling identified a set of genes related to angiogenesis whose expression is altered by compound **22** and that might contribute to the antiangiogenic effects. Furthermore, administration of compound **22** in a xenograft model produced tumor growth reductions ranging from 46 to 55% in the 38% of the treated animals. Importantly, in the responding tumors, a significant reduction in the number of blood vessels and in the levels of VEGF was observed, further supporting the mechanism of action of the compound. Although better efficacy would be desirable, the fact that compound **22** did not induce any toxic effects in vivo and that it was able to effectively block angiogenesis in the tumors of responding animals strongly support the potential of this compound as a lead for the development of new antiangiogenic agents suitable for the treatment of cancer either alone or in combination with other benchmark drugs.

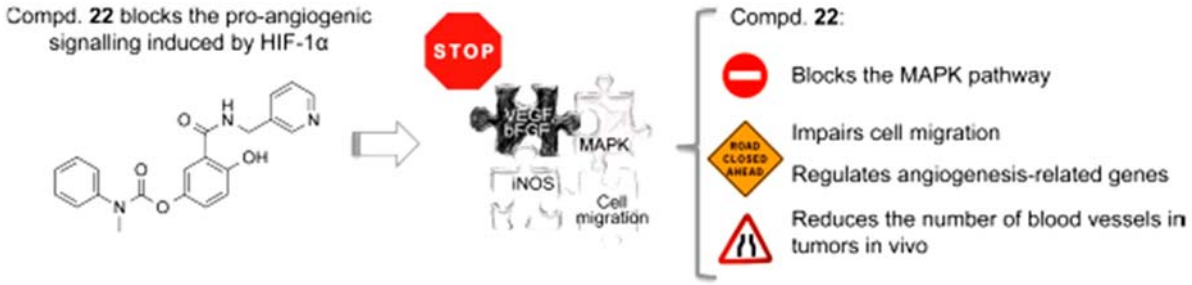


## CHAPTER II: LEAD OPTIMIZATION PROCESS AND BIOLOGICAL CHARACTERIZATION OF A NOVEL INHIBITOR OF ICMT WITH ANTITUMOR ACTIVITY

Single-point mutations of *ras* gene can lead to the production of constitutively activated Ras protein, resulting in a continuous stimulation of cell proliferation and inhibition of apoptotic signaling, thus promoting cancer. However, despite more than three decades of intensive effort, no effective pharmacological inhibitors of the Ras oncoproteins have reached the clinic, prompting the widely held perception that Ras proteins are 'undruggable'.[9,10] Hence, the possibility of blocking Ras activity by interfering with the post-translational modifications responsible for its activation has gained an increasing attention within the last years.

Ras is a member of a large class of proteins known as CAAX proteins, where C is cysteine, A is usually an aliphatic amino acid and X is any amino acid. Their primary translation product ends with a CAAX sequence, which serves as a substrate for three enzymes that modify the sequence in a step-wise manner

to create a lipidated, hydrophobic domain that mediates the association with cellular membranes. First, unmodified CAAX sequences serve as substrates for prenylation by geranylgeranyltransferase type I (GGTase I) or farnesyltransferase (FTase).[11] Second, there is a specific proteolytic removal of the last three amino acids AAX, carried out by the Ras-converting enzyme 1 (Rce1).[12,13] And finally, the newly formed C-terminal prenylcysteine becomes a substrate for a specific protein carboxyl methyltransferase, isoprenylcysteine carboxyl methyltransferase (ICMT), which methylates the free carboxyl group, neutralizing the negative charge of the prenylcysteine and thereby increasing membrane affinity.[14]

In absence of any of these post-translational modifications, Ras losses its ability to induce tumor transformation. However, thus far attempts to abrogate the first two steps of the post-translational modifications have failed.[15-18] Besides, the fact that mammalian genomes encode only one member of the ICMT class of methyltransferases and that it lacks homology to other protein methyltransferases, turns the inhibition of ICMT into a promising alternative for anticancer therapies. In this context, in our research group we have started a project aimed at the design, synthesis and development of new ICMT inhibitors. This has led us to the new lead UCM-1325, which showed the best overall profile in terms of ICMT inhibitory capacity. Thus, the main objectives of the present work are:

3. Optimization of the lead UCM-1325.
4. Study of the mechanism of action of the selected compound(s).

Hence, in this chapter we describe the lead optimization process of UCM-1325 that has led us to the new lead UCM-1336 (**3**), which showed an ICMT inhibition of 93% at 50 $\mu$M ($IC_{50}$ = 2 $\mu$M), hence being selected for in depth biological studies and characterization of its mechanism of action. This new compound enhances programmed cell death, affecting specially those cell lines expressing oncogenic mutant K-Ras; and induces mislocalization of all Ras isoforms. Besides, UCM-1336 (**3**) significantly reduces Ras activity, blocks the activation of the downstream MEK/ERK and PI3K/AKT signaling pathways, and impairs the migratory capacity of tumor cells. Noteworthy, UCM-1336 (**3**) has shown to be more potent than the already validated ICMT inhibitor cysmethynil in all performed assays, suggesting that it could work as a new ICMT inhibitor that would help to definitively validate this enzyme from a mechanistic standpoint as a therapeutic target of interest for the treatment of cancers characterized by high Ras overactivation. All these promising results have prompted us to study the in vivo efficacy of compound UCM-1336 (**3**) in a xenograft mouse model of pancreatic cancer, experiments that are currently ongoing.

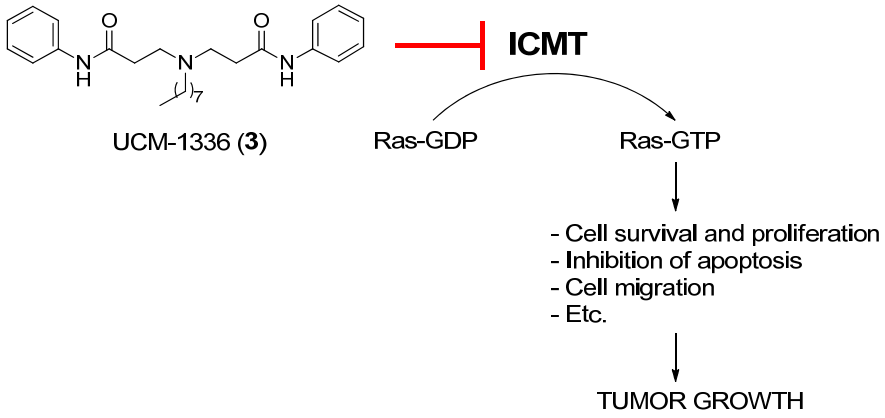


**Bibliography:**

1. Folkman, J. Tumor angiogenesis: therapeutic implications. *New Eng. J. Med.* **1971**, *285*, 1182-1186.

2. Gacche, R. N.; Meshram, R. J. Angiogenic factors as potential drug target: efficacy and limitations of anti-angiogenic therapy. *Biochim. Biophys. Acta* **2014**, *1846*, 161-179.

3. Wu, J. M.; Staton, C. A. Anti-angiogenic drug discovery: lessons from the past and thoughts for the future. *Expert Opin. Drug Discov.* **2012**, *7*, 723-743.

4. Bellou, S.; Pentheroudakis, G.; Murphy, C.; Fotsis, T. Anti-angiogenesis in cancer therapy: Hercules and hydra. *Cancer Lett.* **2013**, *338*, 219-228.

5. Helfrich, I.; Scheffrahn, I.; Bartling, S.; Weis, J.; von Felbert, V.; Middleton, M.; Kato, M.; Ergun, S.; Augustin, H. G.; Schadendorf, D. Resistance to antiangiogenic therapy is directed by vascular phenotype, vessel stabilization, and maturation in malignant melanoma. *J. Exp. Med.* **2010**, *207*, 491-503.

6. Petrillo, M.; Scambia, G.; Ferrandina, G. Novel targets for VEGF-independent anti-angiogenic drugs. *Expert Opin. Investig. Drugs* **2012**, *21*, 451-472.

7. Semenza, G. L. Hypoxia-inducible factors: mediators of cancer progression and targets for cancer therapy. *Trends Pharmacol. Sci.* **2012**, *33*, 207-214.

8. Marín-Ramos, N. I.; Alonso, D.; Ortega-Gutiérrez, S.; Ortega-Nogales, F. J.; Balabasquer, M.; Vázquez-Villa, H.; Andradas, C.; Blasco-Benito, S.; Pérez-Gómez, E.; Canales, Á.; Jiménez-Barbero, J.; Marquina, A.; del Prado, J. M.; Sánchez, C.; Martín-Fontecha, M.; López-Rodríguez, M. L. New inhibitors of angiogenesis with antitumor activity in vivo. *J. Med. Chem.* **2015**, *58*, 3757-3766.

9. Vogelstein, B.; Papadopoulos, N.; Velculescu, V. E.; Zhou, S.; Diaz, L. A.; Kinzler, K. W. Cancer genome landscapes. *Science* **2013**, *339*, 1546-1558.

10. Cox, A. D.; Fesik, S. W.; Kimmelman, A. C.; Luo, J.; Der, C. J. Drugging the undruggable Ras: mission possible? *Nat. Rev. Drug Discov.* **2014**, *13*, 828-851.

11. Wright, L. P.; Philips, M. R. CAAX modification and membrane targeting of Ras. *J. Lipid. Res.* **2006**, *47*, 883-891.

12. Boyartchuk, V. L.; Ashby, M. N.; Rine, J. Modulation of Ras and a-factor function by carboxyl-terminal proteolysis. *Science* **1997**, *275*, 1796-1800.

13. Schmidt, W. K.; Tam, A.; Fujimura-Kamada, K.; Michaelis, S. Endoplasmic reticulum membrane localization of Rce1p and Ste24p, yeast proteases involved in carboxyl-terminal CAAX protein processing and amino-terminal a-factor cleavage. *Proc. Natl. Acad. Sci. U.S.A.* **1998**, *95*, 11175-11180.

14. Dai, Q.; Choy, E.; Chiu, V.; Romano, J.; Slivka, S. R.; Steitz, S. A.; Michaelis, S.; Philips, M. R. Mammalian prenylcysteine carboxyl methyltransferase is in the endoplasmic reticulum. *J. Biol. Chem.* **1998**, *273*, 15030-15034.

15. DeGraw, A. J.; Keiser, M. J.; Ochocki, J. D.; Shoichet, B. K.; Distefano, M. D. Prediction and evaluation of protein farnesyltransferase inhibition by commercial drugs. *J. Med. Chem.* **2010**, *53*, 2464-2471.

16. Niessner, H.; Beck, D.; Sinnberg, T.; Lasithiotakis, K.; Maczey, E.; Gogel, J.; Venturelli, S.; Berger, A.; Mauthe, M.; Toulany, M.; Flaherty, K.; Schaller, M.; Schadendorf, D.; Proikas-Cezanne, T.; Schittek, B.; Garbe, C.; Kulms, D.; Meier, F. The farnesyl transferase inhibitor lonafarnib inhibits mTOR signaling and enforces sorafenib-induced apoptosis in melanoma cells. *J. Invest. Dermatol.* **2011**, *131*, 468-479.

17. Bergo, M. O.; Lieu, H. D.; Gavino, B. J.; Ambroziak, P.; Otto, J. C.; Casey, P. J.; Walker, Q. M.; Young, S. G. On the physiological importance of endoproteolysis of CAAX proteins: heart-specific Rce1 knockout mice develop a lethal cardiomyopathy. *J. Biol. Chem.* **2004**, *279*, 4729-4736.

18. Bhadoriya, K. S.; Sharma, M. C.; Jain, S. V. Pharmacophore modeling and atom-based 3D-QSAR studies on amino derivatives of indole as potent isoprenylcysteine carboxyl methyltransferase (Icmt) inhibitors. *J. Mol. Struct.* **2015**, *1081*, 466-476.

# CHAPTER I:
# NEW INHIBITORS OF ANGIOGENESIS WITH ANTITUMOR ACTIVITY IN VIVO

## 1. INTRODUCTION AND OBJECTIVES

Solid tumors initially grow as avascular nodules by absorbing nutrients and removing waste through simple diffusion, but once they grow beyond approximately 1 mm in diameter, they need to develop a novel network of blood vessels to satisfy their increasing need for nutrients and oxygen, and to remove waste products.[1] Angiogenesis, the process of new blood vessel formation, is then an essential requirement for the survival and proliferation of solid tumors.

The angiogenic process starts when a cell activated by a lack of oxygen releases proangiogenic factors that attract and promote the proliferation of inflammatory cells, which intensify the angiogenic call; and of endothelial cells from existing blood vessels, which proliferate and secrete proteases that break the blood-vessel wall, allowing their migration toward the angiogenic stimuli (Figure 1). Furthermore, one characteristic feature of new tumor vessels is that they fail to become quiescent, enabling the constant growth of tumor vasculature, which consequently becomes distinct from the normal blood supply system, showing irregularly shaped, dilated and tortuous vessels.

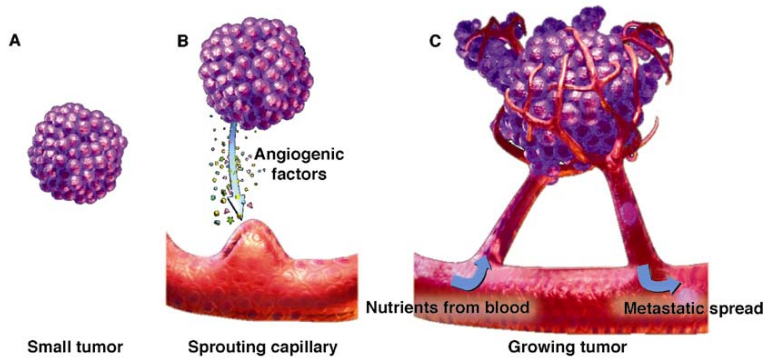


**Figure 1.** The development of new vessels in tumor angiogenesis (from Siemann, D.W. Vascular targeting agents. *Horizons in Cancer Therapeutics* **2002**, *3*, 4-15).

Accordingly, the search for angiogenesis inhibitors has become a leading line of investigation in anticancer research, and it has translated into several drugs in the market that have clearly improved outcomes in patients with different tumor types and metastatic disease.

There are many proangiogenic factors supporting tumor growth, such as vascular endothelial growth factors (VEGF), platelet derived growth factors (PDGF), fibroblast growth factors (FGF), tyrosine-protein kinase KIT (c-KIT or CD117), etc. And consequently, there are a number of possibilities to obtain an angiogenesis blockade. In fact, there are thirteen antiangiogenic drugs approved by the Food and Drug Administration (FDA), categorized as a) monoclonal antibodies or fusion proteins designed against the specific proangiogenic growth factors and/or their receptors; b) tyrosine kinase inhibitors (TKIs) of multiple proangiogenic growth factor receptors; and c) inhibitors of mammalian target of rapamycin (mTOR) (Figure 2).[2]

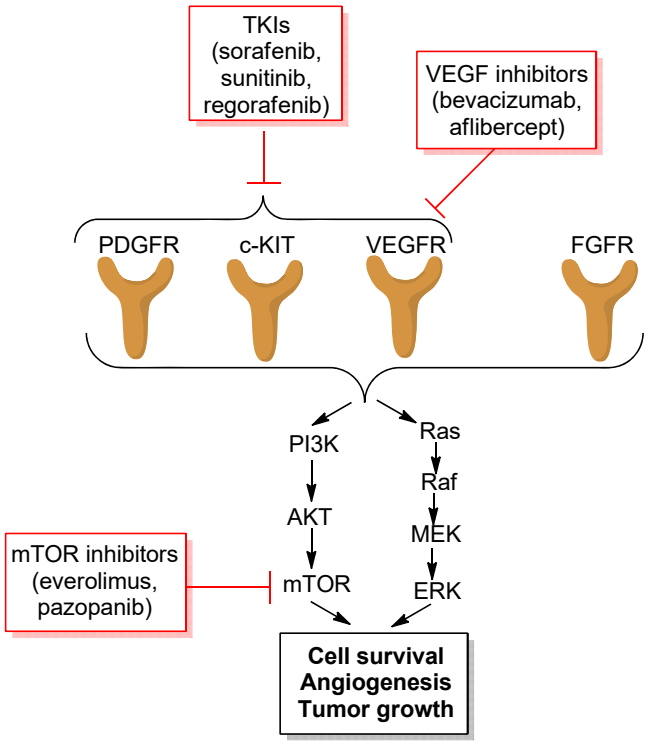


**Figure 2.** Summary of the mode of action of some proangiogenic factors and of major therapeutic agents designed against them (in red boxes).

Among these agents, bevacizumab (Avastin®, Genentech Ltd.) was the first antiangiogenic drug approved by the FDA in 2004.[3] Bevacizumab is a monoclonal antibody that targets VEGF -also known as VEGFA- and hinders it from binding to its corresponding receptor, thus blocking its signaling. Initially considered a first-line treatment for metastatic colorectal cancer, it is also prescribed for the treatment of other types of cancer, and its development still stands out as one of the landmark achievements of anticancer research.[4] With this same target, aflibercept (Zaltrap®, Sanofi/Regeneron), a soluble recombinant fusion receptor composed of VEGFR1 and VEGFR2 fragments, has recently been approved for the second-line treatment of patients with metastatic colorectal cancer in combination with chemotherapy.[5]

On the other hand, some TKIs (Figure 3) have also been approved by the FDA for the treatment of cancer angiogenesis. These compounds exert their effect at the intracellular level, inhibiting the kinase activity of receptors and/or downstream signa transducers of important angiogenic signaling systems. For instance, sorafenib tosylate (Nexavar®, Bayer) inhibits the kinase activity of certain receptors and the downstream transducer rapidly accelerated fibrosarcoma (RAF) blocking both angiogenesis and tumor proliferation, and it was approved for hepatocellular carcinoma and kidney cancer.[6,7] With similar mechanism of action, sunitinib malate (Sutent®, Pfizer) was approved for gastrointestinal stromal tumors and advanced kidney cancer,[8] and regorafenib (Stivarga®, Bayer) has been recently approved for patients with refractory advanced colorectal cancer.[9] However, the main problem of these TKIs is their relatively low specificity, which allows them to inhibit multiple pathways, but with lower efficiency and potential arise of adverse effects.[2]

Besides, some mTOR inhibitors (Figure 3) have been approved by the FDA as antiangiogenic agents for the treatment of cancer, such as everolimus (Afinitor®, Novartis) for both kidney cancer and neuroendocrine tumors, and pazopanib (Votrient®, GlaxoSmithKline/ Novartis) for kidney cancer. However, the activation of phosphoinositide 3-kinase/protein kinase B, also known as Akt- (PI3K/AKT) signaling pathway through the inhibition of mTOR, which could lead to outgrowth of more aggressive lesions; together with the lack of predictive biomarkers of efficacy for tumors treated with these inhibitors is an important concern that limits their clinical applications.[10,11]

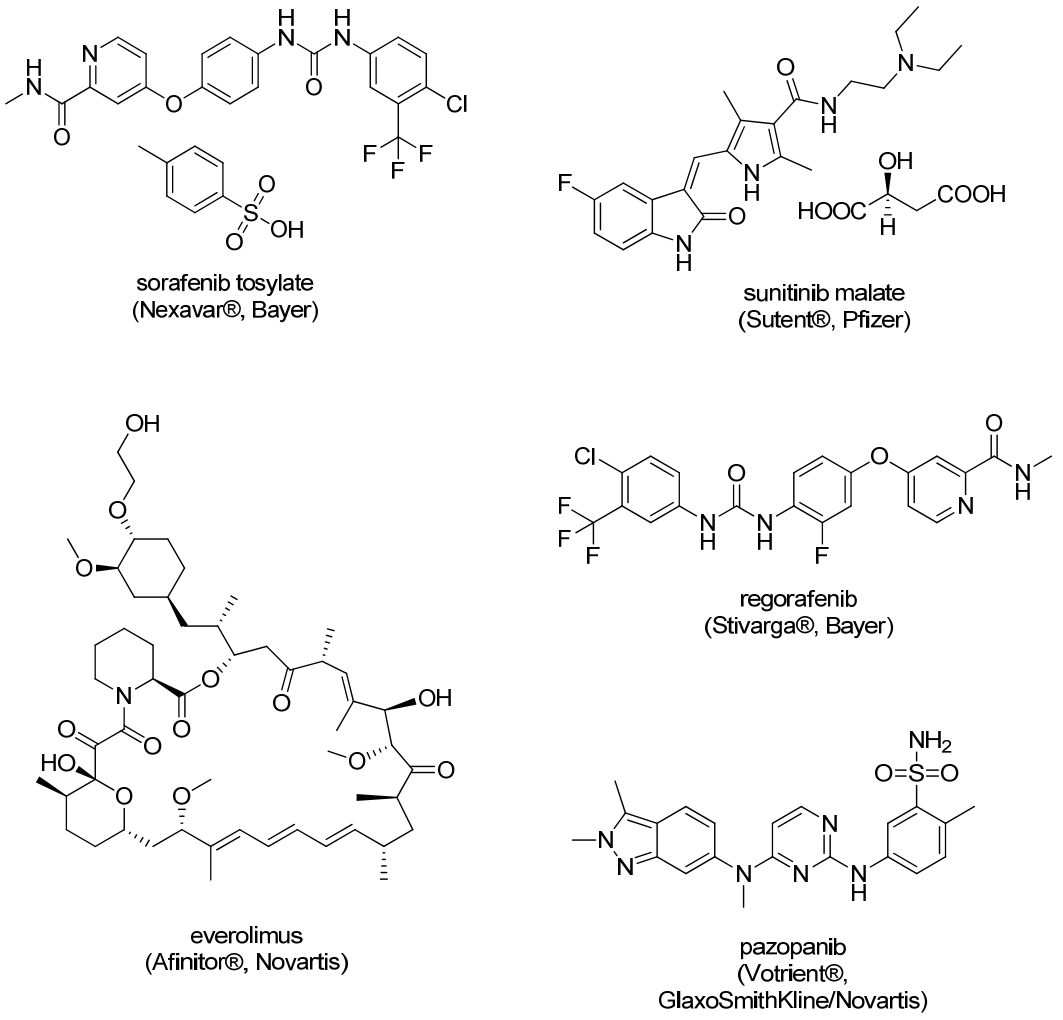


**Figure 3**. Representative examples of antiangiogenic compounds approved by the FDA.

Although the previously mentioned, as well as other drugs with similar mechanisms of action, have progressed into the clinic,[2,12,13] several limitations still exist, such as the lack of efficacy in some patients, the appearance of adverse effects, and drug resistance. Among them, this last one is perhaps the most important efficacy-limiting factor of the current antiangiogenic therapies. This effect has been observed especially for angiogenesis inhibitors targeting VEGF signaling pathways, which

have been clinically used for a longer period of time and in a larger number of patients, thus providing us with more clinical data. Results obtained up to day show that, although they are affording demonstrable therapeutic efficacy in mouse models of cancer and in an increasing number of human cancers, the benefits achieved in both preclinical and clinical studies are at best transitory and are followed by a restoration of tumour growth and progression.[14] A number of factors are behind the appearance of this resistance. For example, it has been suggested that when VEGF signaling is pharmacologically blocked, other proangiogenic factors take over its signaling thereby supporting tumor angiogenesis.[2,15,16] Amid these compensatory angiogenesis pathways, FGF seems to play an integral role in the resistance to anti-VEGF therapy, and different studies have suggested a critical role of the FGF signaling in clinical tumor progression.[17-19] Besides, it has been described that increasing tumor hypoxia during antiangiogenic therapy enhances cell survival through the stimulation of several factors, especially the key regulator hypoxia-inducible factor-1$\alpha$ (HIF-1$\alpha$). Its activation leads to an increase in transcription levels of the VEGF gene, making it even more difficult for the antiangiogenic drugs to achieve their goal.[20]

Although targeting FGF signaling has lagged behind that of other receptor tyrosine kinases, there is now substantial evidence for the importance of FGF signaling in the pathogenesis of diverse tumor types. Hence, the development of compounds that inhibit the FGF pathway is receiving much attention although they are still early in development.[21-23] Among the different FGFs, FGF-2, also known as basic FGF (bFGF), has been functionally implicated in tumor angiogenesis and it is an important target of antiangiogenic therapies.[17,21,23,24] Notwithstanding the importance of blocking angiogenesis for antitumor therapies, it has been shown that prolonged antiangiogenic treatments eventually lead not only to drug resistance but also to enhanced tumor migration and metastasis.[25-27] A main reason for this is that an antiangiogenic compound will eventually generate a hypoxic microenvironment, fact that turns on all pro-anginogenic signaling increasing the levels of factors that promote the acquisition of an invasive and metastatic tumor phenotype such as nitric oxide (NO), VEGF and FGF. In addition, the same cells often express the cognate membrane receptors for these factors, resulting in autocrine signaling.[20] Accordingly, the development of new antitumor compounds that simultaneously block angiogenesis and induce a sustained inhibition of the proangiogenic signaling generated by hypoxia currently remains as an important unmet need, as these agents should be more effective drugs than the ones currently in the clinic and should lack the associated more aggressive recurrence with metastasis and drug resistance.

In this context, the main objective of this work is the identification of new small molecules able to block angiogenesis affecting various proangiogenic factors (especially VEGF and FGF signaling pathways), and inducing a sustained inhibition of the proangiogenic signaling generated by hypoxia.

This overall objective involves the following steps:

1. Hit identification and hit to lead process.
2. Biological characterization of selected compound(s) in terms of impairment of proangiogenic signaling under hypoxia.
3. Antitumor effect of selected compound(s).

## 2. RESULTS AND DISCUSSION

### 2.1. Hit identification and hit to lead process

Selected representative compounds of our in-house library were screened in a bFGF-induced cell proliferation assay using human umbilical vein endothelial cells (HUVECs) in order to identify a hit chemically tractable and with drug-like properties that could be amenable to further optimization. From this screening, carbamate **1** emerged as an initial hit with an $IC_{50}$ value of 317 $\mu$M.

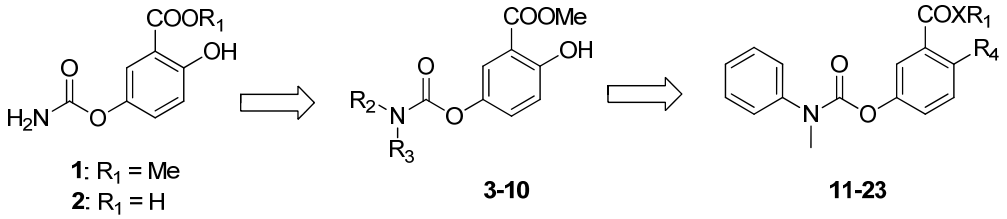


**Figure 4.** Exploration of the scaffold of the initial hit **1.**

We started the exploration of this scaffold (Figure 4) by introducing substituents in the carbamate group and keeping constant the methyl ester moiety (as its removal led to complete inactivity of the corresponding carboxylic acid, derivative **2**, $IC_{50}$ > 500 $\mu$M) as well as the phenolic hydroxyl group (compounds **3-10**). Target compounds were synthesized as depicted in Scheme 1.

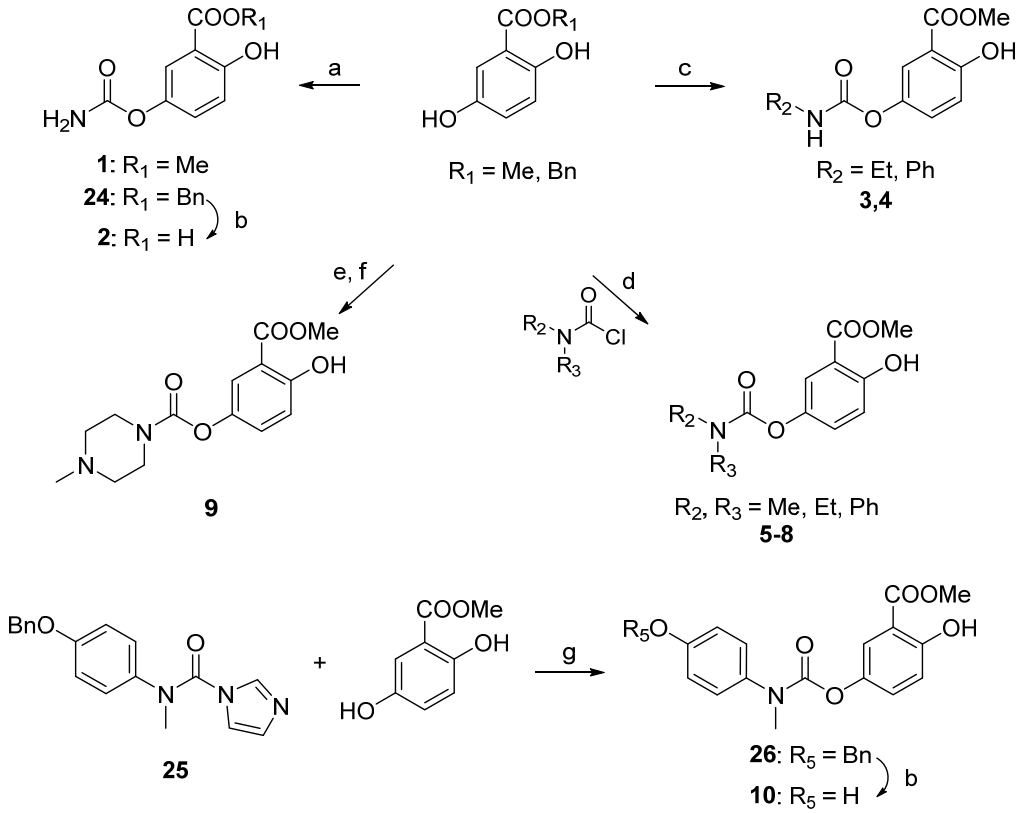


**Scheme 1.** Reagents and conditions: a) CSI, DCM, rt, o/n, 30-34%; b) $H_2$, Pd(C), EtOH, rt, 3 h, 100%; c) $R_2NCO$, DIEA, THF, rt, 16 h, 70-71%; d) NaH, $CH_3CN$, rt, 3 h, 14-64%; e) 4-nitrophenylchloroformate, DABCO, DCM, rt, 5 h, 40%; f) 1-methylpiperazine, DIEA, DCM, 0 °C to rt, 3 h, 67%; g) $CH_3I$, $CH_3CN$, rt, 24 h, 36%.

Reaction of methyl or benzyl 2,5-dihydroxybenzoate with chlorosulfonylisocyanate (CSI), followed by benzyl ester cleavage of intermediate **24** yielded carbamates **1** and **2**, respectively. *N*-monosubstituted carbamates **3** and **4** were obtained by addition of methyl 2,5-dihydroxybenzoate to ethyl and phenyl isocyanate, in the presence of *N,N*-diisopropylethylamine (DIEA) as a base, whereas reaction of methyl 2,5-hydroxybenzoate with the corresponding carbamoylchloride afforded disubstituted carbamates **5-8**. Piperazine derivative **9** was synthesized by nucleophilic substitution of 4-nitrophenylchloroformate with methyl 2,5-dihydroxybenzoate, followed by treatment of the resultant carbonate with 1-methylpiperazine. Alternatively, acylation of methyl 2,5-dihydroxybenzoate with carbonylimidazol derivative **25** gave intermediate **26**, which afforded final compound **10** by benzyl ether deprotection under palladium-catalyzed hydrogenation. Carbamates **2-10** were screened for activity in the bFGF-induced proliferation assay (Table 1).

**Table 1.** Inhibition of bFGF-induced cell proliferation of HUVECs for compounds **1-10**

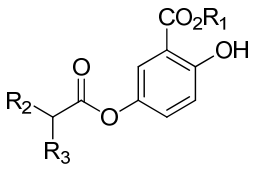


| Cpd | $R_1$ | $R_2$ | $R_3$ | $IC_{50}$ ($\mu$M)[a] |
|---|---|---|---|---|
| **1** | Me | H | H | 317 |
| **2** | H | H | H | >500 |
| **3** | Me | Et | H | 17 |
| **4** | Me | Ph | H | 165 |
| **5** | Me | Me | Me | >500 |
| **6** | Me | Et | Et | >500 |
| **7** | Me | Ph | Me | 48 |
| **8** | Me | Ph | Ph | 35 |
| **9** | Me | $(CH_2)_2NCH_3(CH_2)_2$ | | >500 |
| **10** | Me | *p*-hydroxyphenyl | Me | 96 |

[a] $IC_{50}$ values are the means from two or three independent experiments performed in triplicate. The standard error of the mean (SEM) is in all cases within a 10% of the mean value.

From the obtained results, the main conclusion is that the replacement of a hydrogen of the carbamate group by an ethyl or phenyl group gave active compounds (**3** and **4**), whereas disubstitution of the carbamate with alkyl chains is detrimental for the activity (compounds **5**, **6**, and **9**, $IC_{50}$ >500 $\mu$M). However, when one or both substituents are aromatic rings the antiproliferative activity is restored (**7**, **8**, and **10**). Among this first series of compounds, carbamates **3**, **7**, and **8** deserve special attention as they show the highest potency in the inhibition of cell proliferation, with $IC_{50}$ values of 17, 48, and 35 $\mu$M, respectively. In order to select the best scaffold to continue with the optimization process, we determined some pharmacokinetic parameters (Table 2).

**Table 2.** Pharmacokinetic properties of compounds **3**, **7**, **8**, **21**, and **22**[a]

| | Compound | | | | |
|---|---|---|---|---|---|
| **Property** | **3** | **7** | **8** | **21** | **22** |
| Aqueous solubility (PBS, pH 7.4, μM) | ND | 103.5 | 5.8 | 35 | 175.7 |
| Partition coefficient (LogD, *n*-octanol/PBS, pH 7.4) | ND | 3.13 | 4.46 | 4.19 | 2.95 |
| Chemical stability pH 7.4 (remaining compound, %) | ND | 67 | 24 | 93 | 108 |
| A-B Permeability (TC7, pH 6.5/7.4, $10^{-6}$cm/s) | ND | 46.1 | 7.9 | 35.1 | 53.5 |
| Human plasma stability (remaining compound, %) | <5 | 94 | 105 | 87 | 111 |
| Mouse plasma stability (remaining compound, %) | <5 | 83 | 89 | 78 | 99 |

[a]Data are expressed as the means from two independent experiments performed in duplicate. The SEM in all cases is within a 10% of the mean value. ND, not determined. For stability studies, the percentage of the remaining compound after 1 h is given.

Although the most potent derivative **3** showed a disappointing low stability that disqualified it as a suitable candidate for further optimization, compound **7** showed good properties, especially in terms of aqueous solubility, lipophilicity, permeability and stability. Therefore, it was selected for further structural exploration focused on whether the phenolic hydroxy group was required for activity and if it was possible to replace the methyl ester group without significant activity decrease (compounds **11-23**, Figure 4). These new derivatives were synthesized as depicted in Scheme 2. Disubstituted carbamates **11**, **12** and **14-18** were prepared by reaction of the corresponding 5-hydroxybenzoates with *N*-methyl-*N*-phenylcarbamoyl chloride. Methyl ester **7** was transformed into amide **13** by reaction with methylamine. Finally, phenyl methyl carbamates **19-23** were obtained by condensation of carboxylic acid **28** with the corresponding alcohol or amine in the presence of 1-ethyl-3-(3-dimethylaminopropyl)carbodiimide (EDC) as coupling reagent. All these new compounds were screened for activity (Table 3).

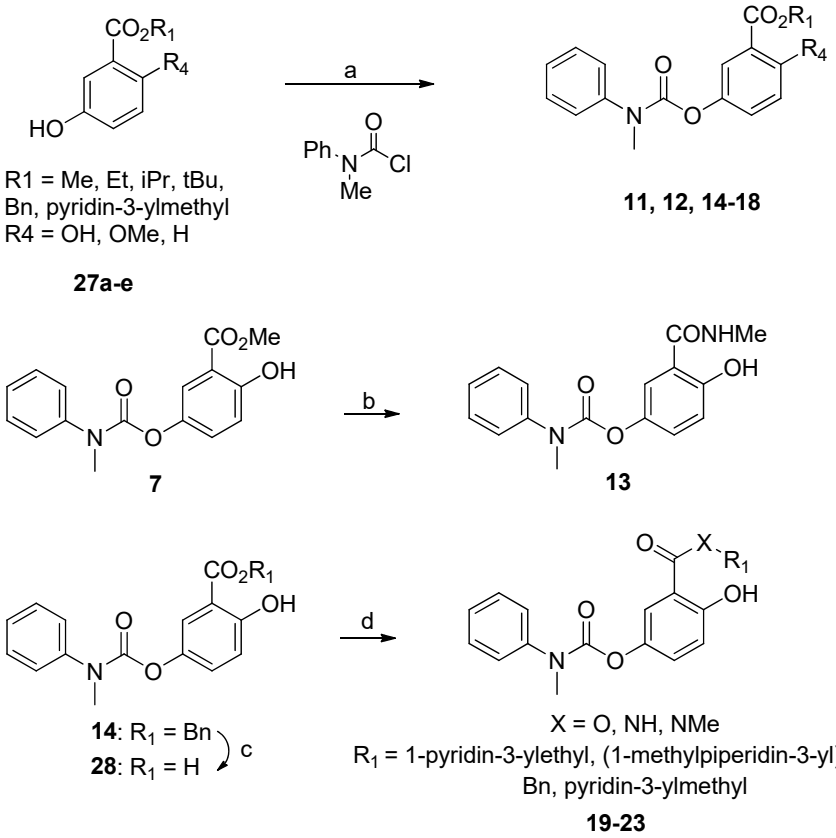


**Scheme 2.** Reagents and conditions: a) NaH, $CH_3CN$, rt, 3 h, 14-64%; b) $CH_3NH_2$, $CH_3OH$, 0 ºC to rt, 3 h, 76%; c) $H_2$, Pd(C), EtOH, rt, 3 h, 100%; d) $R_1OH$, $R_1NH_2$, or $R_1NHMe$, EDC, DMAP, DMF, 0 ºC to rt, 16 h, 27-64%.

**Table 3.** Inhibition of bFGF-induced cell proliferation of HUVECs for compounds **11-23**

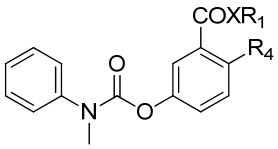


| Cpd | X | $R^1$ | $R^4$ | $IC_{50}$ ($\mu$M)[a] |
|---|---|---|---|---|
| **7** | O | Me | OH | 48 |
| **11** | O | Me | OMe | 118 |
| **12** | O | Me | H | 290 |
| **13** | NH | Me | OH | 67 |
| **14** | O | Bn | OH | 17 |
| **15** | O | Et | OH | 28 |
| **16** | O | Isopropyl | OH | 26 |
| **17** | O | *tert*-Butyl | OH | 25 |
| **18** | O | 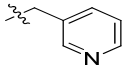 | OH | 16 |
| **19** | O | 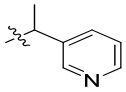 | OH | 39 |
| **20** | O | 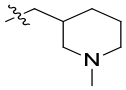 | OH | 74 |
| **21** | NH | Bn | OH | 22 |
| **22** | NH | 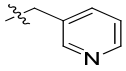 | OH | 14 |
| **23** | N(Me) | | | 90 |

[a] $IC_{50}$ values are the means from two or three independent experiments performed in triplicate. The SEM is in all cases within a 10% of the mean value.

Our results suggest that the phenolic hydroxy group is essential for activity, since both its methylation (compound **11**) or its removal (derivative **12**) led to an important decrease in the activity ($IC_{50}$ (**7**) = 48 $\mu$M vs $IC_{50}$ (**11**) = 118 $\mu$M and $IC_{50}$ (**12**) = 290 $\mu$M, Table 3). Accordingly, the phenolic hydroxy group was kept in carbamates **13-23** and different esters and amides were introduced trying to replace the initial methyl ester group. Our first attempt was to prepare the amide **13**, analogue to **7**, but this change led to a decrease in activity ($IC_{50}$ value for **7** was 48 $\mu$M whereas amide **13** showed

an $IC_{50}$ value of 67 $\mu$M, Table 3). This result suggested that the substitution of the ester by an amide probably would involve some reduction in biological activity, so we first kept the ester bond but replaced the methyl group by other aliphatic and (hetero)aromatic groups searching for better activities. In this case, we could later substitute the ester by an amide group and still keep good activity values. With this idea in mind, esters **14-20** were prepared. Among them, the best results in terms of $IC_{50}$ values were obtained for benzyl and 3-methylpyridinyl groups as $R_1$ substituents, compounds **14** and **18**, with $IC_{50}$ values of 17 and 16 $\mu$M, respectively (Table 3). Hence, these two $R_1$ groups were selected and the analogue amides **21-23** were synthesized. The biological activity of these amides was similar to that of the corresponding esters, as shown, for example, by the $IC_{50}$ values of esters **14** and **18** (17 $\mu$M and 16 $\mu$M, respectively) when compared with the $IC_{50}$ values of amides **21** and **22** (22 $\mu$M and 14 $\mu$M, respectively). Hence, we determined their pharmacokinetic properties in order to select the best candidate to continue with the biological studies. Taking into account all these data (Table 2), amide **22** (UCM-2711) showed the best overall profile with the highest solubility (175.7 $\mu$M), stability (around 100% in the three assayed conditions), and permeability values. Accordingly, this compound was selected for in-depth characterization.

### 2.2. Biological evaluation of compound 22 (UCM-2711)

#### 2.2.1. Proangiogenic signaling in hypoxic MCF7 cells

Tumor hypoxia, a common feature of many solid tumors, has been identified as a key driver for angiogenic regulation mechanisms. Hence, we first explored whether compound **22** is able to inhibit the proangiogenic signaling generated by hypoxia in the MCF7 human breast adenocarcinoma cell line that was chosen as a model. Our results show that compound **22** decreases the levels of important proangiogenic factors VEGF and bFGF in hypoxic MCF7 cells (Figure 5A,B). In addition, this derivative also induces a decrease in the NO levels, which runs parallel to a strong inhibition of iNOS expression (Figure 5C,F).

Considering the importance of the enhancement of autocrine signaling under hypoxic conditions, especially in terms of activation of the corresponding receptors, VEGFR and FGFR, we also assessed whether compound **22** affected their activation. Remarkably, this derivative inhibits the activation of these two receptors, as it decreases their phosphorylated (active) forms (Figure 5D,E).

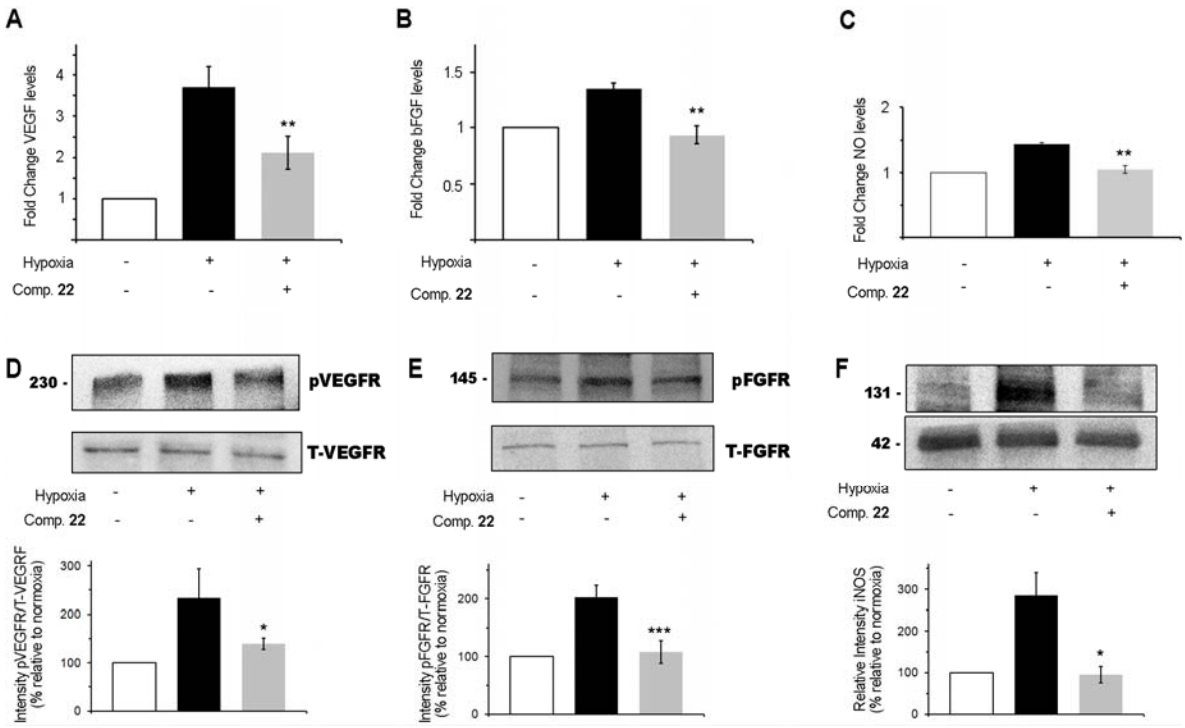


**Figure 5.** Compound **22** (UCM-2711) decreases the production of hypoxia-induced proangiogenic factors VEGF, bFGF, and NO and inhibits the activation of their corresponding receptors. Incubation of MCF7 cells with compound **22** (50 $\mu$M) under hypoxic conditions significantly reduces the levels of (A) VEGF, (B) bFGF, and (C) NO, decreases the activation of the (D) VEGF and (E) FGF receptors, and decreases (F) iNOS expression (131 kDa band). $\beta$-actin (42 kDa) is shown as loading control. Data correspond to the average ± SEM of at least three independent experiments, and representative gels are shown. The bar graphs in panels D and E represent the optical density of the immunoreactive phosphorylated protein normalized to the total corresponding protein, which is expressed as the percentage relative to normoxia. The bar graph in panel F represents the optical density of the immunoreactive protein (iNOS) expressed as the percentage relative to normoxia *, $P$<0.05; **, $P$<0.01; ***, $P$<0.001 (vs hypoxic vehicle-treated cells) (Student's $t$ test).

The main effects of the activation of the FGFR pathway include the induction of proliferation, migration, and antiapoptotic signals. Proliferation enhancement is mainly achieved through activation of the MAPK cascade, whereas the induction of antiapoptotic signals is mediated by activation of the PI3K/AKT pathway.[17,21] This latter cell survival pathway is also reinforced by VEGFR activation. Hence, we explored whether compound **22** was able to suppress the phosphorylation of the downstream kinases AKT, MEK and ERK. As expected, hypoxia activated the AKT and the MEK and ERK signaling pathways as demonstrated by the increased phosphorylation of these kinases and,

remarkably, incubation of the cells with compound **22** prevented this activation (Figure 6A). Importantly, inhibition of these signaling pathways by compound **22** was accompanied by an impairment in hypoxia-stimulated cell migration (Figure 6B).

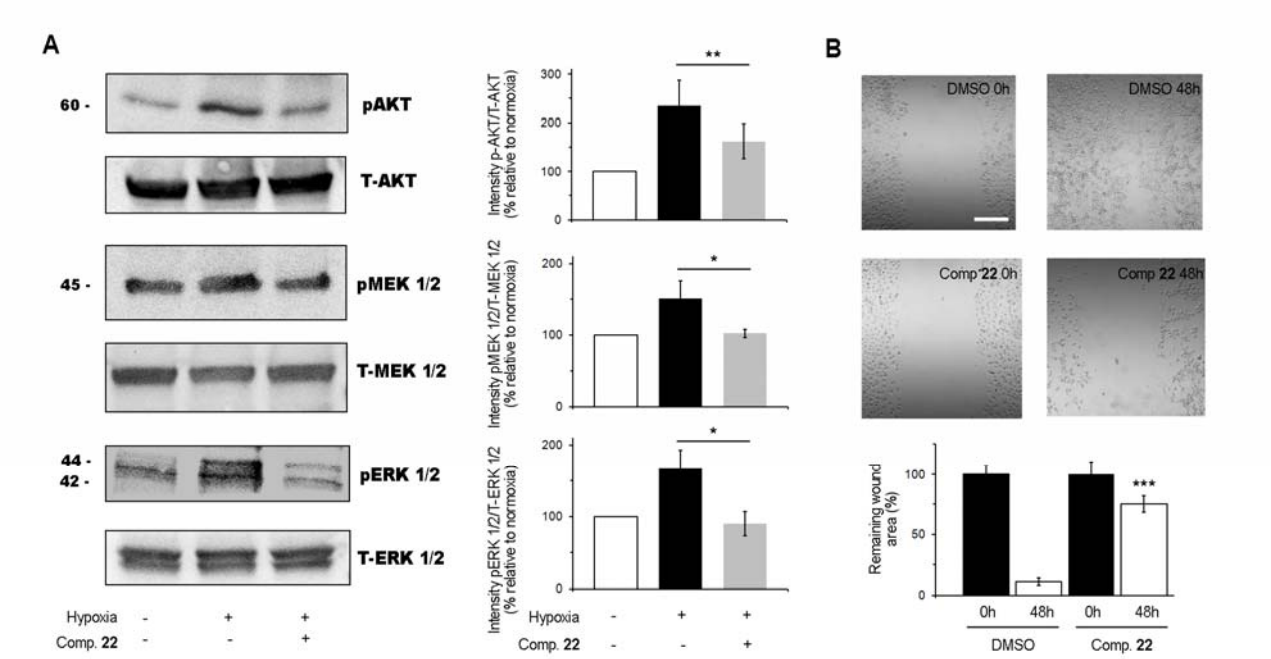


**Figure 6.** Compound **22** (UCM-2711) inhibits hypoxia-activated signaling pathways and suppresses cell migration. (A) Representative western blots of phosphorylated (pAKT) and total AKT (T-AKT), phosphorylated MEK1/2 (pMEK1/2) and total MEK1/2 (T-MEK1/2), and phosphorylated ERK1/2 (pERK1/2) and total ERK1/2 (T-ERK1/2). Lysates were obtained from MCF7 cells treated with compound **22** (50 $\mu$M) under hypoxic conditions. Data correspond to the average ± SEM of at least three independent experiments. The bar graphs in panel A represent the optical density of the immunoreactive phosphorylated protein normalised to the total corresponding protein, which is expressed as the percentage relative to normoxia. *, $P$<0.05; **, $P$<0.01 (Student's $t$ test). (B) In vitro scratches (wounds) were made by scraping confluent cell monolayers with a sterile pipette tip and were visualized by phase contrast microscopy. After 48 h under hypoxic conditions, the remaining wound area was quantified. The bar graph represents the average ± SEM of at least three independent experiments and three different fields. ***, $P$<0.001 (vs DMSO-treated cells) (Student's $t$ test). Bar, 250 $\mu$m.

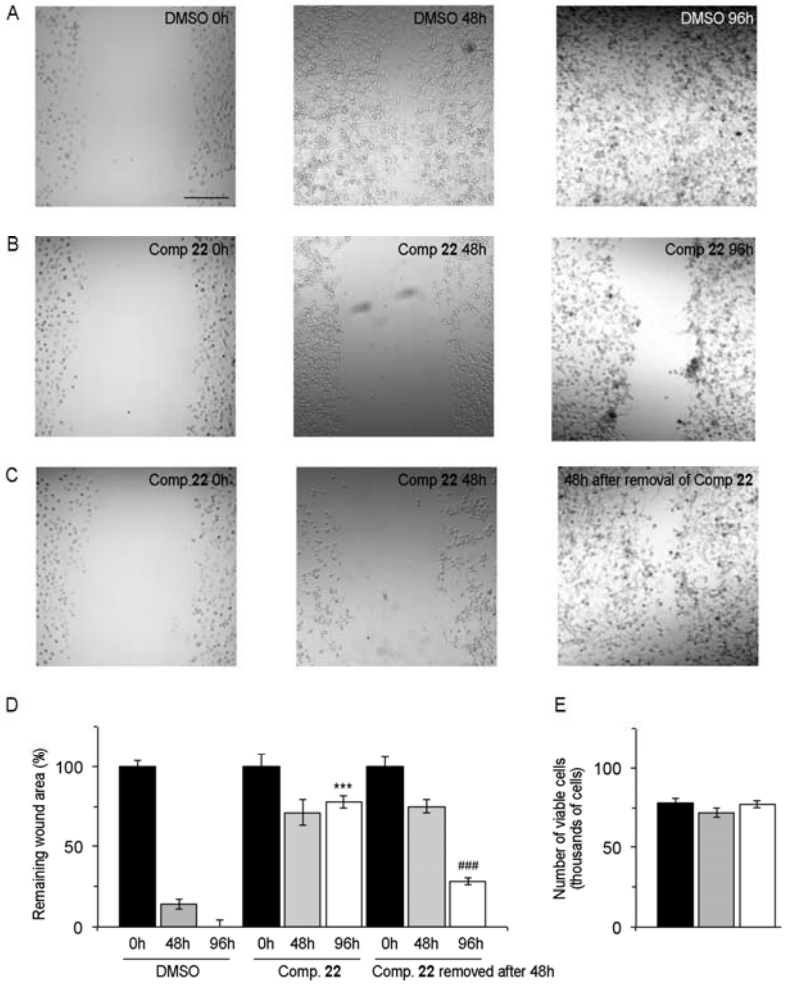


**Figure 7.** Compound **22** (UCM-2711) impairs cell migration without inducing general cytotoxicity. (A-C) Compound **22** prevents cell migration but cells recover their ability to migrate in the absence of compound. In vitro scratches (wounds) were made by scraping confluent cell monolayers with a sterile pipette tip and were visualized by phase contrast microscopy. After the indicated time under hypoxic conditions, remaining wound area was quantified in cells treated with (A) vehicle, (B) 50 $\mu$M of compound **22** during 96 h, and (C) 50 $\mu$M of compound **22** during 48 h and vehicle for additional 48h. Bar, 250 $\mu$m. (D) The bar graph represents the average ± SEM of the remaining wound area of at least three independent experiments and three different fields. ***, $P$<0.001 (vs DMSO-treated cells) (Student's $t$ test). ###, $P$<0.001 (vs cells treated with 50 $\mu$M of compound **22** during 96 h) (Student's $t$ test). (E) Cell viability is not significantly affected by compound **22**. Cells were incubated under hypoxic conditions and the number of viable cells determined after 96 h of incubation with vehicle (black bar), 50 $\mu$M of compound **22** (grey bar) or 50 $\mu$M of compound **22** during 48 h and vehicle for additional 48 h (white bar).

In order to determine whether the decrease in migration was due to general cytotoxicity, we carried out a similar set of experiments in which cells were incubated with compound **22** for 48 h, after which the compound was removed and then the cells were incubated for an additional 48 h. The obtained results show that cells recover their ability to migrate after removal of the compound (Figure 7). In addition, the number of viable cells remains similar to that in the vehicle treated cells (Figure 7E). Taken together, these data strongly suggest that compound **22** is mainly affecting cell migration and not inducing general cytotoxicity.

### 2.2.2. Proangiogenic signaling via hypoxia-inducible factor-1*α* (HIF-1*α*)

Intratumoral hypoxia is one of the major factors that drive tumor angiogenesis, and hypoxia-driven angiogenesis is primarily mediated by HIF-1*α*, often considered to be a master regulator of angiogenesis under hypoxia.[28] In addition, in MCF7 breast cancer cells, HIF-1*α* is the factor that mainly contributes to the expression of genes under hypoxic conditions.[29] Therefore, we analyzed whether HIF-1*α* was involved in the antiangiogenic response elicited by compound **22**. To this end, we knocked-down HIF-1*α* using selective small interfering RNAs (siRNAs) (Figure 8A). As shown in Figure 8B,C, hypoxia induced an increase in bFGF and VEGF levels in MCF7 cells transfected with a nontargeted (control) siRNA (C siRNA), and this effect was prevented by compound **22**. Conversely, genetic silencing of HIF-1*α* abrogated the increase in these two proangiogenic factors upon hypoxia stimulus, and compound 22 did not enhance this effect. These results suggest that the effect of compound **22** on bFGF and VEGF levels is mediated via HIF-1*α*. To further ascribe the effects of compound **22** to HIF-1*α* modulation and not to other members of its family, mainly HIF-2*α*, we selected two proteins, BCL2/adenovirus E1B 19 kDa protein-interacting protein 3 (BNip3) and Angiopoietin 2 (Ang2), which have been described to be mainly regulated by HIF-1*α* and HIF-2*α*, respectively.[30] As expected, and consistent with the literature, hypoxia increased the levels of both proteins, BNip3 and Ang2. Remarkably, compound **22** decreased only the levels of BNip3 (Figure 8D) without affecting the expression of Ang2 (Figure 8E). These results provide further support for the specific involvement of HIF-1*α* in the effects induced by compound **22**. In addition, and to discard potential effects of this derivative upstream of HIFs, we verified that compound **22** did not affect the expression levels either of HIF-1*α* or of HIF-2*α* (Figure 8F).

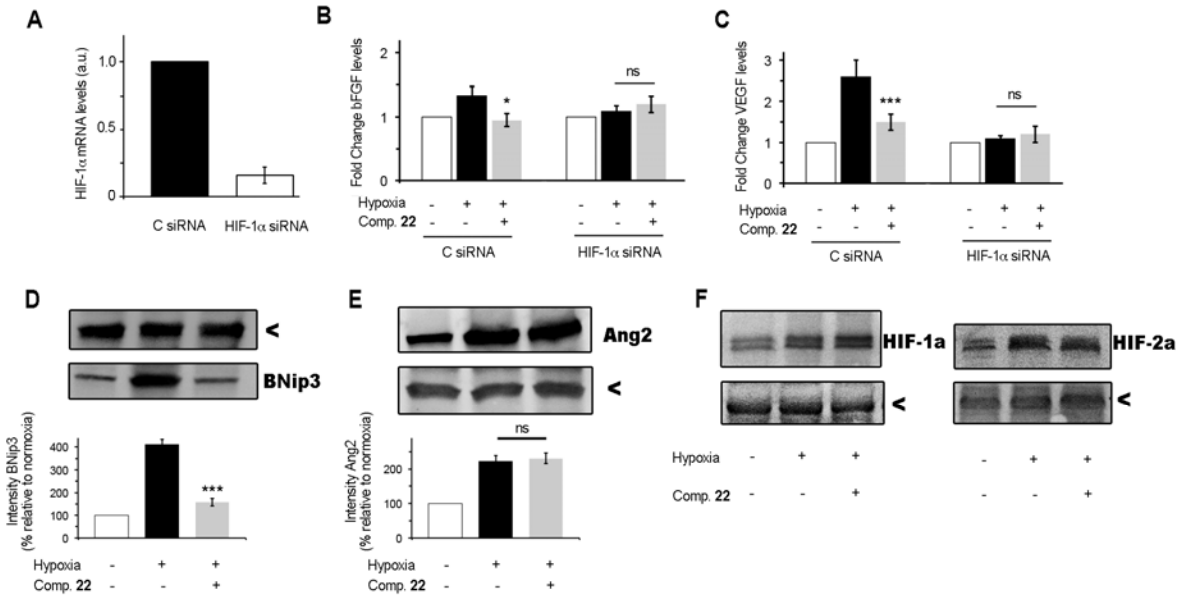


**Figure 8.** Compound **22** (UCM-2711) inhibits the production of the hypoxia-induced proangiogenic factors via HIF-1*α*. (A) HIF-1*α* mRNA levels after transient transfection of MCF7 cells with a siRNA selectively targeting HIF-1*α* (HIF-1*α* siRNA) or with a nontargeted siRNA (C siRNA). Results are expressed in arbitrary units (au). bFGF (B) and VEGF (C) levels in MCF7 cells transiently transfected with the indicated siRNAs under normoxic and hypoxic conditions and in the presence/absence of compound **22**. Representative western blots of (D) BNip3 (22 kDa), (E) Ang2 (65 kDa), (F) HIF-1*α* (132 kDa) and HIF-2*α* (115 kDa). In all cases, *β*-actin (42 kDa), marked with an arrowhead, is used as a loading control. Lysates were obtained from MCF7 cells treated with compound **22** (50 $\mu$M) under normoxic or hypoxic conditions as indicated. Data correspond to the average ± SEM of at least three independent experiments. The bar graphs in panels D and E represent the optical density of the immunoreactive protein (BNip3 or Ang2, respectively) expressed as the percentage relative to normoxia. Ns, not significant; *, $P<0.05$; ***, $P<0.001$ (vs hypoxic vehicle-treated cells) (Student's *t* test).

### 2.2.3. Antiangiogenic gene profile of hypoxic MCF7 cells

To further confirm the antiangiogenic profile of compound **22**, we analyzed the expression of 84 key genes involved in angiogenesis in hypoxic MCF7 cells treated with this compound. We identified 12 genes that were significantly affected by compound **22** (fold change ≥ 2, Figure 9). As expected, several proangiogenic genes were down-regulated in the presence of compound **22**. Among them are several cytokines such as CCL11, IL-1β or the chemokine-like PROK2 that have been linked to angiogenesis in solid tumors[31-33] as well as other known proangiogenic factors such as the vascular endothelial cadherin CDH5, and the receptors VEGFR-2 (also known as KDR) and Notch4.[34] On the other hand, up-regulation of several genes in response to compound **22** was also observed, including the chemokine CXCL9, which has been described to attenuate angiogenesis in some situations.[35] Surprisingly, we observed an increase in the transcript levels of certain proangiogenic factors such as the cell adhesion molecules integrin ITGB3 and PECAM1, the angiopoietin receptor TIE1 and the proangiogenic factors FGF1 and FGF2. These apparently contradictory results may be due to differential regulation at the transcriptional and translational levels. In this regard, for example, it is worth noting that although some increase is observed at the transcriptional level (Figure 9), compound **22** reduces the protein levels of FGF2 (bFGF) as shown in Figure 5B.

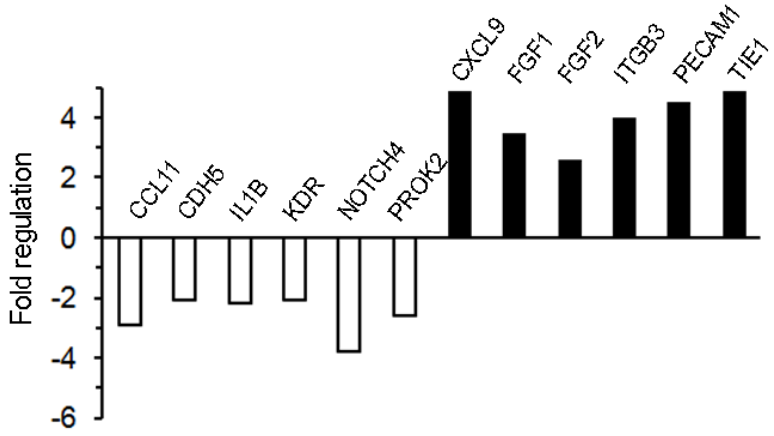


**Figure 9.** Compound **22** (UCM-2711) regulates the expression of angiogenesis-related genes. An angiogenesis PCR array was performed in hypoxic MCF7 cells challenged with compound **22** or the corresponding vehicle. The graph shows the 12 genes that were modulated (threshold = 2 fold increase/decrease) in compound **22**-treated cells vs control cells. Results are expressed as fold regulation.

### 2.2.4. In vivo antitumor effect

In order to assess the in vivo efficacy of compound **22** we used a breast cancer xenograft model. Tumor-bearing mice were injected intraperitoneally with compound **22** (25 mg/kg) once a day for 28 days and tumor volumes were routinely measured (Figure 10A). In vehicle-treated animals, tumors grew in an exponential manner. Treatment of mice with compound **22** produced no effect in 62% of them (5 out of 8), but we observed a significant reduction in tumor growth (ranging from 46% to 55%) in the remaining 38% (3 out of 8) (Figure 10B).

To analyze the in vivo inhibition of angiogenesis, we quantified the number of blood vessels within the tumors by immunofluorescence staining of CD31 (a marker of endothelial cells) in vehicle-treated animals as well as in responding and not-responding individuals (Figure 10C). Significant inhibition of angiogenesis was not detected in non-responding animals. In contrast, in the tumors of compound-responding individuals, a marked reduction in the number of blood vessels was observed. Remarkably, this result correlates with the expression levels of VEFG (Figure 10D). Importantly, the inhibition of angiogenesis and tumor growth induced by compound **22** was not accompanied by any sign of toxicity, as assessed by histopathological analysis of liver, lungs, spleen and heart of compound-treated animals (data not shown). The degree of interindividual variability in the response to compound **22** might be related to a different bioavailability of the compounds caused by the distinct growth and size of each individual tumor or by the existence of clonal variability of xenograft cells, something that has been previously observed for other antitumor targets[36] and also in the clinic after treatment with other angiogenesis inhibitors. In this case, it is possible that increasing the number of individuals would also augment the number of positive cases. In addition, it is important to note that a tumor is a heterogeneous entity, with hypoxic portions but also with other zones, near the blood vessel, which are not hypoxic and each may have different signaling factors. In this context, Figure 9 suggests up-regulation of some proangiogenic genes even in the presence of compound **22**. Hence, it is possible that in the mice in which the drug decreased tumor size the effects of the down-regulated proangiogenic genes predominated, while the increase in tumor size observed in the other mice was dominated by the effect of the proangiogenic genes that remained upregulated even in the presence of the compound.

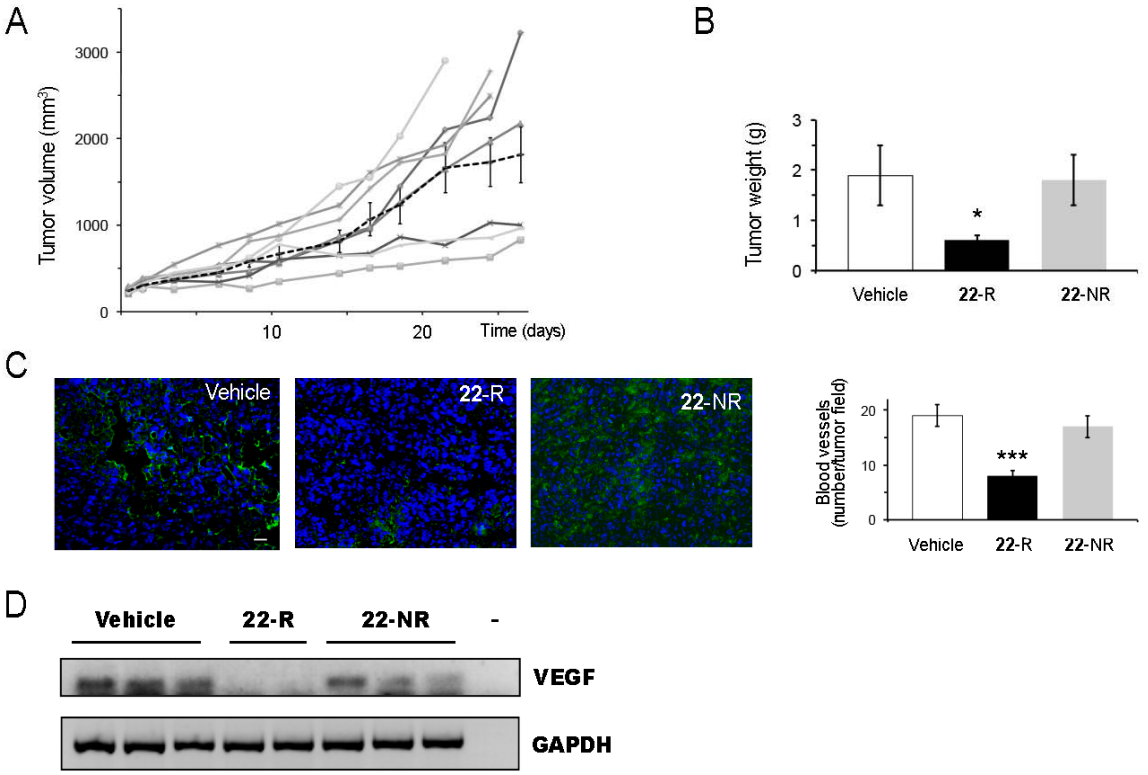


**Figure 10.** Antitumor effects of compound **22** (UCM-2711) in a breast cancer xenograft model. (A) Tumor growth in vehicle-treated (represented as mean ± SEM, grey dashed line, n=8) and compound **22**-treated animals (represented individually, n=8, solid grey lines). (B) Tumor weight at the end of the treatment for vehicle-treated animals (white bar), compound **22**-responding animals (black bar) and compound **22**-treated not-responding animals (grey bar). (C) Compound **22** significantly reduces angiogenesis in responding animals (**22**-R) whereas it does not affect the number of blood vessels in treated but not-responding animals (**22**-NR). Images correspond to representative immunofluorescence stainings of tumor sections of each experimental group. Blood vessels are stained with an antibody against CD31 (in green), and nuclei are shown in blue. Scale bar, 100 $\mu$m. The bar graph represents the number of blood vessels (mean ± SEM, 3 tumors/experimental group and 4 sections/tumor) for vehicle-treated animals (white bar), compound **22**-responding animals (black bar) and not-responding animals (grey bar). *, $P$<0.05; ***, $P$<0.001 (vs compound **22**-treated non-responding mice) (Student's $t$ test). (D) Compound **22** significantly reduces VEGF mRNA levels in responding animals (**22**-R) compared to vehicle-treated mice or to mice treated with compound **22** that are not responding (**22**-NR). Images correspond to representative data obtained from independent samples of tumor sections from each experimental group. Controls include lack of RNA (right lane, labelled -) and GAPDH as housekeeping gene.

## 3. CONCLUSIONS

In conclusion, in this work, we describe a new series of antiangiogenic compounds.[37] Among them, the optimal compound **22** (UCM-2711) inhibits proangiogenic signaling under hypoxic conditions in breast cancer cells. Specifically, administration of **22** decreases the levels of the proangiogenic molecules VEGF, bFGF, and NO. Moreover, this compound inhibits the active forms of the corresponding receptors of these factors (phosphorylated forms of VEGFR and bFGFR) and the levels of the iNOS enzyme. These effects correlate with a blockade of the MEK/ERK and PI3K/AKT pathways and the inhibition of cellular migration, and they are mediated by HIF-1*α*, since the effects of compound **22** mostly disappear when its expression is knocked-down. Additionally, gene profiling identified a set of genes related to angiogenesis whose expression is altered by compound **22** and that might contribute to the antiangiogenic effects. Furthermore, administration of compound **22** in a xenograft model produced tumor growth reductions ranging from 46 to 55% in the 38% of the treated animals. Importantly, in the responding tumors, a significant reduction in the number of blood vessels and in the levels of VEGF was observed, further supporting the mechanism of action of the compound. Although better efficacy would be desirable, the fact that compound **22** did not induce any toxic effects in vivo and that it was able to effectively block angiogenesis in the tumors of responding animals strongly support the potential of this compound as a lead for the development of new antiangiogenic agents suitable for the treatment of cancer either alone or in combination with other benchmark drugs.

## 4. EXPERIMENTAL SECTION

### 4.1. Chemistry

Unless stated otherwise, starting materials, reagents and solvents were purchased as high-grade commercial products from Sigma-Aldrich, Acros, Fluorochem, Abcr, Scharlab or Panreac, and were used without further purification. Anhydrous tetrahydrofuran (THF) and diethyl ether ($Et_2O$) were distilled from sodium benzophenone ketyl and used immediately, dichloromethane (DCM) was distilled from $CaH_2$. All reactions were carried out under an argon atmosphere in oven-dried glassware. Flash chromatography was performed on a Varian 971-FP flash purification system using silica gel cartridges (Varian, particle size 50 $\mu$m, for final compounds). Analytical thin-layer chromatography (TLC) was run on Merck silica gel plates (Kieselgel 60 F-254) with detection by UV light (254 nm), ninhydrin solution, or 10% phosphomolybdic acid solution in ethanol. Melting points (mp, uncorrected) were determined on a Stuart Scientific electrothermal apparatus. Infrared (IR) spectra were measured on a Shimadzu-8300 or Bruker Tensor 27 instrument; frequencies ($\nu$) are expressed in $cm^{-1}$. Nuclear Magnetic Resonance (NMR) spectra were recorded on a Bruker Avance 300-AM ($^1H$, 300 MHz; $^{13}C$, 75 MHz) at the UCM's NMR facilities. Chemical shifts ($\delta$) are expressed in parts per million relative to internal tetramethylsilane; coupling constants ($J$) are in hertz (Hz). The following abbreviations are used to describe peak patterns when appropriate: s (singlet), d (doublet), t (triplet), q (quartet), qt (quintet), sept (septuplet), m (multiplet), br (broad), dd (doublet of doublets), td (triplet of doublets). 2D NMR experiments (HMQC and HMBC) of representative compounds were carried out to assign protons and carbons of the new structures. Elemental analyses (C, H, N) were obtained on a LECO CHNS-932 apparatus at the UCM's analysis services and were within 0.4% of the theoretical values. High Pressure Liquid Chromatography-Mass Spectrometry (HPLC-MS) analysis was performed using an Agilent 1200LC-MSD VL. LC separation was achieved with an Eclipse XDB-C18 column (5 $\mu$m, 4.6 mm x 150 mm) together with a guard column (5 $\mu$m, 4.6 mm x 12.5 mm). The gradient mobile phases consisted of A (95:5 water/MeOH) and B (5:95 water/MeOH) with 0.1% ammonium hydroxide and 0.1% formic acid as the solvent modifiers. MS analysis was performed with an ESI source. The capillary voltage was set to 3.0 kV and the fragmentor voltage

was set at 70 eV. The drying gas temperature was 350 ºC, the drying gas flow was 10 L/min, and the nebulizer pressure was 20 pounds per square inch (psi). Spectra were acquired in positive and negative ionization mode from 100 to 1000 m/z and in UV-mode at four different wavelengths (210, 230, 254, and 280 nm). Spectroscopic data of all described compounds were consistent with the proposed structures. Satisfactory HPLC chromatograms and elemental analyses (C, H, N) were obtained for the final compounds, confirming a purity of at least 95% for all tested compounds. Pharmacokinetic properties of selected compounds **3**, **7**, **8**, **21**, and **22** (UCM-2711) were determined at CEREP (www.cerep.fr).

The free amines **9**, **18-20**, **22**, and **23** were characterized (yield, Rf, IR, NMR), dissolved in anhydrous DCM (6 mL/mmol) and a commercial 1 M HCl(g)/$Et_2O$ solution (1 mL/mmol) was added. The hydrochloride salts were isolated by filtration or evaporation of the solvents, washed with anhydrous $Et_2O$, dried under high vacuum, and characterized (Mp, elemental analysis).

### 4.1.1 Synthesis of final compounds 1- 23

**General procedure for the synthesis of esters 27a and 27b.** A solution of 2,5-dihydroxybenzoic acid (1 g, 6.5 mmol) and 1,1'-carbonyldiimidazole (CDI, 1 g, 6.5 mmol) in anhydrous DMF (16 mL) was heated at 40 ºC for 1 h under an argon atmosphere. Then, isopropanol or *tert*-butanol (13 mmol) and 1,8-diazabicyclo[5.4.0.]undec-7-ene (DBU, 1 mL, 6.5 mmol) were added and the reaction mixture was stirred at 40 ºC for additional 24 h. After cooling to rt, $Et_2O$ (60 mL) was added and the mixture was washed with an aqueous saturated solution of $NaHCO_3$ (3 x 40 mL). The organic layers were dried ($Na_2SO_4$) and evaporated. The residue was purified by column chromatography to afford the title esters.

**Isopropyl 2,5-dihydroxybenzoate (27a).** Obtained from 2,5-dihydroxybenzoic acid (1 g, 6.5 mmol) and isopropanol (1 mL, 13 mmol) in 17% yield. Chromatography: hexane/EtOAc, 7:3; oil. $R_f$ (hexane/EtOAc, 7:3) 0.48. $^1$H NMR (300 MHz, $CDCl_3$) $\delta$ 1.38 (d, 6H, $J$ = 6.3 Hz, $2CH_3$), 4.63 (br s, 1H, OH), 5.27 (sept, 1H, $J$ = 6.3 Hz, C<u>H</u>$(CH_3)_2$), 6.87 (d, 1H, $J$ = 8.9 Hz, $H_3$), 6.99 (dd, 1H, $J$ = 8.9, 3.1 Hz, $H_4$), 7.29 (d, 1H, $J$ = 3.1 Hz, $H_6$), 10.48 (br s, 1H, OH). $^{13}$C NMR (75 MHz, $CDCl_3$) $\delta$ 22.0 ($2CH_3$), 69.5 (CH), 112.9 (C), 115.0, 118.6, 123.9 (3CH), 147.7, 156.1, 169.4 (3C). The spectroscopic data are in agreement with those previously described.[38]

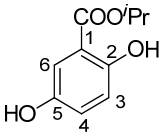


**27a**

***tert*-Butyl 2,5-dihydroxybenzoate (27b).** Obtained from 2,5-dihydroxybenzoic acid (1 g, 6.5 mmol) and *tert*-butanol (1.2 mL, 13 mmol) in 61% yield. Chromatography: hexane/EtOAc, 8:2. Mp 76-77 ºC (Lit.[39] 77-78 ºC). $R_f$ (hexane/EtOAc, 7:3) 0.50. $^1$H NMR (200 MHz, $CDCl_3$) $\delta$ 1.53 (s, 9H, $3CH_3$), 4.47 (br s, 1H, OH), 6.78 (d, 1H, $J$ = 8.9 Hz, $H_3$), 6.90 (dd, 1H, $J$ = 8.9, 3.1 Hz, $H_4$), 7.16 (d, 1H, $J$ = 3.1 Hz, $H_6$), 10.54 (br s, 1H, OH). $^{13}$C NMR (50 MHz, $CDCl_3$) $\delta$ 28.2 ($3CH_3$), 83.2, 113.9 (2C), 115.4, 118.3, 123.6 (3CH), 147.8, 155.4, 169.5 (3C). The spectroscopic data are in agreement with those previously described.[39]

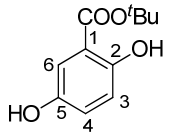


**27b**

**Synthesis of benzyl 2,5-dihydroxybenzoate (27c).** To a solution of 2,5-dihydroxybenzoic acid (2 g, 13 mmol) in anhydrous DMF (17 mL), $KHCO_3$ (1.6 g, 16 mmol) was added, under an argon atmosphere, and the reaction mixture was stirred at rt for 15 min. Then, benzyl bromide (2.3 mL, 19 mmol) was added and the reaction was heated at 40 ºC for 3 h. After cooling to rt, $H_2O$ (10 mL) was added and the mixture was extracted with EtOAc (3 x 40 mL). The organic layers were washed with a saturated aqueous solution of $NaHCO_3$ and brine successively, dried ($Na_2SO_4$) and evaporated to afford the title ester **27c** in 88% yield. Chromatography: hexane/EtOAc, 9:1; oil. $R_f$ (hexane/EtOAc, 7:3) 0.57. $^1$H NMR (200 MHz, $CDCl_3$) $\delta$ 4.62 (br s, 1H, OH), 5.36 (s, 2H, $CH_2$), 6.88 (d, 1H, $J$ = 8.9 Hz, $H_3$), 7.01 (dd, 1H, $J$ = 8.9, 2.9 Hz, $H_4$), 7.31 (d, 1H, $J$ = 2.9 Hz, $H_6$), 7.36-7.44 (m, 5H, Ar), 10.34 (br s, 1H, OH). $^{13}$C NMR (75 MHz, $CDCl_3$) $\delta$ 67.1 ($CH_2$), 112.2 (C), 114.9, 118.6, 124.2 (3CH), 128.3 (2CH), 128.6 (CH), 128.8 (2CH), 135.2, 147.7, 156.0, 169.5 (4C). The spectroscopic data are in agreement with those previously described.[40]

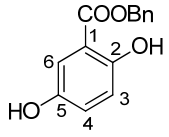


**27c**

**Synthesis of pyridin-3-ylmethyl 2,5-dihydroxybenzoate (27d).** To a solution of 2,5-dihydroxybenzoic acid (700 mg, 4.5 mmol) in DMF (20 mL), pyridin-3-ylmethanol (491 mg, 4.5 mmol), EDC (1.30 g, 6.8 mmol) and DMAP (832 mg, 6.8 mmol) were added. The reaction was warmed to 50 ºC and stirred for 12 h. The mixture was evaporated and the residue was purified by chromatography (DCM/MeOH, 98:2) to afford the title ester as a solid in 27% yield. Mp 173-174 ºC.

*R*$_f$ (DCM/MeOH, 95:5) 0.33. IR (KBr, cm$^{-1}$) ν 3429, 3245 (OH), 1678 (COO), 1627, 1589, 1485 (Ar). $^1$H NMR (300 MHz, $CD_3OD$) δ 5.35 (s, 2H, $CH_2$), 6.71 (d, 1H, *J* = 8.9 Hz, $H_3$), 6.89 (dd, 1H, *J* = 8.9, 3.0 Hz, $H_4$), 7.15 (d, 1H, *J* = 3.0 Hz, $H_6$), 7.40 (dd, 1H, *J* = 7.8, 4.9 Hz, $H_{5'}$), 7.89 (d, 1H, *J* = 7.8 Hz, $H_{4'}$), 8.45 (dd, 1H, *J* = 4.9, 1.4 Hz, $H_{6'}$), 8.58 (d, 1H, *J* = 1.4 Hz, $H_{2'}$). $^{13}$C NMR (75 MHz, $CD_3OD$) δ 65.3 ($CH_2$), 113.0 (C), 115.2, 119.2, 125.4, 125.5 (4CH), 133.9 (C), 138.4 (CH), 150.1 (2CH), 150.9, 156.3, 170.8 (3C).

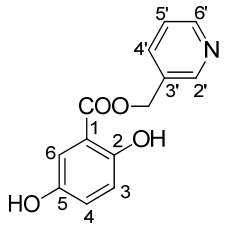


**27d**

**Methyl 5-hydroxy-2-methoxybenzoate (27e).** To a solution of methyl 5-(benzyloxy)-2-hydroxybenzoate[41] (460 mg, 1.8 mmol) in DMF (14 mL), $K_2CO_3$ (738 mg, 5.3 mmol) and methyl iodide (0.1 mL, 1.8 mmol) were added and the mixture was stirred at 80 ºC for 2 h. Then, additional amounts of $K_2CO_3$ (246 mg, 1.8 mmol) and methyl iodide (0.1 mL, 1.8 mmol) were added and the reaction was stirred at 60 ºC for 2 h. The mixture was quenched with $H_2O$ (15 mL) and extracted with DCM (5 x 30 mL). The combined organic layers were dried ($Na_2SO_4$) and evaporated to afford methyl 5-(benzyloxy)-2-methoxybenzoate as an oil in quantitative yield. *R*$_f$ (hexane/EtOAc, 8:2) 0.20. IR (neat, cm$^{-1}$) ν 1728 (COO), 1583, 1528, 1499 (Ar). $^1$H NMR (300 MHz, $CDCl_3$) δ 3.90 (s, 3H, $OCH_3$), 3.93 (s, 3H, $OCH_3$), 5.08 (s, 2H, $CH_2$), 6.95 (d, 1H, *J* = 9.1 Hz, $H_3$), 7.13 (dd, 1H, *J* = 9.1, 3.2 Hz, $H_4$), 7.36-7.49 (m, 6H, $H_6$, $H_{2'}$-$H_{6'}$).$^{13}$C NMR (75 MHz, $CDCl_3$) δ 52.2, 56.8 ($2CH_3$), 70.8 ($CH_2$), 113.8, 117.4 (2CH), 120.5 (C), 120.6 (CH), 127.6 (2CH), 128.1 (CH), 128.7 (2CH), 136.9, 152.2, 153.8, 166.5 (4C).

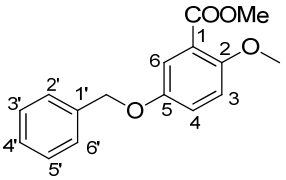


To a solution of methyl 5-(benzyloxy)-2-methoxybenzoate (478 mg, 1.8 mmol) in EtOH (20 mL), 10% Pd(C) (273 mg) was added and the mixture was hydrogenated at rt for 5 h, with an initial hydrogen pressure of 37 psi The reaction was filtered through celite and the solvent was evaporated to afford pure title compound **27e** as a solid in quantitative yield. Mp 75-76 ºC. *R*$_f$ (hexane/EtOAc,

9:1) 0.21. IR (KBr, $cm^{-1}$) ν 3370 (OH), 1710 (COO), 1589, 1502, 1441 (Ar). $^1H$ NMR (300 MHz, $CDCl_3$) δ 3.86 (s, 3H, $OCH_3$), 3.90 (s, 3H, $OCH_3$), 6.88 (d, 1H, *J* = 8.9 Hz, $H_3$), 7.00 (dd, 1H, *J* = 9.0, 3.2 Hz, $H_4$), 7.33 (d, 1H, *J* = 3.2 Hz, $H_3$). $^{13}C$ NMR ($CDCl_3$) δ 52.3, 56.9 ($2CH_3$), 114.2, 118.3, 120.6 (3CH), 149.2 (2C), 153.7, 166.7 (2C).

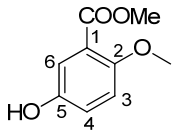


**27e**

**General procedure for the synthesis of compounds 1 and 24.** To a solution of methyl or benzyl 2,5-dihydroxybenzoate (1 equiv) in anhydrous DCM, CSI (1 equiv) was added dropwise and the reaction was stirred at rt for 2 h. Then, the resultant solid was separated by filtration and treated with cold $H_2O$. The solution was stirred overnight to afford a white precipitate which was filtered and washed with $H_2O$ to afford the title compounds, which were purified by chromatography.

**Methyl 5-[(aminocarbonyl)oxy]-2-hydroxybenzoate (1).** Obtained from methyl 2,5-dihydroxybenzoate (1.8 mmol) and CSI (1.8 mmol) in 30% yield. Chromatography: hexane/EtOAc, 8:2. Mp 194-196 ºC. $R_f$ (DCM/EtOH, 9:1) 0.39. IR (KBr, $cm^{-1}$) ν 3423, 3305 (OH, $NH_2$), 1728, 1705 ($NH_2COO$, COO), 1610, 1560, 1493, 1443 (Ar). $^1H$ NMR (300 MHz, acetone-$d_6$) δ 3.75 (s, 3H, $CH_3$), 6.65 (d, 1H, *J* = 8.9 Hz, $H_3$), 6.89 (dd, 1H, *J* = 8.9, 3.0 Hz, $H_4$), 7.09 (d, 1H, *J* = 3.0 Hz, $H_6$), 7.96 (br s, 2H, $NH_2$), 10.01 (br s, 1H, OH). $^{13}C$ NMR (75 MHz, acetone-$d_6$) δ 51.9 ($CH_3$), 123.4 (CH), 124.5 (C), 124.7, 126.8 (2CH), 146.8, 147.5, 154.3, 164.2 (4C). MS (ESI): $[(M-H)^-]$ 210.2.

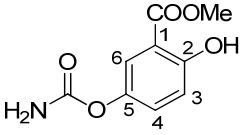


**1**

**Benzyl 5-[(aminocarbonyl)oxy]-2-hydroxybenzoate (24)**. Obtained from benzyl 2,5-dihydroxybenzoate (4.1 mmol) and CSI (4.1 mmol) in 34% yield. Chromatography: hexane/EtOAc, 7:3. Mp 153-154 ºC. $R_f$ (hexane/EtOAc, 6:4) 0.36. IR (KBr, $cm^{-1}$) ν 3429, 3310 (OH, $NH_2$), 1709, 1677 ($NH_2COO$, COO), 1610, 1490, 1430 (Ar). $^1H$ NMR (300 MHz, $CDCl_3$) δ 5.04 (br s, 2H, $NH_2$), 5.29 (s, 2H, $CH_2$), 6.90 (d, 1H, *J* = 9.0 Hz, $H_3$), 7.16 (dd, 1H, *J* = 9.0, 2.8 Hz, $H_4$), 7.31-7.36 (m, 5H, Ph), 7.54 (d, 1H, *J* = 2.8 Hz, $H_6$), 10.60 (br s, 1H, OH). $^{13}C$ NMR (75 MHz, $CDCl_3$) δ 67.2 ($CH_2$), 112.2 (C),

118.4, 122.2 (2CH), 128.4 (2CH), 128.6 (2CH), 128.7, 129.7 (2CH), 134.9, 142.4, 155.1, 159.3, 169.2 (5C).

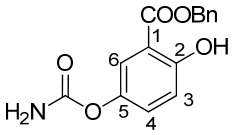


**24**

**Synthesis of 5-[(aminocarbonyl)oxy]-2-hydroxybenzoic acid (2).** To a solution of benzyl ester **24** (117 mg, 0.41 mmol) in absolute EtOH (15 mL), 10% Pd(C) (25 mg) was added and the mixture was hydrogenated at rt for 3 h, with an initial hydrogen pressure of 10 psi. The reaction was filtered over celite and the solvent was evaporated to afford pure title acid **2** as a white solid in quantitative yield. Mp 216-217 ºC. $R_f$ (DCM/EtOH, 8:2) 0.28. IR (KBr, $cm^{-1}$) ν 3450, 3305 (OH, $NH_2$), 1708, 1673 ($NH_2COO$, COO), 1602, 1485, 1400 (Ar).$^1$H NMR (300 MHz, DMSO-$d_6$) δ 6.90 (d, 1H, *J* = 8.9 Hz, $H_3$), 7.15 (br s, 2H, $NH_2$), 7.20 (dd, 1H, *J* = 8.9, 2.9 Hz, $H_4$), 7.41 (d, 1H, *J* = 2.9 Hz, $H_6$). $^{13}$C NMR (75 MHz, DMSO-$d_6$) δ 113.6 (C), 117.2, 122.3, 128.9 (3CH), 142.3, 154.9, 158.1, 171.0 (4C). Elemental analysis: calcd. for $C_8H_7NO_5$: %C: 48.74, %H: 3.58, %N: 7.10; found, %C: 48.49, %H: 3.66, %N: 6.88.

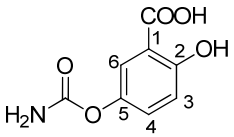


**2**

**General procedure for the synthesis of final compounds 3 and 4.** To a solution of methyl 2,5-dihydroxybenzoate (1 equiv) in anhydrous THF (4 mL/mmol), DIEA (1 equiv) and the proper isocyanate (1 equiv) were added dropwise, and the reaction mixture was stirred at rt for 16 h. The solvent was evaporated and the residue was purified by chromatography to afford the title final compounds as white solids.

**Methyl 5-{[(ethylamino)carbonyl]oxy}-2-hydroxybenzoate (3).** Obtained from methyl 2,5-dihydroxybenzoate (3.9 mmol) and ethyl isocianate (3.9 mmol) in 70% yield. Chromatography: hexane/EtOAc, 8:2. Mp 84-85 ºC. $R_f$ (hexane/EtOAc, 8:2) 0.34. IR (KBr, $cm^{-1}$) ν 3331, 3254 (NH), 1697 (NHCOO), 1653 (COO), 1622, 1593, 1533, 1488 (Ar). $^1$H NMR (300 MHz, $CDCl_3$) δ 1.15 (t, 3H, *J* = 7.2 Hz, $CH_3$), 3.25 (qt, 2H, *J* = 7.2 Hz, $CH_2$), 3.87 (s, 3H, $OCH_3$), 4.89 (br s, 1H, NH), 6.91 (d, 1H, *J* = 9.0 Hz, $H_3$), 7.15 (dd, 1H, *J* = 9.0, 2.9 Hz, $H_4$), 7.54 (d, 1H, *J* = 2.9 Hz, $H_6$), 10.56 (br s, 1H,

OH).[13]C NMR (75 MHz, $CDCl_3$) δ 15.2 ($CH_3$), 36.3 ($CH_2$), 52.5 ($CH_3$), 112.3 (C), 118.4, 122.4, 129.7 (3CH), 142.9, 150.1, 159.1, 170.1 (4C). Elemental analysis: calcd. for $C_{11}H_{13}NO_5$: %C: 55.23, %H: 5.48, %N: 5.86; found, %C: 54.90, %H: 5.32, %N: 5.58.

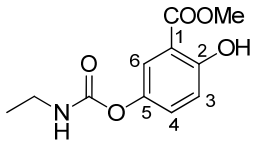


**3**

**Methyl 5-{[(phenylamino)carbonyl]oxy}-2-hydroxybenzoate (4).** Obtained from methyl 2,5-dihydroxybenzoate (3.1 mmol) and phenyl isocianate (3.1 mmol) in 71% yield. Chromatography: hexane/EtOAc, 8:2. Mp 129-130 ºC. $R_f$ (hexane/EtOAc, 7:3) 0.44. IR (KBr, $cm^{-1}$) ν 3354, 3325 (NH), 1724 (NHCOO), 1683 (COO), 1602, 1541, 1485, 1439 (Ar). $^1$H NMR (300 MHz, $CDCl_3$) δ 3.96 (s, 3H, $CH_3$), 6.92 (br s, 1H, NH), 7.02 (d, 1H, *J* = 9.0 Hz, $H_3$), 7.12 (t, 1H, *J* = 7.9 Hz, $H_{4'}$), 7.29 (dd, 1H, *J* = 9.0, 2.9 Hz, $H_4$), 7.34 (t, 2H, *J* = 7.9 Hz, $H_{3'}$, $H_{5'}$), 7.44 (d, 2H, *J* = 7.9 Hz, $H_{2'}$, $H_{6'}$), 7.68 (d, 1H, *J* = 2.9 Hz, $H_6$), 10.69 (br s, 1H, OH). $^{13}$C NMR (75 MHz, $CDCl_3$) δ 52.4 ($CH_3$), 112.2 (C), 118.3 (CH), 118.4 (2CH), 122.3, 123.9 (2CH), 129.0 (2CH), 129.4 (CH), 137.1, 142.1, 151.7, 159.1, 169.8 (5C). Elemental analysis: calcd. for $C_{15}H_{13}NO_5$: %C: 62.72, %H: 4.56, %N: 4.88; found, %C: 62.56, %H: 4.55, %N: 4.94.

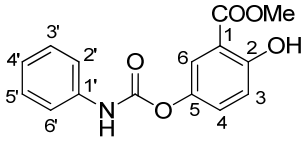


**4**

**General procedure for the synthesis of final compounds 5-8, 11, 12, and 14-18.** To a solution of 1 equiv of the corresponding ester (commercially available or **27a-e**) in anhydrous acetonitrile (4 mL/mmol), 1.3 equiv of NaH (60% in mineral oil) and 1 equiv of the appropriate carbamoyl chloride were added. The reaction mixture was stirred at rt for 3 h and the solvent was evaporated. The residue was purified by chromatography to afford the title final pure compounds.

**Methyl 5-{[(dimethylamino)carbonyl]oxy}-2-hydroxybenzoate (5).** Obtained from methyl 2,5-dihydroxybenzoate (500 mg, 3 mmol) and dimethylcarbamoyl chloride (0.3 mL, 3 mmol) in 21% yield. Chromatography: hexane/EtOAc, 9:1; oil. $R_f$ (hexane/EtOAc, 7:3) 0.24. IR (neat, $cm^{-1}$) ν 3173 (OH), 1725 (NCOO), 1681 (COO), 1621, 1483 (Ar).$^1$H NMR (300 MHz, $CDCl_3$) δ 3.02 (s, 3H, $NCH_3$), 3.10 (s, 3H, $NCH_3$), 3.94 (s, 3H, $OCH_3$), 6.97 (d, 1H, *J* = 9.0 Hz, $H_3$), 7.22 (dd, 1H, *J* = 9.0, 3.0 Hz, $H_4$),

7.61 (d, 1H, *J* = 3.0 Hz, $H_6$), 10.62 (s, 1H, OH). $^{13}$C NMR (75 MHz, $CDCl_3$) δ 36.8, 37.1, 52.8 ($3CH_3$), 112.5 (C), 118.5, 122.8, 130.2 (3CH), 143.7, 155.4, 159.3, 170.4 (4C). MS (ESI): [$(M-H)^-$] 238.1.

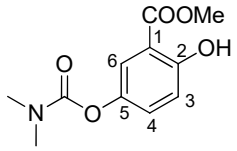


**5**

**Methyl 5-{[(diethylamino)carbonyl]oxy}-2-hydroxybenzoate (6).** Obtained from methyl 2,5-dihydroxybenzoate (500 mg, 3 mmol) and diethylcarbamoyl chloride (0.4 mL, 3 mmol) in 16% yield. Chromatography: hexane/EtOAc, 9:1; oil. $R_f$ (hexane/EtOAc, 7:3) 0.46. IR (KBr, $cm^{-1}$) ν 3191 (OH), 1719 (NCOO), 1683 (COO), 1620, 1480 (Ar).$^1$H NMR (300 MHz, $CDCl_3$) δ 1.18-1.28 (m, 6H, $2CH_3$), 3.38-3.45 (m, 4H, $2CH_2$), 3.94 (s, 3H, $OCH_3$), 6.97 (d, 1H, *J* = 9.0 Hz, $H_3$), 7.23 (dd, 1H, *J* = 9.0, 2.9 Hz, $H_4$), 7.60 (d, 1H, *J* = 2.9 Hz, $H_6$), 10.62 (s, 1H, OH). $^{13}$C NMR (75 MHz, $CDCl_3$) δ 13.8, 14.6 ($2CH_3$), 42.2, 42.7 ($2CH_2$), 52.8 ($CH_3$), 112.5 (C), 118.5, 122.8, 130.2 (3CH), 143.7, 154.7, 159.2, 170.4 (4C). MS (ESI): [$(M-H)^-$] 266.1.

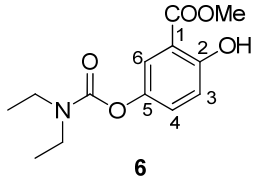


**6**

**Methyl 2-hydroxy-5-({[methyl(phenyl)amino]carbonyl}oxy)benzoate (7).** Obtained from methyl 2,5-dihydroxybenzoate (400 mg, 2.4 mmol) and *N*-methyl-*N*-phenylcarbamoyl chloride (404 mg, 2.4 mmol) in 46% yield. Chromatography: hexane/EtOAc, 9:1; oil. $R_f$ (hexane/EtOAc, 7:3) 0.38. IR (neat, $cm^{-1}$) ν 3168 (OH), 1724 (NCOO), 1680 (COO), 1620, 1597, 1487 (Ar). $^1$H-NMR (300 MHz, $CDCl_3$) δ 3.43 (s, 3H, $NCH_3$), 3.94 (s, 3H, $OCH_3$), 6.96 (d, 1H, *J* = 9.0 Hz, $H_3$), 7.27-7.45 (m, 7H, $H_4$, $H_{2'}$- $H_{6'}$), 7.53 (m, 1H, $H_6$), 10.62 (br s, 1H, OH). $^{13}$C NMR (75 MHz, $CDCl_3$) δ 38.7, 52.8 ($2CH_3$), 112.6 (C), 118.6 (2CH), 122.7, 126.3, 127.1, 129.5 (4CH), 130.0 (2CH), 143.2, 143.5, 154.5, 159.4, 170.4 (5C). MS (ESI): [$(M-H)^-$] 300.1.

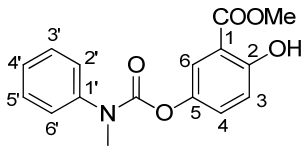


**7**

**Methyl 5-{[(diphenylamino)carbonyl]oxy}-2-hydroxybenzoate (8).** Obtained from methyl 2,5-dihydroxybenzoate (500 mg, 3 mmol) and diphenylcarbamoyl chloride (688 mg, 3 mmol) in 36% yield. Chromatography: hexane/EtOAc, 9:1. Mp 121-123 ºC. $R_f$ (hexane/EtOAc, 8:2) 0.24. IR (KBr, $cm^{-1}$) ν 3179 (OH), 1729 (NCOO), 1682 (COO), 1594, 1488 (Ar).$^1$H NMR (300 MHz, $CDCl_3$) δ 3.95 (s, 3H, $OCH_3$), 6.97 (d, 1H, $J$ = 9.0 Hz, $H_3$), 7.23-7.30 (3H, m, $H_4$, Ph), 7.35-7.42 (8H, m, Ph), 7.66 (d, 1H, $J$ = 2.9 Hz, $H_6$), 10.64 (br s, 1H, OH). $^{13}$C NMR (75 MHz, $CDCl_3$) δ 52.9 ($CH_3$), 112.6 (C), 118.7, 122.6 (2CH), 127.1 (2CH), 127.3 (4CH), 129.6 (4CH), 129.9 (CH), 142.6 (C), 143.3 (2C), 153.7, 159.6, 170.4 (3C). Elemental analysis: calcd. for $C_{21}H_{17}NO_5$: %C: 69.41, %H: 4.72, %N: 3.85; found, %C: 68.99, %H: 4.76, %N: 3.90.

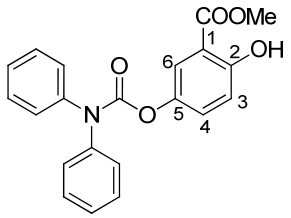


**8**

**Methyl 2-methoxy-5-({[methyl(phenyl)amino]carbonyl}oxy)benzoate (11).** Obtained from methyl ester **27e** (273 mg, 1.5 mmol) and *N*-methyl-*N*-phenylcarbamoyl chloride (254 mg, 1.5 mmol) in 58% yield. Chromatography: DCM/EtOAc, 9:1; oil. $R_f$ (DCM/EtOAc, 9.5:0.5) 0.37. IR (neat, $cm^{-1}$) ν 1723 (NCOO, COO), 1596, 1497, 1437 (Ar).$^1$H NMR (300 MHz, $CDCl_3$) δ 3.43 (s, 3H, $NCH_3$), 3.88 (s, 3H, $OCH_3$), 3.90 (s, 3H, $OCH_3$), 6.95 (d, 1H, $J$ = 9.0 Hz, $H_3$), 7.27-7.44 (m, 6H, $H_4$, $H_{2'}$-$H_{6'}$), 7.58 (m, 1H, $H_6$). $^{13}$C NMR (75 MHz, $CDCl_3$) δ 38.3, 52.1, 56.5 ($3CH_3$), 112.8 (CH), 120.3 (C), 124.8 (CH), 125.9 (2CH), 126.8 (CH), 129.1 (3CH), 142.8, 144.1, 154.0, 156.7, 165.7 (5C). MS (ESI): [$(M+Na)^+$] 338.1.

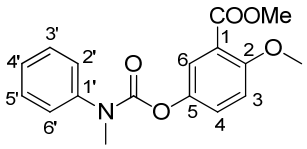


**11**

**Methyl 3-({[methyl(phenyl)amino]carbonyl}oxy)benzoate (12).** Obtained from methyl 5-hydroxybenzoate (477 mg, 3.1 mmol) and *N*-methyl-*N*-phenylcarbamoyl chloride (533 mg, 3.1 mmol) in 64% yield. Chromatography: hexane/EtOAc, 9:1; oil. $R_f$ (hexane/EtOAc, 9:1) 0.23. IR (neat, $cm^{-1}$) ν 1723 (NCOO, COO), 1593, 1495 (Ar). $^1$H NMR (300 MHz, $CDCl_3$) δ 3.47 (s, 3H, $NCH_3$), 3.94 (s, 3H, $OCH_3$), 7.30-7.48 (m, 7H, $H_3$, $H_4$, $H_{2'}$-$H_{6'}$), 7.81 (m, 1H, $H_6$), 7.91 (d, 1H, $J$ = 7.6 Hz, $H_2$). $^{13}$C NMR

(75 MHz, $CDCl_3$) δ 38.3, 52.2 ($2CH_3$), 122.9, 126.0, 126.4, 126.5, 126.8 (5CH), 129.1 (3CH), 129.2 (CH), 131.5, 142.8, 151.3, 153.6, 166.2 (5C). MS (ESI): [$(M-CH_3+Na)^+$] 293.2.

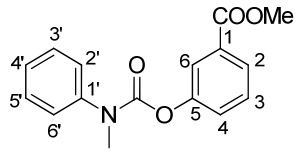


**12**

**Benzyl 2-hydroxy-5-({[methyl(phenyl)amino]carbonyl}oxy)benzoate (14).** Obtained from benzyl ester **27c** (630 mg, 2.6 mmol) and *N*-methyl-*N*-phenylcarbamoyl chloride (437 mg, 2.6 mmol) in 28% yield. Chromatography: hexane/EtOAc, 9:1. Mp 103-105 ºC. $R_f$ (hexane/EtOAc, 7:3) 0.80. IR (KBr, $cm^{-1}$) ν 3194 (OH), 1726 (NCOO), 1679 (COO), 1622, 1599, 1489 (Ar). $^1H$ NMR (300 MHz, $CDCl_3$) δ 3.41 (s, 3H, $NCH_3$), 5.38 (s, 2H, $CH_2$), 6.96 (d, 1H, *J* = 9.0 Hz, $H_3$), 7.20-7.46 (m, 11H, $H_4$, $H_{2'}$-$H_{6'}$, $H_{2''}$-$H_{6''}$), 7.60 (m, 1H, $H_6$), 10.66 (s, 1H, OH).$^{13}C$ NMR (75 MHz, $CDCl_3$) δ 38.3 ($CH_3$), 67.3 ($CH_2$), 112.2 (C), 118.3, 122.3, 126.0, 126.7 (4CH), 128.6 (2CH), 128.7 (CH), 128.8 (3CH), 129.1 (2CH), 129.9 (CH), 135.1, 142.9, 143.2, 154.2, 159.3, 169.5 (6C). MS (ESI): [$(M-H)^-$] 376.1.

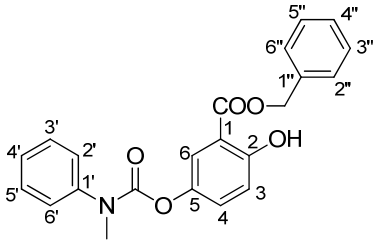


**14**

**Ethyl 2-hydroxy-5-({[methyl(phenyl)amino]carbonyl}oxy)benzoate (15).** Obtained from ethyl 2,5-dihydroxybenzoate (433 mg, 2.4 mmol) and *N*-methyl-*N*-phenylcarbamoyl chloride (404 mg, 2.4 mmol) in 14% yield. Chromatography: hexane/EtOAc, 9:1; oil. $R_f$ (hexane/EtOAc, 7:3) 0.55. IR (neat, $cm^{-1}$) ν 3163 (OH), 1726 (NCOO), 1677 (COO), 1619, 1597, 1487 (Ar). $^1H$ NMR (300 MHz, $CDCl_3$) δ 1.44 (t, 3H, *J* = 7.1 Hz, $CH_3$), 3.46 (s, 3H, $NCH_3$), 4.43 (q, 2H, *J* = 7.1 Hz, $CH_2$), 6.96 (d, 1H, *J* = 8.9 Hz, $H_3$), 7.19-7.45 (m, 6H, $H_4$, $H_{2'}$-$H_{6'}$), 7.62 (m, 1H, $H_6$), 10.77 (s, 1H, OH). $^{13}C$ NMR (75 MHz, $CDCl_3$) δ 14.2, 38.3 ($2CH_3$), 61.7 ($CH_2$), 112.4 (C), 118.2, 122.3, 125.9, 126.7 (4CH), 129.1 (3CH), 129.5 (CH), 142.9, 143.0, 154.2, 159.2, 169.6 (5C). MS (ESI): [$(M-H)^-$] 314.1.

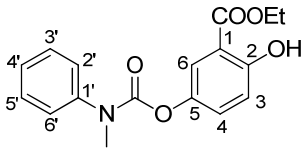


**15**

**Isopropyl 2-hydroxy-5-({[methyl(phenyl)amino]carbonyl}oxy)benzoate (16).** Obtained from isopropyl ester **27a** (211 mg, 1.1 mmol) and *N*-methyl-*N*-phenylcarbamoyl chloride (183 mg, 1.1 mmol) in 28% yield. Chromatography: hexane/EtOAc, 9:1; oil. $R_f$ (hexane/EtOAc, 7:3) 0.57. IR (neat, $cm^{-1}$) ν 3178 (OH), 1728 (NCOO), 1675 (COO), 1622, 1599, 1489 (Ar). $^1H$ NMR (300 MHz, $CDCl_3$) δ 1.42 (d, 6H, *J* = 6.3 Hz, $2CH_3$), 3.47 (s, 3H, $NCH_3$), 5.30 (sept, 1H, *J* = 6.3 Hz, CH), 6.98 (d, 1H, *J* = 9.0 Hz, $H_3$), 7.23-7.33 (m, 2H, Ar), 7.39-7.48 (m, 4H, Ar), 7.61 (m, 1H, $H_6$), 10.97 (br s, 1H, OH). $^{13}C$ NMR (75 MHz, $CDCl_3$) δ 21.8, 38.3 ($2CH_3$), 69.6 (CH), 112.8 (C), 118.2, 122.3, 126.0, 126.7 (4CH), 129.1 (3CH), 129.5 (CH), 142.9, 143.0, 154.2, 159.3, 169.2 (5C). MS (ESI): $[(M-H)^-]$ 328.1.

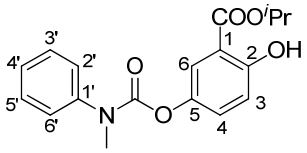


**16**

***tert*-Butyl 2-hydroxy-5-({[methyl(phenyl)amino]carbonyl}oxy)benzoate (17).** Obtained from *tert*-butyl ester **27b** (500 mg, 2.4 mmol) and *N*-methyl-*N*-phenylcarbamoyl chloride (404 mg, 2.4 mmol) in 32% yield. Chromatography: hexane/EtOAc, 9:1; oil. $R_f$ (hexane/EtOAc, 7:3) 0.61. IR (neat, $cm^{-1}$) ν 3070 (OH), 1727 (NCOO), 1673 (COO), 1620, 1599, 1457 (Ar). $^1H$ NMR (300 MHz, $CDCl_3$) δ 1.61 (s, 9H, $3CH_3$), 3.43 (s, 3H, $NCH_3$), 6.93 (d, 1H, *J* = 8.9 Hz, $H_3$), 7.17-7.19 (m, 1H, $H_4$), 7.26-7.30 (m, 2H, Ar), 7.36-7.45 (m, 3H, Ar), 7.49 (m, 1H, $H_6$), 10.95 (br s, 1H, OH). $^{13}C$ NMR (75 MHz, $CDCl_3$) δ 28.1 ($3CH_3$), 38.2 ($CH_3$), 83.2 (C), 113.6 (C), 118.1, 122.4, 125.8, 126.6 (4CH), 129.0 (3CH), 129.1 (CH), 142.8 (2C), 154.2, 159.3, 169.1 (3C). MS (ESI): $[(M-H)^-]$ 342.1.

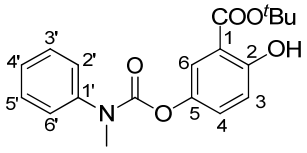


**17**

**Pyridin-3-ylmethyl (2-hydroxy-5-({[methyl(phenyl)amino]carbonyl}oxy)benzoate (18).** Obtained from pyridinyl ester **27d** (272 mg, 1.1 mmol) and *N*-methyl-*N*-phenylcarbamoyl chloride

(188 mg, 1.1 mmol) in 22% yield. The free amine was characterized (yield, Rf, IR, NMR), dissolved in anhydrous $Et_2O$ (4 mL) and treated with a commercial 1 M HCl(g)/$Et_2O$ solution (0.6 mL). The hydrochloride salts was isolated by evaporation of the solvents and characterized (Melting point, elemental analysis). Chromatography: DCM/MeOH, 99:1. Mp 183-185 ºC. $R_f$ (DCM/MeOH, 95:5) 0.56; IR (KBr, $cm^{-1}$) $\nu$ 3170 (OH), 1724 (NCOO), 1680 (COO), 1595, 1488 (Ar). $^1$H-NMR (300MHz, $CDCl_3$) $\delta$ 3.42 (s, 3H, $NCH_3$), 5.40 (s, 2H, $CH_2$), 6.97 (d, 1H, $J$ = 9.0 Hz, $H_3$), 7.22-7.44 (m, 7H, $H_4$, $H_{2'}$-$H_{6'}$, $H_{5''}$), 7.58 (m, 1H, $H_6$), 7.84 (d, 1H, $J$ = 7.8 Hz, $H_{4''}$), 8.66 (m, 1H, $H_{2''}$/$H_{6''}$), 8.76 (m, 1H, $H_{2''}$/$H_{6''}$), 10.51 (s, 1H, OH). $^{13}$C-NMR (75 MHz, $CDCl_3$) $\delta$ 38.8 ($CH_3$), 64.9 ($CH_2$), 112.1 (C), 118.8, 122.6, 124.3, 126.3, 127.2 (5CH), 129.5 (3CH), 130.6 (CH), 132.0 (C), 137.4 (CH), 143.1, 143.5 (2C), 149.7, 149.8 (2CH), 154.5, 159.7, 169.6 (3C). Elemental analysis: calcd. for $C_{21}H_{18}N_2O_5 \cdot HCl \cdot H_2O$: %C: 58.27, %H: 4.89, %N: 6.47; found, %C: 58.64, %H: 5.28, %N: 6.62.

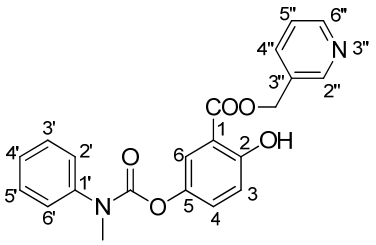


**18**

**Synthesis of 3-(methoxycarbonyl)phenyl 4-methylpiperazine-1-carboxylate (9).** To a solution of methyl 2,5-dihydroxybenzoate (550 mg, 3.3 mmol) and 4-nitrophenyl chloroformate (659 mg, 3.3 mmol) in anhydrous DCM, 1,4-diazabicyclo[2.2.2]octane (DABCO, 734 mg, 6.5 mmol) was added dropwise at 0 ºC and the reaction mixture was stirred for 5 h. The solvent was evaporated and the residue was purified by chromatography (hexane/EtOAc, 9:1) to afford methyl 2-hydroxy-5-{[(4-nitrophenoxy)carbonyl]oxy}benzoate in 40% yield. $R_f$ (hexane/AcOEt, 7:3): 0.57. $^1$H NMR (300 MHz, $CDCl_3$) $\delta$ 3.97 (s, 3H, $OCH_3$), 6.89 (d, 2H, $J$ = 9.1 Hz, $H_{2'}$, $H_{6'}$), 7.03 (d, 1H, $J$ = 9.1 Hz, $H_3$), 7.37 (dd, 1H, $J$ = 9.1, 3.0 Hz, $H_4$), 7.77 (d, 1H, $J$ = 3.0 Hz, $H_6$), 8.13 (d, 2H, $J$ = 9.1 Hz, $H_{3'}$, $H_{5'}$).

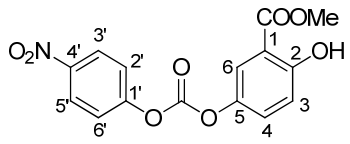


To a solution of methyl 2-hydroxy-5-{[(4-nitrophenoxy)carbonyl]oxy}benzoate (130 mg, 0.4 mmol) and 1-methylpiperazine (0.07 mL, 0.6 mmol) in anhydrous DCM (6 mL), DIEA (0.3 mL, 1.6 mmol) was added dropwise at 0 ºC and the reaction mixture was stirred for 3 h at rt. The solvent was

evaporated and the residue was purified by column chromatography (EtOAc/EtOH, 8:2) to afford the title final compound **9** as a solid in 67% yield. Mp 218-219 ºC. $R_f$ (EtOAc/EtOH, 7:3) 0.32. IR (KBr, $cm^{-1}$) ν 3197 (OH), 1724 (NCOO), 1683 (COO), 1621, 1489 (Ar). $^1$H NMR (300 MHz, $CDCl_3$) δ 2.28 (s, 3H, $NCH_3$), 2.39 (t, 4H, *J* = 5.1 Hz, $2H_{3'}$, $2H_{5'}$), 3.52 (m, 2H, $2H_{2'}/2H_{6'}$), 3.61 (m, 2H, $2H_{2'}/2H_{6'}$), 3.87 (s, 3H, $OCH_3$), 6.90 (d, 1H, *J* = 9.0 Hz, $H_3$), 7.15 (dd, *J* = 9.0, 2.9 Hz, $H_4$), 7.53 (d, 1H, *J* = 2.9 Hz, $H_6$), 10.56 (br s, 1H, OH). $^{13}$C NMR (75 MHz, $CDCl_3$) δ 43.9, 44.4 ($2CH_2$), 46.2, 52.4 ($2CH_3$), 54.6, 54.8 ($2CH_2$), 112.2 (C), 118.3, 122.4, 129.7 (3CH), 143.1, 153.8, 159.0, 170.0 (4C). Elemental analysis: calcd. for $C_{14}H_{18}N_2O_5 \cdot HCl$: %C: 50.84, %H: 5.79, %N: 8.47; found, %C: 50.47, %H: 5.61, %N: 8.68.

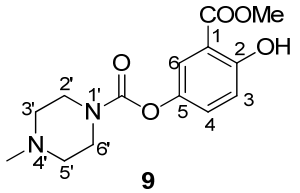


**9**

**Synthesis of *N*-[4-(benzyloxy)phenyl]-*N*-methyl-1-imidazole-1-carboxamide (25).** To a suspension of CDI (750 mg, 3.5 mmol) in anhydrous THF (20 mL), 4-(benzyloxy)-*N*–methylaniline (627 mg, 3.9 mmol) was added. The mixture was refluxed for 16 h. The solvent was evaporated and the residue was dissolved in DCM (20 mL) and washed with $H_2O$ (2 x 30 mL). The organic layers were dried ($Na_2SO_4$) and evaporated to afford the title carbamoylimidazole as a solid in 85% yield. $R_f$ (hexane/ EtOAc, 7:3) 0.37. IR (KBr, $cm^{-1}$) ν 1697 (NCON), 1608, 1510, 1460 (Ar).$^1$H-NMR (300 MHz, $CDCl_3$) δ 3.46 (s, 3H, $NCH_3$), 5.06 (s, 2H, $CH_2$), 6.83-6.84 (m, 1H, $H_{4''}/H_{5''}$), 6.89-6.90 (m, 1H, $H_{4''}/H_{5''}$), 6.97 (d, 2H, *J* = 9.0 Hz, $H_2$,$H_6/H_3$,$H_5$), 7.07 (d, 2H, *J* = 9.0 Hz, $H_2$,$H_6/H_3$,$H_5$), 7.38-7.45 (m, 5H, $H_{2'}$-$H_{6'}$), 7.58 (br s, 1H, $H_{2''}$).

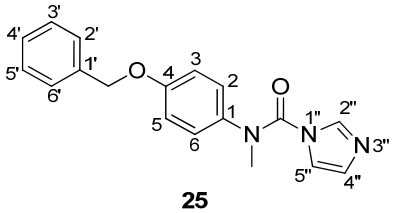


**25**

**Synthesis of methyl 5-({[[4-(benzyloxy)phenyl](methyl)amino]carbonyl}oxy)-2-hydroxybenzoate (26).** To a solution of **25** (937 mg, 3.1 mmol) in acetonitrile (8 mL), methyl iodide (0.9 mL, 12.2 mmol) was added and the mixture was stirred at rt for 24 h. The solvent was evaporated, the residue was dissolved in acetonitrile and methyl 2,5-dihydroxybenzoate (506 mg, 3 mmol) and triethyl amine (0.4 mL, 3 mmol) were added dropwise. The reaction was refluxed for 18 h. The solvent

was evaporated, the residue was dissolved in DCM and an aqueous solution of 0.1 M HCl (50 mL) was added. The aqueous layer was extracted with DCM (3 x 50 mL). The organic layers were dried ($Na_2SO_4$) and evaporated, and the residue was purified by chromatography (hexane/EtOAc, 8:2) to afford the title compound as an oil in 36% yield. $R_f$ (hexane/EtOAc, 7:3) 0.28. IR (neat, $cm^{-1}$) ν 3172 (OH), 1722 (CON), 1681, 1618, 1541, 1484 (Ar).$^1$H NMR (300 MHz, $CDCl_3$) δ 3.36 (s, 3H, $NCH_3$), 3.94 (s, 3H, $OCH_3$), 5.08 (s, 2H, $CH_2$), 6.95 (d, 1H, *J* = 8.9 Hz, $H_3$), 7.01 (d, 2H, *J* = 8.8 Hz, $H_{2'}$, $H_{6'}$), 7.14-7.27 (m, 3H, $H_4$, $H_{3'}$, $H_{5'}$), 7.35-7.46 (m, 5H, $H_{2''}$-$H_{6''}$), 7.57 (m, 1H, $H_6$), 10.63 (br s, 1H, OH). $^{13}$C NMR (75 MHz, $CDCl_3$) δ 37.8, 53.6 ($2CH_3$), 70.7 ($CH_2$), 110.7 (C), 113.7, 116.5, 120.4 (3CH), 125.4 (3CH), 125.4 (C), 125.9 (2CH), 126.5 (2CH), 127.4 (2CH), 134.2, 140.3, 151.0 (3C), 155.4 (2C), 165.9 (C).

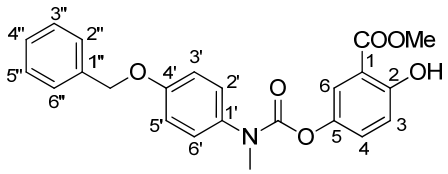


**26**

**Synthesis of 2-hydroxy-5-({[methyl(phenyl)amino]carbonyl}oxy)benzoic acid (28).** To a solution of benzyl ester **14** (120 mg, 0.3 mmol) in absolute EtOH (20 mL), 10% Pd(C) (50 mg) was added and the mixture was hydrogenated at rt for 4 h, with an initial hydrogen pressure of 30 psi. The reaction mixture was filtered through a pad of celite and washed with EtOH. The solvent was evaporated to afford the title pure compound as a solid in quantitative yield. Mp 157-158 ºC. $R_f$ (DCM/EtOH, 95:5) 0.20. IR (KBr, cm-1) ν 3071 (OH), 1699 (NCOO, COO), 1596, 1489 (Ar). $^1$H NMR (300 MHz, $CDCl_3$) δ 3.44 (s, 3H, $NCH_3$), 6.95 (d, 1H, *J* = 8.9 Hz, $H_3$), 7.22-7.45 (m, 6H, $H_4$, $H_{2'}$-$H_{6'}$), 7.61 (m, 1H, $H_6$). $^{13}$C NMR (75 MHz, $CDCl_3$) δ 38.4 ($CH_3$), 114.2 (C), 118.8, 119.1, 126.1, 127.0, 127.3 (5CH), 129.3 (3CH), 142.5, 142.7, 154.8, 159.2, 169.8 (5C).

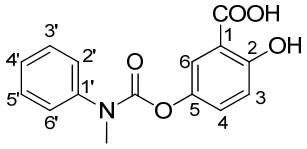


**28**

**Synthesis of methyl 2-hydroxy-5-({[(4-hydroxyphenyl)-(methyl)amino]carbonyl}oxy) benzoate (10).** To a solution of **26** (100 mg, 0.3 mmol) in EtOH (10 mL), 10% Pd(C) (39 mg) was added and the mixture was hydrogenated at rt for 5 h, with an initial hydrogen pressure of 57 psi.

The reaction was filtered through celite and the solvent was evaporated to afford pure the title compound as a solid in quantitative yield. Mp 54-56 ºC. $R_f$ (hexane/EtOAc, 7:3) 0.23. IR (KBr, $cm^{-1}$) ν 3352 (OH), 1687 (NCOO), 1619, 1515, 1485 (Ar). $^1$H NMR (300 MHz, $CD_3OD$) δ 3.32 (s, 3H, $NCH_3$), 3.95 (s, 3H, $OCH_3$), 6.82 (d, 2H, $J$ = 8.7 Hz, $H_{3'}$, $H_{5'}$), 6.93 (d, 1H, $J$ = 7.8 Hz, $H_3$), 7.19 (d, 2H, $J$ = 8.7 Hz, $H_{2'}$, $H_{6'}$), 7.36 (m, 1H, $H_4$), 7.49 (m, 1H, $H_6$).$^{13}$C NMR (75 MHz, $CD_3OD$) δ 39.1, 53.1 ($2CH_3$), 113.5 (C), 116.8 (2CH), 119.1 (2CH), 123.4, 128.7, 130.8 (3CH), 135.9, 144.7, 156.3, 157.7, 160.1, 171.1 (6C). Elemental analysis: calcd. for $C_{16}H_{15}NO_6$: %C: 60.57, %H: 4.77, %N: 4.41; found, %C: 60.29, %H: 4.98, %N: 4.25.

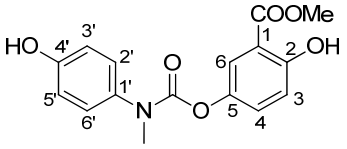


**10**

**Synthesis of 4-hydroxy-3-[(methylamino)carbonyl]phenyl methyl(phenyl)carbamate (13).** To a solution of methyl ester **7** (200 mg, 0.7 mmol) in MeOH (2 mL), a solution of methylamine (40% in $H_2O$) (0.5 mL, 10 mmol) was added dropwise at 0 ºC and the reaction mixture was stirred for 3 h at rt. The solvents were evaporated and the residue was purified by chromatography (hexane/EtOAc, 7:3) to afford the title compound as a solid in 76% yield. Mp 69-70 ºC. $R_f$ (DCM/EtOH, 95:5) 0.43. IR (KBr, $cm^{-1}$) ν 3366 (NH, OH), 1705 (NCOO), 1647 (CON), 1602, 1552, 1494 (Ar).$^1$H NMR (300 MHz, $CDCl_3$) δ 2.92 (d, 3H, $J$ = 4.8 Hz, $NHC\underline{H}_3$), 3.43 (s, 3H, $NCH_3$), 6.41 (br s, 1H, NH), 6.95 (d, 1H, $J$ = 8.8 Hz, $H_3$), 7.10-7.44 (m, 7H, $H_4$, $H_6$, $H_{2'}$-$H_{6'}$), 12.22 (s, 1H, OH). $^{13}$C NMR (75 MHz, $CDCl_3$) δ 26.5, 38.4 ($2CH_3$), 114.2 (C), 118.8, 119.1, 126.1, 127.0, 127.3 (5CH), 129.3 (3CH), 142.5, 142.7, 154.8, 159.2, 169.8 (5C). Elemental analysis: calcd. for $C_{17}H_{18}N_2O_4$: %C: 63.99, %H: 5.37, %N: 9.33; found, %C: 63.70, %H: 5.39, %N: 9.26.

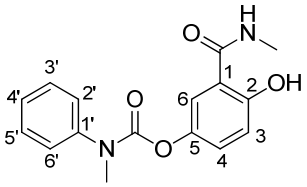


**13**

**General procedure for the synthesis of final compounds 19-23.** To a solution of benzoic acid **28** (1 equiv) in anhydrous DMF (12 mL/mmol), EDC (1.5 equiv) and DMAP (0.3 equiv) were added and the mixture was stirred at rt for 15 min. Then, a solution of the corresponding amine or alcohol

(1 equiv) in DMF (6 mL/mmol) was added at 0 ºC, and the reaction mixture was stirred for 2 h at this temperature and at rt for 14 additional h. The mixture was evaporated and the residue was purified by column chromatography to give the title final compounds.

**1-(Pyridin-3-yl)ethyl 2-hydroxy-5-({[methyl(phenyl)amino]carbonyl}oxy)benzoate (19).** Obtained from acid **28** (201 mg, 0.7 mmol) and 1-pyridin-3-ylethanol (86 mg, 0.7 mmol) in 52% yield. The free amine was characterized (yield, Rf, IR, NMR), dissolved in anhydrous DCM (4 mL) and treated with a commercial 1 M HCl(g)/$Et_2O$ solution (0.6 mL). The hydrochloride salts was isolated by evaporation of the solvents and characterized (Melting point, elemental analysis). Chromatography: DCM/EtOH, 99:1. Mp 80-82 ºC. $R_f$ (DCM/MeOH, 95:5) 0.20. IR (KBr, $cm^{-1}$) ν 3177 (OH), 1723 (NCOO), 1677 (COO), 1620, 1596, 1487 (Ar). $^1$H NMR (300 MHz, $CDCl_3$) δ 1.73 (d, 3H, *J* = 6.7 Hz, $CH_3$), 3.44 (s, 3H, $NCH_3$), 6.17 (q, 1H, *J* = 6.7 Hz, C<u>H</u>$(CH_3)_2$), 6.96 (d, 1H, *J* = 9.0 Hz, $H_3$), 7.25-7.45 (m, 7H, $H_4$, $H_{2'}$-$H_{6'}$, $H_{5''}$), 7.61 (m, 1H, $H_6$), 7.76 (d, 1H, *J* = 7.9 Hz, $H_{4''}$), 8.60 (dd, 1H, *J* = 4.8, 1.6 Hz, $H_{6''}$), 8.73 (d, 1H, *J* = 2.1 Hz, $H_{2''}$). $^{13}$C NMR (75 MHz, $CDCl_3$) δ 22.3, 38.7 ($2CH_3$), 72.1 (CH), 112.4 (C), 118.8, 122.5, 124.0, 126.3, 127.1 (5CH), 129.5 (3CH), 130.5 (CH), 134.2 (C), 136.6 (CH), 143.2, 143.5 (2C), 148.4, 150.1 (2CH), 154.5, 159.8, 169.1 (3C). Elemental analysis: calcd. for $C_{22}H_{20}N_2O_5 \cdot HCl \cdot 5/3H_2O$: %C: 57.58, %H: 5.34, %N: 6.10; found, %C: 57.42, %H: 5.53, %N: 5.99.

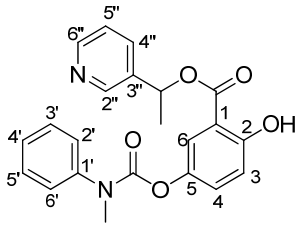


**19**

**(1-Methylpiperidin-3-yl)methyl 3-({[methyl(phenyl)amino]carbonyl}oxy)benzoate (20).** Obtained from acid **28** (230 mg, 0.8 mmol) and (1-methylpiperidin-3-yl)methanol (0.1mL, 0.8 mmol) in 34% yield. The free amine was characterized (yield, Rf, IR, NMR), dissolved in anhydrous DCM (4.5 mL) and treated with a commercial 1 M HCl(g)/$Et_2O$ solution (0.7 mL). The hydrochloride salts was isolated by evaporation of the solvents and characterized (Melting point, elemental analysis). Chromatography: DCM/EtOH, 9:1. Mp 75-77 ºC. $R_f$ (DCM/EtOH, 8:2) 0.55. IR (KBr, $cm^{-1}$) ν 3168 (OH), 1726 (NCOO), 1678 (COO), 1596, 1489 (Ar). $^1$H-NMR (300 MHz, $CDCl_3$) δ 1.00-1.14 (m, 1H, $H_{4''}$), 1.62-1.86 (m, 4H, $H_{4''}$, $2H_{5''}$, $H_{6''}$), 1.99 (td, 1 H, *J* = 11.0, 2.7 Hz, $H_{2''}$), 2.10-2.23 (m, 1H, $H_{3''}$), 2.32 (s, 3H, $NCH_3$), 2.81 (d, 1H, *J* = 10.9 Hz, $H_{6''}$), 2.94 (d, 1H, *J* = 10.1 Hz, $H_{2''}$), 3.44 (s, 3H, PhNC<u>H</u>$_3$), 4.15-4.24 (m, 2H, $CH_2$), 6.96 (d, 1H, *J* = 9.0 Hz, $H_2$), 7.22-7.45 (m, 6H, $H_4$, $H_{2'}$-$H_{6'}$), 7.54 (m, 1H, $H_6$), 10.67 (br s, 1H, OH). $^{13}$C NMR (75 MHz, $CDCl_3$) δ 24.7, 26.6 ($2CH_2$), 35.8 ($CH_3$), 38.3 (CH), 46.7

($CH_3$), 56.1, 59.0, 68.2 ($3CH_2$), 112.2 (C), 118.3, 122.2, 126.0, 126.8 (4CH), 129.1 (3CH), 129.8 (CH), 142.8, 143.1, 154.2, 159.2, 169.5 (5C). Elemental analysis: calcd. for $C_{22}H_{26}N_2O_5 \cdot HCl \cdot 2H_2O$: %C: 56.11, %H: 6.63, %N: 5.95; found, %C: 56.49, %H: 6.36, %N: 6.07.

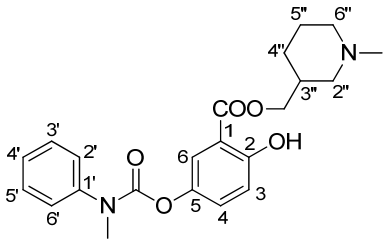

**20**

**3-[(Benzylamino)carbonyl]-4-hydroxyphenyl methyl(phenyl)carbamate (21).** Obtained from acid **28** (230 mg, 0.8 mmol) and benzyl amine (0.09 mL, 0.8 mmol) in 27% yield. Chromatography: hexane/EtOAc, 8:2, oil. $R_f$ (hexane/EtOAc, 95:5) 0.40. IR (neat, $cm^{-1}$) ν 3358, 3068 (NH, OH), 1706 (NCOO), 1646 (CON), 1599, 1545, 1493 (Ar). $^1$H NMR (300 MHz, $CDCl_3$) δ 3.45 (s, 3H, $NCH_3$), 4.62 (d, 2H, $J$ = 5.6 Hz, $CH_2$), 6.56 (br s, 1H, NH), 6.97 (d, 1H, $J$ = 9.0 Hz, $H_3$), 7.14-7.43 (m, 12H, $H_4$, $H_6$, $H_{2'}$-$H_{6'}$, $H_{2''}$-$H_{6''}$), 12.14 (br s, 1H, OH). $^{13}$C NMR (75 MHz, $CDCl_3$) δ 38.3 ($CH_3$), 43.6 ($CH_2$), 114.1 (C), 118.9, 125.8, 126.9, 127.5, 127.6 (5CH), 127.9 (3CH), 128.7 (2CH), 129.2 (3CH), 137.6, 142.5, 142.6, 154.5, 159.1, 169.1 (6C). MS (ESI): [$(M-H)^-$] 375.1.

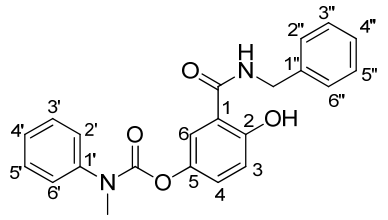

**21**

**4-Hydroxy-3-{[(pyridin-3-ylmethyl)amino]carbonyl}phenyl methyl(phenyl)carbamate (22).** Obtained from acid **28** (228 mg, 0.8 mmol) and pyridin-3-ylmethylamine (87 mg, 0.8 mmol) in 37% yield. The free amine was characterized (yield, Rf, IR, NMR), dissolved in anhydrous DCM (4.5 mL) and treated with a commercial 1 M HCl(g)/$Et_2O$ solution (0.7 mL). The hydrochloride salts was isolated by evaporation of the solvents and characterized (Melting point, elemental analysis). Chromatography: DCM/EtOH, 95:5. Mp 110-112 ºC. $R_f$ (DCM/EtOH, 9:1) 0.32. IR (KBr, cm-1) ν 3348 (NH, OH), 1719 (NCOO), 1646 (CON), 1599, 1545, 1492 (Ar). $^1$H-NMR (300 MHz, $CDCl_3$) δ 3.35 (s, 3H, $NCH_3$), 4.40 (d, 2H, $J$ = 5.7 Hz, $CH_2$), 6.87 (d, 1H, $J$ = 9.0 Hz, $H_3$), 7.04-7.06 (m, 1H, $H_4$), 7.19-7.36 (m, 6H, $H_{5''}$, $H_{2'}$-$H_{6'}$), 7.41 (m, 1H, $H_6$), 7.60 (d, 1H, $J$ = 7.9 Hz, $H_{4''}$), 8.12 (br s, 1H, NH), 8.44 (br

s, 2H, $H_{2''}$, $H_{6''}$). $^{13}$C NMR (75 MHz, $CDCl_3$) δ 38.7 ($CH_3$), 41.3 ($CH_2$), 115.0 (C), 119.1, 120.2, 124.1, 126.3, 127.2, 127.8 (6CH), 129.5 (3CH), 134.3 (C), 136.5 (CH), 142.9, 143.0 (2C), 148.8, 149.3 (2CH), 154.9, 159.0, 169.4 (3C). Elemental analysis: calcd. for $C_{21}H_{19}N_3O_4 \cdot HCl \cdot H_2O$: %C: 58.40, %H: 5.13, %N: 9.73; found, %C: 58.01, %H: 5.19, %N: 9.75.

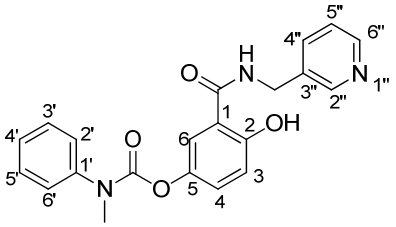

**22**

**4-Hydroxy-3-{[methyl(pyridin-3-ylmethyl)amino]carbonyl}phenylmethyl(phenyl)-carbamate (23).** Obtained from acid **28** (144 mg, 0.5 mmol) and *N*-methyl-*N*-(pyridin-3-yl)methylamine (61 mg, 0.5 mmol) in 64% yield. The free amine was characterized (yield, Rf, IR, NMR), dissolved in anhydrous DCM (2 mL) and treated with a commercial 1 M HCl(g)/$Et_2O$ solution (0.3 mL). The hydrochloride salts was isolated by evaporation of the solvents and characterized (Melting point, elemental analysis). Chromatography: DCM/EtOH, 95:5. Mp 207-209 ºC. $R_f$ (DCM/EtOH, 95:5) 0.14. IR (KBr, $cm^{-1}$) ν 3062 (OH), 1721 (NCOO), 1629 (CON), 1601, 1493 (Ar). $^1$H NMR (300 MHz, $CDCl_3$) δ 3.05 (s, 3H, $NCH_3$), 3.39 (s, 3H, $PhNC\underline{H}_3$), 4.73 (s, 2H, $CH_2$), 6.93 (d, 1H, *J* = 8.7 Hz, $H_3$), 7.02-7.09 (m, 2H, $H_4$, $H_{5''}$), 7.26-7.41 (m, 6H, $H_6$, $H_{2''}$-$H_{6''}$), 7.69 (d, 1H, *J* = 7.7 Hz, $H_{4''}$), 8.56 (d, 1H, *J* = 4.1 Hz, $H_{6''}$ ), 8.62 (m, 1H, $H_{2''}$). $^{13}$C NMR (75 MHz, $CDCl_3$) δ 37.0, 38.7 ($2CH_3$), 60.8 ($CH_2$), 118.3 (CH), 119.2 (C), 121.6, 124.3, 125.8, 126.3, 127.1 (5CH), 129.5 (3CH), 132.8 (C), 136.5 (CH), 143.2 (2C), 149.1, 149.4 (2CH), 154.5, 155.3, 171.4 (3C). Elemental analysis: calcd. for $C_{22}H_{21}N_3O_4 \cdot HCl \cdot 1/2H_2O$: %C: 60.48, %H: 5.31, %N: 9.62; found, %C: 60.16, %H: 5.12, %N: 9.51.

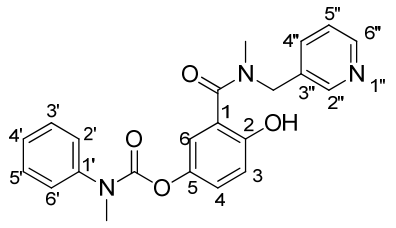

**23**

### 4.2. Biological experiments

**4.2.1. Inhibition of bFGF-induced cell proliferation of HUVECs.** HUVECs, obtained from American Type Culture Collection (ATCC, Rockville, MD), were cultured in a humidified atmosphere of 95% air and 5% $CO_2$ at 37 °C in M199 medium containing 10% fetal bovine serum (FBS) and 10 $\mu$g/mL heparin. Cells were incubated in the presence of bFGF (1 $\mu$g/mL) and the appropiate concentration of compound or vehicle (0.4% DMSO) for 2 days, and cell proliferation was quantified spectrofluorimetrically. $IC_{50}$ values are the mean from at least two independent experiments carried out in triplicate. In all cases, the SEM is within a 10% of the mean value.

**4.2.2. Determination of VEGF and bFGF levels.** Cells were seeded in 12-well plates at a density of 5 x $10^4$ cells per well and were grown for 24 h to obtain a 70-80% confluent monolayer. Then, medium was replaced with fresh Dulbecco's Modified Eagle Medium (DMEM) with or without 150 $\mu$M $CoCl_2$. After 5 h, compound **22** or vehicle (DMSO) were added to the culture medium, and cells were incubated for 4 h more. Supernatants were then collected and used straightaway or stored at -80 ºC for further use. Concentrations of VEGF and bFGF in the culture medium were measured using an enzyme-linked immunosorbent assay (ELISA), according to the manufacturer's instructions (VEGF human ELISA kit and FGF-basic human ELISA kit, Invitrogen, Carlsbad, CA). Absorbance was measured at 450 nm using an Asys UVM 340 (Biochrom Ltd., Cambridge, UK) microplate reader, and data were normalized to the kit controls and the number of producing cells. Data from three to five independent experiments carried out in triplicate were represented as mean fold ± SEM with bar graphs.

**4.2.3. Nitric oxide (NO) quantification.** Nitric oxide production was measured through determination of nitrite concentration in the culture medium using the Griess test. Briefly, cells were seeded in 96-well plates at a density of 1 x $10^4$ cells per well in DMEM with 10% FBS and incubated for 24 h prior to treatments. The medium was then replaced with fresh DMEM with or without 150 $\mu$M $CoCl_2$; after 5 h of incubation, compound **22** or vehicle was added, and incubation was continued for another 4 h. Then, 100 $\mu$L of supernatant from each condition was mixed with 100 $\mu$L of Griess reagent (1% sulphanilamide, 0.1% *N*-(1-naphthyl)ethylendiamine dihydrochloride, 2.5% phosphoric acid). After 15 min at rt in the dark, absorbance was measured at 548 nm in an Asys UVM 340 (Biochrom Ltd., Cambridge, UK) microplate reader. The concentration of nitrite, a stable oxidized derivative of NO in cell cultures, was determined from a sodium nitrite ($NaNO_2$, Sigma-Aldrich) standard curve. Data from three independent experiments performed in triplicate were presented as mean ± SEM.

**4.2.4. Western blot analysis.** MCF7 cells were plated at a density of 2 x $10^6$ cells in 15-cm dishes and allowed to grow 24 h in DMEM with 1% FBS, to a 80% confluent monolayer. The medium was then replaced by fresh DMEM with or without 150 $\mu$M $CoCl_2$ and cells were incubated for 5 h to allow hypoxic response. After that, compound **22** or vehicle were added and cells were incubated during 4 h. Cells were washed with phosphate buffered saline (PBS) and lysed with ice-cold RIPA buffer (50 mM Tris-HCl pH 7.4, 150 mM NaCl, 1% Igepal) containing protease and phosphatase inhibitors (Roche and Sigma-Aldrich, respectively). Lysates were clarified by centrifugation at 10000*g* for 10 min at 4 ºC and used straightaway or stored at -80 ºC until use. Protein concentration was measured (DC protein assay kit, Bio-Rad), and samples with equal amounts of total protein were diluted into Laemmli reducing sample buffer (Bio-Rad) and denatured at 95 ºC for 5 min. Samples were then resolved on 4-20% SDS-PAGE gels (Bio-Rad), and proteins were transferred to nitrocellulose membranes (GE Healthcare, Amersham). After 1 h of incubation in blocking buffer [10 mM Tris-HCl pH 8.0, 150 mM NaCl, 0.05% Tween-20 (TBS-T) with 1% BSA], membranes were incubated overnight at 4 ºC with the corresponding primary antibody. Then, membranes were washed three times (5 min each) with TBS-T and incubated with the corresponding secondary antibody for 1 h at rt. Protein bands were visualized using enhanced chemiluminescence detection reagents (GE Healthcare, Amersham) in a Fujifilm LAS-3000 developer (Tokyo, Japan) and quantified by densitometry using ImageJ software (NIH).

Primary antibodies were from Cell Signaling and used at 1:1000 dilution (rabbit anti-phospho-AKT (pS473), rabbit anti-AKT, rabbit anti-phospho-ERK1/2, rabbit anti-ERK1/2, rabbit anti-phospho-MEK1/2, rabbit anti-MEK1/2, rabbit anti-VEGFR, rabbit anti-phospho-VEGFR, rabbit anti-FGFR, rabbit anti-phospho-FGFR) or from Santa Cruz Biotechnology and used at 1:200 dilution (mouse anti-HIF-1$\alpha$, mouse anti-HIF-2$\alpha$, mouse anti-iNOS, rabbit anti-$\beta$-actin). Secondary antibodies used were goat anti-mouse or goat anti-rabbit IgG HRP conjugates (1:5000, Sigma-Aldrich) accordingly. Relative phosphorylation levels from three independent experiments were presented as mean ± SEM with bar graphs.

**4.2.5. Migration or wound healing assay.** Cells were seeded in 96-well plates at a density of 1.5 x $10^4$ cells per well in DMEM with 10% FBS and grown for 24 h at 37 ºC and 5% of $CO_2$ to obtain a 90-100% confluent monolayer. Wounds were made with a sterile p20 pipette tip and each well was washed twice with PBS to eliminate nonadherent cells and cell debris. Fresh DMEM with or without 150 $\mu$M $CoCl_2$ was then added and after 5 h of incubation, compound **22** (50 $\mu$M) or vehicle was added. At this time (0 h) and after 48 h, cells were photographed under phase contrast with an Olympus FW1200 microscope. Empty area in each wound was quantified using ImageJ software (NIH) and compared with the corresponding area of the initial wound. The percentage of area from

three independent experiments performed in triplicate was presented as mean ± SEM with bar graphs.

**4.2.6. RNA interference-mediated silencing of the HIF-1*α* gene.** Cells were transfected with specific siRNA duplexes using DharmaFECT 1 as transfection reagent according to the manufacturer's instructions (Dharmacon-Thermo Scientific, Lafayette, CO). Selective siRNA against human HIF-1*α* was a smart pool from Dharmacon-Thermo Scientific, and the sequences were: 5'-GAACAAAUACAUGGGAUUA-3'; 5'-AGAAUGAAGUGUACCCUAA-3'; 5'-GAUGGAAGCACUAGACAAA-3'; 5'-CAAGUAGCCUCUUUGACAA-3'. The nontargeted control sequence, 5'-UUCUCCGAACGUGUCACGU-3', was from Applied Biosystems-Ambion (Austin, TX). Twenty-four hours after transfection, cells were seeded for ELISA assays, which performed as described below.

**4.2.7. Quantitive polymerase chain reaction (qPCR).** RNA from cell cultures or tumor tissues was isolated with TRIzol reagent (Sigma-Aldrich). cDNA was subsequently obtained with Transcriptor reverse transcriptase (Roche). Real-time quantitative PCR assays were performed using the FastStart master mix with Rox (Roche), and probes were obtained from the Universal Probe Library (Roche). The primers used for human HIF-1*α* were as follows: sense, 5'-GATAGCAAGACTTTCCTCAGTCG-3'; and antisense, 5'-TGGCTCATATCCCATCAATTC-3'. Amplifications were run in a 7900 HT-fast real-time PCR system (Applied Biosystems). Each value was normalized to human *β*-actin RNA levels as an internal control: sense, 5'-CCAACCGCGAGAAGATGA-3'; and anti-sense, 5'-CCAGAGGCGTACAGGGATAG-3'.

**4.2.8. Gene expresssion analysis.** The $RT^2$ profiler PCR array of human angiogenesis (Qiagen, Valencia, CA), which analyzes the expression of 84 key genes involved in modulating the biological processes of angiogenesis, was used. RNA from cell cultures was isolated with TRIzol reagent (Sigma-Aldrich), including a DNA digestion step with genomic DNA elimination mix (Qiagen). cDNA was subsequently obtained with a $RT^2$ first strand kit according to manufacturer's instructions (Qiagen). Real-time PCR assay was performed using the $RT^2$ profiler PCR array of human angiogenesis in combination with RT2 SYBR Green master mix (Qiagen). Amplifications were run in a 7900 HT-fast real-time PCR system (Applied Biosystems) and data were analyzed using the SABiosciences PCR array data analysis template Excel (Qiagen).

**4.2.9. VEGF expression analysis.** RNA was isolated from tumors with TRIzol reagent (Invitrogen) with the real star kit (Durviz, Valencia, Spain), and cDNA was obtained with Transcriptor reverse transcriptase (Roche). The primers used for VEGF-A amplification were: sense, 5'-GTCCTGTGTGCCGCTGAT-3'; antisense, 5'-AGGTTTGATCCGCATGATCT-3'. GAPDH was used

as reference (sense, 5'-GGGAAGCTCACTGGCATGGCCTTCC-3'; antisense, 5'-CATGTGGGCCATGAGGTCCACCAC-3').

**4.2.10. Subcutaneous xenografts.** All procedures involving animals were performed with the approval of the Complutense University Animal Experimentation Committee in compliance with European official regulations. Five million MDA-MB-231 breast cancer cells in 100 $\mu$L of PBS were subcutaneously injected into the flank of 6-week-old athymic mice (Harlan Interfauna Iberica, Barcelona, Spain). Tumors were routinely measured with external caliper, and volume was calculated as $(4\pi/3)$ x $(width/2)^2$ x (length/2). When tumors reached ca. 200 $mm^3$, the mice were treated intraperitoneally three times a week with compound **22** (25 mg/kg) or vehicle (DMSO 0.2 mg/$\mu$L in PBS) for 4 weeks. After treatment, animals were sacrificed, and tumors and organs were collected. Tumors were divided into different portions for preparation of tissue sections for immunofluorescent staining [frozen in Tissue-Tek (Sakura Finetek Europe, Zoeterwoude, The Netherlands)] or snap frozen for RNA extraction (and stored at -80 ºC until use). Organs collected were fixed in formaldehyde and stained with hematoxylin-eosin for analysis.

For immunofluorescence analysis, Tissue-Tek frozen sections were fixed in PFA 4% and were subjected to heat-induced antigen retrieval in citrate buffer. Then, sections were blocked with PBS containing 0.25% TritonX-100 and 10% goat serum, and incubated with anti-CD31 (Pharmingen/BD Biosciences, San Jose, CA). Secondary anti-mouse antibodies conjugated with Alexa Flour 488 were from Invitrogen (Carlsbad, CA). Cell nuclei were stained with DAPI (Invitrogen). Images were acquired using a Leica DM400B microscope (Leica, Wetzlar, Germany).

## 7. BIBLIOGRAPHY


1. Folkman, J. Tumor angiogenesis: therapeutic implications. *New Eng. J. Med.* **1971**, *285*, 1182-1186.

2. Gacche, R. N.; Meshram, R. J. Angiogenic factors as potential drug target: efficacy and limitations of anti-angiogenic therapy. *Biochim. Biophys. Acta* **2014**, *1846*, 161-179.

3. Ferrara, N.; Hillan, K. J.; Gerber, H.-P.; Novotny, W. Discovery and development of bevacizumab, an anti-VEGF antibody for treating cancer. *Nat. Rev. Drug Discov.* **2004**, *3*, 391-400.

4. Folkman, J. Angiogenesis: an organizing principle for drug discovery? *Nat. Rev. Drug Discov.* **2007**, *6*, 273-286.

5. Ciombor, K. K.; Berlin, J.; Chan, E. Aflibercept. *Clin. Cancer Res.* **2013**, *19*, 1920-1925.

6. Kane, R. C.; Farrell, A. T.; Madabushi, R.; Booth, B.; Chattopadhyay, S.; Sridhara, R.; Justice, R.; Pazdur, R. Sorafenib for the treatment of unresectable hepatocellular carcinoma. *The Oncologist* **2009**, *14*, 95-100.

7. Kane, R. C.; Farrell, A. T.; Saber, H.; Tang, S.; Williams, G.; Jee, J. M.; Liang, C.; Booth, B.; Chidambaram, N.; Morse, D.; Sridhara, R.; Garvey, P.; Justice, R.; Pazdur, R. Sorafenib for the treatment of advanced renal cell carcinoma. *Clin. Cancer Res.* **2006**, *12*, 7271-7278.

8. Goodman, V. L.; Rock, E. P.; Dagher, R.; Ramchandani, R. P.; Abraham, S.; Gobburu, J. V. S.; Booth, B. P.; Verbois, S. L.; Morse, D. E.; Liang, C. Y.; Chidambaram, N.; Jiang, J. X.; Tang, S.; Mahjoob, K.; Justice, R.; Pazdur, R. Approval summary: Sunitinib for the treatment of Imatinib refractory or intolerant gastrointestinal stromal tumors and advanced renal cell carcinoma. *Clin. Cancer Res.* **2007**, *13*, 1367-1373.

9. Ettrich, T. J.; Seufferlein, T., Regorafenib. In *Small Molecules in Oncology*, Springer Berlin Heidelberg: 2014; *201*, pp 185-196.

10. Ballou, L. M.; Lin, R. Z. Rapamycin and mTOR kinase inhibitors. *J. Chem. Biol.* **2008**, *1*, 27-36.

11. Delbaldo, C.; Albert, S.; Dreyer, C.; Sablin, M. P.; Serova, M.; Raymond, E.; Faivre, S. Predictive biomarkers for the activity of mammalian target of rapamycin (mTOR) inhibitors. *Target. Oncol.* **2011**, *6*, 119-124.

12. Wu, J. M.; Staton, C. A. Anti-angiogenic drug discovery: lessons from the past and thoughts for the future. *Expert Opin. Drug Discov.* **2012**, *7*, 723-743.

13. Bellou, S.; Pentheroudakis, G.; Murphy, C.; Fotsis, T. Anti-angiogenesis in cancer therapy: Hercules and hydra. *Cancer Lett.* **2013**, *338*, 219-228.

14. Bergers, G.; Hanahan, D. Modes of resistance to anti-angiogenic therapy. *Nat. Rev. Cancer* **2008**, *8*, 592-603.

15. Helfrich, I.; Scheffrahn, I.; Bartling, S.; Weis, J.; von Felbert, V.; Middleton, M.; Kato, M.; Ergun, S.; Augustin, H. G.; Schadendorf, D. Resistance to antiangiogenic therapy is directed by vascular phenotype, vessel stabilization, and maturation in malignant melanoma. *J. Exp. Med.* **2010**, *207*, 491-503.

16. Petrillo, M.; Scambia, G.; Ferrandina, G. Novel targets for VEGF-independent anti-angiogenic drugs. *Expert Opin. Investig. Drugs* **2012**, *21*, 451-472.

17. Turner, N.; Grose, R. Fibroblast growth factor signalling: from development to cancer. *Nat. Rev. Cancer* **2010**, *10*, 116-129.

18. Lieu, C.; Heymach, J.; Overman, M.; Tran, H.; Kopetz, S. Beyond VEGF: inhibition of the fibroblast growth factor pathway and antiangiogenesis. *Clin. Cancer Res.* **2011**, *17*, 6130-6139.

19. Liang, G.; Chen, G.; Wei, X.; Zhao, Y.; Li, X. Small molecule inhibition of fibroblast growth factor receptors in cancer. *Cytokine Growth Factor Rev.* **2013**, *24*, 467-475.

20. Semenza, G. L. Hypoxia-inducible factors: mediators of cancer progression and targets for cancer therapy. *Trends Pharmacol. Sci.* **2012**, *33*, 207-214.

21. Dieci, M. V.; Arnedos, M.; Andre, F.; Soria, J. C. Fibroblast growth factor receptor inhibitors as a cancer treatment: from a biologic rationale to medical perspectives. *Cancer Discov.* **2013**, *3*, 264-279.

22. Bono, F.; De Smet, F.; Herbert, C.; De Bock, K.; Georgiadou, M.; Fons, P.; Tjwa, M.; Alcouffe, C.; Ny, A.; Bianciotto, M.; Jonckx, B.; Murakami, M.; Lanahan, A. A.; Michielsen, C.; Sibrac, D.; Dol-

Gleizes, F.; Mazzone, M.; Zacchigna, S.; Herault, J. P.; Fischer, C.; Rigon, P.; Ruiz de Almodovar, C.; Claes, F.; Blanc, I.; Poesen, K.; Zhang, J.; Segura, I.; Gueguen, G.; Bordes, M. F.; Lambrechts, D.; Broussy, R.; van de Wouwer, M.; Michaux, C.; Shimada, T.; Jean, I.; Blacher, S.; Noel, A.; Motte, P.; Rom, E.; Rakic, J. M.; Katsuma, S.; Schaeffer, P.; Yayon, A.; Van Schepdael, A.; Schwalbe, H.; Gervasio, F. L.; Carmeliet, G.; Rozensky, J.; Dewerchin, M.; Simons, M.; Christopoulos, A.; Herbert, J. M.; Carmeliet, P. Inhibition of tumor angiogenesis and growth by a small-molecule multi-FGF receptor blocker with allosteric properties. *Cancer Cell* **2013**, *23*, 477-488.

23. Li, D.; Wei, X.; Xie, K.; Chen, K.; Li, J.; Fang, J. A novel decoy receptor fusion protein for FGF-2 potently inhibits tumour growth. *Br. J. Cancer* **2014**, *111*, 68-77.

24. Wang, Y.; Becker, D. Antisense targeting of basic fibroblast growth factor and dibroblast growth factor receptor-1 in human melanomas blocks intratumoral angiogenesis and tumor growth. *Nat. Med.* **1997**, *3*, 887-893.

25. Ebos, J. M.; Lee, C. R.; Cruz-Munoz, W.; Bjarnason, G. A.; Christensen, J. G.; Kerbel, R. S. Accelerated metastasis after short-term treatment with a potent inhibitor of tumor angiogenesis. *Cancer Cell* **2009**, *15*, 232-239.

26. Loges, S.; Mazzone, M.; Hohensinner, P.; Carmeliet, P. Silencing or fueling metastasis with VEGF inhibitors: antiangiogenesis revisited. *Cancer Cell* **2009**, *15*, 167-170.

27. Paez-Ribes, M.; Allen, E.; Hudock, J.; Takeda, T.; Okuyama, H.; Vinals, F.; Inoue, M.; Bergers, G.; Hanahan, D.; Casanovas, O. Antiangiogenic therapy elicits malignant progression of tumors to increased local invasion and distant metastasis. *Cancer Cell* **2009**, *15*, 220-231.

28. Philip, B.; Ito, K.; Moreno-Sanchez, R.; Ralph, S. J. HIF expression and the role of hypoxic microenvironments within primary tumours as protective sites driving cancer stem cell renewal and metastatic progression. *Carcinogenesis* **2013**, *34*, 1699-1707.

29. Mole, D. R.; Blancher, C.; Copley, R. R.; Pollard, P. J.; Gleadle, J. M.; Ragoussis, J.; Ratcliffe, P. J. Genome-wide association of hypoxia-inducible factor (HIF)-1alpha and HIF-2alpha DNA binding with expression profiling of hypoxia-inducible transcripts. *J. Biol. Chem.* **2009**, *284*, 16767-16775.

30. Keith, B. J., R.S.; Simon, M.C. HIF1α and HIF2α: sibling rivalry in hypoxic tumor growth and progression. *Nat. Rev. Cancer* **2012**, *12*, 9-22.

31. Levina, V.; Nolen, B. M.; Marrangoni, A. M.; Cheng, P.; Marks, J. R.; Szczepanski, M. J.; Szajnik, M. E.; Gorelik, E.; Lokshin, A. E. Role of eotaxin-1 signaling in ovarian cancer. *Clin. Cancer Res.* **2009**, *15*, 2647-2656.

32. Naldini, A.; Filippi, I.; Miglietta, D.; Moschetta, M.; Giavazzi, R.; Carraro, F. Interleukin-1beta regulates the migratory potential of MDAMB231 breast cancer cells through the hypoxia-inducible factor-1alpha. *Eur. J. Cancer* **2010**, *46*, 3400-3408.

33. Curtis, V. F.; Wang, H.; Yang, P.; McLendon, R. E.; Li, X.; Zhou, Q. Y.; Wang, X. F. A PK2/Bv8/PROK2 antagonist suppresses tumorigenic processes by inhibiting angiogenesis in glioma and blocking myeloid cell infiltration in pancreatic cancer. *PLoS One* **2013**, *8*, e54916.

34. Leong, K. G.; Karsan, A. Recent insights into the role of Notch signaling in tumorigenesis. *Blood* **2006**, *107*, 2223-2233.

35. Sahin, H.; Borkham-Kamphorst, E.; Kuppe, C.; Zaldivar, M. M.; Grouls, C.; Al-samman, M.; Nellen, A.; Schmitz, P.; Heinrichs, D.; Berres, M. L.; Doleschel, D.; Scholten, D.; Weiskirchen, R.; Moeller, M. J.; Kiessling, F.; Trautwein, C.; Wasmuth, H. E. Chemokine Cxcl9 attenuates liver fibrosis-associated angiogenesis in mice. *Hepatology* **2012**, *55*, 1610-1619.

36. Puig, T.; Aguilar, H.; Cufi, S.; Oliveras, G.; Turrado, C.; Ortega-Gutiérrez, S.; Benhamú, B.; López-Rodríguez, M. L.; Urruticoechea, A.; Colomer, R. A novel inhibitor of fatty acid synthase shows activity against HER2+ breast cancer xenografts and is active in anti-HER2 drug-resistant cell lines. *Breast Cancer Res.* **2011**, *13*, R131.

37. Marín-Ramos, N. I.; Alonso, D.; Ortega-Gutiérrez, S.; Ortega-Nogales, F. J.; Balabasquer, M.; Vázquez-Villa, H.; Andradas, C.; Blasco-Benito, S.; Pérez-Gómez, E.; Canales, Á.; Jiménez-Barbero, J.; Marquina, A.; del Prado, J. M.; Sánchez, C.; Martín-Fontecha, M.; López-Rodríguez, M. L. New inhibitors of angiogenesis with antitumor activity in vivo. *J. Med. Chem.* **2015**, *58*, 3757-3766.

38. Carta, F.; Vullo, D.; Maresca, A.; Scozzafava, A.; Supuran, C. T. Mono-/dihydroxybenzoic acid esters and phenol pyridinium derivatives as inhibitors of the mammalian carbonic anhydrase isoforms I, II, VII, IX, XII and XIV. *Bioorg. Med. Chem.* **2013**, *21*, 1564-1569.

39. Sunasee, R.; Clive, D. L. J. A Route to 1,4-disubstituted aromatics and its application to the synthesis of the antibiotic culpin. *J. Org. Chem.* **2008**, *73*, 8016-8020.

40. Thomsen, D. L.; Keller, P.; Naciri, J.; Pink, R.; Jeon, H.; Shenoy, D.; Ratna, B. R. Liquid crystal elastomers with mechanical properties of a muscle. *Macromolecules* **2001**, *34*, 5868-5875.

41. Pérez-Álvarez, M.; Raymo, F. M.; Rowan, S. J.; Schiraldi, D.; Stoddart, J. F.; Wang, Z. H.; White, A. J. P.; Williams, D. J. The balance between electronic and steric effects in the template-directed syntheses of [2]catenanes. *Tetrahedron* **2001**, *57*, 3799-3808.

# CHAPTER II:
# LEAD OPTIMIZATION PROCESS AND BIOLOGICAL CHARACTERIZATION OF A NOVEL INHIBITOR OF ICMT WITH ANTITUMOR ACTIVITY

## 1. INTRODUCTION AND OBJECTIVES

The Ras protein family members are monomeric low-molecular-weight GTP-binding proteins that play a role in regulating cell differentiation, proliferation, and survival. To do so, Ras proteins act as binary molecular switches, exchanging guanosine 5'-triphosphate (GTP, active form) for guanosine 5'-diphosphate (GDP, inactive form), or vice versa. GTP binding induces a marked conformational change in Ras that allows it to bind effectors via their Ras binding domains (RBD). This switch is regulated by guanine nucleotide exchange factors (GEFs) and GTPase activating proteins (GAPs), which change the activation state of Ras without covalently modifying it (Figure 1).[1]

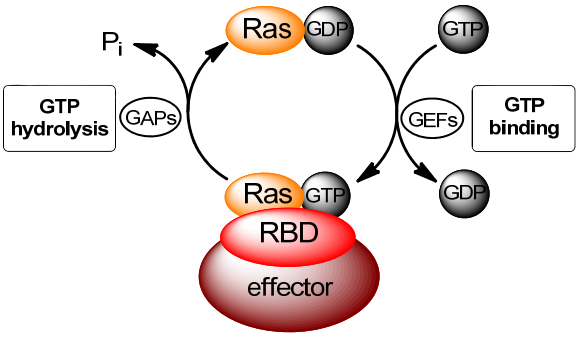


**Figure 1.** The GTP/GDP cycle of Ras.

Single-point mutations of *ras* gene can lead to the production of constitutively activated Ras protein, with impaired GTPase activity. These activating mutations of *ras* result in continuous stimulation of cell proliferation and inhibition of apoptotic signaling, thus promoting cancer. In fact, intensive sequencing of the cancer genome has revealed that, despite the identification of more than 500 validated cancer genes, the three *ras* genes (*hras*, *nras* and *kras*) still constitute the most frequently mutated oncogene family in human cancers. Considering also that mutations in *ras* are

found in some of the most lethal cancers -they have been found in almost 30% of all cancers, including 50% of colon and up to 90% of pancreatic tumors-,[2,3] it is easy to understand the interest that has been spurred in developing Ras inhibitors. However, despite more than three decades of intensive effort, no effective pharmacological inhibitors of the Ras oncoproteins have reached the clinic, prompting the widely held perception that Ras proteins are 'undruggable'.[4,5] Hence, the possibility of blocking Ras activity by interfering with the post-translational modifications responsible for its activation has gained an increasing attention within the last years.

Ras is a member of a large class of proteins known as CAAX proteins, where C is cysteine, A is usually an aliphatic amino acid and X is any amino acid. The primary translation product of CAAX protein genes ends with a CAAX sequence, which serves as a substrate for three enzymes that modify the sequence in a step-wise manner to create a lipidated, hydrophobic domain that mediates the association with cellular membranes. First, unmodified CAAX sequences serve as substrates for prenylation by one of the cytosolic prenyltransferases: geranylgeranyltransferase type I (GGTase I) if the X amino acid is leucine or phenylalanine, or farnesyltransferase (FTase), for any other amino acid.[6] For Ras protein, this first modification means the addition of a farnesyl moiety, turning an otherwise globular and hydrophilic protein into one that binds to the cytoplasmic leaflet of cellular membranes, which is an essential process required for Ras biological activation.[1] However, it has been demonstrated that upon inhibition of FTase, N-Ras and K-Ras (but not H-Ras) can also be geranylgeranylated.[7]

The second step for prenylated proteins consists in a specific proteolytic removal of the last three amino acids AAX, which is carried out by the Ras-converting enzyme 1 (Rce1), an integral membrane protease of the endoplasmic reticulum.[8,9] Finally, the newly formed C-terminal prenylcysteine becomes a substrate for a specific protein carboxyl methyltransferase, isoprenylcysteine carboxyl methyltransferase (ICMT), also localized in the endoplasmic reticulum,[10] which methylates the free carboxyl group, neutralizing the negative charge of the prenylcysteine and thereby increasing membrane affinity (Figure 2).[6]

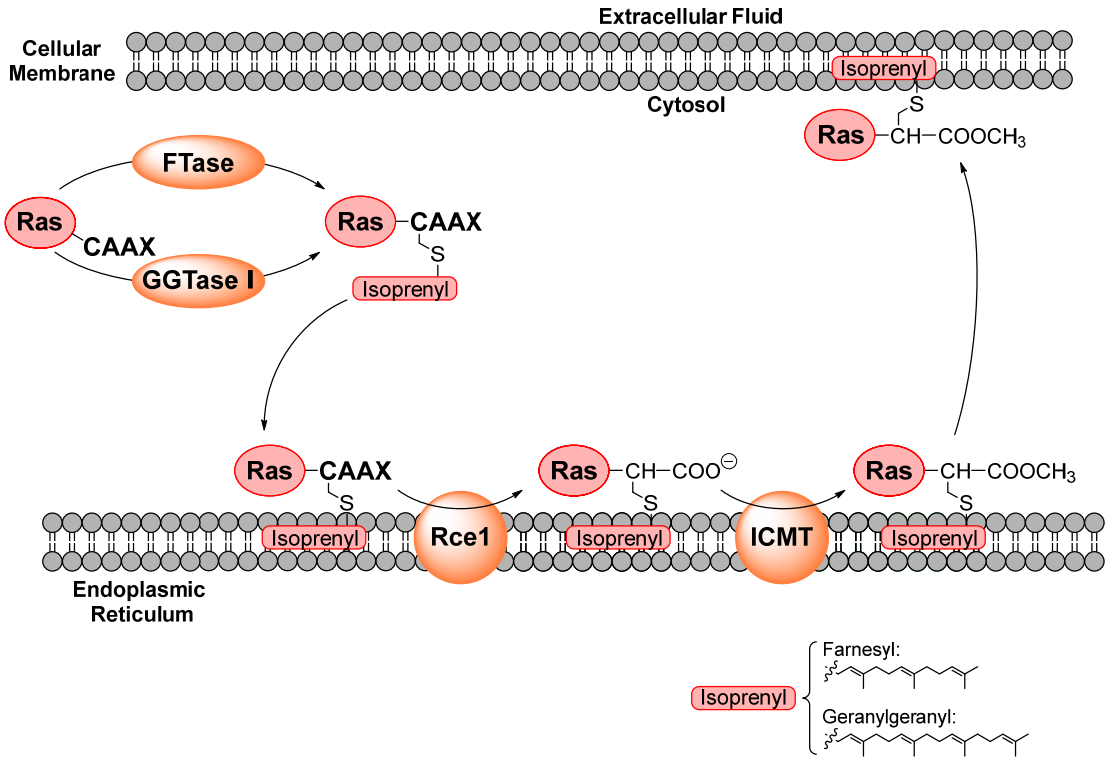


**Figure 2.** Post-translational modifications of Ras.

In absence of any of these post-translational modifications, Ras losses its ability to induce tumor transformation. Therefore, the blockade of the enzymes involved in these modifications represents an attractive strategy to inhibit Ras activity. However, thus far attempts to abrogate the plasma membrane binding of Ras by FTase[11,12] have failed because N-Ras and K-Ras are also good substrates for GGTase I.[7] Meanwhile, inactivation of Rce1 has been shown to promote the development of lethal cardiomyopathy in mice,[13] as well as to accelerate the growth of some malignancies, such as myeloproliferative disease.[14] Besides, mammalian genomes encode only one member of the ICMT class of methyltransferases and it lacks homology to other protein methyltransferases,[10] thus resulting in a more specific target than Rce1, and turning the inhibition of ICMT into a promising alternative for anticancer therapies.[15]

Up to date, few structurally distinct inhibitors of ICMT have been disclosed and only two compounds have been studied for their potential use as anticancer agents. First, cysmethynil (CYSM, Figure 3) was discovered in 2005 by high-throughput screening (HTS), and it has been characterized

as an ICMT inhibitor ($IC_{50}$ = 2.4 $\mu$M) able to impact on tumor growth, but its in vitro antiproliferative activity and in vivo antitumor efficacy are still quite modest.[16,17]

More recently, and also from a HTS followed by structure-activity relationship (SAR) studies, some tetrahydropyrane derivatives have been described (general structure referred as THP, Figure 3). However, none of the cellular effects observed using these ICMT inhibitors were very pronounced,[18] so no further biological characterization -either in vitro or in vivo- has been carried out regarding these derivatives.

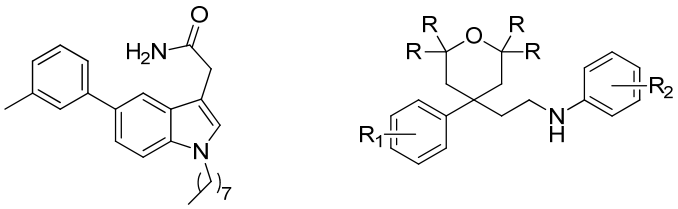


CYSM
$IC_{50}$ = 2.4 $\mu$M

THP
$IC_{50}$ = 0.0013-0.31 $\mu$M

**Figure 3.** Representative synthetic inhibitors of ICMT.

Given the interest of ICMT and the paucity of inhibitors, in our research group we have started a project aimed at the design, synthesis and development of new ICMT inhibitors. For the initial design, we built a 3D pharmacophore model that was subsequently refined by homology models based on the ICMT prokaryotic ortologue,[19] and followed by virtual screening of the Natural Cancer Institute database. This work first led us to the hit UCM-1310 (Figure 4),[20] which showed 30% of ICMT inhibition at 50 $\mu$M. The subsequent hit to lead process yielded the lead UCM-1325 (Figure 4), with 54% of ICMT inhibition at 50 $\mu$M.

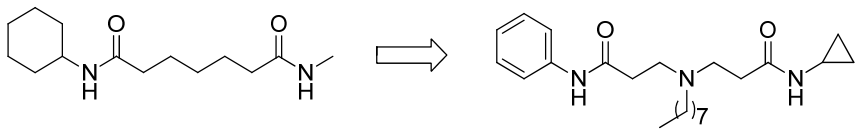


UCM-1310
30% inhibition of ICMT at 50 $\mu$M

UCM-1325
54% inhibition of ICMT at 50 $\mu$M

**Figure 4.** Hit to lead process carried out in our research group.

Thus, the main objectives of this work are:

1. Optimization of the lead UCM-1325.
2. Study of the mechanism of action of the selected compound(s).

## 2. RESULTS AND DISCUSSION

### 2.1. Optimization of the lead compound UCM-1325

We have carried out an optimization process aimed at the improvement of the inhibitory capacity of lead compound UCM-1325, while keeping good pharmacokinetic properties. For this purpose, the three types of structural modifications depicted in Figure 5 were carried out: substitution of the cyclopropyl ring for different aromatic rings (compounds **1-15**); modifications in the hydrophobic chain (compounds **16-27**); and modifications in the amide group (compounds **28-30**).

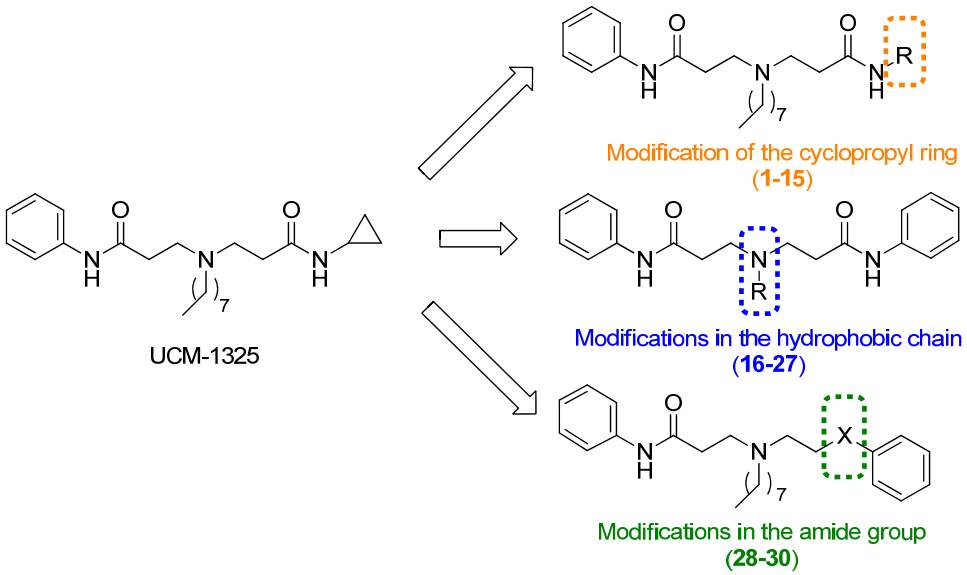


**Figure 5.** Structural modifications in compound UCM-1325.

### 2.1.1. Modification of the cyclopropyl ring

To start the exploration of compound UCM-1325 with the aim of increasing the ICMT inhibitory capacity, we first designed compounds **1-3** (Scheme 1), where the cyclopropyl ring was substituted by an aromatic moiety (pyridine or benzene).

The synthesis of compounds **1-3** was carried out following the approach depicted in Scheme 1, starting from acryloyl chloride, which through reaction with the corresponding amine in the presence of a base (triethylamine or pyridine) gave acrylamides **31-33**. The aza-Michael reaction of 1 equivalent of acrylamide **33** with 3 equivalents of octylamine in the presence of 1,8-diazabicycloundec-7-ene (DBU) for 5 h gave secondary amine **34**, which through reaction with the acrylamides **31** and **32** in the presence of DBU afforded the final compounds **1** and **2**, respectively. The aza-Michael reaction of 3 equivalents of acrylamide **33** with 1 equivalent of octylamine in the presence of DBU for 24 h gave final compound **3**.

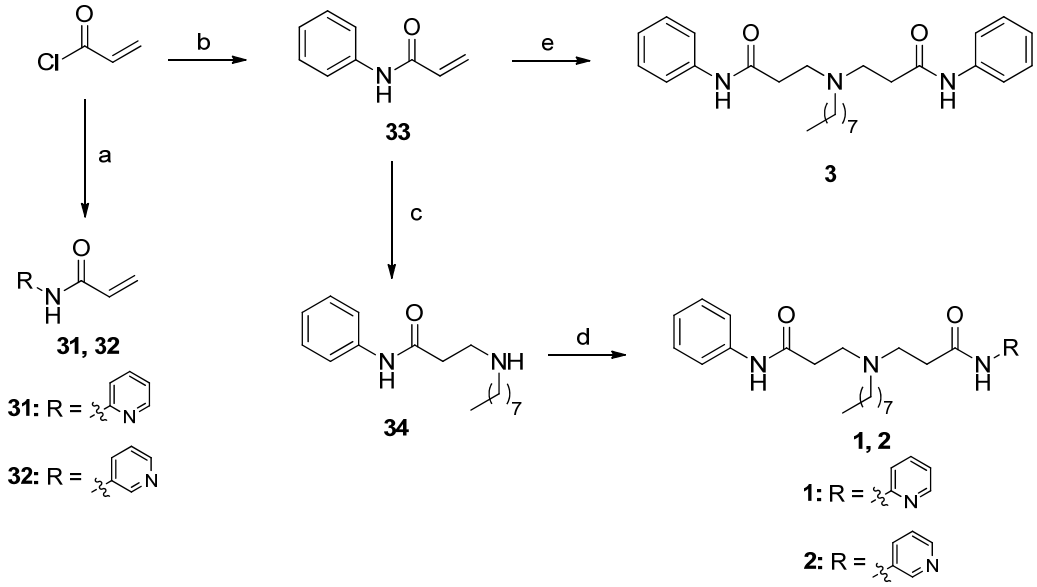


**Scheme 1.** Reagents and conditions: a) 2- or 3-aminopyridine, $Et_3N$, DCM, -78 to 0 ºC, 57-68%; b) aniline, pyridine, DCM, 0 ºC to rt, 2 h, 84%; c) $CH_3(CH_2)_7NH_2$, DBU, $CH_3CN$, 60 ºC, 5 h, 79%; d) **31** or **32**, DBU, $CH_3CN$, 60 ºC, 24 h, 37-45%; e) $CH_3(CH_2)_7NH_2$, DBU, $CH_3CN$, 60 ºC, 24 h, 83%.

The synthetized compounds were screened for ICMT inhibitory capacity and for cell antiproliferative effect in a panel of cancer cell lines (Table 1).

To determine the capacity of these new derivatives to inhibit the activity of ICMT, we used as a source of enzyme membranes from Sf9 insect cells that overexpressed ICMT, biotinyl-*S*-farnesylcysteine (BFC) as substrate, and [$^3$H]-*S*-adenosylmethionine ([$^3$H]-SAM) as cosubstrate. Incubation of the enzyme with BFC and [$^3$H]-SAM in the presence of the compound under study allowed us to quantify the percentage of inhibition of the methyl esterification reaction, in which the tritiated methyl group of [$^3$H]-SAM was transferred to the substrate BFC. The incorporated radioactivity was measured by liquid scintillation spectrometry.

The antiproliferative effect of the compounds in breast cancer MCF7 and MDA-MB-231 cells, as well as in prostate cancer PC-3 cells, was measured through MTT assays. Cells were incubated with different concentrations of the compounds for 48 h and then, the formation of formazan crystals by the remaining viable cells was measured and compared to the vehicle-treated cells.

**Table 1.** Biological activity of compounds UCM-1325 and **1-3**[a]

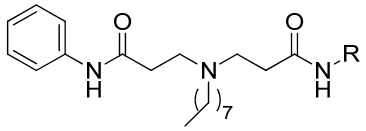

| Cpd | R | Antiproliferative effect ($IC_{50}$, $\mu$M) | | | ICMT inhibition (%, 50 $\mu$M) |
|---|---|---|---|---|---|
| | | MCF7 | MDA-MB-231 | PC-3 | |
| UCM-1325 |  | 34 | 36 | 34 | 54 |
| **1** |  | 19 | 28 | 22 | 24 |
| **2** | 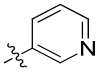 | 37 | 48 | 54 | 18 |
| **3** |  | 10 | 17 | 22 | 93 |

[a]Data from three independent experiments performed in triplicate; the standard error of the mean (SEM) is in all cases within a 10% of the mean value.

As can be deduced from the biological data obtained for compounds **1-3** (Table 1), while the introduction of pyridine rings does not improve the ICMT inhibitory capacity of derivatives **1** and **2**, the opposite occurs when a phenyl ring is introduced (**3**). In this last case, we can observe a significant increase in the inhibitory capacity (93% ICMT inhibition at 50 $\mu$M), which comes along with an improvement in the antiproliferative effect of the resulting derivative, compound **3**.

We hence decided to keep the phenyl group and analyze the influence of the introduction of different substituents, which led to derivatives **4-15**. The synthesis of the compounds was achieved following the conditions depicted in Scheme 2. The aza-Michael reaction between amine **34** and the corresponding acrylamide (**37-47**) in the presence of DBU afforded asymmetric amides **4-14**. The hydrolysis of the ethyl ester **14** with lithium hydroxide gave final compound **15**. Synthesis of acrylamides (**37-47**) was carried out as previously described in Scheme 1, starting from acryloyl chloride, which afforded the corresponding acrylamides by reaction with the adequate anilines in the presence of a base.

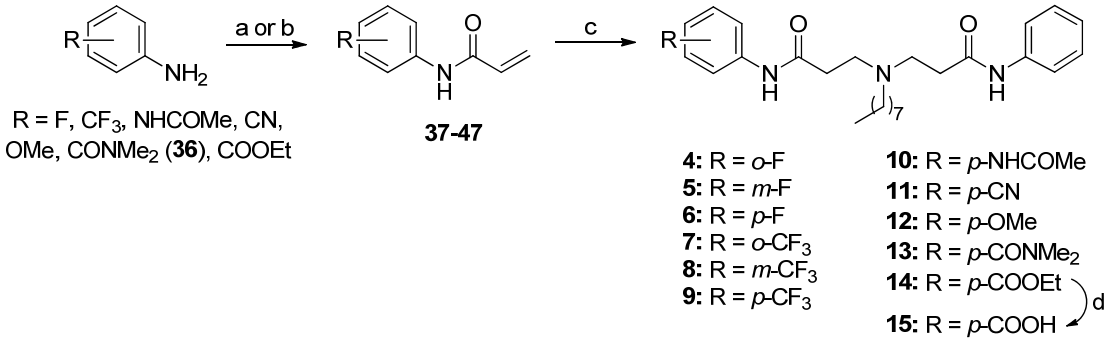


**Scheme 2.** Reagents and conditions: a) acryloyl chloride, pyridine, DCM, 0 ºC to rt, 2 h, 35-93%; b) acryloyl chloride, $Et_3N$, THF/DMF, 0 ºC to rt, o/n, 41%; c) $N^1$-phenyl-$N^3$-octyl-β-alaninamide (**34**), DBU, $CH_3CN$, 77 ºC, 24 h, 32-100%; d) $LiOH \cdot H_2O$, $THF/H_2O$, reflux, 3h, 28%.

All the anilines used in Scheme 2 were commercial except for derivative **36**, which was prepared as described in Scheme 3.

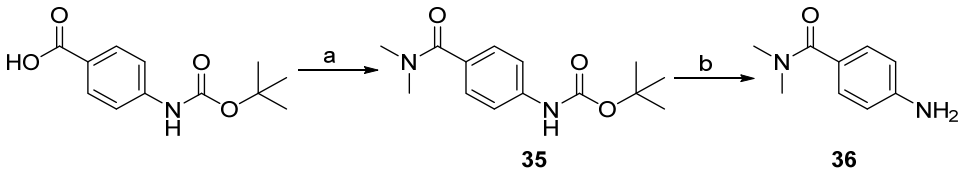


**Scheme 3.** Reagents and conditions: a) $NHMe_2 \cdot HCl$, *O*-(benzotriazol-1-yl)-*N,N,N′,N′*-tetramethyluronium tetrafluoroborate (TBTU), $Et_3N$, rt, 2 h, 75%; b) TFA/DCM, rt, 1 h, 93%.

We then determined the antiproliferative activity and the ICMT inhibitory capacity of compounds **4-15** (Table 2). First, we analyzed the influence of the position of the substitution in the phenyl ring (*ortho*, *meta* or *para*) for F and $CF_3$ substituents (compounds **4-9**). Regarding the antiproliferative

effect, both *meta* and *para* positions led to similar biological activity ($IC_{50}$ = 10-15 $\mu$M for F substituted derivatives **5** and **6**, and 8-22 $\mu$M for $CF_3$ substituted compounds **8** and **9**), better than the *ortho* substitution ($IC_{50}$ = 21-38 $\mu$M for F substituted derivative **4**, and 25-36 $\mu$M for $CF_3$ substituted derivative **7**). However, the inhibition of ICMT was much higher for the derivatives with the substituent at *para* position rather than for those with *ortho* or *meta* substitutions, as observed when comparing *para* substituted compounds **6** and **9** (with percentages of ICMT inhibition at 50 $\mu$M of 84% and 63%, respectively) with the *meta* substituted **5** and **8** (23% and 35%), or the *ortho* substituted **4** and **7** (23% and 30%, respectively). Hence, the *para* position was chosen for the rest of substituents (compounds **10-15**).

With respect to the influence of the electronic effects we could not observe any clear correlation between the biological activity (antiproliferative activity and ICMT inhibitory capacity) and the electron donor or acceptor character of the different substituents. In any case, none of the modifications improved the 93% inhibition obtained with derivative **3**, and their antiproliferative activity in cancer cells was clearly decreased (Table 2).

**Table 2.** Biological activity of compounds **3-15**[a]

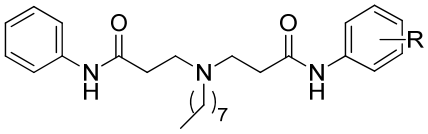

| Cpd | R | Antiproliferative effect ($IC_{50}$ $\mu$M) | | | ICMT Inhibition (%, 50 $\mu$M) |
|---|---|---|---|---|---|
| | | MCF7 | MDA-MB-231 | PC-3 | |
| **3** | H | 10 | 17 | 23 | 93 |
| **4** | *o*-F | 22 | 38 | 21 | 23 |
| **5** | *m*-F | 14 | 13 | 10 | 23 |
| **6** | *p*-F | 15 | 14 | 14 | 84 |
| **7** | *o*-$CF_3$ | 36 | 25 | 30 | 30 |
| **8** | *m*-$CF_3$ | 15 | 20 | 22 | 35 |
| **9** | *p*-$CF_3$ | 11 | 8 | 12 | 63 |
| **10** | *p*-$NHCOCH_3$ | 32 | 38 | 31 | 40 |
| **11** | *p*-CN | 14 | 25 | 27 | 68 |
| **12** | *p*-$OCH_3$ | 16 | 25 | 25 | 53 |
| **13** | *p*-$CON(CH_3)_2$ | 22 | 33 | 25 | 47 |
| **14** | *p*-$COOCH_2CH_3$ | 17 | 21 | 15 | 21 |
| **15** | *p*-COOH | >50 | 48 | >50 | 15 |

[a]Data from three independent experiments performed in triplicate; the SEM is in all cases within a 10% of the mean value.

### 2.1.2. Influence of the hydrophobic chain

In order to study the influence of the hydrophobic chain, we designed a new series of compounds (**16-27**) with lower calculated logarithm of the octanol/water partition coefficient (clogP) values by replacing the hydrophobic *n*-octyl chain by shorter alkyl chains or more polar substituents. First, the importance of the length of the alkyl chain was evaluated in order to check whether it is possible to

decrease the lipophilicity of compounds by shortening it, while keeping a good biological activity. This led us to compounds **16-18**. Next, we analyzed the influence of the introduction of oxygen atoms in the hydrophobic chain (**19-22**) or its replacement by more polar groups (**23-27**).

The synthesis of compounds **16-27** was carried out following the approach depicted in Scheme 4. The nucleophilic substitution of **48** with $NH_3$ gave compound **16**, whereas its reaction with piperidinyl or piperazinyl amines in the presence of triethylamine afforded compounds **26** and **27**. Intermediate phenylamide **48** was obtained by nucleophilic substitution of 3-bromopropanoyl chloride and aniline using pyridine as a base. The aza-Michael reaction of acrylamide **33** (Scheme 1) with the appropriate primary amine in the presence of DBU gave compounds **17-25**.

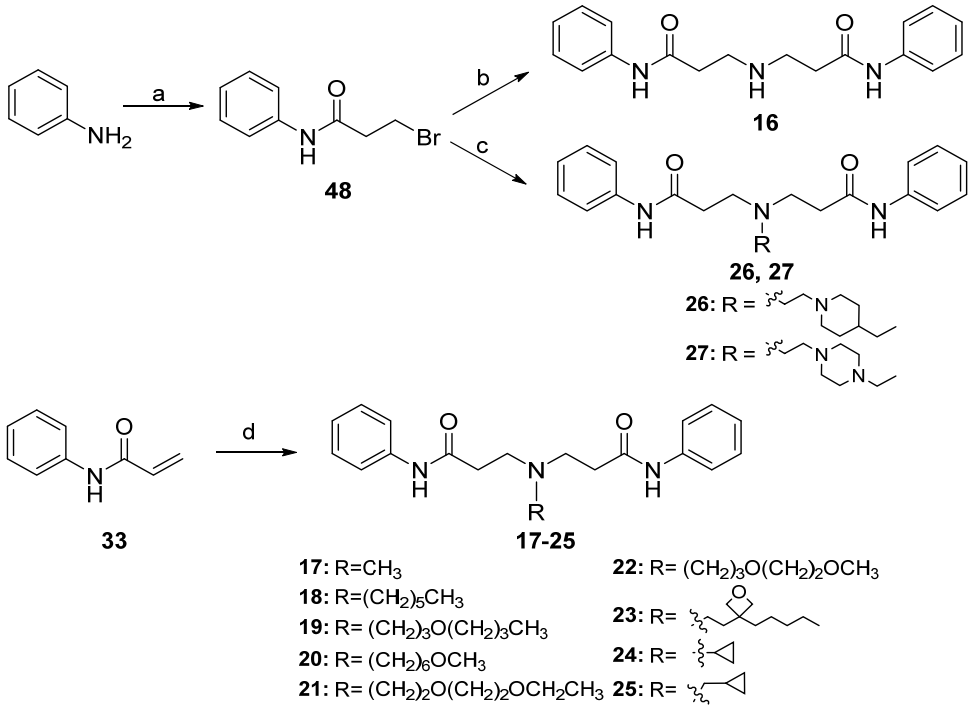


**Scheme 4.** Reagents and conditions: a) 3-bromopropanoyl chloride, pyridine, DCM, rt, 2 h, 92%; b) $NH_3$ (2 M in MeOH), DCM, rt, o/n, 15%; c) $RNH_2$, $Et_3N$, 10% KI, DCM, 60 ºC, 24 h, 48-54%; d) $RNH_2$, DBU, $CH_3CN$, 60 ºC or 45 ºC, 24 h, 21-100%.

This synthetic route involved the previous preparation of the non-commercial amines 6-methoxyhexyl-1-amine (**52**), 2-(2-ethoxyethoxy)ethylamine (**54**), 3-(2-methoxyethoxy)propyl-1-amine (**56**), 2-(3-pentyloxetan-3-yl)ethylamine (**59**) and (4-ethylpiperazin-1-yl)ethylamine (**61**).

Amines **52**, **54**, and **56**, with oxygen atoms introduced in their alkyl chains, were synthetized as depicted in Scheme 5. 6-Methoxyhexyl-1-amine (**52**) was obtained using 2-methoxycyclohexyl-1-one as starting material. This ketone was transformed into the corresponding oxime (**49**) by reaction with hydroxylamine, and further acetylated to give intermediate **50**. Later reductive Beckman fragmentation and reduction with $BH_3$ finally provided amine **52**. 2-(2-Ethoxyethoxy)ethylamine (**54**) was prepared through Mitsunobu reaction of 2-(2-ethoxyethoxy)ethanol and phthalimide, in the presence of diisopropylazodicarboxylate (DIAD) and triphenylphosphine, followed by deprotection with hydrazine and sodium borohydride. 3-(2-Methoxyethoxy)propyl-1-amine (**56**) was synthetized starting from 2-methoxyethanol, by addition of acrylonitrile in the presence of KOH, followed by reduction of the resulting nitrile (**55**) with $BH_3$.

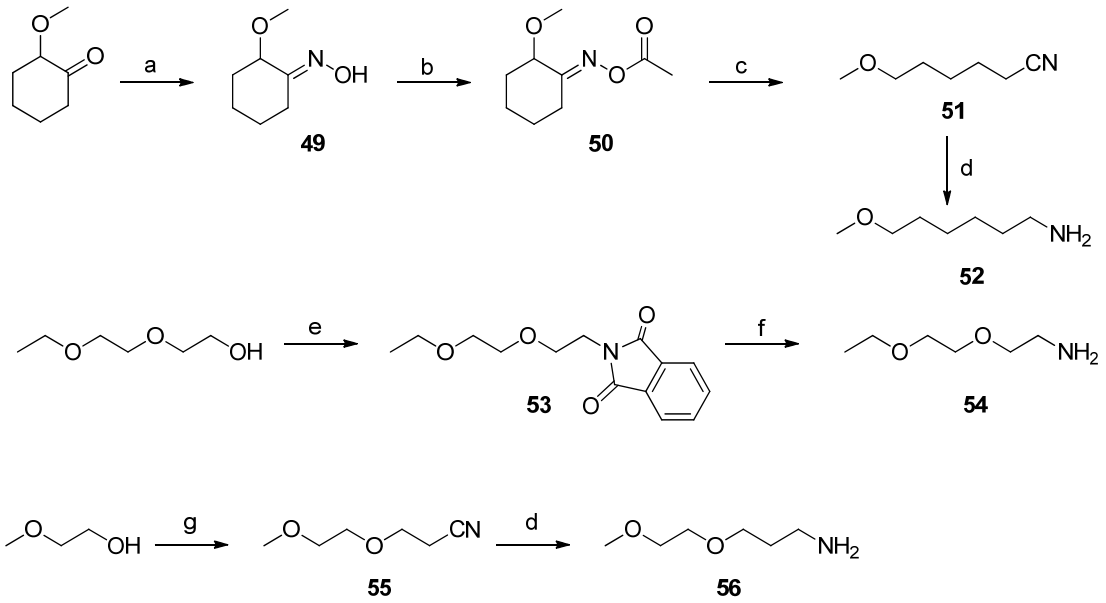


**Scheme 5.** Reagents and conditions: a) $NH_2OH{\cdot}HCl$, NaOAc, $H_2O$, MeOH, 60 ºC, 24 h, 99%; b) $Ac_2O$, pyridine, rt, 16 h, 95%; c) $Et_3SiH$, $CF_3SO_3SiMe_3$, DCM, 0 ºC, 6 h, 83%; d) $BH_3$, THF, reflux, 3.5 h, 68-89%; e) DIAD, $PPh_3$, phthalimide, MeOH, toluene, 0 ºC to rt, o/n, 58%; f) $N_2H_4{\cdot}H_2O$, $NaBH_4$, MeOH, rt, o/n, 71%; g) acrylonitrile, KOH, HCl, 0 ºC, 1.5 h, 100%.

2-(3-Pentyloxetan-3-yl)ethylamine (**59**) was prepared as shown in Scheme 6. The intermediate nitrile **57**, obtained by a Wittig reaction between oxetan-3-one and the appropriate phosphorane, was reacted with pentylmagnesium bromide in the presence of copper (I). Reduction of the resulting product **58** with lithium aluminium hydride (LAH) gave the desired amine **59**.

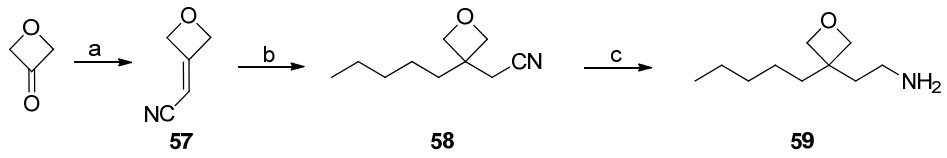


**57** **58** **59**

**Scheme 6.** Reagents and conditions: a) $Ph_3P$=CHCN, DCM, rt, 6 h, 79%; b) $C_5H_{11}MgBr$, CuI, $Et_2O$, 0 ºC, 2 h, 26%; c) LAH, $Et_2O$, 0 ºC, 2 h, 59%.

(4-Ethylpiperazin-1-yl)ethylamine (**61**) was obtained through formation of nitrile **60** by reaction of 1-ethylpiperazine and bromoacetonitrile in the presence of $K_2CO_3$, followed by reduction with LAH, as previously described in the literature (Scheme 7).[21]

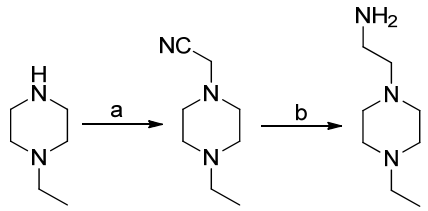


**60** **61**

**Scheme 7.** Reagents and conditions: a) $BrCH_2CN$, $K_2CO_3$, $CH_3CN$, rt, o/n, 100%; b) LAH, THF, 0 ºC, 4 h, 86%.

The biological activity of compounds **16-27** was also determined. The obtained results (Table 3) show that a decrease in the length of the alkyl chain (compounds **16-18**), despite it significantly improves cLogP values, involves important reductions in the inhibitory activity of the compounds, ranging from 0% to 30% inhibition. Neither the introduction of oxygen atoms in the alkyl chain (**19-22**), nor the introduction of the oxetane group (**23**) allows to keep good inhibition values, compared to the 93% inhibition induced by derivative **3** at the same concentration. Finally, replacement of the *n*-octyl chain by cyclopropane, methylcyclopropane, (4-ethylpiperidin-1-yl)ethane or (4-ethylpiperazin-1-yl)ethane (**24-27**) also implies an important decrease in the antiproliferative and inhibitory activities of the resulting compounds.

**Table 3.** cLogP and biological activity of compounds **3** and **16-27**

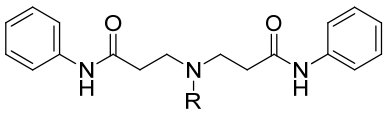

| Cpd | R | cLogP[a] | Antiproliferative effect ($IC_{50}$ $\mu$M)[b] | | | ICMT inhibition[b] (%, 50 $\mu$M) |
|---|---|---|---|---|---|---|
| | | | MCF7 | MDA-MB-231 | PC-3 | |
| **3** | $-(CH_2)_7CH_3$ | 4.11 | 10 | 17 | 23 | 93 |
| **16** | -H | 1.92 | >50 | >50 | >50 | 30 |
| **17** | $-CH_3$ | 0.39 | ND | ND | ND | 0 |
| **18** | $-(CH_2)_5CH_3$ | 2.52 | >50 | >50 | >50 | 9 |
| **19** | $-(CH_2)_3O(CH_2)_3CH_3$ | 2.21 | >50 | 40 | >50 | 14 |
| **20** | $-(CH_2)_6OCH_3$ | 1.68 | >50 | >50 | >50 | 30 |
| **21** | $-(CH_2)_2O(CH_2)_2OCH_2CH_3$ | 0.26 | >50 | >50 | >50 | 15 |
| **22** | $-(CH_2)_3O(CH_2)_2OCH_3$ | 0.26 | >50 | >50 | >50 | 45 |
| **23** | 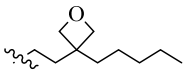 | 2.90 | ND | ND | ND | 0 |
| **24** |  | 0.76 | 24 | 29 | >50 | 33 |
| **25** |  | 1.29 | >50 | >50 | >50 | 36 |
| **26** | 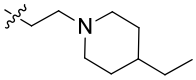 | 2.83 | 39 | >50 | >50 | 13 |
| **27** | 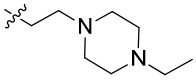 | 0.41 | >50 | >50 | >50 | 15 |

[a]Parameter calculated using ACD/Labs Percepta. [b]Data from three independent experiments performed in triplicate; the SEM is in all cases within a 10% of the mean value. ND, not determined.

Taken together, the data obtained suggest that a long hydrophobic chain attached to the nitrogen atom is needed, so we decided to keep the *n*-octyl chain and continued with the exploration of the amide group.

### 2.1.3. Influence of the amide group

Previous experiments carried out in our research group have shown that the amide group present in both UCM-1325 and compound **3** is necessary for a good inhibitory activity. However, when we studied the metabolic stability of derivative **3** in mouse serum, we observed that it was only moderate, with a half-life value ($t_{1/2}$) of 27 min. Thus, we decided to introduce a methyl substituent in one of the amide groups of compound **3** (derivative **28**), since it has been described that tertiary amides tend to have increased metabolic stabilities. We also replaced the initial amide by a sulfonamide (**29**) or by an oxadiazole heterocyclic ring (**30**), considering that they have been reported as more stable isosteres of the amide group.[22]

Compounds **28-30** were obtained as described in Scheme 8, starting from secondary amine **34** and following a similar approach to the previously described (Scheme 1).

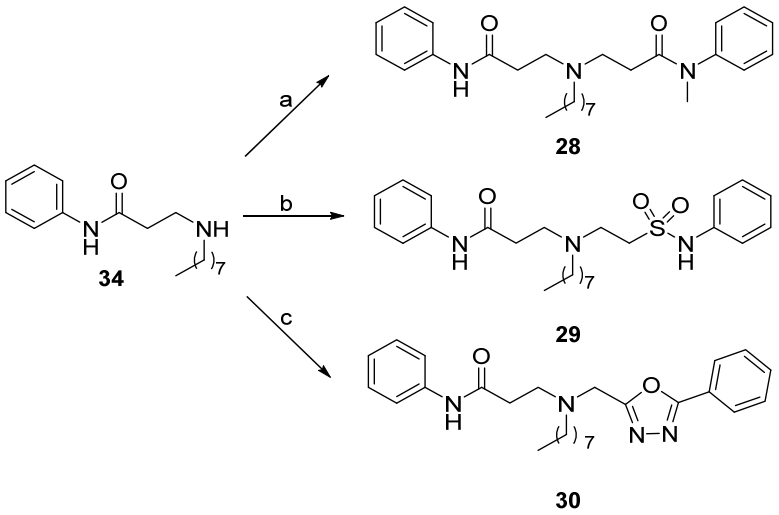


**Scheme 8.** Reagents and conditions: a) *N*-methyl-*N*-phenylacrylamide (**62**), DBU, $CH_3CN$, 60 ºC, 24 h, 58%; b) *N*-phenylethylensulfonamide (**63**), DBU, $CH_3CN$, 60 ºC, 24 h, 12%; c) 2-(chloromethyl)-5-phenyl-1,3,4-oxadiazole, $Et_3N$, $CH_3CN$, 60 ºC, 24 h, 62%.

The reaction of secondary amine **34** with either *N*-methyl-*N*-phenylacrylamide (**62**), *N*-phenylethylensulfonamide (**63**) or 2-(chloromethyl)-5-phenyl-1,3,4-oxadiazole in the presence of a base (DBU or triethylamine), afforded final compounds **28-30.** Intermediates **62** and **63** were obtained as previously described (Scheme 1). Thus, acrylamide **62** was prepared using *N*-methylaniline and acryloyl chloride as starting materials, whereas sulfonamide **63** was obtained from aniline and 2-chloroethanesulfonyl chloride.

The biological evaluation of compounds **28-30** as ICMT inhibitors and antiproliferative agents in the selected panel of cancer cell lines, suggested that none of these modifications in the amide group improved the inhibitory capacity of the resulting derivatives in comparison to the reference compound **3**, as can be observed in Table 4.

**Table 4.** Biological activity of compounds **3** and **28-30**[a]

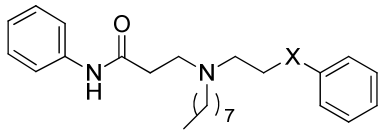


| Cpd | X | Antiproliferative effect ($IC_{50}$ $\mu$M) | | | ICMT Inhibition (%, 50 $\mu$M) |
|---|---|---|---|---|---|
| | | MCF7 | MDA-MB-231 | PC-3 | |
| **3** | NHCO | 10 | 17 | 23 | 93 |
| **28** | $NCH_3CO$ | 6 | 7 | 8 | 68 |
| **29** | $NHSO_2$ | 30 | 34 | 25 | 22 |
| **30** | 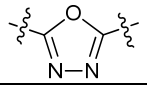 | >50 | >50 | >50 | 13 |



[a]Data from three independent experiments performed in triplicate; the SEM is in all cases within a 10% of the mean value.

Taken together the inhibitory capacity, the antiproliferative effect, and the pharmacokinetic parameters of this derivative, compound **3** (UCM-1336) deserves special attention as a structurally new inhibitor of the ICMT enzyme that could be a promising lead for anticancer treatment, so it was selected for its further biological characterization.

In order to compare the biological results obtained with compound **3**, we decided to use 2-[5-(3-methylphenyl)-1-octyl-1*H*-indol-3-yl]acetamide (cysmethynil) as a positive control for ICMT inhibition. The synthesis of cysmethynil was carried out following the route previously described in the literature (Scheme 9).[16]

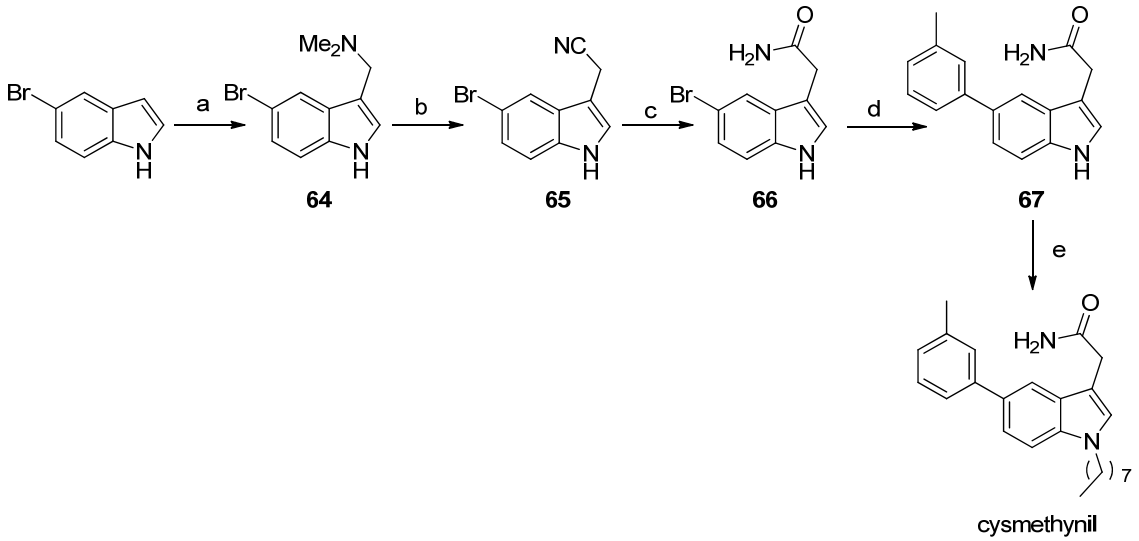


**Scheme 9.** Reagents and conditions: a) $CH_2O$, $(CH_3)_2NH$, 1,4-dioxane, AcOH, $H_2O$, 0 ºC to rt, o/n, 83%; b) KCN, $(CH_3)_2SO_4$, THF, 10 ºC to 60 ºC, 2h, 95%; c) KOH, *t*-BuOH, reflux, 1.5 h, 74%; d) *m*-tolylboronic acid, $Pd(PPh_3)_4$, $NaHCO_3$, toluene, EtOH, reflux, o/n, 23%; e) NaH , $Br(CH_2)_7CH_3$, DMF, 55 ºC, o/n, 43%.

Hence, we analyzed the ICMT inhibitory capacity and antiproliferative effect of compound **3** in comparison to the already validated ICMT inhibitor cysmethynil. As can be observed in Table 5, the values obtained with compound **3** (UCM-1336) were very similar or even better than those of cysmethynil, reinforcing the potential of compound **3** as an ICMT inhibitor.

**Table 5.** Biological activity of cysmethynil (CYSM) and compound **3** (UCM-1336)[a]

| Cpd | Antiproliferative effect ($IC_{50}$, $\mu$M) | | | ICMT inhibition at 50 $\mu$M (%) | $IC_{50}$ values of ICMT inhibition |
|---|---|---|---|---|---|
| | MCF7 | MDA-MB-231 | PC-3 | | |
| CYSM | 24 | 24 | 23 | 90 | 2.4 $\mu$M |
| **3** (UCM-1336) | 10 | 17 | 22 | 93 | 2 $\mu$M |

[a]Data from three independent experiments performed in triplicate; SEM is in all cases within a 10% of the mean value.

### 2.2. Biological evaluation of compound 3 (UCM-1336)

Validation of the new lead **3** (UCM-1336) as an ICMT inhibitor required not only to check that it effectively blocked the enzyme activity, but also to demonstrate its significant in vivo efficacy in cancer cell lines through the blockade of the activity of downstream Ras protein. In order to confirm the mechanism of action of this compound and the relevance of ICMT inhibition for Ras inactivation, we assessed whether UCM-1336 affects specifically tumor cell lines characterized by oncogenic Ras activity, enhances programmed cell death, induces mislocalization of Ras protein, inactivates all Ras isoforms, blocks the downstream signaling pathways, and impairs cell migration.

#### 2.2.1. Determination of cytotoxicity in a panel of cancer cell lines

First, we established the antiproliferative activity of UCM-1336 using the MTT assay. The panel of cells was chosen to include multiple examples of cell lines that express wild-type or oncogenic mutant K-Ras, which was selected for being the most frequently mutated Ras isoform in cancer. It is remarkable that regardless of the origin of the tumor, UCM-1336 inhibited the proliferation of cells expressing oncogenic mutant K-Ras (breast cancer MDA-MB-231 cells, pancreatic cancer MIA PaCa-2 and PANC-1 cells, and colon cancer SW620 cells) more potently than cells expressing wild-type K-Ras (pancreatic cancer BxPC-3 cells, breast cancer MCF7 cells, prostate cancer PC-3 cells, and melanoma SK-Mel-28 cells), as can be observed in Table 6. Interestingly, UCM-1336 did not induce significant cytotoxic effects at concentrations up to 100 $\mu$M in non tumoral cell lines such as NIH3T3 and 142BR fibroblasts, suggesting that the mechanism of action of the compound is specific for cancer cell lines.

**Table 6.** Cytotoxicity of UCM-1336 in a panel of cancer cell lines

| **Mutant K-Ras**[a] | | **Wild-type K-Ras**[b] | |
|---|---|---|---|
| **Cell Line** | **$IC_{50}$[c] ($\mu$M)** | **Cell Line** | **$IC_{50}$[c] ($\mu$M)** |
| MDA-MB-231 | 10 | MCF7 | 17 |
| MIA PaCa-2 | 2 | BxPC-3 | > 50 |
| PANC-1 | 7 | PC-3 | 23 |
| SW620 | 3 | SK-Mel-28 | 15 |

[a]Mutant K-Ras and wild-type H- and N-Ras; [b]wild-type H,K,N-Ras [Ras status according to the Catalog of Somatic Mutations in Cancer (Wellcome Trust Sanger Institute)]; [c]all errors are less than 10%.

### 2.2.2. Induction of autophagy and apoptosis

An important property of anticancer agents is the ability to induce cell death, and many current antitumoral drugs enhance either autophagy (eg. tamoxifen) or apoptosis (eg. rapamycin) in cancer cells.[23,24] Besides, it has been recently reported that both knockdown of ICMT and treatment of cells with cysmethynil increase protein levels and aggregation of microtubule-associated protein light chain 3 (LC-3) into vesicular structures characteristic of autophagosomes; as well as elevation of cleaved poly(ADP-ribose) polymerase (cPARP) levels and caspase 3 activity, suggesting that the inhibition of ICMT promotes both autophagy and apoptosis in cancer cell lines.[17,25] Hence, we studied the cell death mechanism of action of UCM-1336.

Autophagy was assessed by determining the vesicular accumulation of LC-3, using a fusion protein with mCherry in a live cell imaging assay. To do so, we chose two different cell lines: human embryonic kidney AD-293 cells, as they are easily transfected and were hence selected as our model for transient transfections; and osteosarcoma U2OS cells, as they have been described in the literature as a model of cells that use autophagy as a protective mechanism to survive treatment with antineoplasic drugs such as doxorubicin.[26] Our results show that both UCM-1336 and cysmethynil used at 5 $\mu$M cause a dramatic increase in total abundance of LC-3, which also aggregates into vesicular structures characteristic of autophagosome formation in AD-293 cells and in U2OS cells (Figure 6A). Noteworthy, the observed effect was greater for treatment with UCM-1336 than for cysmethynil. This was further supported by immunoblot analysis of LC-3, which showed a significant elevation of this protein in PC-3 cells treated with 10 $\mu$M UCM-1336 or 25 $\mu$M cysmethynil, included as a positive control (Figure 6B).

Apoptosis was assessed by measurement of caspase 3 activation using a colorimetric assay, and by the appearance of cPARP through immunoblot analysis (Figure 6C and D). Caspases are cysteine aspartyl proteases that serve as the central engine of apoptosis. In particular, caspase 3 is used as a control of the overall levels of apoptosis, as it is activated both by extrinsic and intrinsic pathways.[27] PC-3 cells were incubated in the presence of 10 $\mu$M UCM-1336 or 25 $\mu$M cysmethynil. Our results showed that exposure of cells to either UCM-1336 or cysmethynil increased caspase 3 activity in a 4-5 fold (Figure 6C). In addition, caspase 3 is responsible, either wholly or partially, for the proteolytic cleavage of a large number of substrates during apoptosis, including PARP -a family of proteins involved in DNA repair and programmed cell death-,[27] so we confirmed the previous results by measuring the levels of cPARP in cells treated with UCM-1336. Immunoblot analysis showed the appearance of cPARP after 48 h in UCM-1336 or cysmethynil exposed cells (Figure 6D), whose levels revealed a 4-8 fold increase. These data provide clear evidence that UCM-1336 treatment induces both apoptosis and autophagy.

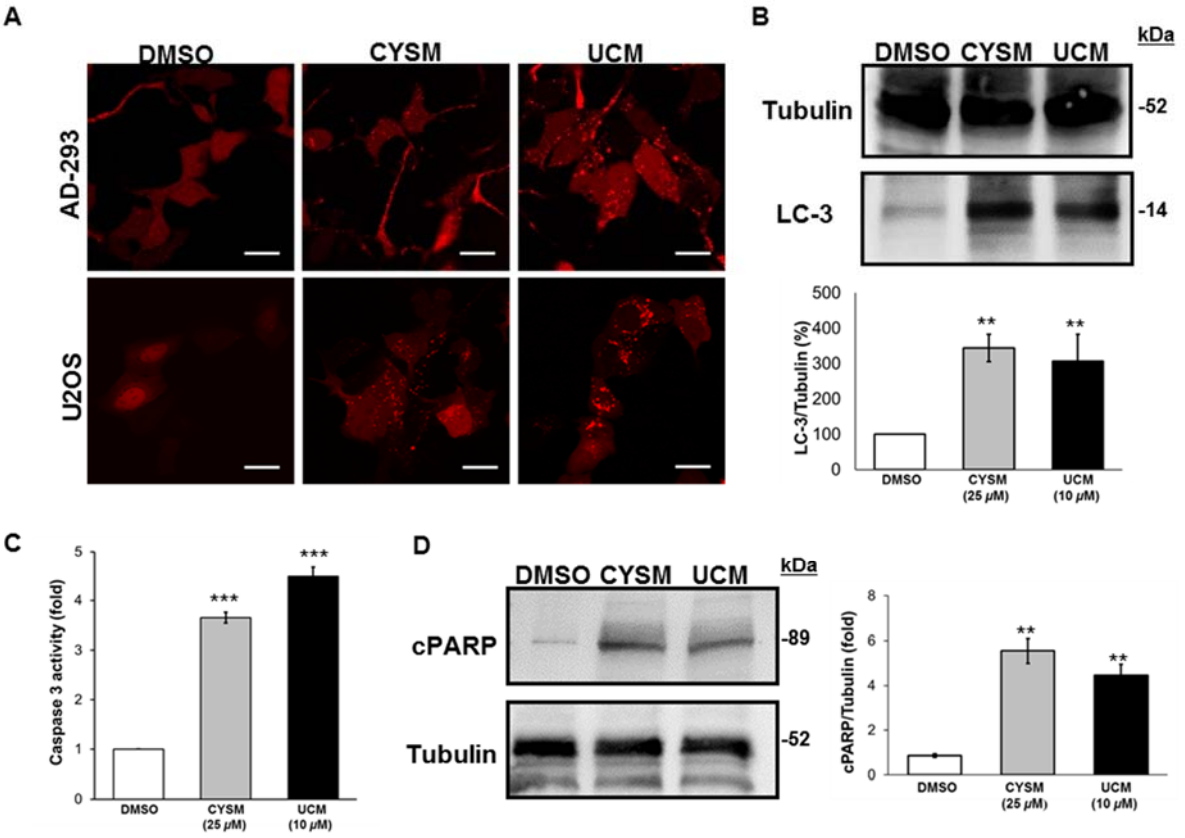


**Figure 6.** Treatment with UCM-1336 induces autophagy and apoptosis in cancer cells. (A) Confocal images of live AD-293 (upper) and U2OS (lower) cells transiently transfected with mChery-LC-3 plasmid and treated overnight with vehicle (DMSO), 5 $\mu$M cysmethynil (CYSM) or 5 $\mu$M UCM-1336 (UCM). Images were taken using an inverted Zeiss LSM 510 Meta laser scanning confocal microscope and are representative of two independent transfections performed in triplicate. Bars, 10 $\mu$m. (B) Representative immunoblot analysis of LC-3. PC-3 cells were treated with either vehicle (DMSO), 25 $\mu$M cysmethynil (CYSM) or 10 $\mu$M UCM-1336 (UCM) for 48 h. The bar graphs represent the optical density of the LC-3 protein normalised to the tubulin (loading control), and expressed as the percentage relative to DMSO. (C) Caspase 3 activity induction. PC-3 cells were treated for 48 h with vehicle (DMSO), 25 $\mu$M cysmethynil (CYSM) or 10 $\mu$M UCM-1336 (UCM) before being harvested and lysed. Lysates were assayed for caspase 3 activity and results are presented as the percentage relative to DMSO. (D) Representative immunoblot analysis of cPARP. PC-3 cells were treated with either vehicle (DMSO), 25 $\mu$M cysmethynil (CYSM) or 10 $\mu$M UCM-1336 (UCM) for 48 h. cPARP protein was quantified as the indication for the level of apoptosis and tubulin protein was used as loading control. In all cases, data correspond to the average ± SEM of three independent experiments performed in triplicate. **, $P$<0.01; ***, $P$<0.001 vs DMSO treated cells (Student's $t$ test).

### 2.2.3. Mislocalization of endogenous Ras in PC-3 cells

Then, we determined whether inhibition of ICMT leads to Ras mislocalization in tumor cells. PC-3 cells were incubated with increasing concentrations of compound UCM-1336 or cysmethynil for 96 h. This time frame was chosen to allow trafficking of newly synthesized Ras proteins and turnover of Ras proteins that were already present when treatments started. As expected, in the absence of compounds, Ras was localized along the plasma membrane (Figure 7, 0 $\mu$M). In contrast, a large fraction of Ras in the UCM-1336 or cysmethynil treated cells was trapped within the cytoplasm, and fluorescence at the plasma membrane was reduced (Figure 7, 1-25 $\mu$M). Remarkably, this effect was higher for UCM-1336 than for cysmethynil at the same concentration, and increased in a dose-dependent manner. These data are consistent with previous observations of Ras mislocalization caused by knockout of ICMT[28] and by the ICMT inhibitor cysmethynil.[16]

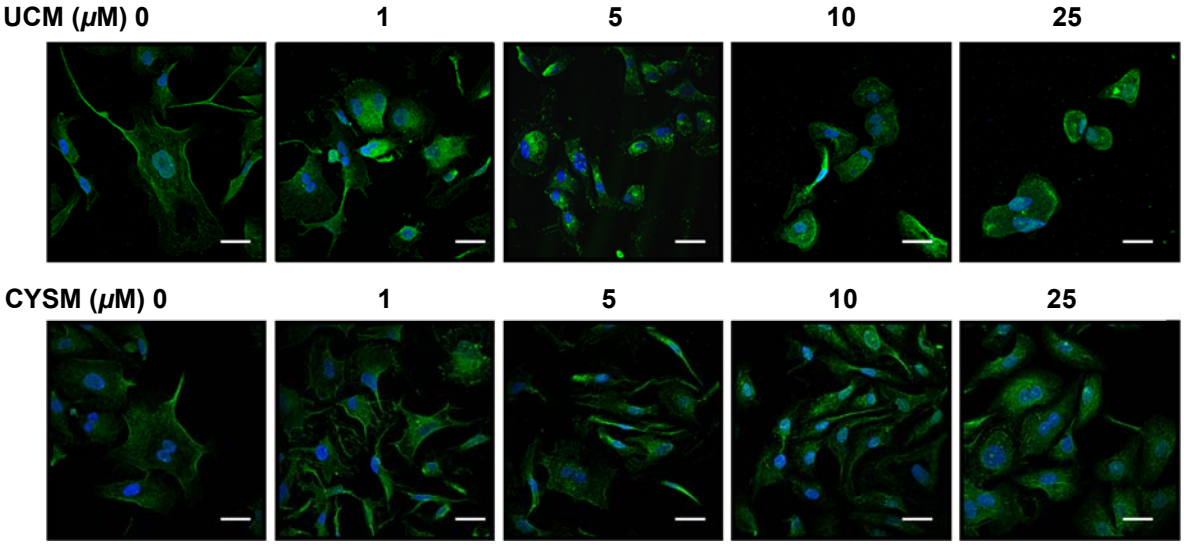


**Figure 7.** Compound UCM-1336 induces Ras mislocalization from the cellular membrane (far-left image) to intracellular locations in PC-3 cells in a dose-dependent manner. The observed effect is higher for UCM-1336 than for cysmethynil at the same concentration. Immunofluorescence images show Ras in green stained using an anti-Ras primary antibody followed by the appropriate secondary FITC-labelled antibody. Nuclei (in blue) were stained with Hoechst 33258. Images were obtained in a Leica confocal microscope under the same conditions and are representative of three to five independent experiments. Bars, 30 $\mu$m.

### 2.2.4. Mislocalization of the four isoforms of Ras

There are three *ras* genes in mammals: *hras*, *kras*, and *nras*, but through alternative splicing of exon 4, the *kras* gene gives rise to two isoforms: K-Ras4A and K-Ras4B.[1] To determine whether the observed effects of UCM-1336 on the localization of Ras affected equally all isoforms, we used confocal live cell fluorescent imaging of AD-293 cells transfected with the four Ras isoforms tagged with green fluorescent protein (GFP).

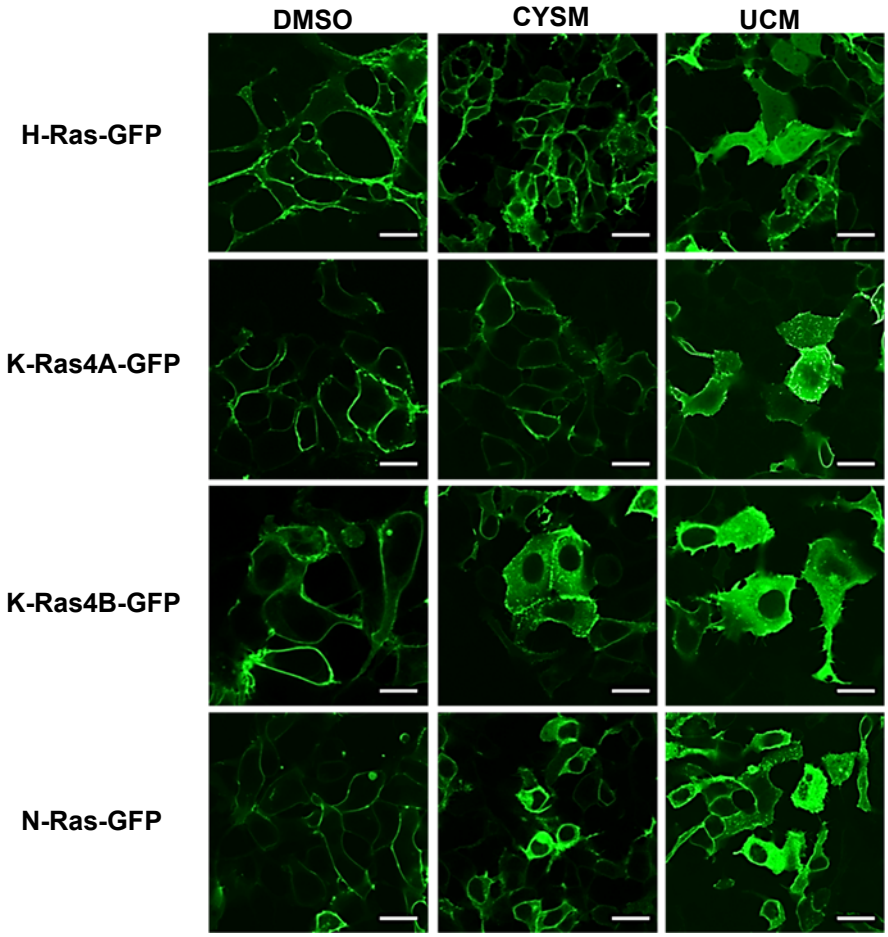


**Figure 8.** UCM-1336 impairs plasma localization of the four Ras isoforms in live cells. Confocal images of live AD-293 cells that had been transiently transfected with H-Ras, K-Ras4A, K-Ras4B, and N-Ras GFP fusion plasmids, and treated overnight with vehicle (DMSO), 5 $\mu$M cysmethynil (CYSM), or 5 $\mu$M UCM-1336 (UCM). Live cells were imaged with an inverted Zeiss LSM 510 Meta laser scanning confocal microscope. Similar results were obtained with three independent transfections performed in triplicate. Bars, 10 $\mu$m.

Transfected cells were treated overnight with 5 $\mu$M cysmethynil or UCM-1336, or with DMSO. While the vehicle-treated cells showed a predominant localization of Ras in the plasma membrane, all four isoforms of Ras were substantially mislocalized to the cytosolic region after treatment with UCM-1336 (Figure 8). Furthermore, this effect was more significant for UCM-1336 than for cysmethynil, included for comparison, at the same concentration.

### 2.2.5. Study of the specificity of the mechanism of action of UCM-1336

To confirm that the effect of mislocalization of the Ras isoforms is due to ICMT inhibition, and not to any other unspecific mechanism, we performed two additional sets of tranfections: with Fyn protein, to discard potential detergent-like effects; and with a geranylgeranylated K-Ras, to confirm that the mislocalization of Ras is not caused by inhibition of any other upstream enzyme rather than ICMT.

As a control to discard any possible nonspecific detergent-like effects of the compounds, cells were transfected with GFP-tagged Fyn, a member of the Src family of tyrosine protein kinases that targets the plasma membrane after myristoylation and palmitoylation, but which is not processed by ICMT (Figure 9). In this case, neither UCM-1336 nor cysmethynil affected the localization pattern of Fyn.

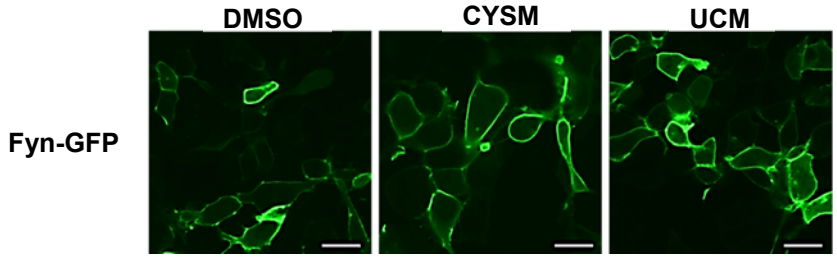


**Figure 9.** UCM-1336 does not affect Fyn localization. To discard any possible nonspecific detergent-like effects, AD-293 cells were transfected with GFP-tagged Fyn, which is not processed by ICMT, and treated overnight with vehicle (DMSO), 5 $\mu$M cysmethynil (CYSM), or 5 $\mu$M UCM-1336 (UCM). After treatments, GFP-tagged Fyn showed the same localization pattern in all cases. Live cells were imaged with an inverted Zeiss LSM 510 Meta laser scanning confocal microscope. Similar results were obtained with three independent transfections performed in triplicate. Bars, 10 $\mu$m.

Furthermore, it has been previously demonstrated that CAAX proteolysis and carboxyl methylation by ICMT are required only for previously farnesylated Ras proteins to proper localize in the plasma membrane, but not for geranylgeranylated proteins. The substrate specificity for FTase versus GGTase I is determined by the residue in the X position of the CAAX motif: S and M specifies farnesylation whereas L specifies geranylgeranylation.[29] Using a GFP-tagged K-Ras4B protein with

a CAAX motif point mutation expected to switch the chain length of the isoprenyl modification (farnesylation for geranylgeranylation), we studied the effect of derivative UCM-1336 on its cellular localization. Geranylgeranylated K-Ras4B (K-Ras4B-CVIL-GFP) localized in the plasma membrane of AD-293 cells with an indistinguishable pattern in both vehicle and compound treated cells, whereas farnesylated K-Ras4B-GFP was mislocalized to the cytosol in the presence of compound UCM-1336 (Figure 10). This further confirmed the specific effect of UCM-1336 on farnesylated GTPases through inhibition of ICMT, as geranylgeranylated Ras should not be affected by an ICMT inhibition.

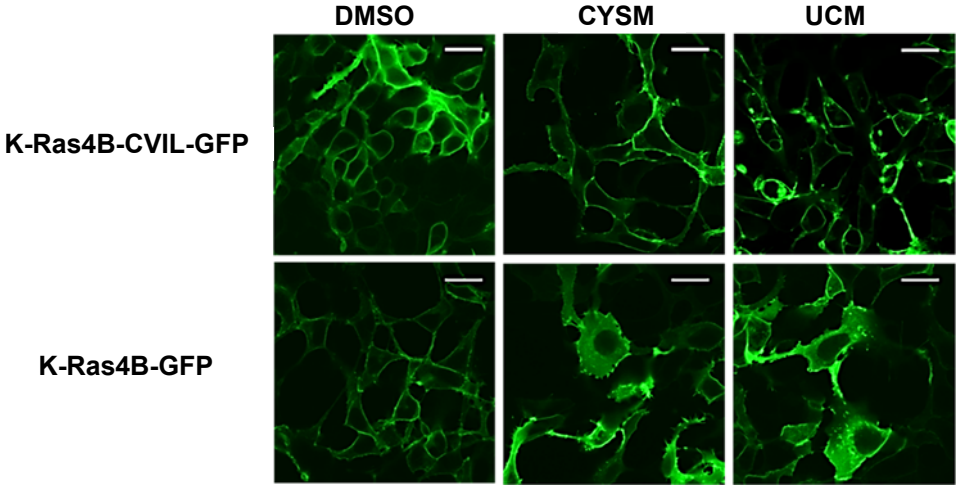


**Figure 10.** UCM-1336 affects the membrane association of farnesylated K-Ras, but not geranylgeranylated K-Ras. Confocal images of live AD-293 cells transiently transfected with a GFP-tagged K-Ras4B plasmid with a CAAX motif point mutation that switches farnesylation for geranylgeranylation, or with wild-type K-Ras4B-GFP. Geranylgeranylated K-Ras4B (K-Ras4B-CVIL-GFP) localizes in the plasma membrane with an indistinguishable pattern in both vehicle and compound treated cells, whereas farnesylated K-Ras4B-GFP mislocalizes to the cytosol in the presence of cysmethynil or compound UCM-1336. Live cells were imaged with an inverted Zeiss LSM 510 Meta laser scanning confocal microscope. Images are representative of two to three independent experiments performed in triplicate. Bars, 10 $\mu$m.

These results supported the specificity of the mechanism of action of UCM-1336 through inhibition of signaling pathways upstream of Ras.

### 2.2.6. Study of the activation status of Ras

As Ras signaling is dependent on membrane association, we next explored the ability of our compound to prevent Ras activation, by analysing the GTP loading capacity of Ras using a pulldown assay, and studying its effects on the activation of the downstream MAP kinase pathways. Figure 11A shows that UCM-1336 at 10 $\mu$M significantly reduces pan-Ras GTP loading to a greater extent than treatment with 25 $\mu$M cysmethynil. This reduction in Ras activation correlates closely with a concomitant reduction in the phosphorylation of MEK/ERK and PI3K/AKT signaling pathways (Figure 11B). After activation of PC-3 cells with epidermal growth factor (EGF), the phosphorylated levels of MEK1/2 (p-MEK1/2), ERK1/2 (p-ERK1/2), and AKT (p-AKT) were decreased in cells treated with 10 $\mu$M UCM-1336, and this reduction was greater than the one produced by 25 $\mu$M cysmethynil.

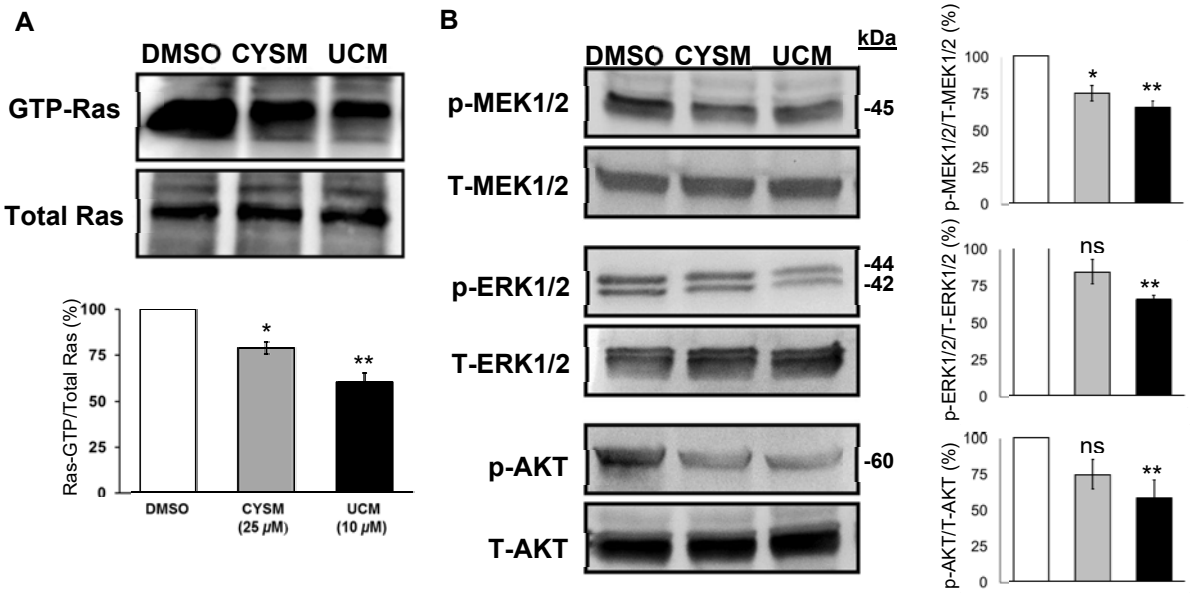


**Figure 11.** Compound UCM-1336 significantly reduces the Ras-GTP (active form) levels and its downstream MEK/ERK and PI3K/AKT signaling pathways. (A) Ras-GTP complex from PC-3 cells treated with DMSO, 25 $\mu$M cysmethynil or 10 $\mu$M UCM-1336 were immunoprecipitated and visualized by western blot. The bar graph shows the ratio Ras-GTP/total Ras, expressed as percentage relative to DMSO. (B) Representative western blots of phosphorylated MEK1/2 (p-MEK1/2) and total MEK1/2 (T-MEK1/2), phosphorylated ERK1/2 (p-ERK1/2) and total ERK1/2 (T-ERK1/2), and phosphorylated AKT (p-AKT) and total AKT (T-AKT). Lysates were obtained from PC-3 cells treated with DMSO, 25 $\mu$M cysmethynil (CYSM) or 10 $\mu$M UCM-1336 (UCM). The bar graphs represent the optical density of the immunoreactive phosphorylated protein normalised to the total corresponding protein, and expressed as the percentage relative to DMSO. White bars, DMSO; grey bars, 25 $\mu$M cysmethynil; black bars, 10 $\mu$M UCM-1336. In all cases, data correspond to the average ± SEM of three to five independent experiments. ns, not significant; *, $P$<0.05; **, $P$<0.01 vs DMSO (Student's $t$ test).

### 2.2.7. Study of the impairment of cellular migration

Importantly, inhibition of Ras signaling pathways by compound UCM-1336 was accompanied by a reduced invasive phenotype as measured by in vitro wound-healing assays, where MDA-MB-231 cells expressing oncogenic mutant K-Ras treated with UCM-1336 or cysmethynil showed a significantly reduced capacity for wound closing at 48 h, which decreased in a dose-dependent manner and was much higher in cells treated with UCM-1336 than in those treated with the same concentrations of cysmethynil (Figure 12). However, the number of viable cells remained similar to the vehicle-treated cells (data not shown), meaning that the inhibition of cell migration was not simply due to a cytotoxic effect caused by the compound.

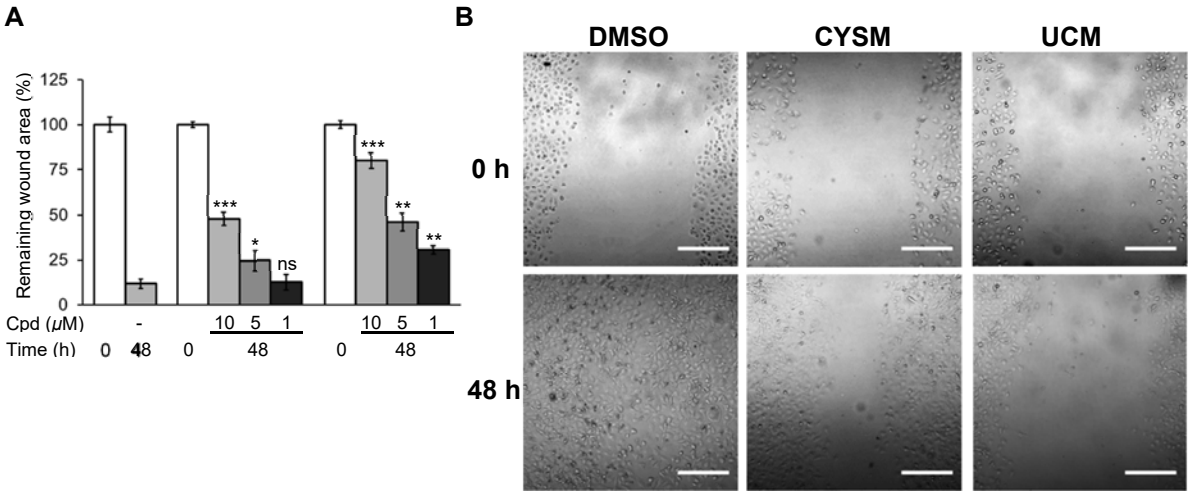


**Figure 12.** Compound UCM-1336 significantly impairs cellular migration in a dose-dependent manner. (A) After wound scratching, MDA-MB-231 cells were treated with vehicle or different concentrations of cysmethynil (CYSM) or UCM-1336 (UCM), and after 48 h cells were visualized under the microscope. The percentage of the remaining wound area was quantified and expressed as percentage of initial wound area. The bar graph represents the average ± SEM of at least three independent experiments performed in triplicate and three different fields. ns, not significant; *, $P<0.05$; **, $P<0.01$; ***, $P<0.001$ (vs DMSO treated cells at 48 h) (Student's *t* test). (B) Representative images of at least three independent experiments performed in triplicate, taken at time 0 h and after 48 h of treatment with vehicle (DMSO), 10 $\mu$M cysmethynil (CYSM) or 10 $\mu$M UCM-1336 (UCM), under phase contrast with an Olympus FW1200 microscope. Bars, 250 $\mu$m.

The main effects of the activation of the Ras pathway include the induction of proliferation, migration, and antiapoptotic signals; so its inhibition should lead to an arrest of all these processes, and consequently, of tumor growth. All these promising results have prompted us to study the in vivo efficacy of compound UCM-1336 in a xenograft mouse model of pancreatic cancer, experiments that are currently ongoing in our laboratory.

## 3. CONCLUSIONS

In this work we have started the lead optimization process of UCM-1325 (54% inhibition of ICMT at 50 $\mu$M) that has led us to the new compound UCM-1336 (**3**), which showed an ICMT inhibition of 93% at 50 $\mu$M ($IC_{50}$ = 2 $\mu$M), hence being selected for in depth biological studies and characterization of its mechanism of action. This new compound enhances programmed cell death, affecting specially those cell lines expressing oncogenic mutant K-Ras; and induces mislocalization of all Ras isoforms. Besides, UCM-1336 (**3**) significantly reduces Ras activity, blocks the activation of the downstream MEK/ERK and PI3K/AKT signaling pathways, and impairs the migratory capacity of tumor cells. Noteworthy, UCM-1336 (**3**) has shown to be more potent than cysmethynil in all performed assays, suggesting that it could work as a new ICMT inhibitor that would help to definitively validate this enzyme from a mechanistic standpoint as a therapeutic target of interest for the treatment of cancers characterized by high Ras overactivation, a current unmet clinical need. All these promising results have prompted us to study the in vivo efficacy of compound UCM-1336 in a xenograft mouse model of pancreatic cancer, experiments that are currently ongoing.

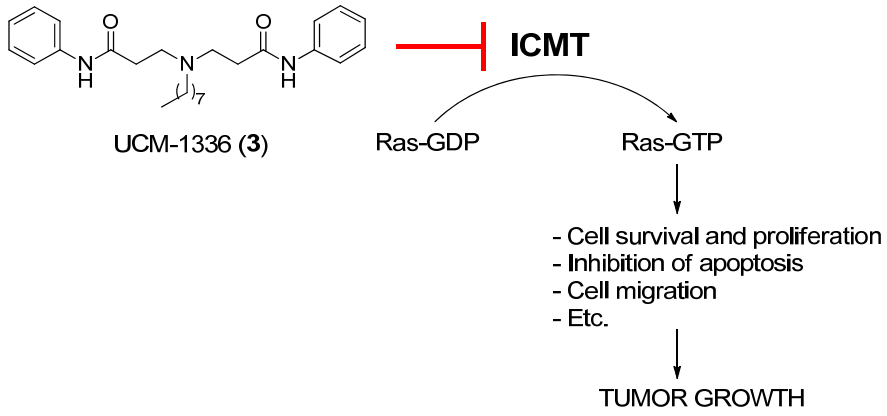

## 4. EXPERIMENTAL SECTION

### 4.1. Chemistry

Unless stated otherwise, starting materials, reagents and solvents were purchased as high-grade commercial products from Sigma-Aldrich, Acros, Fluorochem, Abcr, Scharlab or Panreac, and were used without further purification. Dichloromethane (DCM) and tetrahydrofuran (THF) were dried using a Pure Solv™ Micro 100 Liter solvent purification system. All non-aqueous reactions were carried out under an argon atmosphere in oven-dried glassware. Chromatography was performed on glass column using silica gel type 60 (Merck, particle 230-400 mesh) or using a VARIAN 971-FP system with cartridges of silica gel (Varian, size particle 50 $\mu$m). Analytical thin-layer chromatography (TLC) was run on Merck silica gel plates (Kieselgel 60 F-254) with detection by UV light (254 nm), ninhydrin solution, or 10% phosphomolybdic acid solution in ethanol. Melting points (mp, uncorrected) were determined on a Stuart Scientific electrothermal apparatus. Infrared (IR) spectra were measured on a Shimadzu-8300 or Bruker Tensor 27 instrument equipped with a Specac ATR accessory of 5200-650 $cm^{-1}$ transmission range; frequencies ($\nu$) are expressed in $cm^{-1}$. Nuclear Magnetic Resonance (NMR) spectra were recorded on a Bruker Avance 300-AM ($^{1}H$, 300 MHz; $^{13}C$, 75 MHz) at the UCM's NMR facilities. Chemical shifts ($\delta$) are expressed in parts per million relative to internal tetramethylsilane; coupling constants (*J*) are in hertz (Hz). The following abbreviations are used to describe peak patterns when appropriate: app (apparent), s (singlet), d (doublet), t (triplet), q (quartet), qt (quintet), m (multiplet), br (broad), dd (doublet of doublets), ddd (doublet of doublets of doublets), tt (triplet of triplets). 2D NMR experiments (HMQC and HMBC) of representative compounds were carried out to assign protons and carbons of the new structures. Elemental analyses (C, H, N) were obtained on a LECO CHNS-932 apparatus at the UCM's analysis services and were within 0.4% of the theoretical values. High Performance Liquid Chromatography-Mass Spectrometry (HPLC-MS) analysis was performed using an Agilent 1200LC-MSD VL. LC separation was achieved with an Eclipse XDB-C18 column (5 $\mu$m, 4.6 mm x 150 mm) together with a guard column (5 $\mu$m, 4.6 mm x 12.5 mm). The gradient mobile phases consisted of A (95:5 water/MeOH) and B (5:95 water/MeOH) with 0.1% ammonium hydroxide and 0.1% formic acid as the solvent

modifiers. MS analysis was performed with an ESI source. The capillary voltage was set to 3.0 kV and the fragmentor voltage was set at 70 eV. The drying gas temperature was 350 ºC, the drying gas flow was 10 L/min, and the nebulizer pressure was 20 psi. Spectra were acquired in positive or negative ionization mode from 100 to 1000 m/z and in UV-mode at four different wavelengths (210, 230, 254, and 280 nm). High resolution mass spectrometry (HRMS) was carried out on a FTMS Bruker APEX Q IV (UCM) spectrometer in electrospray ionization (ESI) mode at UCM's spectrometry facilities. Spectroscopic data of all described compounds were consistent with the proposed structures. Satisfactory HPLC chromatograms and elemental analyses (C, H, N) were obtained for the final compounds, confirming a purity of at least 95% for all tested compounds.

#### 4.1.1. Synthesis of asymmetric diamides 1, 2, 4-15 and 28-30

**Synthesis of *tert*-butyl 4-[(dimethylamino)carbonyl]phenylcarbamate (35).**[30] To a solution of 4-(Boc-amino)benzoic acid (261 mg, 1.1 mmol), dimethylamine hydrochloride (269 mg, 3.3 mmol) and TBTU (459 mg, 1.4 mmol) in DMF (1.3 mL) was added, under argon atmosphere, triethylamine (0.92 mL, 6.6 mmol) and the reaction mixture was stirred for 2 h at rt. Then, the reaction crude was washed with $H_2O$ (10 mL) and extracted with EtOAc (3 x 10 mL). The organic phase was dried over $Na_2SO_4$ and the solvent was evaporated under reduced pressure to obtain the title compound as an oil in 75% yield. Chromatography: hexane/EtOAc, 3:7; oil. $R_f$ (EtOAc) 0.56. IR (ATR) ν 3256 (NH), 1725, 1612 (CO), 1535, 1494, 1454 (Ar). $^1$H NMR (300 MHz, $CD_3OD$) δ Mixture of rotamers A:B 1:1; 1.52 (s, 9H, $3CH_3C$), 3.05, 3.07 (2br s, 6H, $2CH_3N$, rotamers A and B), 7.35 (d, $J$ = 8.7 Hz, 2H, $H_3$, $H_5$), 7.49 (d, $J$ = 8.6 Hz, 2H, $H_2$, $H_6$). $^{13}$C NMR (75 MHz, $CD_3OD$) δ 28.6 ($3CH_3$), 35.8, 40.2 ($2CH_3$), 81.2 (C), 119.0 (2CH), 129.1 (2CH), 130.7, 142.6, 154.9, 173.7 (4C). MS (ESI): [$(M+H)^+$] 265.1.

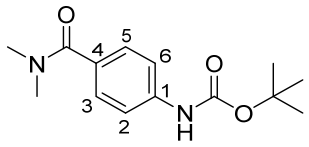


**35**

**Synthesis of 4-amino-*N,N*-dimethylbenzamide (36).** A solution of **35** (216 mg, 0.8 mmol) in TFA/DCM 1:1 (8.7 mL) was stirred 1 h at rt under argon atmosphere. The reaction crude was washed with saturated solutions of $NaHCO_3$ (2 x 10 mL) and NaCl (10 mL); dried over $Na_2SO_4$ and the solvent was evaporated under reduced pressure to obtain the title compound as a white solid in 93% yield. Chromatography: EtOAc. Mp 147-148 ºC (Lit.[31] 151-154 ºC) . $R_f$ (EtOAc) 0.35. IR (ATR) ν 3462, 3344 (NH), 1604 (CO), 1525, 1490, 1444 (Ar). $^1$H NMR (300 MHz, $CD_3OD$) δ 3.06 (s, 6H, $2CH_3N$), 6.69 (d,

*J* = 8.6 Hz, 2H, $H_3$, $H_5$), 7.22 (d, *J* = 8.6 Hz, 2H, $H_2$, $H_6$). MS (ESI): [$(M+H)^+$] 165.1. The spectroscopic data are in agreement with those previously described.[32]

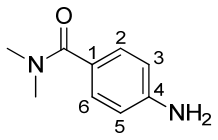

**36**

**General procedure for the synthesis of pyridinylacrylamides 31 and 32.**[33] A solution of the corresponding amine (1 equiv.) and triethylamine (1 equiv.) in anhydrous DCM (9 mL/mmol) was stirred, under argon atmosphere and at -78 ºC, for 10 min. Then was added dropwise the acryloyl chloride (1 equiv.). The mixture was stirred for 3 h, warming it up to 0 ºC, and the solvent was removed under reduced pressure.

***N*-Pyridin-2-ylacrylamide (31).** Obtained following the general procedure for the synthesis of pyridinylacrylamides from acryloyl chloride (0.22 mL, 2.8 mmol) and 2-aminopyridine (260 mg, 2.8 mmol) in 68% yield. Chromatography: EtOAc. Mp 66-68 ºC (Lit.[33] 71 ºC). $R_f$ (hexane/EtOAc, 1:1) 0.44. $^1$H NMR (300 MHz, $CDCl_3$) $\delta$ 5.84 (dd, *J* = 10.2, 1.2 Hz, 1H, 1/2$CH_2$), 6.28 (dd, *J* = 16.9, 10.2 Hz, 1H, CHCO), 6.48 (dd, *J* = 16.9, 1.1 Hz, 1H, 1/2$CH_2$), 7.08 (ddd, *J* = 7.2, 5.0, 0.9 Hz, 1H, $H_5$), 7.75 (td, *J* = 7.9, 1.9 Hz, 1H, $H_4$), 8.23 (br s, 1H, NH), 8.28-8.34 (m, 2H, $H_3$, $H_6$). MS (ESI): [$(M+H)^+$] 149.0. The spectroscopic data are in agreement with those previously described.[33]

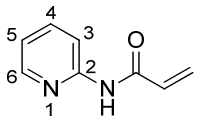

**31**

***N*-Pyridin-3-ylacrylamide (32).** Obtained following the general procedure for the synthesis of pyridinylacrylamides from acryloyl chloride (0.45 mL, 5.5 mmol) and 3-aminopyridine (520 mg, 5.5 mmol) in 57% yield. Chromatography: EtOAc/MeOH, 9:1. Mp 121-123 ºC (Lit.[33] 118-121 ºC). $R_f$ (hexane/EtOAc, 1:1) 0.25. $^1$H NMR (300 MHz, $CDCl_3$) $\delta$ 5.84 (dd, *J* = 10.1, 1.2 Hz, 1H, 1/2$CH_2$), 6.29 (dd, *J* = 16.9, 10.2 Hz, 1H, 1/2$CH_2$), 6.49 (dd, *J* = 16.8, 1.2 Hz, 1H, CHCO), 7.31 (dd, *J* = 8.3, 4.8 Hz, 1H, $H_5$), 7.59 (br s, 1H, NH), 8.28 (d, *J* = 9.4 Hz, 1H, $H_4$), 8.38 (dd, *J* = 4.7, 1.3 Hz, 1H, $H_6$), 8.61 (d, *J* = 2.5 Hz, 1H, $H_2$). MS (ESI): [$(M+H)^+$] 148.9. The spectroscopic data are in agreement with those previously described.[33]

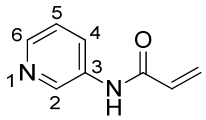

**32**

**General procedure for the synthesis of phenylacrylamides 33, 37-47 and 62-63.** To a solution of the corresponding aniline (1 equiv) in anhidrous DCM (2 mL/mmol) was added, under argon atmosphere and at 0 ºC, acryloyl chloride (1.1 equiv) and pyridine (1.1 equiv), consecutively. Then, the reaction mixture was stirred 2 h at rt. In the case of *N*-[4-(acetylamino)phenyl]acrylamide (**43**), triethylamine was used as the base, THF with the minimum volume required of DMF as the solvent, and the reaction was stirred overnight at rt. For the synthesis of *N*-phenylethylensulfonamide (**63**), 2-chloroethanesulfanoyl chloride was added instead of acryloyl chloride, anhydrous acetone was used as the solvent, and the reaction was stirred overnight at 0 ºC. In all cases, the reaction crude was washed with saturated solutions of $NaHCO_3$, $CuSO_4$ (when pyridine was used) and NaCl; dried over $Na_2SO_4$, and the solvent was evaporated under reduced pressure to afford title compounds as white solids. In some cases, the solid was purified by column chromatography (hexane/EtOAc).

***N*-Phenylacrylamide (33).** Obtained following the general procedure for the synthesis of phenylacrylamides from aniline (0.98 mL, 10.7 mmol) and acryloyl chloride (0.95 mL, 11.8 mmol) in 84% yield. Chromatography: hexane/EtOAc, 7:3. Mp 107-108 ºC (Lit.[34] 105-106 ºC). $R_f$ (hexane/EtOAc, 7:3) 0.39. $^1$H NMR (300 MHz, $CDCl_3$) $\delta$ 5.71 (dd, $J$ = 9.6, 2.0 Hz, 1H, 1/2$CH_2$), 6.31 (dd, $J$ = 16.9, 9.7 Hz, 1H, CHCO), 6.42 (dd, $J$ = 16.9, 1.9 Hz, 1H, 1/2$CH_2$), 7.10 (t, $J$ = 7.4 Hz, 1H, $H_4$), 7.30 (t, $J$ = 7.9 Hz, 2H, $H_3$, $H_5$), 7.60 (d, $J$ = 7.9 Hz, 2H, $H_2$, $H_6$), 8.16 (br s, 1H, NH). MS (ESI): [$(M+H)^+$] 147.9. The spectroscopic data are in agreement with those previously described.[35]

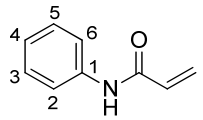

**33**

***N*-(2-Fluorophenyl)acrylamide (37)**.[36] Obtained following the general procedure for the synthesis of phenylacrylamides from 2-fluoroaniline (0.5 mL, 5.2 mmol) and acryloyl chloride (0.46 mL, 5.8 mmol) in 87% yield. Mp 102-103 ºC. $R_f$ (hexane/EtOAc, 7:3) 0.53. IR (ATR) $\nu$ 3276, 3209 (NH), 1669 (CO), 1616, 1547, 1490 (Ar). $^1$H NMR (300 MHz, $CDCl_3$) $\delta$ 5.80 (dd, $J$ = 10.0, 1.4 Hz, 1H, 1/2$CH_2$), 6.30 (dd, $J$ = 16.9, 10.1 Hz, 1H, CHCO), 6.45 (dd, $J$ = 16.9, 1.4 Hz, 1H, 1/2$CH_2$), 7.02-7.17 (m, 3H, $H_3$, $H_4$, $H_6$), 7.54 (br s, 1H, NH), 8.40 (t, $J$ = 7.6 Hz, 1H, $H_5$). $^{13}$C NMR (75 MHz, $CDCl_3$) $\delta$ 114.9

(d, *J* = 19.2 Hz, CH), 122.0 (CH), 124.7 (d, *J* = 13.5 Hz, CH), 124.8 (d, *J* = 8.8 Hz, CH), 126.4 (d, *J* = 10.0 Hz, C), 128.5 ($CH_2$), 131.0 (CH), 152.6 (d, *J* = 244.7 Hz, C), 163.6 (C). $^{19}F$ NMR (282 MHz, $CDCl_3$) δ -131.9. MS (ESI): [$(M+H)^+$] 166.1.

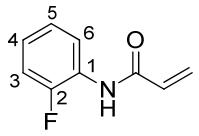


**37**

***N*-(3-Fluorophenyl)acrylamide (38).** Obtained following the general procedure for the synthesis of phenylacrylamides from 3-fluoroaniline (0.5 mL, 5.2 mmol) and acryloyl chloride (0.46 mL, 5.8 mmol) in 70% yield. Mp 119-120 ºC (Lit.[36] 125-126 ºC). $R_f$ (hexane/EtOAc, 7:3) 0.51. $^1H$ NMR (300 MHz, $CDCl_3$) δ 5.79 (dd, *J* = 10.1, 1.3 Hz, 1H, 1/2$CH_2$), 6.27 (dd, *J* = 16.9, 10.1 Hz, 1H, CHCO), 6.45 (dd, *J* = 16.8, 1.3 Hz, 1H, 1/2$CH_2$), 6.79-6.86 (m, 1H, $H_4$), 7.20-7.30 (m, 2H, $H_5$, $H_6$), 7.56 (d, *J* = 10.9 Hz, 1H, $H_2$), 7.70 (br s, 1H, NH). MS (ESI): [$(M+H)^+$] 166.1. The spectroscopic data are in agreement with those previously described.[36]

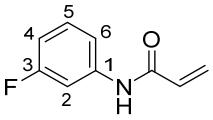


**38**

***N*-(4-Fluorophenyl)acrylamide (39).** Obtained following the general procedure for the synthesis of phenylacrylamides from 4-fluoroaniline (0.22 mL, 2 mmol) and acryloyl chloride (0.18 mL, 2.2 mmol) in 35% yield. Mp 152-153 ºC. $R_f$ (hexane/EtOAc, 7:3) 0.41. $^1H$ NMR (300 MHz, $CDCl_3$) δ 5.80 (dd, *J* = 10.2, 1.3 Hz, 1H, 1/2$CH_2$), 6.24 (dd, *J* = 16.8, 10.2 Hz, 1H, CHCO), 6.46 (dd, *J* = 16.8, 1.3 Hz, 1H, 1/2$CH_2$), 7.05 (t, *J* = 8.7 Hz, 2H, $H_3$, $H_5$), 7.24 (br s, 1H, NH), 7.53-7.58 (m, 2H, $H_2$, $H_6$). MS (ESI): [$(M+H)^+$] 166.0. The spectroscopic data are in agreement with those previously described.[37]

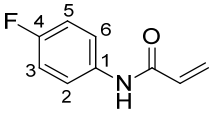


**39**

***N*-[2-(Trifluoromethyl)phenyl]acrylamide (40).** Obtained following the general procedure for the synthesis of phenylacrylamides from 2-(trifluoromethyl)aniline (0.5 mL, 3.9 mmol) and acryloyl

chloride (0.35 mL, 4.3 mmol) in 62% yield. Chromatography: hexane/EtOAc, 7:3. Mp 115-116 ºC. $R_f$ (hexane/EtOAc, 7:3) 0.39. IR (ATR) ν 3275 (NH), 1664 (CO), 1634, 1613, 1591, 1534 (Ar). $^1$H NMR (300 MHz, $CDCl_3$) δ 5.82 (dd, *J* = 10.1, 1.2 Hz, 1H, 1/2$CH_2$), 6.29 (dd, *J* = 16.9, 10.0 Hz, 1H, CHCO), 6.44 (dd, *J* = 16.9 Hz, 1.2 Hz, 1H, 1/2$CH_2$), 7.25 (t, *J* = 7.7 Hz, 1H, $H_3$), 7.56 (t, *J* = 7.8 Hz, 1H, $H_4$), 7.61 (d, *J* = 7.9 Hz, 1H, $H_5$), 7.67 (br s, 1H, NH), 8.24 (d, *J* = 7.9 Hz, 1H, $H_6$). $^{13}$C NMR (75 MHz, $CDCl_3$) δ 120.3 (q, *J* = 28.9 Hz, C), 124.2 (q, *J* = 273.2 Hz, C), 124.5, 124.8 (2CH), 126.2 (q, *J* = 5.4 Hz, CH), 128.6 ($CH_2$), 131.1, 133.1 (2CH), 135.2, 163.7 (2C). $^{19}$F NMR (282 MHz, $CDCl_3$) δ -60.8. MS (ESI): [$(M+H)^+$] 216.0.

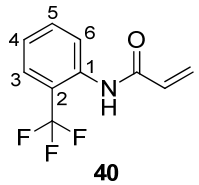


**40**

***N*-[3-(Trifluoromethyl)phenyl]acrylamide (41).**[37] Obtained following the general procedure for the synthesis of phenylacrylamides from 3-(trifluoromethyl)aniline (0.5 mL, 4 mmol) and acryloyl chloride (0.35 mL, 4.4 mmol) in 84% yield. Chromatography: hexane/EtOAc, 7:3. Mp 85-86 ºC. $R_f$ (hexane/EtOAc, 7:3) 0.38. IR (ATR) ν 3285 (NH), 1671 (CO), 1608, 1557, 1492, 1447 (Ar). $^1$H NMR (300 MHz, $CDCl_3$) δ 5.82 (dd, *J* = 10.2, 1.2 Hz, 1H, 1/2$CH_2$), 6.26 (dd, *J* = 16.8, 10.2 Hz, 1H, CHCO), 6.48 (dd, *J* = 16.8 Hz, 1.2 Hz, 1H, 1/2$CH_2$), 7.38 (d, *J* = 7.8 Hz, 1H, $H_4$), 7.45 (t, *J* = 7.9 Hz, 1H, $H_5$), 7.51 (br s, 1H, NH), 7.79 (d, *J* = 8.1 Hz, 1H, $H_6$), 7.88 (s, 1H, $H_2$). $^{13}$C NMR (75 MHz, $CDCl_3$) δ 116.9, 121.2, 123.3 (3CH), 123.9 (q, *J* = 272.5 Hz, C), 128.9 ($CH_2$), 129.7, 130.8 (2CH), 131.5 (q, *J* = 32.6 Hz, C), 138.3, 164.0 (2C). $^{19}$F NMR (282 MHz, $CDCl_3$) δ -63.1. MS (ESI): [$(M+H)^+$] 215.9.

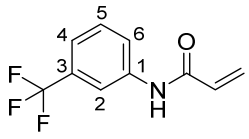


**41**

***N*-[4-(Trifluoromethyl)phenyl]acrylamide (42).** Obtained following the general procedure for the synthesis of phenylacrylamides from 4-(trifluoromethyl)aniline (0.3 mL, 2.4 mmol) and acryloyl chloride (0.21 mL, 2.6 mmol) in 64% yield. Chromatography: hexane/EtOAc, 7:3. Mp 171-172 ºC. $R_f$ (hexane/EtOAc, 7:3) 0.33. $^1$H NMR (300 MHz, $CDCl_3$) δ 5.84 (dd, *J* = 10.2, 1.2 Hz, 1H, 1/2$CH_2$), 6.25 (dd, *J* = 16.8, 10.2 Hz, 1H, CHCO), 6.48 (dd, *J* = 16.8, 1.1 Hz, 1H, 1/2$CH_2$), 7.35 (br s, 1H, NH), 7.60

(d, *J* = 8.7 Hz, 2H, $H_3$, $H_5$), 7.72 (d, *J* = 8.7 Hz, 2H, $H_2$, $H_6$). MS (ESI): [$(M+H)^+$] 216.1. The spectroscopic data are in agreement with those previously described.[37]

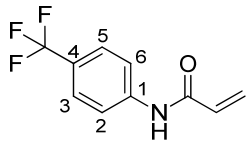

**42**

***N*-[4-(Acetylamino)phenyl]acrylamide (43).**[38] Obtained following the general procedure for the synthesis of phenylacrylamides from 4-(acetylamino)aniline (1 g, 6.7 mmol) and acryloyl chloride (0.94 mL, 11.7 mmol) in 41% yield. $R_f$ (hexane/EtOAc, 1:1) 0.18. Mp >220 ºC (decomposed). IR (ATR) ν 3277 (NH), 1665 (CO), 1616, 1583, 1517 (Ar). $^1$H NMR (300 MHz, $CDCl_3$) δ 2.02 (s, 3H, $CH_3$), 5.73 (dd, *J* = 10.0, 2.2 Hz, 1H, 1/2$CH_2$), 6.23 (dd, *J* = 17.0, 2.2 Hz, 1H, 1/2$CH_2$), 6.42 (dd, *J* = 17.0, 10.0 Hz, 1H, CHCO), 7.51 (d, *J* = 9.0 Hz, 2H, $H_2$, $H_6$ / $H_3$, $H_5$), 7.58 (d, *J* = 9.0 Hz, 2H, $H_2$, $H_6$ / $H_3$, $H_5$), 9.90 (br s, 1H, NH), 10.08 (br s, 1H, NH). $^{13}$C NMR (75 MHz, $CDCl_3$) δ 23.9 ($CH_3$), 119.3 (2CH), 119.7 (2CH), 126.5 ($CH_2$), 131.9 (CH), 134.2, 135.1, 162.8, 168.0 (4C). MS (ESI): [$(M)^+$] 204.8.

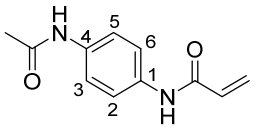

**43**

***N*-(4-Cyanophenyl)acrylamide (44).** Obtained following the general procedure for the synthesis of phenylacrylamides from 4-aminobenzonitrile (550 mg, 4.6 mmol) and acryloyl chloride (0.41 mL, 5 mmol) in 68% yield. Chromatography: hexane/EtOAc, 7:3. Mp 197-199 ºC. $R_f$ (hexane/EtOAc, 7:3) 0.18. $^1$H NMR (300 MHz, $CDCl_3$) δ 5.87 (dd, *J* = 10.2, 1.0 Hz, 1H, 1/2$CH_2$), 6.26 (dd, *J* = 16.8, 10.2 Hz, 1H, CHCO), 6.50 (dd, *J* = 16.8, 1.0 Hz, 1H, 1/2$CH_2$), 7.44 (br s, 1H, NH), 7.63 (d, *J* = 8.8 Hz, 2H, $H_3$, $H_5$), 7.73 (d, *J* = 8.8 Hz, 2H, $H_2$, $H_6$). MS (ESI): [$(M+H)^+$] 173.0**.** The spectroscopic data are in agreement with those previously described.[39]

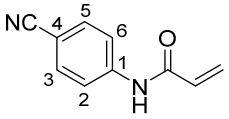

**44**

***N*-(4-Methoxyphenyl)acrylamide (45).** Obtained following the general procedure for the synthesis of phenylacrylamides from 4-methoxyaniline (680 mg, 5.5 mmol) and acryloyl chloride (0.49 mL, 6 mmol) in 72% yield. Chromatography: hexane/EtOAc, 7:3. Mp 98-99 ºC (Lit.[33] 97-98 ºC). $R_f$ (hexane/EtOAc, 6:4) 0.27. $^1$H NMR (300 MHz, $CDCl_3$) $\delta$ 3.78 (s, 3H, $CH_3$), 5.71 (dd, *J* = 10.0, 1.4 Hz, 1H, 1/2$CH_2$), 6.24 (dd, *J* = 16.8, 10.0 Hz, 1H, CHCO), 6.40 (dd, *J* = 16.8, 1.4 Hz, 1H, 1/2$CH_2$), 6.85 (d, *J* = 9.0 Hz, 2H, $H_3$, $H_5$), 7.48 (d, *J* = 8.9 Hz, 2H, $H_2$, $H_6$), 7.63 (br s, 1H, NH). MS (ESI): [(M+H)$^+$] 178.1. The spectroscopic data are in agreement with those previously described.[35]

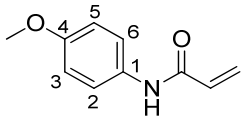

**45**

**4-(Acryloylamino)-*N*,*N*-dimethylbenzamide (46).** Obtained following the general procedure for the synthesis of phenylacrylamides from **36** (69 mg, 0.4 mmol) and acryloyl chloride (0.04 mL, 0.5 mmol) in 72% yield. Chromatography: hexane/EtOAc, 4:6. Mp 149-151 ºC. $R_f$ (hexane/EtOAc, 6:4) 0.23. IR (ATR) $\nu$ 3265 (NH), 1688 (CO), 1608, 1532, 1492 (Ar). $^1$H NMR (300 MHz, $CDCl_3$) $\delta$ 2.99 (s, 3H, $CH_3$), 3.10 (s, 3H, $CH_3$), 5.74 (dd, *J* = 9.8, 1.8 Hz, 1H, 1/2$CH_2$), 6.32 (dd, *J* = 16.9, 9.8 Hz, 1H, CHCO), 6.44 (dd, *J* = 16.9, 1.8 Hz, 1H, 1/2$CH_2$), 7.29 (d, *J* = 8.5 Hz, 2H, $H_3$, $H_5$), 7.52 (d, *J* = 8.5 Hz, 2H, $H_2$, $H_6$), 8.45 (br s, 1H, NH). $^{13}$C NMR (75 MHz, $CDCl_3$) $\delta$ 35.7, 39.9 (2$CH_3$), 120.0 (2CH), 128.1 (2CH+$CH_2$), 131.2 (CH), 131.7, 139.5, 164.1, 171.6 (4C). MS (ESI): [(M+H)$^+$] 219.1.

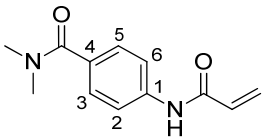

**46**

**Ethyl 4-acrylamidobenzoate (47).[40]** Obtained following the general procedure for the synthesis of phenylacrylamides from ethyl 4-aminobenzoate (550 mg, 3.3 mmol) and acryloyl chloride (0.29 mL, 3.6 mmol) in 86% yield. Chromatography: hexane/EtOAc, 8:2. Mp 119-121 ºC. $R_f$ (hexane/EtOAc, 7:3) 0.31. IR (ATR) $\nu$ 3312 (NH), 1716, 1674 (CO), 1603, 1541, 1474 (Ar). $^1$H NMR (300 MHz, $CDCl_3$) $\delta$ 1.38 (t, *J* = 7.1 Hz, 3H, $CH_3$), 4.35 (q, *J* = 7.1 Hz, 2H, $CH_2O$), 5.79 (dd, *J* = 10.0, 1.4 Hz, 1H, 1/2$CH_2$), 6.31 (dd, *J* = 16.8, 10.0 Hz, 1H, CHCO), 6.46 (dd, *J* = 16.8, 1.4 Hz, 1H, 1/2$CH_2$), 7.69 (d, *J* = 8.8 Hz, 2H, $H_2$, $H_6$), 8.00 (d, *J* = 8.8 Hz, 2H, $H_3$, $H_5$), 8.07 (br s, 1H, NH). $^{13}$C NMR (75

MHz, $CDCl_3$) δ 14.5 ($CH_3$), 61.1 ($CH_2$), 119.2 (2CH), 126.2 (C), 128.8 ($CH_2$), 130.9 (2CH), 131.0 (CH), 142.1, 164.0, 166.4 (3C). MS (ESI): [$(M+H)^+$] 220.0.

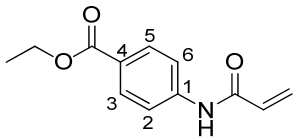

**47**

***N*-Methyl-*N*-phenylacrylamide (62).** Obtained following the general procedure for the synthesis of phenylacrylamides from methylaniline (0.5 mL, 4.5 mmol) and acryloyl chloride (0.4 mL, 5 mmol) in quantitative yield. Mp 75-76 ºC (Lit.[41] 74-76 ºC). $R_f$ (hexane/EtOAc, 7:3) 0.26. $^1$H NMR (300 MHz, $CDCl_3$) δ 3.37 (s, 3H, $CH_3N$), 5.52 (dd, *J* = 10.3, 2.0 Hz, 1H, 1/2$CH_2$), 6.08 (dd, *J* = 16.8, 10.4 Hz, 1H, CHCO), 6.37 (dd, *J* = 16.8, 2.0 Hz, 1H, 1/2$CH_2$), 7.19 (d, *J* = 7.1 Hz, 2H, $H_2$, $H_6$), 7.34 (t, *J* = 7.3 Hz, 1H, $H_4$), 7.42 (t, *J* = 7.4 Hz, 2H, $H_3$, $H_5$). MS (ESI): [$(M+H)^+$] 162.1. The spectroscopic data are in agreement with those previously described.[41]

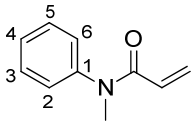

**62**

***N*-Phenylethylensulfonamide (63).** Obtained following the general procedure for the synthesis of phenylacrylamides from aniline (0.24 mL, 2.7 mmol) and 2-chloroethanesulfanoyl chloride (0.31 mL, 3 mmol) in 30% yield. Chromatography: hexane/ EtOAc, 6:4. Mp 67-68 ºC. $R_f$ (hexane/EtOAc, 7:3) 0.29. IR (ATR) ν 3262 (NH), 1599, 1495 (Ar), 1338, 1147 ($SO_2$). $^1$H NMR (300 MHz, $CDCl_3$) δ 5.94 (d, *J* = 10.0 Hz, 1H, ½$CH_2$), 6.09 (d, *J* = 16.5 Hz, 1H, ½$CH_2$), 6.66 (dd, *J* = 16.5, 10.0 Hz, 1H, CHCO), 7.06 (tt, *J* = 6.9, 1.8 Hz, 1H, $H_4$), 7.21-7.32 (m, 4H, $H_2$, $H_3$, $H_5$, $H_6$), 8.69 (br s, 1H, NH). The spectroscopic data are in agreement with those previously described.[42]

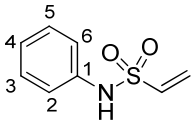

**63**

**Synthesis of $N^1$-phenyl-$N^3$-octyl-β-alaninamide (34).** To a solution of acrylamide **33** (230 mg, 1.6 mmol) and octylamine (0.78 mL, 4.7 mmol) in anhidrous acetonitrile (0.8 mL) was added DBU (0.71 mL, 4.7 mmol) and the reaction mixture was stirred 5 h at 60 ºC. Then, the solvent was removed under reduced pressure to give the secondary amine in 79% yield. Chromatography: EtOAc/MeOH, 9:1; oil. $R_f$ (EtOAc) 0.12. IR (ATR) ν 3297 (NH), 1667 (CO), 1601, 1551, 1497, 1444 (Ar). $^1$H NMR (300 MHz, $CDCl_3$) δ 0.86-0.88 (m, 3H, $CH_3$), 1.29 (m, 10H, $(C\underline{H}_2)_5CH_3$), 1.54-1.58 (m, 2H, $C\underline{H}_2(CH_2)_5CH_3$), 2.48 (t, $J$ = 5.2 Hz, 2H, $CH_2CO$), 2.69 (t, $J$ = 6.8 Hz, 2H, $(CH_2)_6C\underline{H}_2N$), 2.97 (t, $J$ = 5.4 Hz, 2H, $NC\underline{H}_2CH_2CO$), 3.48 (br s, 1H, NH), 7.06 (t, $J$ = 7.3 Hz, 1H, $H_4$), 7.29 (t, $J$ = 7.7 Hz, 2H, $H_3$, $H_5$), 7.53 (d, $J$ = 7.8 Hz, 2H, $H_2$, $H_6$). $^{13}$C NMR (75 MHz, $CDCl_3$) δ 14.1 ($CH_3$), 22.7, 27.5, 29.3, 29.5, 30.1, 31.8, 36.1, 45.5, 49.3 ($9CH_2$), 119.7 (2CH), 123.6 (CH), 128.9 (2CH), 138.8, 171.1 (2C). MS (ESI): [$(M+H)^+$] 277.2.

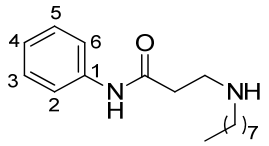


**34**

**General procedure for the synthesis of asymmetric diamides 1, 2, 4-15 and 28-30.** To a solution of the corresponding acrylamide, sulfonamide, or 2-(chloromethyl)-5-phenyl-1,3,4-oxadiazole (1.5 equiv) and secondary amine **34** (1 equiv) in anhidrous acetonitrile (0.5 mL/mmol), was added DBU (1.5 equiv), and the reaction mixture was stirred 24 h at 60 ºC. Then, the solvent was removed under reduced pressure and the residue was purified by column chromatography to give the title compounds. For the synthesis of $N^3$-octyl-$N^1$-phenyl-$N^3$-[(5-phenyl-1,3,4-oxadiazol-2-yl)methyl]-β-alaninamide (**30**) triethylamine was used as a base.

***$N^3$*-(3-Anilino-3-oxopropyl)-*$N^3$*-octyl-*$N^1$*-pyridin-2-yl-β-alaninamide (1).** Obtained following the general procedure for the synthesis of asymmetric diamides from amine **34** (75 mg, 0.3 mmol) and acrylamide **31** (60 mg, 0.4 mmol) in 45% yield. Chromatography: EtOAc; oil. $R_f$ (EtOAc/MeOH, 98:2) 0.28. IR (ATR) ν 3274 (NH), 1665, 1540 (CO), 1600, 1436 (Ar). $^1$H NMR (300 MHz, $CDCl_3$) δ 0.83 (t, $J$ = 6.9 Hz, 3H, $CH_3$), 1.04-1.34 (m, 10H, $(C\underline{H}_2)_5CH_3$), 1.51 (m, 2H, $C\underline{H}_2(CH_2)_5CH_3$), 2.51-2.60 (m, 6H, $(CH_2)_6C\underline{H}_2N$ , $2CH_2CO$), 2.90 (t, $J$ = 6.0 Hz, 4H, $2NC\underline{H}_2CH_2CO$), 6.98-7.01 (m, 2H, $H_5$, $H_{4'}$), 7.20 (t, $J$ = 7.8 Hz, 2H, $H_{3'}$, $H_{5'}$), 7.47 (d, $J$ = 7.8 Hz, 2H, $H_{2'}$, $H_{6'}$), 7.66 (t, $J$ = 7.9 Hz, 1H, $H_4$), 8.17-8.22 (m, 2H, $H_3$, $H_6$), 9.89 (br s, 1H, NH), 10.55 (br s, 1H, NH). $^{13}$C NMR (75 MHz, $CDCl_3$) δ 14.1 ($CH_3$), 22.6, 26.7, 27.5, 29.2, 29.5, 31.7, 34.1, 36.3, 50.0, 51.0, 54.1 ($11CH_2$), 114.5, 119.7 (2CH), 120.0 (2CH), 123.9

(CH), 128.8 (2CH), 138.5 (C), 138.6, 147.5 (2CH), 151.6, 170.9, 171.0 (3C). HRMS (ESI): [(M)$^+$] calcd. for $C_{25}H_{36}N_4O_2$, 424.2833; found, 424.2832.

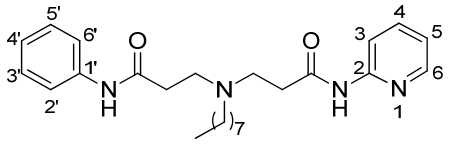

**1**

***N*$^3$-(3-Anilino-3-oxopropyl)-*N*$^3$-octyl-*N*$^1$-pyridin-3-yl-β-alaninamide (2).** Obtained following the general procedure for the synthesis of asymmetric diamides from amine **34** (100 mg, 0.4 mmol) and acrylamide **32** (80 mg, 0.5 mmol) in 37% yield. Chromatography: EtOAc/MeOH, 9:1; oil. $R_f$ (EtOAc/MeOH, 9:1) 0.28. IR (ATR) ν 3265 (NH), 1664, 1546 (CO), 1600, 1489, 1444 (Ar). $^1$H NMR (300 MHz, $CDCl_3$) δ 0.84 (t, *J* = 6.8 Hz, 3H, $CH_3$), 1.07-1.34 (m, 10H, $(C\underline{H}_2)_5CH_3$), 1.51 (m, 2H, $C\underline{H}_2(CH_2)_5CH_3$), 2.50-2.59 (m, 6H, $(CH_2)_6C\underline{H}_2N$, $2CH_2CO$), 2.82 (t, *J* = 6.4 Hz, 2H, $NC\underline{H}_2CH_2CO$), 2.84 (d, *J* = 6.4 Hz, 2H, $NC\underline{H}_2CH_2CO$), 6.99 (t, *J* = 7.4 Hz, 1H, $H_{4'}$), 7.10 (dd, *J* = 8.3, 4.8 Hz, 1H, $H_5$), 7.15 (t, *J* = 7.8 Hz, 2H, $H_{3'}$, $H_{5'}$), 7.41 (d, *J* = 7.8 Hz, 2H, $H_{2'}$, $H_{6'}$), 7.99 (d, *J* = 8.5 Hz, 1H, $H_4$), 8.21 (d, *J* = 5.8 Hz, 1H, $H_6$), 8.54 (d, *J* = 2.4 Hz, 1H, $H_2$), 9.52 (br s, 1H, NH), 9.98 (br s, 1H, NH). $^{13}$C NMR (75 MHz, $CDCl_3$) δ 14.1 ($CH_3$), 22.6, 26.7, 27.7, 29.3, 29.5, 31.8 ($6CH_2$), 34.3 ($2CH_2$), 49.6, 49.8, 53.7 ($3CH_2$), 119.9 (2CH), 123.7, 124.1, 127.1 (3CH), 128.8 (2CH), 135.4, 138.0 (2C), 140.9, 144.4 (2CH), 170.6, 171.4 (2C). HRMS (ESI): [(M)$^+$] calcd. for $C_{25}H_{36}N_4O_2$, 424.2833; found, 424.2831.

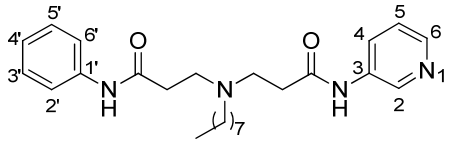

**2**

***N*$^3$-{3-[(2-Fluorophenyl)amino]-3-oxopropyl}-*N*$^3$-octyl-*N*$^1$-phenyl-β-alaninamide (4).** Obtained following the general procedure for the synthesis of asymmetric diamides from amine **34** (60 mg, 0.2 mmol) and acrylamide **37** (54 mg, 0.2 mmol) in 85% yield. Chromatography: EtOAc/MeOH, 95:5; oil. $R_f$ (EtOAc/hexane, 7:3) 0.38. IR (ATR) ν 3287 (NH), 1663 (CO), 1600, 1543, 1497, 1449 (Ar). $^1$H NMR (300 MHz, $CDCl_3$) δ 0.84 (t, *J* = 6.8 Hz, 3H, $CH_3$), 1.19-1.25 (m, 10H, $(C\underline{H}_2)_5CH_3$), 1.53 (m, 2H, $C\underline{H}_2(CH_2)_5CH_3$), 2.52-2.59 (m, 6H, $2CH_2CO$, $(CH_2)_6C\underline{H}_2N$), 2.83-2.92 (m, 4H, $2NC\underline{H}_2CH_2CO$), 6.95-7.07 (m, 4H, $H_3$, $H_4$, $H_6$, $H_{4'}$), 7.18 (t, *J* = 7.8 Hz, 2H, $H_{3'}$, $H_{5'}$), 7.43 (d, *J* = 7.7 Hz, 2H, $H_{2'}$, $H_{6'}$), 8.25 (t, *J* = 7.9 Hz, 1H, $H_5$), 8.80 (br s, 1H, NH), 9.61 (br s, 1H, NH). $^{13}$C NMR

(75 MHz, $CDCl_3$) δ 14.2 ($CH_3$), 22.7, 26.5, 27.7, 29.4, 29.6, 31.9, 34.3, 34.7, 49.7, 49.8, 53.7 (11$CH_2$), 114.9 (d, *J* = 19.3 Hz, CH), 119.8 (2CH), 122.1, 124.1 (2CH), 124.3 (d, *J* = 34.5 Hz, CH), 124.4 (d, *J* = 30.5 Hz, CH), 126.6 (d, *J* = 10.4 Hz, C), 128.9 (2CH), 138.1 (C), 152.6 (d, *J* = 243.0 Hz, C), 170.3, 171.7 (2C). $^{19}$F NMR (282 MHz, $CDCl_3$) δ -130.4. HRMS (ESI): [(M+Na)$^+$] calcd. for $C_{26}H_{36}FN_3O_2Na$, 464.26892; found, 464.27185.

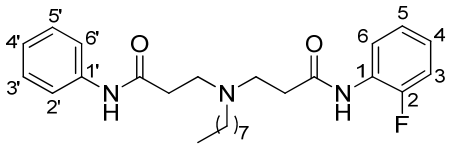

**4**

***N*$^3$-{3-[(3-Fluorophenyl)amino]-3-oxopropyl}-*N*$^3$-octyl-*N*$^1$-phenyl-β-alaninamide (5).** Obtained following the general procedure for the synthesis of asymmetric diamides from amine **34** (80 mg, 0.3 mmol) and acrylamide **38** (72 mg, 0.4 mmol) in 88% yield. Chromatography: EtOAc/MeOH, 8:2; oil. $R_f$ (EtOAc/MeOH, 95:5) 0.50. IR (ATR) ν 1685 (CO), 1604, 1543, 1492, 1443 (Ar). $^1$H NMR (300 MHz, $CDCl_3$) δ 0.83 (t, *J* = 6.8 Hz, 3H, $CH_3$), 1.16-1.27 (m, 10H, (C$\underline{H}_2$)$_5$$CH_3$), 1.49 (m, 2H, C$\underline{H}_2$($CH_2$)$_5$$CH_3$), 2.47-2.51 (m, 6H, 2$CH_2$CO, ($CH_2$)$_6$C$\underline{H}_2$N), 2.77-2.81 (m, 4H, 2NC$\underline{H}_2$$CH_2$CO), 6.65-6.72 (m, 1H, $H_4$), 6.99-7.06 (m, 3H, $H_5$, $H_6$, $H_{4'}$), 7.17 (t, *J* = 7.8 Hz, 2H, $H_{3'}$, $H_{5'}$), 7.41-7.47 (m, 3H, $H_2$, $H_{2'}$, $H_{6'}$), 9.32 (br s, 1H, NH), 9.65 (br s, 1H, NH). $^{13}$C NMR (75 MHz, $CDCl_3$) δ 14.1 ($CH_3$), 22.7, 26.8, 27.7, 29.4, 29.6, 31.9, 34.2, 34.4, 49.6, 49.9, 53.6 (11$CH_2$), 107.3 (d, *J* = 26.2 Hz, CH), 110.6 (d, *J* = 21.3 Hz, CH), 115.2 (d, *J* = 2.6 Hz, CH), 120.1 (2CH), 124.2 (CH), 128.9 (2CH), 129.9 (d, *J* = 9.4 Hz, CH), 138.0 (C), 139.8 (d, *J* = 10.8 Hz, C), 162.9 (d, *J* = 244.1 Hz, C), 170.7, 171.0 (2C). $^{19}$F NMR (282 MHz, $CDCl_3$) δ -112.0. HRMS (ESI): [(M+H)$^+$] calcd. for $C_{26}H_{37}FN_3O_2$, 442.28698; found, 442.28703.

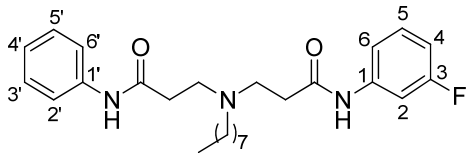

**5**

.

***N*$^3$-{3-[(4-Fluorophenyl)amino]-3-oxopropyl}-*N*$^3$-octyl-*N*$^1$-phenyl-β-alaninamide (6).** Obtained following the general procedure for the synthesis of asymmetric diamides from amine **34** (44.8 mg, 0.3 mmol) and acrylamide **39** (50 mg, 0.2 mmol) in 58% yield. Chromatography: EtOAc/MeOH, 8:2. Mp 79-80 ºC. $R_f$ (EtOAc) 0.32. IR (ATR) ν 3290 (NH), 1659 (CO), 1604, 1550,

1508, 1445 (Ar). $^{1}$H NMR (300 MHz, $CD_3OD$) δ 0.87 (t, *J* = 7.0 Hz, 3H, $CH_3$), 1.08-1.41 (m, 10H, $(C\underline{H}_2)_5CH_3$), 1.51 (m, 2H, $C\underline{H}_2(CH_2)_5CH_3$), 2.52-2.61 (m, 6H, $2CH_2CO$, $(CH_2)_6C\underline{H}_2N$), 2.85-2.90 (m, 4H, $2NC\underline{H}_2CH_2CO$), 6.90 (t, *J* = 8.8 Hz, 2H, $H_{3'}$, $H_{5'}$), 7.07 (t, *J* = 7.4 Hz, 1H, $H_{4'}$), 7.23 (t, *J* = 7.9 Hz, 2H, $H_3$, $H_5$), 7.43-7.50 (m, 4H, $H_2$, $H_6$, $H_{2'}$, $H_{6'}$). $^{13}$C NMR (75 MHz, $CD_3OD$) δ 14.4 ($CH_3$), 23.7, 28.3, 28.8, 30.5, 30.8, 33.0, 35.5, 37.9, 51.0, 51.1, 54.7 ($11CH_2$), 116.1 (d, *J* = 22.4 Hz, 2CH), 121.4 (2CH), 123.1 (d, *J* = 7.8 Hz, 2CH), 125.1 (CH), 129.7 (2CH), 135.8 (d, *J* = 2.8 Hz, C), 139.6 (C), 160.5 (d, *J* = 240.0 Hz, C), 173.2, 173.3 (2C). $^{19}$F NMR (282 MHz, $CD_3OD$) δ -121.2. Elemental analysis: calcd. for $C_{26}H_{36}FN_3O_2$: %C: 70.72, %H: 8.22, %N: 9.52; found, %C: 70.23, %H: 8.23, %N: 9.29.

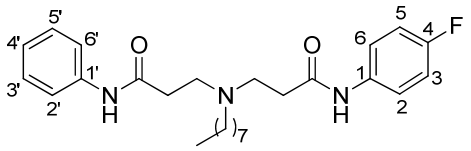


**6**

***N*$^3$-(3-Anilino-3-oxopropyl)-*N*$^3$-octyl-*N*$^1$-[2-(trifluoromethyl)phenyl]-β-alaninamide (7).** Obtained following the general procedure for the synthesis of asymmetric diamides from amine **34** (50 mg, 0.2 mmol) and acrylamide **40** (58 mg, 0.3 mmol) in 89% yield. Chromatography: EtOAc/MeOH, 9:1; oil. $R_f$ (EtOAc) 0.35. IR (ATR) ν 3301 (NH), 1663 (CO), 1600, 1546, 1499, 1456 (Ar). $^{1}$H NMR (300 MHz, $CDCl_3$) δ 0.84 (t, *J* = 6.8 Hz, 3H, $CH_3$), 1.20-1.27 (m, 10H, $(C\underline{H}_2)_5CH_3$), 1.49 (m, 2H, $C\underline{H}_2(CH_2)_5CH_3$), 2.49-2.60 (m, 6H, $2CH_2CO$, $(CH_2)_6C\underline{H}_2N$), 2.87-2.92 (m, 4H, $2NC\underline{H}_2CH_2CO$), 6.99 (t, *J* = 7.4 Hz, 1H, $H_{4'}$), 7.14-7.21 (m, 3H, $H_{3'}$, $H_{5'}$, $H_6$), 7.38-7.47 (m, 3H, $H_5$, $H_{2'}$, $H_{6'}$), 7.55 (d, *J* = 7.8 Hz, 1H, $H_3$), 7.96 (d, *J* = 8.1 Hz, 1H, $H_4$), 8.80 (br s, 1H, NH), 9.02 (br s, 1H, NH). $^{13}$C NMR (75 MHz, $CDCl_3$) δ 14.2 ($CH_3$), 22.7, 26.0, 27.7, 29.3, 29.6, 31.9, 34.1, 34.2, 49.1, 49.7, 53.3 ($11CH_2$), 119.8 (2CH), 121.2 (q, *J* = 28.3 Hz, C), 123.9 (CH), 124.0 (q, *J* = 273.3 Hz, C), 124.8, 125.8 (2CH), 126.1 (q, *J* = 5.5 Hz, CH), 128.9 (2CH), 132.8 (CH), 135.1, 138.2, 170.5, 170.8 (4C). $^{19}$F NMR (282 MHz, $CDCl_3$) δ -60.9. HRMS (ESI): [$(M+H)^+$] calcd. for $C_{27}H_{37}F_3N_3O_2$: 492.28324; found, 492.28235.

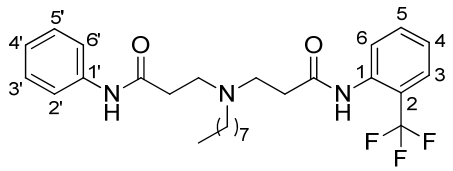


**7**

***N*³-(3-Anilino-3-oxopropyl)-*N*³-octyl-*N*¹-[3-(trifluoromethyl)phenyl]-β-alaninamide (8).** Obtained following the general procedure for the synthesis of asymmetric diamides from amine **34** (50 mg, 0.2 mmol) and acrylamide **41** (26 mg, 0.2 mmol) in 49% yield. Chromatography: EtOAc/MeOH, 9:1; oil. $R_f$ (EtOAc/MeOH, 9:1) 0.50. IR (ATR) ν 3299 (NH), 1661 (CO), 1601, 1554, 1498, 1446 (Ar). $^1$H NMR (300 MHz, $CDCl_3$) δ 0.83 (t, *J* = 6.8 Hz, 3H, $CH_3$), 1.17-1.25 (m, 10H, $(C\underline{H}_2)_5CH_3$), 1.51 (m, 2H, $C\underline{H}_2(CH_2)_5CH_3$), 2.49-2.56 (m, 6H, $2CH_2CO$, $(CH_2)_6C\underline{H}_2N$), 2.78-2.84 (m, 4H, $2NC\underline{H}_2CH_2CO$), 6.99 (t, *J* = 7.4 Hz, 1H, $H_{4'}$), 7.12-7.25 (m, 4H, $H_{3'}$, $H_{5'}$, $H_5$, $H_6$), 7.40 (d, *J* = 7.8 Hz, 2H, $H_{2'}$, $H_{6'}$), 7.52 (d, *J* = 7.3 Hz, 1H, $H_6$), 7.87 (s, 1H, $H_2$), 9.22 (br s, 1H, NH), 9.70 (br s, 1H, NH). $^{13}$C NMR (75 MHz, $CDCl_3$) δ 14.2 ($CH_3$), 22.7, 26.7, 27.7, 29.4, 29.6, 31.9, 34.2, 34.4, 49.6, 49.9, 53.8 ($11CH_2$), 116.5 (d, *J* = 3.9 Hz, CH), 120.0 (2CH), 120.4 (d, *J* = 3.8 Hz, CH), 122.9 (CH), 124.0 (q, *J* = 272.7 Hz, C), 124.3 (CH), 129.0 (2CH), 129.4 (CH), 131.1 (q, *J* = 32.2 Hz, C), 137.9, 138.8, 170.7, 171.1 (4C). $^{19}$F NMR (282 MHz, $CDCl_3$) δ -63.0. HRMS (ESI): [$(M+H)^+$] calcd. for $C_{27}H_{37}F_3N_3O_2$: 492.28324; found, 492.28379.

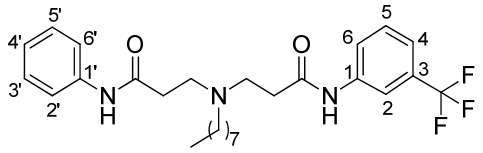


**8**

***N*³-(3-Anilino-3-oxopropyl)-*N*³-octyl-*N*¹-[4-(trifluoromethyl)phenyl]-β-alaninamide (9).** Obtained following the general procedure for the synthesis of asymmetric diamides from amine **34** (94 mg, 0.3 mmol) and acrylamide **42** (110 mg, 0.5 mmol) in quantitative yield. Chromatography: EtOAc/MeOH, 7:3. Mp 77-78 ºC. $R_f$ (EtOAc/MeOH, 8:2) 0.58. IR (ATR) ν 3286 (NH), 1660 (CO), 1603, 1544, 1499, 1444 (Ar). $^1$H NMR (300 MHz, $CDCl_3$) δ 0.84 (t, *J* = 6.8 Hz, 3H, $CH_3$), 1.15-1.28 (m, 10H, $(C\underline{H}_2)_5CH_3$), 1.46-1.51 (m, 2H, $C\underline{H}_2(CH_2)_5CH_3$), 2.50-2.57 (m, 6H, $2CH_2CO$, $(CH_2)_6C\underline{H}_2N$), 2.81-2.89 (m, 4H, $2NC\underline{H}_2CH_2CO$), 7.05 (t, *J* = 7.4 Hz, 1H, $H_{4'}$), 7.20 (t, *J* = 7.8 Hz, 2H, $H_{3'}$, $H_{5'}$), 7.33 (d, *J* = 8.6 Hz, 2H, $H_3$, $H_5$), 7.38 (d, *J* = 8.1 Hz, 2H, $H_{2'}$, $H_{6'}$), 7.50 (d, *J* = 8.6 Hz, 2H, $H_2$, $H_6$), 8.32 (br s, 1H, NH), 9.44 (br s, 1H, NH). $^{13}$C NMR (75 MHz, $CDCl_3$) δ 14.1 ($CH_3$), 22.7, 26.7, 27.8, 29.4, 29.6, 31.8, 34.3, 34.5, 49.6, 50.0, 53.6 ($11CH_2$), 119.5 (2CH), 120.1 (2CH), 124.2 (q, *J* = 271.5 Hz, C), 124.4 (CH), 125.4 (q, *J* = 32.6 Hz, C), 126.0 (q, *J* = 3.9 Hz, 2CH), 128.9 (2CH), 137.9, 141.3, 170.7, 171.3 (4C). $^{19}$F NMR (282 MHz, $CDCl_3$) δ -62.4. Elemental analysis: calcd. for $C_{27}H_{36}F_3N_3O_2$: %C: 65.97, %H: 7.38, %N: 8.55; found, %C: 66.43, %H: 7.36, %N: 8.45.

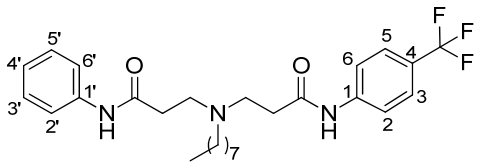

**9**

***N*³-(3-{[4-(Acetylamino)phenyl]amino}-3-oxopropyl)-*N*³-octyl-*N*¹-phenyl-β-alaninamide (10).** Obtained following the general procedure for the synthesis of asymmetric diamides from amine **34** (36 mg, 0.13 mmol) and acrylamide **43** (40 mg, 0.2 mmol) in 32% yield. Chromatography: EtOAc/MeOH, 8:2; oil. $R_f$ (EtOAc/MeOH, 9:1) 0.33. IR (ATR) ν 3291 (NH), 1664 (CO), 1600, 1550, 1515, 1499, 1444 (Ar). $^1$H NMR (300 MHz, $CDCl_3$) δ 0.84 (t, *J* = 6.8 Hz, 3H, $CH_3$), 1.13-1.28 (m, 10H, $(CH_2)_5CH_3$), 1.51 (m, 2H, $CH_2(CH_2)_5CH_3$), 2.12 (s, 3H, $CH_3CO$), 2.52-2.55 (m, 6H, $2CH_2CO$, $(CH_2)_6CH_2N$), 2.82-2.86 (m, 4H, $2NCH_2CH_2CO$), 7.01 (t, *J* = 7.4 Hz, 1H, $H_{4'}$), 7.19 (t, *J* = 7.8 Hz, 2H, $H_{3'}$, $H_{5'}$), 7.26 (d, *J* = 8.9 Hz, 2H, $H_2$, $H_6$/ $H_3$, $H_5$), 7.32 (d, *J* = 8.9 Hz, 2H, $H_2$, $H_6$/ $H_3$, $H_5$), 7.44 (d, *J* = 7.4 Hz, 2H, $H_{2'}$, $H_{6'}$), 7.74 (br s, 1H, NH), 9.32 (br s, 1H, NH), 9.37 (br s, 1H, NH). $^{13}$C NMR (75 MHz, $CDCl_3$) δ 14.2 ($CH_3$), 22.7 ($CH_2$), 24.5 ($CH_3$), 26.6, 27.7, 29.4, 29.6, 31.9, 34.1, 34.4 ($7CH_2$), 49.9 ($2CH_2$), 53.7 ($CH_2$), 120.0 (2CH), 120.7 (2CH), 121.0 (2CH), 124.1 (CH), 129.0 (2CH), 134.1, 134.6, 138.2, 168.8 (4C), 170.6 (2C). HRMS (ESI): [$(M+Na)^+$] calcd. for $C_{28}H_{40}N_4O_3Na$: 503.29981; found, 503.30008.

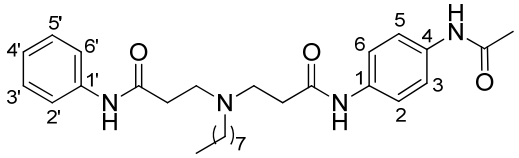

**10**

***N*³-(3-Anilino-3-oxopropyl)-*N*¹-(4-cyanophenyl)-*N*³-octyl-β-alaninamide (11).** Obtained following the general procedure for the synthesis of asymmetric diamides from amine **34** (80 mg, 0.3 mmol) and acrylamide **44** (75 mg, 0.4 mmol) in 59% yield. Chromatography: EtOAc/MeOH, 95:5. Mp 99-100 ºC. $R_f$ (EtOAc) 0.24. IR (ATR) ν 3294 (NH), 2926 (CN), 1664 (CO), 1597, 1531, 1500, 1444 (Ar). $^1$H NMR (300 MHz, $CDCl_3$) δ 83 (t, *J* = 6.9 Hz, 3H, $CH_3$), 1.14-1.25 (m, 10H, $(CH_2)_5CH_3$), 1.48 (m, 2H, $CH_2(CH_2)_5CH_3$), 2.47-2.57 (m, 6H, $2CH_2CO$, $(CH_2)_6CH_2N$), 2.77-2.85 (m, 4H, $2NCH_2CH_2CO$), 7.07 (t, *J* = 7.3 Hz, 1H, $H_{4'}$), 7.20 (t, *J* = 7.8 Hz, 2H, $H_{3'}$, $H_{5'}$), 7.31 (d, *J* = 8.7 Hz, 2H, $H_3$, $H_5$), 7.38 (d, *J* = 7.9 Hz, 2H, $H_{2'}$, $H_{6'}$), 7.52 (d, *J* = 8.6 Hz, 2H, $H_2$, $H_6$), 8.66 (br s, 1H, NH), 9.83 (br s, 1H, NH). $^{13}$C NMR (75 MHz, $CDCl_3$) δ 14.2 ($CH_3$), 22.7, 26.8, 27.8, 29.4, 29.6, 31.9, 34.4, 34.8, 49.4, 50.3, 53.7

(11$CH_2$), 106.2, 119.2 (2C), 119.6 (2CH), 120.2 (2CH), 124.6 (CH), 129.1 (2CH), 133.0 (2CH), 137.7, 142.5, 170.5, 171.5 (4C). HRMS (ESI): [(M+Na)$^+$] calcd. for $C_{27}H_{36}N_4O_2Na$: 471.27359; found, 471.27339.

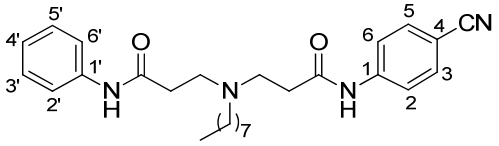

**11**

***N*$^3$-(3-Anilino-3-oxopropyl)-*N*$^1$-(4-methoxyphenyl)-*N*$^3$-octyl-β-alaninamide (12).** Obtained following the general procedure for the synthesis of asymmetric diamides from amine **34** (85 mg, 0.3 mmol) and acrylamide **45** (82 mg, 0.5 mmol) in 59% yield. Chromatography: EtOAc/MeOH, 95:5; oil. *R*$_f$ (EtOAc/MeOH) 0.26. IR (ATR) ν 3279 (NH), 1658 (CO), 1601, 1544, 1510, 1464, 1443 (Ar). $^1$H NMR (300 MHz, $CDCl_3$) δ 0.82 (t, *J* = 6.8 Hz, 3H, $CH_3$), 1.16-1.26 (m, 10H, (C$\underline{H}_2$)$_5$$CH_3$), 1.48 (m, 2H, C$\underline{H}_2$($CH_2$)$_5$$CH_3$), 2.45-2.50 (m, 6H, 2$CH_2$CO, ($CH_2$)$_6$C$\underline{H}_2$N), 2.78 (t, *J* = 6.0 Hz, 4H, 2NC$\underline{H}_2$$CH_2$CO), 3.71 (s, 3H, $CH_3$O), 6.67 (d, *J* = 9.0 Hz, 2H, $H_3$, $H_5$), 7.00 (t, *J* = 7.4 Hz, 1H, $H_{4'}$), 7.16 (t, *J* = 7.8 Hz, 2H, $H_{3'}$, $H_{5'}$), 7.32 (d, *J* = 9.0 Hz, 2H, $H_2$, $H_6$), 7.43 (d, *J* = 7.6 Hz, 2H, $H_{2'}$, $H_{6'}$), 9.30 (br s, 1H, NH), 9.45 (br s, 1H, NH). $^{13}$C NMR (75 MHz, $CDCl_3$) δ 14.1 ($CH_3$), 22.7, 26.8, 27.7, 29.4, 29.6, 31.8, 34.1, 34.3 (8$CH_2$), 49.8 (2$CH_2$), 53.6 ($CH_2$), 55.4 ($CH_3$), 114.0 (2CH), 119.9 (2CH), 121.7 (2CH), 123.9 (CH), 128.8 (2CH), 131.4, 138.3, 156.1, 170.5, 170.8 (5C)**.** HRMS (ESI): [(M+H)$^+$] calcd. for $C_{27}H_{39}N_3O_3Na$: 454.30696; found, 454.30446.

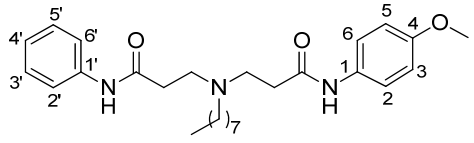

**12**

***N*$^3$-(3-Anilino-3-oxopropyl)-*N*$^3$-octyl-*N*$^1$-[4-(dimethylbenzamide)phenyl]-β-alaninamide (13).** Obtained following the general procedure for the synthesis of asymmetric diamides from amine **34** (42 mg, 0.15 mmol) and acrylamide **46** (33 mg, 0.23 mmol) in 56% yield. Chromatography: EtOAc/MeOH, 9:1; oil. *R*$_f$ (EtOAc/MeOH/$NH_3$, 9:1:0.1) 0.35. IR (ATR) ν 3302 (NH), 1683, 1605 (CO), 1542, 1496, 1446, 1401 (Ar). $^1$H NMR (300 MHz, $CDCl_3$) δ 0.83 (t, *J* = 6.6 Hz, 3H, C$\underline{H}_3$$CH_2$), 1.18-1.24 (m, 10H, (C$\underline{H}_2$)$_5$$CH_3$), 1.51 (m, 2H, C$\underline{H}_2$($CH_2$)$_5$$CH_3$), 2.50-2.53 (m, 6H, 2$CH_2$CO, ($CH_2$)$_6$C$\underline{H}_2$N), 2.83 (t, *J* = 5.3 Hz, 4H, 2NC$\underline{H}_2$$CH_2$CO), 2.94 (s, 3H, $CH_3$N), 3.06 (s, 3H, $CH_3$N), 6.99 (t, *J* = 7.3 Hz,

1H, $H_{4'}$), 7.17 (m, 4H, $H_3$, $H_5$, $H_{3'}$, $H_{5'}$), 7.41 (m, 4H, $H_2$, $H_6$, $H_{2'}$, $H_{6'}$), 9.39 (br s, 1H, NH), 9.70 (br s, 1H, NH). $^{13}$C NMR (75 MHz, $CDCl_3$) δ 14.2 ($CH_3$), 22.7, 26.7, 27.7, 29.4, 29.6, 31.9, 34.3, 34.4 ($8CH_2$), 35.6, 39.8 ($2CH_3$) 49.8, 49.9, 53.6 ($3CH_2$), 119.4 (2CH), 120.0 (2CH), 124.0 (CH), 128.1 (2CH), 128.9 (2CH), 131.0, 138.3, 138.8, 170.7, 171.0, 171.6 (6C). HRMS (ESI): [(M+H)$^+$] calcd. for $C_{29}H_{43}N_4O_3$: 495.33351; found, 495.33450.

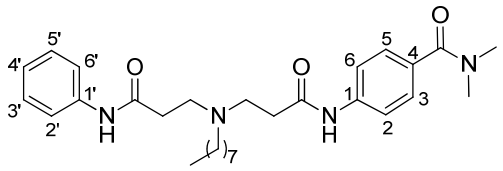

**13**

**Ethyl 4-{[*N*-(3-anilino-3-oxopropyl)-*N*-octyl-β-alanyl]amino}benzoate (14).** Obtained following the general procedure for the synthesis of asymmetric diamides from amine **34** (190 mg, 0.7 mmol) and acrylamide **47** (226 mg, 1 mmol) in 84% yield. Chromatography: EtOAc/MeOH, 9:1; oil. $R_f$ (EtOAc/MeOH, 9:1) 0.50. IR (ATR) ν 3309 (NH), 1712, 1664 (CO), 1599, 1537, 1444, 1409 (Ar). $^1$H NMR (300 MHz, $CDCl_3$) δ 0.83 (t, $J$ = 6.8 Hz, 3H, $CH_3$), 1.17-1.28 (m, 10H, $(C\underline{H}_2)_5CH_3$), 1.38 (t, $J$ = 7.1 Hz, 3H, $C\underline{H}_3CH_2O$), 1.47-1.54 (m, 2H, $C\underline{H}_2(CH_2)_5CH_3$), 2.50-2.58 (m, 6H, $2CH_2CO$, $(CH_2)_6C\underline{H}_2N$), 2.83-2.90 (m, 4H, $2NC\underline{H}_2CH_2CO$), 4.34 (q, $J$ = 7.1 Hz, 2H, $CH_2O$), 7.05 (t, $J$ = 7.4 Hz, 1H, $H_{4'}$), 7.21 (t, $J$ = 7.9 Hz, 2H, $H_{3'}$, $H_{5'}$), 7.41 (d, $J$ = 7.7 Hz, 2H, $H_2$, $H_6$), 7.49 (d, $J$ = 8.7 Hz, 2H, $H_{2'}$, $H_{6'}$), 7.83 (d, $J$ = 8.7 Hz, 2H, $H_3$, $H_5$), 8.47 (br s, 1H, NH), 9.39 (br s, 1H, NH). $^{13}$C NMR (75 MHz, $CDCl_3$) δ 14.1, 14.4 ($2CH_3$), 22.7, 26.8, 27.7, 29.3, 29.6, 31.8, 34.2, 34.5, 49.6, 49.9, 53.5, 60.8 ($12CH_2$), 118.9 (2CH), 120.0 (2CH), 124.2 (CH), 125.4 (C), 128.9 (2CH), 130.6 (2CH), 138.0, 142.5, 166.3, 170.7, 171.1 (5C). HRMS (ESI): [(M+H)$^+$] calcd. for $C_{29}H_{42}N_3O_4$: 496.31753; found, 496.31665.

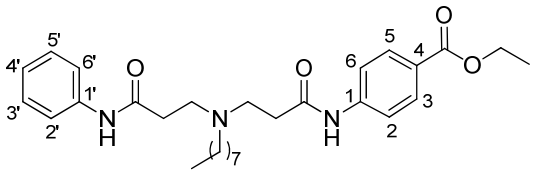

**14**

***N*$^3$-{3-[Methyl(phenyl)amino]-3-oxopropyl}-*N*$^3$-octyl-*N*$^1$-phenyl-β-alaninamide (28).** Obtained following the general procedure for the synthesis of asymmetric diamides from amine **34** (100 mg, 0.24 mmol) and acrylamide **62** (87 mg, 0.54 mmol) in 58% yield. Chromatography: EtOAc/MeOH, 9:1; oil. $R_f$ (EtOAc/MeOH, 9:1) 0.31. IR (ATR) ν 3306 (NH), 1658 (CO), 1599, 1547, 1497 (Ar). ). $^1$H

NMR (300 MHz, $CDCl_3$) δ 0.88 (t, *J* = 6.8 Hz, 3H, $C\underline{H}_3CH_2$), 1.23 (m, 10H, $(C\underline{H}_2)_5CH_3$), 1.47 (m, 2H, $C\underline{H}_2(CH_2)_5CH_3$), 2.30 (t, *J* = 6.8 Hz, 2H, $CH_2CO$), 2.39 (t, *J* = 7.5 Hz, 2H, $(CH_2)_6C\underline{H}_2N$), 2.46 (app t, 2H, $CH_2CO$), 2.63 (app t, 2H, $NC\underline{H}_2CH_2CO$), 2.84 (t, *J* = 6.8 Hz, 2H, $NC\underline{H}_2CH_2CO$), 3.18 (s, 3H, $CH_3N$), 7.07 (t, *J* = 7.4 Hz, 1H, $H_4$), 7.10 (d, *J* = 6.7 Hz, 2H, $H_{2'}$, $H_{6'}$), 7.27-7.42 (m, 5H, $H_3$, $H_5$, $H_{3'}$-$H_{5'}$), 7.50 (d, *J* = 7.9 Hz, 2H, $H_2$, $H_6$), 10.40 (br s, 1H, NH). $^{13}C$ NMR (75 MHz, $CDCl_3$) δ 14.1 ($CH_3$), 22.6, 26.6, 27.6, 29.3, 29.5, 31.5, 31.8, 33.9 ($8CH_2$), 37.3 ($CH_3$), 49.1, 50.3, 53.4 ($3CH_2$), 119.8 (2CH), 123.5 (CH), 127.1 (2CH), 128.0 (CH), 128.8 (2CH), 129.9 (2CH), 138.7, 143.7, 170.9, 171.2 (4C). HRMS (ESI): [$(M+H)^+$] calcd. for $C_{27}H_{39}N_3O_2$: 437.3042; found, 437.3041.

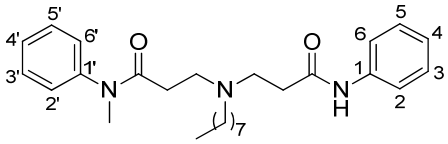

**28**

***N*³-[2-(Anilinosulfonyl)ethyl]-*N*³-octyl-*N*¹-phenil-β-alaninamide (29).** Obtained following the general procedure for the synthesis of asymmetric diamides from amine **34** (151 mg, 0.8 mmol) and sulfonamide **63** (150 mg, 0.8 mmol) in 12% yield. Chromatography: hexane/EtOAc, 7:3; oil. $R_f$ (hexane/EtOAc, 7:3) 0.35. IR (ATR) ν 3253 (NH), 1661, 1545 (CO), 1599, 1498, 1466 (Ar), 1376, 1148 ($SO_2$). $^1H$ NMR (300 MHz, $CDCl_3$) δ 0.81 (t, *J* = 6.8 Hz, 3H, $CH_3$), 1.04-1.29 (m, 10H, $(C\underline{H}_2)_5CH_3$), 1.36 (m, 2H, $C\underline{H}_2(CH_2)_5CH_3$), 2.35 (app t, *J* = 7.7 Hz, 2H, $(CH_2)_6C\underline{H}_2N$), 2.44 (t, *J* = 5.8 Hz, 2H, $CH_2CO$), 2.71 (t, *J* = 5.7 Hz, 2H, $NC\underline{H}_2CH_2CO$), 2.96 (t, *J* = 6.5 Hz, 2H, $CH_2SO_2$), 3.21 (t, *J* = 6.5 Hz, 2H, $NC\underline{H}_2CH_2SO_2$), 6.99-7.12 (m, 4H, $H_4$, $H_{2'}$, $H_{4'}$, $H_{6'}$), 7.19-7.32 (m, 5H, $H_3$, $H_5$, $H_{3'}$, $H_{5'}$, NH), 7.48 (d, *J* = 7.7 Hz, 2H, $H_2$, $H_6$), 9.12 (br s, 1H, NH). $^{13}C$ NMR (75 MHz, $CDCl_3$) δ 14.1 ($CH_3$), 22.6, 26.3, 27.5, 29.2, 29.4, 31.8, 34.6, 47.4, 48.1, 50.5, 53.7 ($11CH_2$), 119.9 (2CH), 120.5 (2CH), 124.1, 125.0 (2CH), 128.9 (2CH), 129.6 (2CH), 136.9, 138.1, 170.8 (3C). HRMS (ESI): [$(M+H)^+$] calcd. for $C_{25}H_{38}N_3O_3S$: 460.26284; found, 460.26383.

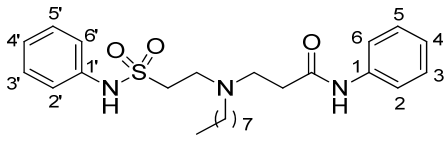

**29**

**Synthesis of *N*³-octyl-*N*¹-phenyl-*N*³-[(5-phenyl-1,3,4-oxadiazol-2-yl)methyl]-β-alaninamide (30).** Obtained following the general procedure for the synthesis of asymmetric diamides from amine

**34** (200 mg, 0.73 mmol) and 2-(chloromethyl)-5-phenyl-1,3,4-oxadiazole (117 mg, 0.6 mmol) in 62% yield. Chromatography: DCM/EtOAc, 8:2; oil. $R_f$(DCM/EtOAc, 8:2) 0.40. IR (ATR) ν 3304 (NH), 1728 (CO), 1599, 1550, 1499, 1444 (Ar). $^1$H NMR (300 MHz, $CDCl_3$) δ 0.85 (t, *J* = 6.9 Hz, 3H, $CH_3$), 1.25-1.30 (m, 10H, ($C\underline{H}_2$)$_5CH_3$), 1.50-1.60 (m, 2H, $C\underline{H}_2(CH_2)_5CH_3$), 2.63 (t, *J* = 6.3 Hz, 2H, $CH_2CO$), 2.70 (app t, *J* = 7.3 Hz, 2H, $NCH_2$), 3.00 (t, *J* = 6.3 Hz, 2H, $NC\underline{H}_2CH_2CO$), 4.10 (s, 2H, $NCH_2C_{het}$), 7.07 (tt, *J* = 7.7 Hz, 1.8, 1H, $H_4$), 7.28 (t, *J* = 7.2 Hz, 2H, $H_3$, $H_5$), 7.44 (t, *J* = 7.7 Hz, 2H, $H_{3'}$, $H_{5'}$), 7.50 (d, *J* = 7.3 Hz, 1H, $H_{4'}$), 7.57 (d, *J* = 8.6 Hz, 2H, $H_2$, $H_6$), 7.93 (d, *J* = 8.6 Hz, 2H, $H_{2'}$, $H_{6'}$), 10.17 (br s, 1H, NH). $^{13}$C NMR (75 MHz, $CDCl_3$) δ 14.5 ($CH_3$), 23.0, 27.2, 27.8, 29.6, 29.8, 32.1, 34.2, 47.7, 51.0, 54.4 (10$CH_2$), 120.3 (2CH), 123.8, 124.3 (2CH), 127.3 (2CH), 129.3 (2CH), 129.5 (2CH), 132.3, 138.8, 163.8, 165.9, 170.4 (5C). HRMS (ESI): [(M+H)$^+$] calcd. for $C_{26}H_{35}N_4O_2$: 435.2755; found, 435.2752.

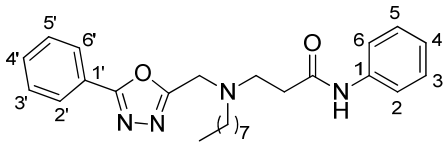


**30**

**Synthesis of 4-{[*N*-(3-anilino-3-oxopropyl)-*N*-octyl-β-alanyl]amino}benzoic acid (15)**.[43] To a solution of **14** (34 mg, 0.07 mmol) in THF/$H_2O$ 2:1 (1.2 mL) was added LiOH·$H_2O$ (6.5 mg, 0.3 mmol) and the reaction mixture was stirred at reflux for 3 h. Then, the solvent was removed under reduced pressure, and the residue was taken up in EtOAc and washed with saturated solution of NaCl (3 x 10 mL). The organic phase was dried over $Na_2SO_4$ and the solvent was evaporated under reduced pressure to obtain the title compound in 28% yield. Chromatography: EtOAc/MeOH, 1:1; oil. $R_f$ (EtOAc/MeOH/$NH_3$, 7:3:0.2) 0.34. IR (ATR) ν 3275, 3193, 3057 (NH, OH), 1685 (CO), 1602, 1544, 1502, 1446 (Ar). $^1$H NMR (300 MHz, $CD_3OD$) δ 0.86 (t, *J* = 6.7 Hz, 3H, $CH_3$), 1.25-1.29 (m, 10H, ($C\underline{H}_2$)$_5CH_3$), 1.67-1.72 (m, 2H, $C\underline{H}_2(CH_2)_5CH_3$), 2.52 (q, *J* = 6.3 Hz, 4H, $2CH_2CO$), 3.00 (t, *J* = 7.5 Hz, 2H, $(CH_2)_6C\underline{H}_2N$), 3.34 (m, 4H, $2NC\underline{H}_2CH_2CO$), 7.07 (t, *J* = 7.4 Hz, 1H, $H_{4'}$), 7.24 (t, *J* = 7.4 Hz, 2H, $H_{3'}$, $H_{5'}$), 7.51 (d, *J* = 7.6 Hz, 2H, $H_2$, $H_6$), 7.62 (d, *J* = 8.6 Hz, 2H, $H_{2'}$, $H_{6'}$), 7.89 (d, *J* = 8.6 Hz, 2H, $H_3$, $H_5$). $^{13}$C NMR (75 MHz, $CD_3OD$) δ 14.4 ($CH_3$), 23.7, 26.3, 28.0, 30.3, 30.4, 30.8, 32.5, 32.9 (8$CH_2$), 51.1 (2$CH_2$), 55.1 ($CH_2$), 120.2 (2CH), 121.3 (2CH), 124.3 (C), 125.4 (CH), 129.8 (2CH), 131.7 (2CH), 139.5, 143.4, 170.5, 171.6, 171.8 (5C). HRMS (ESI): [(M-H)$^-$] calcd. for $C_{27}H_{36}N_3O_4$: 466.27058; found, 466.27198.

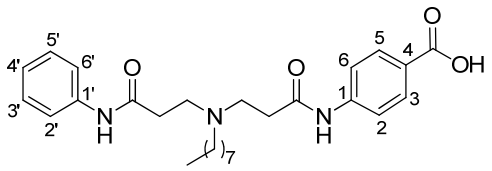

**15**

### 4.1.2. Synthesis of symmetric diamides 3 and 16-27

**Synthesis of 3-bromo-*N*-phenylpropanamide (48).** To a solution of aniline (4.1 mL, 45 mmol) in anhidrous DCM (225 mL) was added, under argon atmosphere and at 0 ºC, 3-bromopropanoyl chloride (5 mL, 50 mmol) and pyridine (4 mL, 50 mmol), consecutively. The reaction mixture was stirred for 1 h at rt, and the crude was washed with saturated solution of $NaHCO_3$, $H_2O$ and saturated solution of NaCl, sequentially. The aqueous phase was dried over $Na_2SO_4$ and the solvent was evaporated at reduced pressure, giving the compound as a solid in 71% yield. $R_f$ (DCM/MeOH, 95:5) 0.56. Mp: 118-122 ºC (Lit.[44] 123-124 ºC). $^1$H NMR (300 MHz, $CDCl_3$) $\delta$ 2.96 (t, $J$ = 6.5 Hz, 2H, $CH_2CO$), 3.65 (t, $J$ = 6.5 Hz, 2H, $CH_2Br$), 7.10 (t, $J$ = 7.4 Hz, 1H, $H_4$), 7.27 (t, $J$ = 7.8 Hz, 2H, $H_3$, $H_5$), 7.55 (d, $J$ = 7.8 Hz, 2H, $H_2$, $H_6$), 8.63 (br s, 1H, NH). The spectroscopic data are in agreement with those previously described.[44]

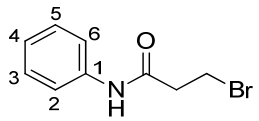

**48**

**Synthesis of (1*E*)-*N*-hydroxy-2-methoxycyclohexylimine (49).** To a solution of sodium acetate (192 mg, 2.3 mmol) and hydroxylamine hydrochloride (163 mg, 2.3 mmol) in $H_2O$ (5.8 mL) previously heated at 60 ºC, was added a solution of 2-methoxycyclohexyl-1-one (0.15 mL, 1.1 mmol) in methanol (0.6 mL) under argon atmosphere. The reaction mixture was stirred overnight at 60 ºC, and the crude was washed with $H_2O$ (5.5 mL) and extracted with $Et_2O$. The organic phase was washed with saturated aqueous solutions of $NaHCO_3$ and NaCl, dried over $Na_2SO_4$, and the solvent was removed under reduced pressure to obtain the title compound in quantitative yield. Chromatography: hexane/EtOAc, 7:3; oil. $R_f$ (hexane/EtOAc, 7:3) 0.40. $^1$H NMR (300 MHz, $CDCl_3$) $\delta$ 1.35-1.94 (m, 5H, $2CH_2$, $1/2CH_2$), 2.03-2.14 (m, 2H, $CH_2$), 3.01-3.05 (m, 1H, $1/2CH_2$), 3.27 (s, 3H, $CH_3$), 3.75 (m, 1H, CH), 6.05 (br s, 1H, OH). MS (ESI): [$(M+H)^+$] 143.9. The spectroscopic data are in agreement with those previously described.[45]

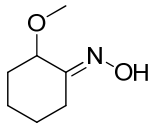

**49**

**Synthesis of 1-{[(*E*)-(2-methoxycyclohexylidene)amino]oxy}bethanone (50).** A solution of ketoxime **49** (166 mg, 1.2 mmol), pyridine (0.34 mL, 4.2 mmol) and acetic anhydride (0.68 mL, 7.2 mmol) was stirred overnight under argon atmosphere at rt. The solvent was removed under reduced pressure and coevaporated with toluene to obtain the title compound in 85% yield. Chromatography: hexane/EtOAc, 7:3; oil. $R_f$ (hexane/EtOAc, 7:3) 0.42. IR (ATR) ν 1769 (COO), 1702 (CN), 1193 (COC). $^1$H NMR (300 MHz, $CDCl_3$) δ 1.34-1.70 (m, 5H, $2CH_2$, $1/2CH_2$), 1.73-2.02 (m, 2H, $CH_2$), 2.07-2.26 (m, 5H, $CH_2$, $CH_3CO$), 3.03-3.08 (m, 1H, $1/2CH_2$), 3.30 (s, 3H, $OCH_3$), 3.95 (m, 1H, CH). $^{13}$C NMR (75 MHz, $CDCl_3$) δ 19.3 ($CH_3$ diastereomers), 19.4 ($CH_2$ diastereomers), 19.4 ($CH_3$ diastereomers), 19.6, 23.2, 25.5, 26.8, 28.0, 31.8, 32.7 ($7CH_2$ diastereomers), 56.0, 56.2 ($CH_3$ diastereomers), 70.1, 77.0 (CH diastereomers), 166.9, 167.4, 168.3, 168.5 (2C diastereomers). MS (ESI): [$(M\text{-}OCOCH_3)^+$] 125.9.

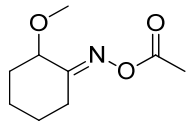

**50**

**Synthesis of 6-methoxyhexanenitrile (51).**[46] A solution of **50** (120 mg, 0.7 mmol), trimethylsilane (0.12 mL, 0.8 mmol) and catalytic quantities of trimethylsilyl trifluoromethanesulfonate (TMSOTf) (12 μL, 70.0 nmol) was stirred at 0 ºC for 6 h. Then, the solvent was removed under reduced pressure to give the title compound in 87% yield. Chromatography: hexane/EtOAc, 8:2; oil. $R_f$ (hexane/EtOAc, 8:2) 0.33. IR (ATR) ν 2246 (CN), 1120 (CO). $^1$H NMR (300 MHz, $CDCl_3$) δ 1.47-1.75 (m, 6H, $(C\underline{H}_2)_3CH_2CN$), 2.36 (t, $J$ = 7.1 Hz, 2H, $CH_2CN$), 3.34 (s, 3H, $CH_3$), 3.39 (t, $J$ = 6.1 Hz, 2H, $CH_2O$). $^{13}$C NMR (75 MHz, $CDCl_3$) δ 17.3, 25.4, 25.6, 29.0 ($4CH_2$), 58.8 ($CH_3$), 72.3 ($CH_2$), 119.8 (C). MS (ESI): [$(M\text{-}CH_3\text{+}H)^+$] 113.0.

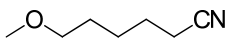

**51**

**Synthesis of 6-methoxyhexyl-1-amine (52).** To a solution of nitrile **51** (100 mg, 0.8 mmol) in anhydrous THF (1 mL) was added under argon atmosphere a solution of 1M $BH_3$ in THF (3.2 mL, 3.2 mmol) and the mixture was stirred at reflux for 3.5 h. Once at rt, the reaction was quenched by slow addition of MeOH (1.8 mL) and concentrated HCl (0.2 mL), and the product was extracted with DCM, dried over $Na_2SO_4$, and the solvent was removed under reduced pressure. The title amine was obtained in 66% yield. Chromatography: EtOAc/MeOH, 9:1; oil. $R_f$ (hexane/EtOAc, 1:1) 0.13. IR (ATR) $\nu$ 3332 (NH). $^1$H NMR (300 MHz, $CDCl_3$) $\delta$ 1.34-1.49 (m, 4H, $2CH_2$), 1.56 (qt, *J* = 6.6 Hz, 2H, $CH_2$), 1.79 (qt, *J* = 7.4 Hz, 2H, $CH_2$), 2.99 (t, *J* = 7.7 Hz, 2H, $CH_2N$), 3.32 (s, 3H, $CH_3$), 3.37 (t, *J* = 6.4 Hz, 2H, $CH_2O$). $^{13}$C NMR (75 MHz, $CDCl_3$) $\delta$ 25.7, 26.4, 27.6, 29.4, 40.0 ($5CH_2$), 58.6 ($CH_3$), 72.6 ($CH_2$). MS (ESI): [$(M+H)^+$] 132.0.

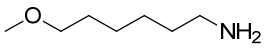


**52**

**Synthesis of 2-[2-(2-ethoxyethoxy)ethyl]-1*H*-isoindol-1,3(2*H*)-dione (53).** To a solution of 2-(2-ethoxyethoxy)ethanol (0.5 mL, 3.7 mmol), phthalimide (549 mg, 3.7 mmol) and triphenylphosphine (977 mg, 3.7 mmol) in anhydrous toluene (11 mL) was added, under argon atmosphere and at 0 ºC, DIAD (0.8 mL, 4 mmol). The reaction mixture was stirred at 0 ºC for 50 min and at rt for 1 h. Then, was added methanol (2.9 mL) and the mixture was stirred overnight at rt. Solvent was removed under reduced pressure and precipitate was washed with hexane, filtered and dried over $Na_2SO_4$, to obtain the title compound in 58% yield. Chromatography: hexane/EtOAc, 7:3; oil. $R_f$ (hexane/EtOAc, 7:3) 0.22. $^1$H NMR (300 MHz, $CDCl_3$) $\delta$ 1.13 (t, *J* = 7.0 Hz, 3H, $CH_3$), 3.45 (q, *J* = 7.0 Hz, 2H, $CH_3C\underline{H}_2O$), 3.52-3.55 (m, 2H, $CH_2N$), 3.62-3.65 (m, 2H, $CH_2O$), 3.74 (t, *J* = 5.8 Hz, 2H, $CH_2O$), 3.90 (t, *J* = 5.8 Hz, 2H, $CH_2O$), 7.70 (m, 2H, $2H_3$), 7.84 (m, 2H, $2H_2$). MS (ESI): [$(M+H)^+$] 264.0. The spectroscopic data are in agreement with those previously described.[47]

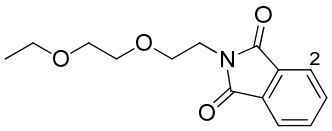


**53**

**Synthesis of 2-(2-ethoxyethoxy)ethylamine (54).** To a solution of **53** (295 mg, 1.1 mmol) in dry methanol (4.9 mL) was added, under argon atmosphere, hydrazine (0.1 mL, 2.2 mmol) and the reaction mixture was stirred for 2 h. Then, $NaBH_4$ (42 mg, 1.1 mmol) and a second portion of hydrazine (0.1 mL, 2.2 mmol) were added and stirring was continued overnight at rt. The suspension was filtered and the solvent was removed under reduced pressure. The residue was dissolved in

EtOAc (20 mL), warmed to 50 °C, sonicated, and filtered. The filtrate was evaporated, redissolved in $Et_2O$ (20 mL), filtered, and the solvent was removed under reduced pressure to afford the title compound as a yellowish oil in quantitative yield. $R_f$ (EtOAc/MeOH, 9:1) 0.35. $^1$H NMR (300 MHz, $CDCl_3$) $\delta$ 1.20 (t, $J$ = 7.0 Hz, 3H, $CH_3$), 1.95 (br s, 2H, $NH_2$ ), 2.85 (t, $J$ = 5.2 Hz, 2H, $CH_2N$), 3.42-3.53 (m, 4H, $2CH_2O$), 3.56-3.62 (m, 4H, $2CH_2O$). The spectroscopic data are in agreement with those previously described.[47]

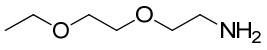

**54**

**Synthesis of 3-(2-methoxyethoxy)propanenitrile (55).** A solution of 2-methoxyethanol (2 mL, 26 mmol) in acrylonitrile (15 mL, 229 mmol) was stirred under argon atmosphere at 0 ºC for 10 min. Then, KOH (133 mg, 2.4 mmol) was added and the mixture was stirred at 0 ºC for 1.5 h. Four drops of an aqueous solution of concentrated HCl were added and the solvent was removed under reduced pressure. The residue was dissolved in chloroform, filtered and the solvent was removed under reduced pressure to obtain the title nitrile as a colorless oil in 94% yield. $R_f$ (hexane/EtOAc, 7:3) 0.28. $^1$H NMR (300 MHz, $CDCl_3$) $\delta$ 2.64 (t, $J$ = 6.5 Hz, 2H, $CH_2CN$), 3.40 (s, 3H, $CH_3$), 3.55-3.58 (m, 2H, $CH_2O$), 3.66-3.69 (m, 2H, $CH_2O$), 3.73 (t, $J$ = 6.5 Hz, 2H, $CH_2O$). MS (ESI): [$(M+H)^+$] 130.0. The spectroscopic data are in agreement with those previously described.[48]

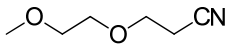

**55**

**Synthesis of 3-(2-methoxyethoxy)propyl-1-amine (56).** To a solution of nitrile **55** (440 mg, 31.8 mmol) in anhydrous THF (41.6 mL) was added, dropwise and under argon atmosphere, a solution of 1M $BH_3$ in THF (7.7 mL, 7.7 mmol) and the mixture was stirred at reflux for 3.5 h. Once at rt, the reaction was quenched by slow addition of MeOH (73 mL) and concentrated HCl (8 mL), the product was extracted with DCM, dried over $Na_2SO_4$, and the solvent was removed under reduced pressure to obtain the title amine as an oil in 89% yield. $R_f$ (hexane/EtOAc, 9:1) 0.25. $^1$H NMR (300 MHz, $CDCl_3$) $\delta$ 1.74 (qt, $J$ = 6.5 Hz, 2H, $C\underline{H}_2CH_2N$), 2.78 (t, $J$ = 6.8 Hz, 2H, $CH_2N$), 3.38 (s, 3H, $CH_3$), 3.52-3.60 (m, 6H, $3CH_2O$). MS (ESI): [$(M+H)^+$] 134.1. The spectroscopic data are in agreement with those previously described.[48]

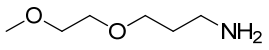

**56**

**Synthesis of (oxetan-3-ylidene)acetonitrile (57).** To a solution of oxetan-3-one (0.67 mL, 10.4 mmol) in dry DCM (3 mL) was added, dropwise and under an argon atmosphere, a solution of $Ph_3P$=CHCN (3.14 g, 10.4 mmol) in dry DCM (15 mL). The mixture was stirred for 6 h at rt, and the solvent was evaporated under reduced pressure. The residue was dissolved in hexane/$Et_2O$ (3:2), filtered over a plug of silica gel and washed with $Et_2O$ (2 x 50 mL). The solvents were removed under reduced pressure to give the nitrile in 79% yield. Chromatography: hexane/EtOAc, 8:2; oil. $R_f$ (hexane/EtOAc, 7:3) 0.40. IR (ATR) $\nu$ 2218 (CN), 1690 (C=C). $^1$H NMR (300 MHz, $CDCl_3$) $\delta$ 5.30 (m, 1H, CH), 5.25-5.28 (m, 2H, $CH_2O$), 5.29-5.32 (m, 2H, $CH_2O$).

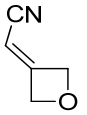

**57**

**Synthesis of (3-pentyloxetan-3-yl)acetonitrile (58).** To a suspension of CuI (200 mg, 1 mmol) in anhydrous $Et_2O$ (1 mL), pentylmagnesium bromide (2 M in $Et_2O$, 1.3 mL) was added dropwise under argon atmosphere. The mixture was cooled to 0 ºC before a solution of nitrile **57** (210 mg, 2.2 mmol) in $Et_2O$ (4 mL) was added within 15 min. The reaction mixture was stirred at this temperature for 2 h, quenched with saturated $NH_4Cl$, and extracted with EtOAc (2 x 50 mL). The organic layers were washed with saturated aqueous solution of NaCl and dried over $Na_2SO_4$. The solvent was removed under reduced pressure to give the title compound in 26% yield. Chromatography: hexane/EtOAc, 8:2; oil. $R_f$ (hexane) 0.20. IR (ATR) $\nu$ 2245 (CN). $^1$H NMR (300 MHz, $CDCl_3$) $\delta$ 0.84 (t, $J$ = 6.7 Hz, 3H, $CH_3$), 1.16-1.29 (m, 6H, $(CH_2)_3CH_3$), 1.74 (m, 2H, $CH_2C$), 2.75 (s, 2H, $CH_2CN$), 4.43 (d, $J$ = 6.4 Hz, 2H, $CH_2O$), 4.51 (d, $J$ = 6.4 Hz, 2H, $CH_2O$). $^{13}$C NMR (75 MHz, $CDCl_3$) $\delta$ 14.0 ($CH_3$), 22.5, 23.9, 25.0, 31.9, 35.7 ($5CH_2$), 41.1 (C), 79.9 ($2CH_2$), 118.3 (C).

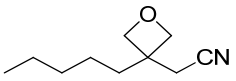

**58**

**Synthesis of 2-(3-pentyloxetan-3-yl)ethylamine (59).** To a suspension of LAH (96 mg, 2.5 mmol) in anhydrous $Et_2O$, nitrile **58** (200 mg, 1.2 mmol) was added dropwise at 0º C and under argon

atmosphere. The reaction was stirred for 2 h at this temperature and the crude was quenched by adding $H_2O$ (2.5 mL), NaOH 1 M (2.5 mL), and $H_2O$ (5 mL). The reaction mixture was extracted with EtOAc (2 x 50 mL) and the organic layers were washed with saturated aqueous solution of NaCl and dried over $Na_2SO_4$. Then, the solvent was removed under reduced pressure to obtain the amine as an oil in 59% yield. $R_f$ (EtOAc/MeOH, 85:15) 0.10. IR (ATR) ν 3360 (NH). $^1$H NMR (300 MHz, $CDCl_3$) δ 0.90 (t, *J* = 6.7 Hz, 3H, $CH_3$), 1.18-1.35 (m, 6H, $(C\underline{H}_2)_3CH_3$), 1.54 (br s, 2H, $NH_2$), 1.65 (app t, *J* = 7.3, 2H, $CH_2C$), 1.84 (app t, *J* = 8.1 Hz, 2H, $C\underline{H}_2CH_2N$), 2.69 (t, *J* = 7.3 Hz, 2H, $CH_2N$), 4.40 (AB system, *J* = 5.7 Hz, 4H, $2CH_2O$). $^{13}$C NMR (75 MHz, $CDCl_3$) δ 14.1 ($CH_3$), 22.6, 23.7, 31.0 ($3CH_2$), 32.3 (C), 34.3, 35.9, 41.5 ($3CH_2$), 81.9 ($2CH_2$). MS (ESI): $[(M+H)^+]$ 172.1.

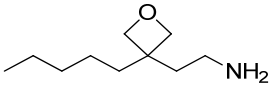


**59**

**Synthesis of (4-ethylpiperazin-1-yl)acetonitrile (60).**[21] A mixture of 1-ethylpiperazine (0.7 mL, 5.4 mmol), bromoacetonitrile (0.43 mL, 6.0 mmol) and $K_2CO_3$ (1.7 g, 12 mmol) in anhidrous acetonitrile (0.5 mL/mmol) was stirred overnight at rt. The product was isolated by filtration with celite, washed with acetonitrile, and the solvent was evaporated under reduced pressure to give the title compound as a pure orange oil in quantitative yield. $R_f$ (EtOAc/MeOH, 8:2) 0.28. IR (ATR) ν 2231 (CN). $^1$H NMR (300 MHz, $CDCl_3$) δ 1.08 (t, *J* = 7.2 Hz, 3H, $CH_3$), 2.42 (q, *J* = 7.2 Hz, 2H, $CH_3C\underline{H}_2$), 2.51 (m, 4H, $2CH_2N$), 2.64 (t, *J* = 4.6 Hz, 4H, $2CH_2N$), 3.50 (s, 2H, $CH_2CN$). $^{13}$C NMR (75 MHz, $CDCl_3$) δ 11.9 ($CH_3$), 45.7 ($CH_2$), 51.7 ($2CH_2$), 52.0 ($CH_2$), 52.1 ($2CH_2$), 114.7 (C). MS (ESI): $[(M+H)^+]$ 154.1.

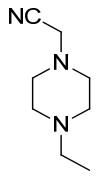


**60**

**Synthesis of (4-ethylpiperazin-1-yl)ethylamine (61).**[21] A mixture of nitrile **60** (465 mg, 3 mmol) in THF (3 mL/mmol) was treated with LAH (242 mg, 6 mmol) at 0 ºC for 4 h. After completion, the reaction was quenched with $Na_2SO_4 \cdot 10H_2O$ (8.4 g, excess) and stirred for 30 min. The product was isolated by filtration with celite, washed with THF and dried under reduced pressure to give the title compound as a pure orange oil in 86% yield. IR (ATR) ν 3311 ($NH_2$). $^1$H NMR (300 MHz, $CDCl_3$) δ

1.07 (t, *J* = 7.2 Hz, 3H, $CH_3$), 2.36-2.48 (m, 12H, $C\underline{H}_2CH_3$+$4CH_2N$+$C\underline{H}_2CH_2NH_2$), 2.78 (t, *J* = 6.3 Hz, 4H, $C\underline{H}_2NH_2$). $^{13}C$ NMR (75 MHz, $CDCl_3$) δ 12.1 ($CH_3$), 38.9, 52.4 ($2CH_2$), 52.9 ($2CH_2$), 53.3 ($2CH_2$), 61.3 ($CH_2$). MS (ESI): [$(M+H)^+$] 158.2.

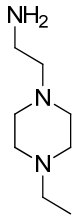

**61**

**General procedure A for the synthesis of symmetric diamides 3 and 17-25.** To a solution of *N*-phenylacrylamide **33** (3 equiv) and the corresponding amine (1 equiv) in anhidrous acetonitrile (0.5 mL/mmol), was added DBU (3 equiv), and the reaction mixture was stirred 24 h at 60 ºC (except for **24**). The solvent was removed under reduced pressure and the crude was purified by column chromatography (EtOAc/MeOH) to obtain the title compounds as yellowish oils.

***N*$^3$-(3-Anilino-3-oxopropyl)-*N*$^1$-phenyl-*N*$^3$-octyl-β–alaninamide (3).** Obtained following the general procedure A for the synthesis of symmetric diamides from acrylamide **33** (500 mg, 3.4 mmol) and octylamine (0.18 mL, 1.1 mmol) in 83% yield. Chromatography: hexane/EtOAc, 1:1; oil. $R_f$ (hexane:EtOAc, 1:1) 0.45. IR (ATR) ν 3294 (NH), 1659 (CO), 1601, 1546, 1497 (Ar). $^1H$ NMR (300 MHz, $CDCl_3$) δ 0.85 (t, *J* = 6.7 Hz, 3H, $CH_3$), 1.08 (m, 2H, $C\underline{H}_2CH_3$), 1.19-1.25 (m, 8H, $(C\underline{H}_2)_4CH_2CH_3$), 1.52 (m, 2H, $C\underline{H}_2(CH_2)_5CH_3$), 2.53 (t, *J* = 6.3 Hz, 6H, $2CH_2CO$, $(CH_2)_6C\underline{H}_2N$), 2.85 (t, *J* = 6.2 Hz, 4H, $2NC\underline{H}_2CH_2CO$), 7.02 (t, *J* = 7.3 Hz, 2H, $2H_4$), 7.20 (t, *J* = 7.8 Hz, 4H, $2H_3$, $2H_5$), 7.43 (d, *J* = 7.8 Hz, 4H, $2H_2$, $2H_6$), 8.90 (br s, 2H, 2NH). $^{13}C$ NMR (75 MHz, $CDCl_3$) δ 14.0 ($CH_3$), 22.6, 26.8, 27.7, 29.3, 29.5, 31.8 ($6CH_2$), 34.5 ($2CH_2$), 49.9 ($2CH_2$), 53.7 ($CH_2$), 119.9 (4CH), 124.0 (2CH), 128.9 (4CH), 138.1 (2C), 170.4 (2C). HRMS (ESI): [$(M+H)^+$] calcd. for $C_{26}H_{38}N_3O_2$, 424.2959; found, 424.2959.

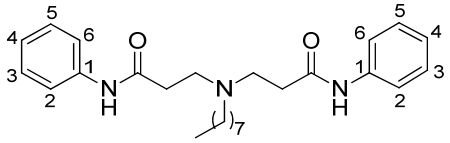

**3**

***N*$^3$-(3-Anilino-3-oxopropyl)-*N*$^1$-phenyl-*N*$^3$-methyl-β-alaninamide (17).** Obtained following the general procedure A for the synthesis of symmetric diamides from acrylamide **33** (500 mg, 3.4 mmol)

and methylamine (2 M solution in THF, 1.1 mmol) in 95% yield. Chromatography: DCM/MeOH, 95:5; oil. $R_f$ (DCM/MeOH, 95:5) 0.13; IR (ATR) ν 3298 (NH), 1660 (CO), 1600, 1547, 1497, 1443 (Ar). $^1$H NMR (300 MHz, $CDCl_3$) δ 2.30 (s, 3H, $CH_3$), 2.52 (t, $J$ = 5.9 Hz, 4H, $2CH_2CO$), 2.75 (t, $J$ = 5.9 Hz, 4H, $2CH_2N$), 7.01 (t, $J$ = 7.2 Hz, 2H, $2H_4$), 7.17 (t, $J$ = 7.6 Hz, 4H, $2H_3$, $2H_5$), 7.46 (d, $J$ = 7.8 Hz, 4H, $2H_2$, $2H_6$), 9.36 (br s, 2H, 2NH). $^{13}$C NMR (75 MHz, $CDCl_3$) δ 34.3 ($2CH_2$), 41.3 ($CH_3$), 53.0 ($2CH_2$), 120.1 (4CH), 124.0 (2CH), 128.8 (4CH), 138.2 (2C), 170.5 (2C). HRMS (ESI): [(M+H)$^+$] calcd. for $C_{19}H_{24}N_3O_2$, 326.1863; found, 326.1866.

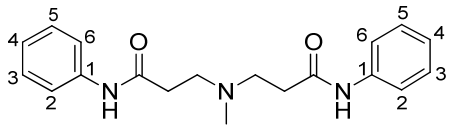

**17**

***N*$^3$-(3-Anilino-3-oxopropyl)-*N*$^3$-hexyl-*N*$^1$-phenyl-β-alaninamide (18).** Obtained following the general procedure A for the synthesis of symmetric diamides from acrylamide **33** (500 mg, 3.4 mmol) and hexylamine (111 mg, 1.1 mmol) in 76% yield. Chromatography: EtOAc/MeOH, 9:1; oil. $R_f$ (EtOAc/MeOH, 9:1) 0.21. IR (ATR) ν 3298 (NH), 1660 (CO), 1601, 1547, 1498, 1443 (Ar). $^1$H NMR (300 MHz, $CDCl_3$) δ 0.82 (t, $J$ = 6.9 Hz, 3H, $CH_3$), 1.20-1.28 (m, 6H, $(C\underline{H}_2)_3CH_3$), 1.50-1.54 (m, 2H, $C\underline{H}_2(CH_2)_3CH_3$), 2.52 (t, $J$ = 6.2 Hz, 6H, $2C\underline{H}_2CO$, $(CH_2)_4C\underline{H}_2N$), 2.83 (t, $J$ = 6.2 Hz, 4H, $2NC\underline{H}_2CH_2CO$), 7.02 (t, $J$ = 7.4 Hz, 2H, $2H_4$), 7.19 (t, $J$ = 7.8 Hz, 4H, $2H_3$, $2H_5$), 7.44 (d, $J$ = 7.9 Hz, 4H, $2H_2$, $2H_6$), 9.08 (br s, 2H, 2NH). $^{13}$C NMR (75 MHz, $CDCl_3$) δ 14.4 ($CH_3$), 23.0, 27.1, 27.7, 32.1 ($4CH_2$), 34.7 ($2CH_2$), 50.1 ($2CH_2$), 54.0 ($CH_2$), 120.2 (4CH), 124.4 (2CH), 129.3 (4CH), 138.5 (2C), 170.9 (2C). HRMS (ESI): [(M+H)$^+$] calcd. for $C_{24}H_{34}N_3O_2$, 396.2646; found, 369.2648.

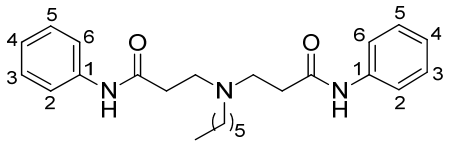

**18**

***N*$^3$-(3-Anilino-3-oxopropyl)-*N*$^3$-(3-butoxypropyl)-*N*$^1$-phenyl-β-alaninamide (19).** Obtained following the general procedure A for the synthesis of symmetric diamides from acrylamide **33** (336 mg, 2.3 mmol) and 3-butoxypropyl-1-amine (0.1 mL, 0.76 mmol) in 25% yield. Chromatography: EtOAc; oil. $R_f$ (EtOAc) 0.30. IR (ATR) ν 3287 (NH), 1661 (CO), 1600, 1547, 1498, 1443 (Ar). $^1$H NMR (300 MHz, $CDCl_3$) δ 0.76 (t, $J$ = 7.3 Hz, 3H, $CH_3$), 1.10-1.37 (m, 4H, $(C\underline{H}_2)_2CH_3$), 1.64 (qt, $J$ = 6.6 Hz,

2H, $NCH_2C\underline{H}_2CH_2O$), 2.44-2.52 (m, 6H, $2CH_2CO$, $NC\underline{H}_2(CH_2)_2O$), 2.75 (t, *J* = 6.3 Hz, 4H, $2NC\underline{H}_2CH_2CO$), 3.13 (t, *J* = 6.6 Hz, 2H, $CH_2O$), 3.30 (t, *J* = 6.4 Hz, 2H, $CH_2O$), 6.93 (t, *J* = 7.4 Hz, 2H, $2H_4$), 7.10 (t, *J* = 7.9 Hz, 4H, $2H_3$, $2H_5$), 7.37 (dd, *J* = 8.8, 1.0 Hz, 4H, $2H_2$, $2H_6$). $^{13}$C NMR (75 MHz, $CDCl_3$) δ 14.4 ($CH_3$), 20.4, 28.3, 32.9 ($3CH_2$), 35.6 ($2CH_2$), 51.2 ($2CH_2$), 51.3, 69.8, 71.7 ($3CH_2$), 121.3 (4CH), 125.1 (2CH), 129.8 (4CH), 139.7 (2C), 173.4 (2C). HRMS (ESI): [$(M+Na)^+$] calcd. for $C_{25}H_{35}N_3O_3Na$, 448.25761; found, 448.25641.

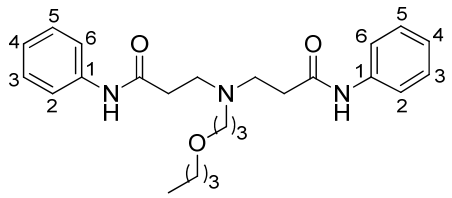

**19**

***N*$^3$-[3-(Phenylamino)-3-oxopropyl]-*N*$^3$-[6-(methoxyhexyl)]-*N*$^1$-phenyl-β-alaninamide (20).** Obtained following the general procedure A for the synthesis of symmetric diamides from acrylamide **33** (168 mg, 1.1 mmol) and amine **52** (60 mg, 0.46 mmol) in 21% yield. Chromatography: EtOAc/MeOH, 9:1; oil. $R_f$ (EtOAc/MeOH, 9:1) 0.42. IR (ATR) ν 3238 (NH), 1678, 1645 (CO), 1601, 1548, 1495, 1443 (Ar). $^1$H NMR (300 MHz, $CDCl_3$) δ 1.18-1.58 (m, 8H, $OCH_2(C\underline{H}_2)_4$), 2.51 (t, *J* = 7.1 Hz, 2H, $(CH_2)_5C\underline{H}_2N$), 2.53 (t, *J* = 5.9 Hz, 4H, $2CH_2CO$), 2.83 (t, *J* = 6.1 Hz, 4H, $2NC\underline{H}_2CH_2CO$), 3.29-3.33 (m, 5H, $CH_2OCH_3$), 7.02 (t, *J* = 7.4 Hz, 2H, $2H_4$), 7.18 (t, *J* = 7.8 Hz, 4H, $2H_3$, $2H_5$), 7.44 (d, *J* = 7.8 Hz, 4H, $2H_2$, $2H_6$), 9.20 (br s, 2H, 2NH). $^{13}$C NMR (75 MHz, $CDCl_3$) δ 25.9, 26.6, 27.2, 29.5 ($4CH_2$), 34.6 ($2CH_2$), 50.0 ($2CH_2$), 53.4 ($CH_2$), 58.6 ($CH_3$), 72.8 ($CH_2$), 119.9 (4CH), 124.0 (2CH), 128.9 (4CH), 138.3 (2C), 170.7 (2C). HRMS (ESI): [$(M-H)^-$] calcd. for $C_{25}H_{34}N_3O_3$, 424.26001; found, 424.26106.

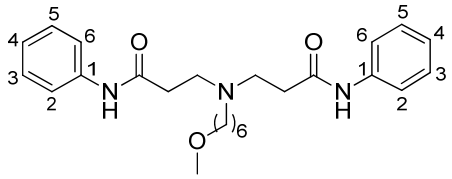

**20**

***N*$^3$-(3-Anilino-3-oxopropyl)-*N*$^3$-[2-(2-ethoxyethoxy)ethyl]-*N*$^1$-phenyl-β-alaninamide (21).** Obtained following the general procedure A for the synthesis of symmetric diamides from acrylamide **33** (332 mg, 2.3 mmol) and amine **54** (100 mg, 0.8 mmol) in 53% yield. Chromatography: EtOAc/MeOH, 8:2; oil. $R_f$ (EtOAc/MeOH, 9:1) 0.30. IR (ATR) ν 3303 (NH), 1660, 1547 (CO), 1601,

1496, 1443 (Ar). $^{1}$H NMR (300 MHz, $CDCl_3$) δ 1.14 (t, *J* = 7.0 Hz, 3H, $CH_3$), 2.53 (t, *J* = 6.0 Hz, 4H, $2CH_2CO$), 2.74 (t, *J* = 4.9 Hz, 2H, $NC\underline{H}_2CH_2O$), 2.87 (t, *J* = 6.0 Hz, 4H, $2NC\underline{H}_2CH_2CO$), 3.44-3.49 (m, 4H, $NCH_2C\underline{H}_2O$, $OC\underline{H}_2CH_3$), 3.54-3.59 (m, 4H, $O(CH_2)_2O$), 6.98 (t, *J* = 7.4 Hz, 2H, $2H_4$), 7.13 (t, *J* = 7.8 Hz, 4H, $2H_3$, $2H_5$), 7.43 (d, *J* = 7.7 Hz, 4H, $2H_2$, $2H_6$), 9.24 (br s, 2H, 2NH). $^{13}$C NMR (75 MHz, $CDCl_3$) δ 15.0 ($CH_3$), 35.2 ($2CH_2$), 51.4 ($2CH_2$), 54.7, 66.6, 69.3, 69.6, 70.3 ($5CH_2$), 120.0 (4CH), 123.8 (2CH), 128.7 (4CH), 138.3 (2C), 171.0 (2C). HRMS (ESI): [$(M+Na)^+$] calcd. for $C_{24}H_{33}N_3O_4Na$, 450.23688; found, 450.23663.

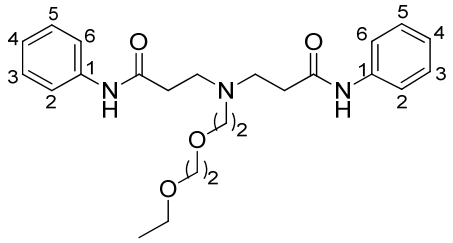

**21**

***N*$^{3}$-(3-Anilino-3-oxopropyl)-*N*$^{3}$-[3-(2-methoxyethoxy)propyl]-*N*$^{1}$-phenyl-β-alaninamide (22).** Obtained following the general procedure A for the synthesis of symmetric diamides from acrylamide **33** (332 mg, 2.3 mmol) and amine **56** (100 mg, 0.8 mmol) in 39% yield. Chromatography: EtOAc/MeOH, 8:2; oil. $R_f$ (EtOAc/MeOH, 9:1) 0.29. IR (ATR) ν 3305 (NH), 1662, 1545 (CO), 1600, 1497, 1443 (Ar). $^{1}$H NMR (300 MHz, $CDCl_3$) δ 1.59 (qt, *J* = 5.7 Hz, 2H, $NCH_2C\underline{H}_2CH_2O$), 2.51 (app t, 4H, $2CH_2CO$), 2.54 (t, *J* = 5.4 Hz, 2H, $NC\underline{H}_2CH_2CH_2O$), 2.75 (t, *J* = 5.4 Hz, 4H, $NC\underline{H}_2CH_2CO$), 3.28 (t, *J* = 5.5 Hz, 2H, $NCH_2CH_2C\underline{H}_2O$), 3.39-3.42 (m, 2H, $OC\underline{H}_2CH_2O$), 3.45 (s, 3H, $CH_3$), 3.60-3.63 (m, 2H, $OCH_2C\underline{H}_2O$), 6.98 (t, *J* = 7.3 Hz, 2H, $2H_4$), 7.11 (t, *J* = 7.7 Hz, 4H, $2H_3$, $2H_5$), 7.39 (d, *J* = 8.1 Hz, 4H, $2H_2$, $2H_6$), 8.89 (br s, 2H, 2NH). $^{13}$C NMR (75 MHz, $CDCl_3$) δ 27.1 ($CH_2$), 35.5 ($2CH_2$), 49.3 ($CH_2$), 50.6 ($2CH_2$), 58.9 ($CH_3$), 67.2, 69.4, 72.5 ($3CH_2$), 119.8 (4CH), 123.6 (2CH), 128.7 (4CH), 138.4 (2C), 171.9 (2C). HRMS (ESI): [$(M+H)^+$] calcd. for $C_{24}H_{34}N_3O_4$, 428.25493; found, 428.25429.

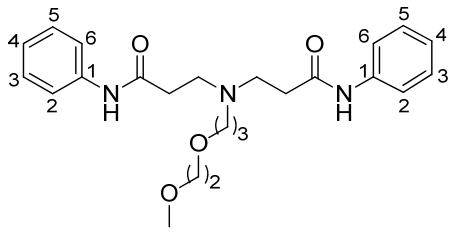

**22**

***N*³-(3-Anilino-3-oxopropyl)-*N*³-[(3-pentyloxetan-3-yl)ethyl]-*N*¹-phenyl-β-alaninamide (23).** Obtained following the general procedure A for the synthesis of symmetric diamides from acrylamide **33** (275 mg, 1.9 mmol) and amine **59** (98 mg, 0.62 mmol) in 21% yield. Chromatography: EtOAc/MeOH, 9:1; oil. $R_f$ (EtOAc/MeOH, 95:5) 0.60. IR (ATR) ν 3304 (NH), 1657 (CO), 1598, 1542, 1498, 1442 (Ar). $^1$H NMR (300 MHz, $CDCl_3$) δ 0.88 (t, *J* = 7.1 Hz, 3H, $CH_3$), 1.15-1.31 (m, 6H, $(C\underline{H}_2)_3CH_3$), 1.56 (app t, *J* = 7.3 Hz, 2H, $CH_2C$), 1.78 (t, *J* = 7.1 Hz, 2H, $CC\underline{H}_2CH_2N$), 2.56 (t, *J* = 5.8 Hz, 4H, $2CH_2CO$), 2.63 (t, *J* = 7.1 Hz, 2H, $CCH_2C\underline{H}_2N$), 2.87 (t, *J* = 5.8 Hz, 4H, $2NC\underline{H}_2CH_2CO$), 4.30 (d, *J* = 5.9 Hz, 2H, $CH_2O$), 4.45 (d, *J* = 5.9 Hz, 2H, $CH_2O$), 7.02 (t, *J* = 7.5 Hz, 2H, $2H_4$), 7.16 (t, *J* = 7.5 Hz, 4H, $2H_3$, $2H_5$), 7.38 (d, *J* = 8.1 Hz, 4H, $2H_2$, $2H_6$), 8.63 (br s, 2H, 2NH). $^{13}$C NMR (75 MHz, $CDCl_3$) δ 14.1 ($CH_3$), 22.6, 23.8, 31.6, 32.2 ($4CH_2$), 35.1 ($2CH_2$), 36.9 ($CH_2$), 41.4 (C), 49.2 ($CH_2$), 50.1 ($2CH_2$), 80.9 ($2CH_2$), 119.8 (4CH), 124.0 (2CH), 128.8 (4CH), 138.0 (2C), 170.6 (2C). HRMS (ESI): [$(M+H)^+$] calcd. for $C_{28}H_{39}N_3O_2$, 466.3025; found, 466.3050.

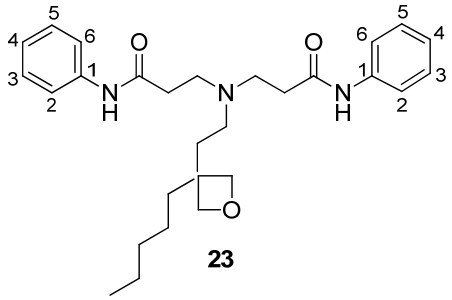

**23**

***N*³-(3-Anilino-3-oxopropyl)-*N*³-cyclopropyl-*N*¹-phenyl-β-alaninamide (24**). Obtained following the general procedure A for the synthesis of symmetric diamides from acrylamide **33** (100 mg, 0.7 mmol) and cyclopropylamine (16 μL, 0.2 mmol) at 45 ºC in 27% yield. Chromatography: EtOAc/MeOH, 9:1; oil. $R_f$ (EtOAc/MeOH, 9:1) 0.51. IR (ATR) ν 3296 (NH), 1659 (CO), 1598, 1546, 1498, 1443 (Ar). $^1$H NMR (300 MHz, $CDCl_3$) δ 0.50-0.55 (m, 2H, $CH_{2cyc}$), 0.58-0.61 (m, 2H, $CH_{2cyc}$), 1.78-1.83 (m, 1H, $CH_{cyc}$), 2.63 (t, *J* = 6.2 Hz, 4H, $2CH_2CO$), 3.02 (t, *J* = 6.2 Hz, 4H, $2CH_2N$), 7.03 (t, *J* = 7.4 Hz, 2H, $2H_4$), 7.19 (t, *J* = 7.8 Hz, 4H, $2H_3$, $2H_5$), 7.41 (d, *J* = 7.7 Hz, 4H, $2H_2$, $2H_6$), 8.70 (br s, 2H, 2NH). $^{13}$C NMR (75 MHz, $CDCl_3$) δ 6.9 ($2CH_2$), 34.5 ($2CH_2$), 37.2 (CH), 51.7 ($2CH_2$), 119.6 (4CH), 124.1 (2CH), 129.0 (4CH), 138.1 (2C), 170.6 (2C). HRMS (ESI): [$(M+Na)^+$] calcd. for $C_{21}H_{25}N_3O_2Na$: 374.18445; found, 374.17157.

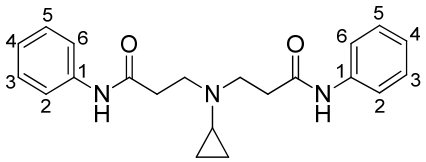

**24**

***N*³-(3-Anilino-3-oxopropyl)-*N*³-(cyclopropylmethyl)-*N*¹-phenyl-β-alaninamide (25).** Obtained following the general procedure A for the synthesis of symmetric diamides from acrylamide **33** (100 mg, 0.7 mmol) and aminomethylcyclopropane (0.02 mL, 0.2 mmol) in quantitative yield. Chromatography: EtOAc/MeOH, 9:1; oil. $R_f$ (EtOAc/MeOH, 9:1) 0.42. IR (ATR) ν 3306 (NH), 1658 (CO), 1599, 1548, 1498, 1444 (Ar). $^1$H NMR (300 MHz, $CDCl_3$) δ 0.13 (q, *J* = 5.0 Hz, 2H, $CH_{2cyc}$), 0.49-0.55 (m, 2H, $CH_{2cyc}$), 0.88-0.94 (m, 1H, $CH_{cyc}$), 2.43 (d, *J* = 6.7 Hz, 2H, $CHC\underline{H}_2N$), 2.52 (t, *J* = 6.3 Hz, 4H, $2CH_2CO$), 2.90 (t, *J* = 6.3 Hz, 4H, $2NC\underline{H}_2CH_2CO$), 7.01 (t, *J* = 7.4 Hz, 2H, $2H_4$), 7.18 (t, *J* = 7.8 Hz, 4H, $2H_3$, $2H_5$), 7.46 (d, *J* = 7.7 Hz, 4H, $2H_2$, $2H_6$), 9.53 (br s, 2H, 2NH). $^{13}$C NMR (75 MHz, $CDCl_3$) δ 4.3 ($2CH_2$), 8.6 (CH), 34.3 ($2CH_2$), 49.7 ($2CH_2$), 58.5 ($CH_2$), 119.9 (4CH), 124.1 (2CH), 128.9 (4CH), 138.3 (2C), 170.7 (2C). HRMS (ESI): [$(M+Na)^+$] calcd. for $C_{22}H_{27}N_3O_2Na$: 388.20010; found, 388.19619.

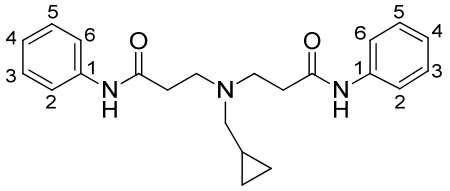

**25**

**Synthesis of *N*³-(3-anilino-3-oxopropyl)-*N*¹-phenyl-β-alaninamide (16).** To a solution of **48** (500 mg, 2.2 mmol) in anhydrous DCM (4 mL) was added a 2 M solution of $NH_3$ in methanol (1.1 mL, 2.2 mmol), and the mixture was stirred overnight at rt. The solvent was removed under reduced pressure, and the residue was dissolved in DCM, washed in saturated aqueous solutions of $NaHCO_3$ and NaCl, dried over $Na_2SO_4$, and the solvent removed under reduced pressure to give final compound **16** in 15% yield. Chromatography: EtOAc/MeOH 95:5; oil. $R_f$ (DCM/MeOH, 95:5) 0.18. IR (ATR) ν 3285 (NH), 1733 (CO), 1668, 1602 (Ar). $^1$H NMR (300 MHz, $CDCl_3$) δ 2.59 (t, *J* = 6.3 Hz, 4H, $2CH_2CO$), 2.89 (t, *J* = 6.3 Hz, 4H, $2CH_2N$), 6.97 (t, *J* = 7.4 Hz, 2H, $2H_4$), 7.10 (t, *J* = 7.7 Hz, 4H, $2H_3$, $2H_5$), 7.37 (d, *J* = 7.7 Hz, 4H, $2H_2$, $2H_6$). $^{13}$C NMR (75 MHz, $CDCl_3$) δ 35.6 ($2CH_2$), 50.9 ($2CH_2$), 121.5 (4CH), 125.0 (2CH), 129.7 (4CH), 139.5 (2C), 173.3 (2C). HRMS (ESI): [$(M+H)^+$] calcd. for $C_{18}H_{22}N_3O_2$: 312.1706; found, 312.1706.

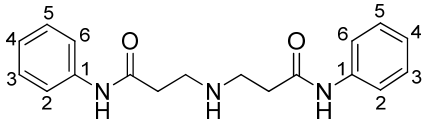

**16**

**General procedure B for the synthesis of symmetric diamides 26 and 27.** To a solution of 3-bromo-*N*-phenylpropanamide **48** (3 equiv) and the corresponding amine (1 equiv) in DCM (0.5 mL/mmol), was added triethylamine (2.5 equiv) and 10% of KI, and the reaction mixture was stirred 24 h at 60 ºC. The solvent was removed under reduced pressure and the crude was purified by column chromatography (EtOAc/MeOH/$NH_3$) to give the title compounds as colorless oils.

***N*$^3$-(3-Anilino-3-oxopropyl)-*N*$^3$-[2-(4-ethylpiperidin-1-yl)ethyl]-*N*$^1$-phenyl-β-alaninamide (26).** Obtained following the general procedure B for the synthesis of symmetric diamides from **48** (185 mg, 0.8 mmol) and 2-(4-ethylpiperidin-1-yl)ethanamine (42 mg, 0.3 mmol) in 48% yield. Chromatography: EtOAc/MeOH/$NH_3$, 9:1:0.2; oil. $R_f$ (EtOAc/MeOH/$NH_3$, 9:1:0.2) 0.43. IR (ATR) ν 3310 (NH), 1675 (CO), 1602, 1551, 1498, 1445 (Ar). $^1$H NMR (300 MHz, $CDCl_3$) δ 0.76 (t, *J* = 7.3 Hz, 3H, $CH_3$), 1.04-1.12 (m, 5H, $C\underline{H}_2CH_3$+CH+2x1/2$CH_{2cyc}$), 1.48 (d, *J* = 11.2 Hz, 2H, 2x1/2$CH_{2cyc}$), 1.92 (t, *J* = 11.1 Hz, 2H, 2x1/2$CH_{2cyc}$N), 2.52-2.54 (m, 6H, $N_{cyc}C\underline{H}_2CH_2N$+ $2CH_2CO$), 2.71 (t, *J* = 6.1 Hz, 2H, $N_{cyc}CH_2C\underline{H}_2N$), 2.85 (t, *J* = 6.0 Hz, 4H, $2NC\underline{H}_2CH_2CO$), 2.95 (d, *J* = 11.3 Hz, 2H, 2x1/2$CH_{2cyc}$N), 7.01 (t, *J* = 7.4 Hz, 2H, $2H_4$), 7.17 (t, *J* = 7.8 Hz, 4H, $2H_3$, $2H_5$), 7.44 (d, *J* = 7.9 Hz, 4H, $2H_2$, $2H_6$), 8.84 (br s, 2H, 2NH). $^{13}$C NMR (75 MHz, $CDCl_3$) δ 14.3 ($CH_3$), 29.2 ($CH_2$), 31.6 ($2CH_2$), 35.2 ($2CH_2$), 37.3 (CH), 50.8 ($2CH_2$), 51.5 ($CH_2$), 54.9 ($2CH_2$), 56.8 ($CH_2$), 120.2 (4CH), 124.1 (2CH), 128.9 (4CH), 138.2 (2C), 170.8 (2C). HRMS (ESI): [$(M+H)^+$] calcd. for $C_{27}H_{39}N_4O_2$: 451.30730; found, 451.30714.

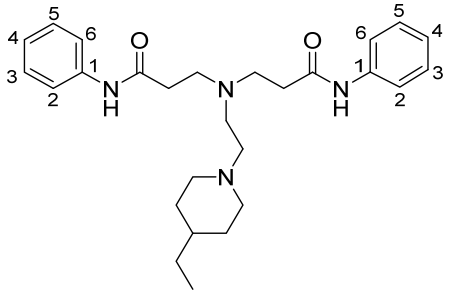

**26**

***N*$^3$-(3-Anilino-3-oxopropyl)-*N*$^3$-[2-(4-ethylpiperazin-1-yl)ethyl]-*N*$^1$-phenyl-β-alaninamide (27).** Obtained following the general procedure B for the synthesis of symmetric diamides from **48** (218 mg, 0.9 mmol) and amine **61** (50 mg, 0.3 mmol) in 54% yield. Chromatography: EtOAc/MeOH/$NH_3$, 7:3:0.2. Mp 70-72 ºC. $R_f$ (EtOAc/MeOH/$NH_3$, 8:2:0.2) 0.22. IR (ATR) ν 3276 (NH), 1664 (CO), 1601, 1548, 1498, 1445 (Ar). $^1$H NMR (300 MHz, $CDCl_3$) δ 0.96 (t, *J* = 7.2 Hz, 3H, $CH_3$), 2.23 (q, *J* = 7.2 Hz, 2H, $C\underline{H}_2CH_3$), 2.19-2.53 (m, 14H, $2CH_2CO$+$4CH_{2cyc}$+$N_{cyc}C\underline{H}_2CH_2N$), 2.64 (t, *J* = 5.9 Hz, 2H, $N_{cyc}CH_2C\underline{H}_2N$), 2.80 (t, *J* = 6.1 Hz, 4H, $2NC\underline{H}_2CH_2CO$), 7.00 (t, *J* = 7.4 Hz, 2H, $2H_4$), 7.16 (t, *J* = 7.8 Hz, 4H, $2H_3$, $2H_5$), 7.44 (d, *J* = 7.7 Hz, 4H, $2H_2$, $2H_6$), 9.24 (br s, 2H, 2NH). $^{13}$C NMR (75 MHz, $CDCl_3$) δ 11.9 ($CH_3$), 34.8 ($2CH_2$), 50.6 ($2CH_2$), 50.8, 52.2 ($2CH_2$), 52.4 ($2CH_2$), 53.8 ($2CH_2$), 56.3 ($CH_2$), 120.3 (4CH), 124.1 (2CH), 128.9 (4CH), 138.3 (2C), 170.7 (2C). HRMS (ESI): [$(M+H)^+$] calcd. for $C_{26}H_{38}N_5O_2$: 452.30255; found, 452.30104.

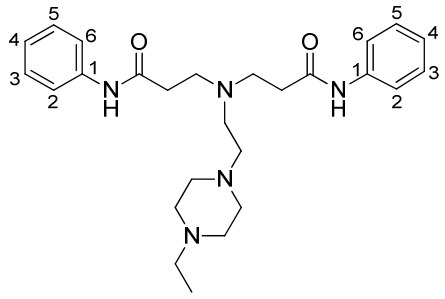

**27**

### 4.1.3. Synthesis of cysmethynil

**Synthesis of *N*-[(5-bromo-1*H*-indol-3-yl)methyl]-*N*,*N*-dimethylamine (64).** To a solution of 1,4-dioxane (10.4 mL) and acetic acid (10.4 mL), were added sequentially at 0 ºC, formaldehyde (0.8 mL, 11.1 mmol), $H_2O$ (0.8 mL), $NHMe_2$ (1.4 mL, 11.1 mmol), and 5-bromoindole (2 g, 10.1 mmol) previously solved in 10.4 mL of 1,4-dioxane. The reaction mixture was stirred at 0 ºC for 2 h after which time it was removed from the ice bath and allowed to stir overnight at rt. Then, the reaction crude was diluted with $H_2O$ (130 ml), and active charcoal (0.6 g) and celite (0.6 g) were added. The mixture was stirred for 10 min, filtered, and a 20% solution of NaOH (200 mL) was added to the filtrate to precipitate it. The resulting precipitate was filtered in vacuo, washed with $H_2O$ (3 x 50 mL), and dried under reduced pressure to give a white solid in 83% yield. Mp 149-150 ºC (Lit.[16] 149-152 ºC). $^1$H NMR (300 MHz, $CDCl_3$) δ 2.27 (s, 6H, $2CH_3$), 3.57 (s, 2H, $CH_2$), 7.06 (d, *J* = 2.0 Hz, 1H, $CH_{Ar}$), 7.20-7.29 (m, 2H, $2CH_{Ar}$), 7.84 (d, *J* = 0.8 Hz, 1H, $CH_{Ar}$), 8.24 (br s, 1H, NH). The spectroscopic data are in agreement with those previously described.[16]

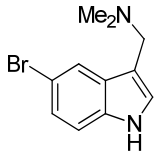


**64**

**Synthesis of (5-bromo-1*H*-indol-3-yl)acetonitrile (65).** To a solution of $Me_2SO_4$ (7.6 mL, 39.5 mmol) in THF (5.4 mL) and acetic acid (0.16 mL) under argon atmosphere, was added dropwise the bromoindol **64** (2 g, 7.9 mmol), previously solved in THF (13.8 mL) and acetic acid (0.16 mL). The reaction mixture was stirred for 1 h at 10 ºC, and the crude was filtered in vacuo, washed with $Et_2O$ and dried under reduced pressure. Then, the precipitate was solved in a solution of KCN (1.5 g, 23.7 mmol) in $H_2O$ (20 mL); and the mixture was stirred vigorously for 1 h at 60-70 ºC, and then allowed to cool down to rt. The product was extracted with $Et_2O$ (2 x 50 mL) and dried under reduced pressure to give a pale solid in 95% yield. Mp 100-101 ºC (Lit.[16] 100-102 ºC). $^1$H NMR (300 MHz, $CDCl_3$) $\delta$ 3.80 (s, 2H, $CH_2$), 7.23-76 (m, 3H, $3CH_{Ar}$), 7.75 (s, 1H, $CH_{Ar}$), 8.23 (br s, 1H, NH). The spectroscopic data are in agreement with those previously described.[16]

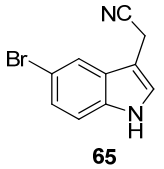


**65**

**Synthesis of 2-(5-bromo-1*H*-indol-3-yl)acetamide (66).** To a solution of nitrile **65** (1.77 g, 7.53 mmol) refluxed in *t*-BuOH (16 mL), was added under argon atmosphere KOH (3.98 g, 60.2 mmol), and the reaction mixture was stirred at reflux for 1.5 h. Then, the reaction crude was cooled down to rt, diluted with $H_2O$ (16 mL), and acidified with 1N HCl (65 mL) in order precipitate the product as a brown solid. The resulting suspension was filtered, washed with $H_2O$ (16 ml) and dried under reduced pressure to give the title compound in 74% yield. $^1$H NMR (300 MHz, DMSO-$d_6$) $\delta$ 3.44 (s, 2H, $CH_2$), 6.86 (s, 1H, $CH_{Ar}$), 7.15-7.38 (m, 4H, $2CH_{Ar}$+$NH_2$), 7.73 (s, 1H, $CH_{Ar}$), 11.08 (br s, 1H, NH). The spectroscopic data are in agreement with those previously described.[16]

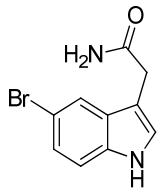

**66**

**Synthesis of 2-[5-(3-methylphenyl-1*H*-indol-3-yl]acetamide (67).** To a suspension of bromoindole **66** (1.36 g, 5.37 mmol) in anhydrous toluene (107 ml) was added $Pd(PPh_3)_4$ (0.35 g, 0.31 mmol) and the reaction mixture was stirred for 1 h at rt under argon atmosphere. Hence, were added a solution of *m*-tolylboronic acid (1.13 g, 8 mmol) in ethanol (20 mL), and a saturated aqueous solution of $NaHCO_3$ (50 mL). The mixture was refluxed overnight, the reaction crude was washed with saturated aqueous solution of NaCl (2 x 50 mL), and the organic fraction was extracted with EtOAc (3 x 100 mL), dried over $Na_2SO_4$, and the solvent was removed under reduced pressure. The product appeared as a yellow solid in 23% yield. Chromatography: DCM/MeOH, 1:1. $^1$H NMR (300 MHz, $CDCl_3$) $\delta$ 2.40 (s, 3H, $CH_3$), 3.70 (s, 2H, $CH_2$), 5.49 (br s, 1H, NH), 5.62 (br s, 1H, NH), 7.05-7.42 (m, 7H, $7CH_{Ar}$), 7.68 (s, 1H, $CH_{Ar}$), 8.23 (br s, 1H, NH). The spectroscopic data are in agreement with those previously described.[16]

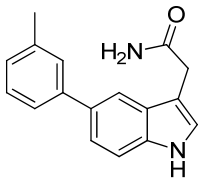

**67**

**Synthesis of 2-[5-(3-methylphenyl)-1-octyl-1*H*-indol-3-yl]acetamide (cysmethynil).** To a suspension of NaH (25 g, 0.63 mmol) in DMF (0.8 mL) was added dropwise indol **67** (139 mg, 0,53 mmol) in DMF (1.1 mL) and the mixture was stirred for 1.5 h at rt under argon atmosphere. Then 1-bromooctane (309 mg, 1.6 mmol) was added dropwise and the reaction was stirred overnight at 55 ºC. The reaction crude was poured into ice water (23 mL) and was stirred for 10 min. The product was extracted with $Et_2O$ (6 x 10mL), washed with saturated aqueous solution of NaCl (4 x 15 mL), and dried over $Na_2SO_4$. The solvent was evaporated under reduced pressure to give the title compound as a yellowish oil in 43% yield. Chromatography: DCM/MeOH, 95:5; oil. $^1$H NMR (300 MHz, $CDCl_3$) $\delta$ 0.85 (t, *J* = 6.7 Hz, 3H, $C\underline{H}_3CH_2$), 1.25-1.34 (m, 10H, $(C\underline{H}_2)_5CH3$), 1.86 (m, 2H, $C\underline{H}_2(CH_2)_5CH_3$), 2.44 (s, 3H, $C\underline{H}_3C$), 3.76 (s, 2H, $CH_2CO$), 4.11 (t, *J* = 7.1 Hz, 2H, $(CH_2)_6C\underline{H}_2N$), 5.60 (br s, 1H, NH), 5.71 (br s, 1H, NH), 7.08 (s, 1H, $CH_{Ar}$), 7.14 (d, *J* = 7.1 Hz, 1H, $CH_{Ar}$), 7.31-7.53 (m,

5H, 5$CH_{Ar}$), 7.76 (s, 1H, $CH_{Ar}$). HRMS (ESI): [$(M+Na)^+$] calcd. for $C_{25}H_{32}N_2ONa$, 399.24123; found, 399.24078.

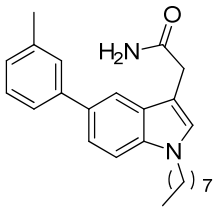


**cysmethynil**

### 4.2. Biological experiments

**4.2.1. ICMT activity assay.** ICMT activity was determined as previously described[49] with slight modifications. Briefly, membranes that overexpress ICMT enzyme were incubated in the presence of the corresponding concentration of the compound under study in assay buffer (100 mM Hepes, 5 mM $MgCl_2$, pH 7.4) for 10 min, with shaking, at rt. Then, BFC and [$^3$H]-SAMt were added at final concentrations of 5 and 2 $\mu$M, respectively (final volume 45 $\mu$L). Reactions were carried out for 30 min at 37 ºC after which they were terminated by addition of 5 $\mu$L of 10% Tween 20 in phosphate buffered saline (PBS). Then, the reaction mixture was transferred to a 96-well plate containing streptavidin beads (10 $\mu$L of packed beads, Thermofisher, suspended in 500 $\mu$L of PBS), and mixed by gentle shaking overnight at 4 °C. Finally, the radioactivity bound to the beads was counted in a Microbeta TopCount instrument (Perkin-Elmer). The percentage of inhibition was determined with respect to the 100% activity obtained in the absence of compounds. For the determination of $IC_{50}$ values, the percentage of ICMT activity was plotted against log concentration of the compound on GraphPad Prism (Version 5.0, GraphPad Software, San Diego, CA). In all cases, the reported data corresponded to the average obtained from three independent experiments carried out in duplicate.

**4.2.2. Cell lines and culture.** MDA-MB-231, MIA PaCa-2, PANC-1, SW620, MCF7, SK-Mel-28, NIH3T3, AD-293, and U2OS cells from American Type Culture Collection (ATCC, Rockville, MD) and 142BR fibroblasts from Sigma-Aldrich, were grown in Dulbecco's Modified Eagle medium (DMEM, Invitrogen) supplemented with 10% heat-inactivated fetal bovine serum (FBS, HyClone), 1% L-glutamine (Invitrogen), 1% sodium pyruvate (Invitrogen), 50 U/mL penicillin and 50 $\mu$g/mL streptomycin (Invitrogen). BxPC-3 and PC-3 cells were obtained from ATCC and maintained in Roswell Park Memorial Institute medium (RPMI) supplemented with 10% heat-inactivated FBS, 1% L-glutamine, 1% sodium pyruvate, 50 U/mL penicillin, and 50 $\mu$g/mL streptomycin. Cells were incubated in a humidified atmosphere at 37 ºC in the presence of 5% of $CO_2$.

**4.2.3. MTT citotoxicity assay.** The sensitivity of MDA-MB-23, MIA PaCa-2, PANC-1, SW620, BxPC-3, PC-3, MCF7, SK-Mel-28, NIH3T3, and 142BR cell lines to compounds was tested through a standard MTT assay. Briefly, cells were seeded in 96-well plates at a density of 5 or 10 x $10^3$ cells per well in the corresponding medium with 10% FBS for 24 h prior to treatments. The medium was then replaced by fresh medium containing different concentrations of compounds or the equivalent volume of DMSO. Cells were treated for 48 h, when medium was replaced by fresh medium with 2 mg/mL of MTT (3-(4,5-dimethylthiazol-2-yl)-2,5-diphenyltetrazolium bromide, Sigma-Aldrich) and cells were incubated for 4 h at 37 ºC in the dark. Once supernatants were removed, formazan crystals previously formed by viable cells were dissolved in DMSO (100 $\mu$L/well) and absorbance was measured at 570 nm (OD570-630) using an Asys UVM 340 microplate reader (Biochrom Ltd., Cambridge, UK). Background absorbance from blank wells containing only media with compound or vehicle were substracted from each test well. For the determination of the $IC_{50}$ values, the percentage of absorbance was plotted against log concentration of the compound on GraphPad Prism (Version 5.0, GraphPad Software, San Diego, CA). Results were reported as $IC_{50}$ from three independent experiments carried out in triplicate.

**4.2.4. Serum stability assay.** To 900 $\mu$L of mouse serum (Europa Bioproducts) previously warmed at 37 ºC, were added 300 $\mu$L of a 2 mM solution of the compound in phosphate buffered saline (PBS), and the mixture was incubated at 37 ºC for different times (0, 5, 10, 20, 40 and 60 min). Then, 200 $\mu$L of each mixture were added over 200 $\mu$L of cold acetonitrile, mixed, and incubated for 10 min on ice to precipitate proteins. Supernatants were separated by centrifugation at 39000*g* for 10 min, filtered (0.22 $\mu$m); and 50 $\mu$L of each filtered supernatant were analyzed by HPLC-MS in an spectrometer Agilent 1200LC-MSD VL, using a column Eclipse XDB-C18 (5 $\mu$m, 4.6 mm x 150 mm) together with a guard column (5 $\mu$m, 4.6 mm x 12.5 mm). The gradient mobile phases consisted of A (95:5 water/MeOH) and B (5:95 water/MeOH), with 0.1% ammonium hydroxide and 0.1% formic acid as the solvent modifiers. In all cases, a constant flow of 0.5 mL/min was used for a total time of 15 min. MS analysis was performed with an ESI source. The capillary voltage was set to 3.0 kV and the fragmentor voltage was set at 70 eV. The drying gas temperature was 350 ºC, the drying gas flow was 10 L/min, and the nebulizer pressure was 20 psi.

**4.2.5. Intracellular imaging of endogenous pan-Ras in PC-3 fixed cells.** PC-3 cells were seeded at a density of 2 x $10^4$ cells per well on 12-mm coverslips previously treated with poly-D-lysine hydrobromide (Sigma-Aldrich) and grown for 24 h at 37 ºC and 5 % of $CO_2$ in RPMI medium with 10% FBS. Medium was replaced with fresh medium with the indicated concentrations of compounds or DMSO and cells were incubated for 96 h, replacing the medium after the first 48 h. Cells were washed twice with PBS, fixed with 4% paraformaldehyde (Sigma-Aldrich) and permeabilized with PBS-T (PBS with 0.1% Triton X-100, Sigma-Aldrich). Incubation with primary

antibody mouse anti-Ras (1:200, Thermo Scientific) in PBS with 4% normal goat serum (NGS) was performed at rt with gentle shaking for 2 h. Then, cells were washed twice with PBS-T and incubated for 1 h in the dark with Alexa Fluor 488 goat anti-mouse (1:1500, Life Technologies) diluted in PBS with 1% NGS. Afterwards cells were washed twice with PBS-T and incubated with 5 $\mu$g/mL Hoechst 33258 (Sigma-Aldrich) in PBS for 10 min at rt to visualize cell nuclei. Finally, cells were washed thrice with PBS-T and coverslips were carefully mounted with Immumount (Thermo Scientific). Visualization was performed using an Olympus IX83 inverted confocal microscope fitted with the appropriate excitation and emission filters and a 60X oil immersion objective. Images shown are representative of three to five independent experiments.

**4.2.6. Plasmid constructs.** The coding sequences of K-Ras4A, K-Ras4B, N-Ras and H-Ras cDNAs were amplified by polymerase chain reaction (PCR) and cloned in-frame into pEGFPC1 (Clontech, Mountain View, CA), producing a fusion between the Ras proteins and a monomeric form of green fluorescent protein (GFP), as previously described.[50] Point mutation in CAAX motif in order to obtain the K-Ras-CVIL-GFP plasmid was generated by PCR with primers incorporating the desired mutation, and the resulting DNA was cloned into pEGFP-C3 (BD Biosciences Clontech, PaloAlto, CA).[29] The coding sequence of LC-3 was amplified by PCR and cloned in-frame into mCherry (Clontech, Mountain View, CA).[51] All plasmid constructs were verified by bidirectional DNA sequencing.

**4.2.7. Transfection of cells and live cell imaging.** AD-293 and U2OS cells were seeded at 2 x $10^5$ cells in 35-mm plastic dishes with a 1-cm round glass coverslip (MatTek, Ashland, MA) 24 h before transfection. Transient transfections were performed with Lipofectamine Plus (Invitrogen, Carlsbad, CA) according to the manufacturer's instructions. In all cases, 2 $\mu$g of DNA total was used for each 35-mm dish. After 4 h of incubation at 37 ºC, media was replaced by fresh DMEM supplemented with 10% FBS containing 5 $\mu$M cysmethynil, UCM-1336 or an equivalent volume of DMSO, and incubated overnight. Live cells were imaged the next day with an inverted Zeiss LSM 510 Meta laser scanning confocal microscope (63 Plan-Neofluar 1.25-numerical-aperture oil).

**4.2.8. Active Ras pulldown assay.** PC-3 cells were plated at a density of 2 x $10^6$ cells in 15-cm dishes and grown in RPMI medium with 10% FBS at 37 ºC and 5% of $CO_2$. After 24 h, medium was replaced by fresh medium with 25 $\mu$M cysmethynil, 10 $\mu$M UCM-1336 or an equivalent volume of DMSO for vehicle control, and cells were incubated for 48 h at 37 ºC and 5% of $CO_2$. At this point, medium was replaced once again by fresh medium with compounds or DMSO, and the incubation was kept for additional 48 h. After 5 min of stimulation with EGF (10 ng/mL), cells were washed with PBS and lysed with ice-cold lysis buffer provided by the manufacturer. Lysates were clarified by centrifugation at 16000*g* for 15 min and protein concentration was measured using bicinchoninic acid

method (Thermo Scientific). Before performing the assay, 50 $\mu$L of each lysate were separated to analyze the total Ras expression. For the analysis of active Ras, a Ras-GTP pulldown assay kit (Thermo Scientific) was used following manufacturer's instructions. Briefly, lysates were incubated with a glutathione *S*-transferase fusion of the RBD of Raf1 along with glutathione agarose resin to pull down active Ras. The entire samples obtained after the pulldown assay were boiled for 5 min and loaded onto 4-20% SDS-PAGE gels (Bio-Rad). Ras proteins were visualized by immunoblotting on nitrocellulose membranes using a mouse anti-Ras antibody provided by the manufacturer. Blots were analyzed by densitometry using ImageJ software (NIH). Data from four independent experiments were presented as mean ± SEM with bar graphs.

**4.2.9. Western blot analysis.** PC-3 cells were plated at a density of 2 x $10^6$ cells in 15-cm dishes and allowed to grow for 24 h in RPMI medium with 10% FBS, to obtain a 80% confluent monolayer. The medium was then replaced by fresh RPMI with 10 $\mu$M cysmethynil or UCM-1336, or an equivalent volume of DMSO, and cells were incubated overnight, except for LC-3 and PARP immunoblots, where the incubation times were prolonged up to 48 h following previously described results.[25] Five minutes prior to lysis, cells were stimulated with EGF (10 ng/mL). Cells were washed with PBS and lysed with ice-cold RIPA buffer (50 mM Tris-HCl pH 7.4, 150 mM NaCl, 1% Igepal) containing protease and phosphatase inhibitors (Roche and Sigma-Aldrich, respectively). Lysates were clarified by centrifugation at 16000*g* for 10 min at 4 ºC and used immediately or stored at -80 ºC until use. Protein concentration was measured (DC Protein Assay Kit, Bio-Rad) and samples with equal amounts of total protein were diluted into a Laemmli reducing sample buffer (Bio-Rad) and denatured at 95 ºC for 5 min. Samples were then resolved on 4-20% SDS-PAGE gels (Bio-Rad) and proteins transferred to nitrocellulose membranes (GE Healthcare, Amersham). After 1 h of incubation in a blocking buffer [10 mM Tris-HCl pH 8.0, 150 mM NaCl, 0.05% Tween-20 (TBS-T) with 1% BSA], membranes were incubated overnight at 4 ºC with the corresponding primary antibody. Then, membranes were washed three times (5 min each) with TBS-T and incubated with the corresponding secondary antibody for 1 h at rt. Protein bands were visualized using enhanced chemiluminescence detection reagents (GE Healthcare, Amersham) in a Fujifilm LAS-3000 developer (Tokyo, Japan) and quantified by densitometry using ImageJ software (NIH).

Primary antibodies used were rabbit anti-phospho-AKT, rabbit anti-AKT, rabbit anti-phospho-ERK1/2, rabbit anti-ERK1/2, rabbit anti-phospho-MEK1/2, rabbit anti-MEK1/2, rabbit anti-PARP, rabbit anti-α/β tubulin (1:1000, Cell Signalling), rabbit anti-LC-3 (1:1000, Abgent), or mouse anti-Ras (1:1000, Thermo Scientific). Secondary antibodies used were goat anti-mouse or goat anti-rabbit IgG HRP conjugates (1:5000, Sigma-Aldrich). Relative phosphorylation levels from at least three independent experiments performed in triplicate were presented as mean ± SEM with bar graphs.

**4.2.10. Migration or wound healing assay.** MDA-MB-231 cells were seeded in 96-well plates at a density of 1.5 x $10^4$ cells per well in DMEM with 10% FBS for 24 h at 37 ºC and 5% of $CO_2$ to a 90-100% confluent monolayer. Wounds were made with a sterile p20 pipette tip and each well was washed twice with PBS to eliminate non adherent cells and cell debris. Fresh DMEM with indicated concentrations of cysmethynil or UCM-1336**,** or with an equivalent volume of DMSO was then added. At this time (0 h) and after 48 h, cells were photographed under phase contrast with an Olympus FW1200 microscope. Empty area in each wound was quantified using ImageJ software (NIH) and compared with the corresponding initial wound. Percentage of the areas from three independent experiments performed in triplicate was presented as mean ± SEM with bar graphs.

**4.2.11. Caspase 3 enzyme activity assay**. PC-3 cells were seeded at 5 x $10^4$ cells per well in a 24-well plate and grown for 24 h before treatments in RPMI medium with 10% FBS. The medium was then replaced by fresh RPMI with 10 $\mu$M cysmethynil or UCM-1336, or an equivalent volume of DMSO, and cells were incubated for 48 h. After this time, cells were washed with ice-cold PBS, counted and harvested by centrifugation at 400*g* for 5 min. The activity of caspase 3 was determined by a caspase colorimetric assay kit (Clontech, Mountain View, CA), according to the manufacturer's protocol. Briefly, the protease activity was tested using a caspase 3 specific peptide, conjugated to the color reporter molecule *p*-nitroaniline (p-NA). The chromophore p-NA, cleaved by caspase 3, was quantified with a spectrophotometer at a wavelength of 405 nm. The caspase enzymatic activities in cell lysates are directly proportional to the color reaction. Data from three independent experiments performed in triplicate were presented as mean ± SEM with bar graphs.

## 7. BIBLIOGRAPHY


1. Ahearn, I. M. H., K.; Bar-Sagi, D.; Philips, M.R. Regulating the regulator: post-translational modification of Ras. *Nat. Rev. Mol. Cell Biol.* **2012**, *13*, 39-51.
2. Bos, J. L. Ras oncogenes in human cancer: a review. *Cancer Res.* **1989**, *49*, 4682-4689.
3. Adjei, A. A. Blocking oncogenic Ras signaling for cancer therapy. *J. Natl. Cancer Inst.* **2001**, *93*, 1062-1074.
4. Vogelstein, B.; Papadopoulos, N.; Velculescu, V. E.; Zhou, S.; Diaz, L. A.; Kinzler, K. W. Cancer genome landscapes. *Science* **2013**, *339*, 1546-1558.
5. Cox, A. D.; Fesik, S. W.; Kimmelman, A. C.; Luo, J.; Der, C. J. Drugging the undruggable Ras: mission possible? *Nat. Rev. Drug Discov.* **2014**, *13*, 828-851.
6. Wright, L. P.; Philips, M. R. CAAX modification and membrane targeting of Ras. *J. Lipid. Res.* **2006**, *47*, 883-891.
7. Whyte, D. B.; Kirschmeier, P.; Hockenberry, T. N.; Nunez-Oliva, I.; James, L.; Catino, J. J.; Bishop, W. R.; Pai, J.-K. K- and N-Ras are geranylgeranylated in cells treated with farnesyl protein transferase inhibitors. *J. Biol. Chem.* **1997**, *272*, 14459-14464.
8. Boyartchuk, V. L.; Ashby, M. N.; Rine, J. Modulation of Ras and a-factor function by carboxyl-terminal proteolysis. *Science* **1997**, *275*, 1796-1800.
9. Schmidt, W. K.; Tam, A.; Fujimura-Kamada, K.; Michaelis, S. Endoplasmic reticulum membrane localization of Rce1p and Ste24p, yeast proteases involved in carboxyl-terminal CAAX protein processing and amino-terminal a-factor cleavage. *Proc. Natl. Acad. Sci. U.S.A.* **1998**, *95*, 11175-11180.
10. Dai, Q.; Choy, E.; Chiu, V.; Romano, J.; Slivka, S. R.; Steitz, S. A.; Michaelis, S.; Philips, M. R. Mammalian prenylcysteine carboxyl methyltransferase is in the endoplasmic reticulum. *J. Biol. Chem.* **1998**, *273*, 15030-15034.

11. DeGraw, A. J.; Keiser, M. J.; Ochocki, J. D.; Shoichet, B. K.; Distefano, M. D. Prediction and evaluation of protein farnesyltransferase inhibition by commercial drugs. *J. Med. Chem.* **2010**, *53*, 2464-2471.

12. Niessner, H.; Beck, D.; Sinnberg, T.; Lasithiotakis, K.; Maczey, E.; Gogel, J.; Venturelli, S.; Berger, A.; Mauthe, M.; Toulany, M.; Flaherty, K.; Schaller, M.; Schadendorf, D.; Proikas-Cezanne, T.; Schittek, B.; Garbe, C.; Kulms, D.; Meier, F. The farnesyl transferase inhibitor lonafarnib inhibits mTOR signaling and enforces sorafenib-induced apoptosis in melanoma cells. *J. Invest. Dermatol.* **2011**, *131*, 468-479.

13. Bergo, M. O.; Lieu, H. D.; Gavino, B. J.; Ambroziak, P.; Otto, J. C.; Casey, P. J.; Walker, Q. M.; Young, S. G. On the physiological importance of endoproteolysis of CAAX proteins: heart-specific Rce1 knockout mice develop a lethal cardiomyopathy. *J. Biol. Chem.* **2004**, *279*, 4729-4736.

14. Bhadoriya, K. S.; Sharma, M. C.; Jain, S. V. Pharmacophore modeling and atom-based 3D-QSAR studies on amino derivatives of indole as potent isoprenylcysteine carboxyl methyltransferase (Icmt) inhibitors. *J. Mol. Struct.* **2015**, *1081*, 466-476.

15. Berndt, N.; Hamilton, A. D.; Sebti, S. M. Targeting protein prenylation for cancer therapy. *Nat. Rev. Cancer* **2011**, *11*, 775-791.

16. Winter-Vann, A. M.; Baron, R. A.; Wong, W.; dela Cruz, J.; York, J. D.; Gooden, D. M.; Bergo, M. O.; Young, S. G.; Toone, E. J.; Casey, P. J. A small-molecule inhibitor of isoprenylcysteine carboxyl methyltransferase with antitumor activity in cancer cells. *Proc. Natl. Acad. Sci. U.S.A.* **2005**, *102*, 4336-4341.

17. Wang, M.; Tan, W.; Zhou, J.; Leow, J.; Go, M.; Lee, H. S.; Casey, P. J. A small molecule inhibitor of isoprenylcysteine carboxymethyltransferase induces autophagic cell death in PC3 prostate cancer cells. *J. Biol. Chem.* **2008**, *283*, 18678-18684.

18. Judd, W. R.; Slattum, P. M.; Hoang, K. C.; Bhoite, L.; Valppu, L.; Alberts, G.; Brown, B.; Roth, B.; Ostanin, K.; Huang, L.; Wettstein, D.; Richards, B.; Willardsen, J. A. Discovery and SAR of methylated tetrahydropyranyl derivatives as inhibitors of isoprenylcysteine carboxyl methyltransferase (ICMT). *J. Med. Chem.* **2011**, *54*, 5031-5047.

19. Yang, J.; Kulkarni, K.; Manolaridis, I.; Zhang, Z.; Dodd, Roger B.; Mas-Droux, C.; Barford, D. Mechanism of isoprenylcysteine carboxyl methylation from the crystal structure of the integral membrane methyltransferase ICMT. *Mol. Cell* **2011**, *44*, 997-1004.

20. López-Rodríguez, M. L.; Ortega-Gutiérrez, S.; Martín-Fontecha, M.; Balabasquer, M.; Ortega, F. J.; Marín-Ramos, N. I. Novel inhibitors of the enzyme isoprenylcysteine carboxyl methyltransferase (ICMT). PCT Int. Appl. WO2014118418 A1, **2014**.

21. Andreas, B.; Nicole, B.; Pascal, F.; Jean-Marc, G.; Joanna, H. L.; Joerg, K.; Keiichi, M.; Lorenz, M.; Andrea, V. 3-imidazolyl-indoles for the treatment of proliferative diseases. PCT Int. Appl. WO2012176123 A1, **2008**.

22. Boström, J.; Hogner, A.; Llinàs, A.; Wellner, E.; Plowright, A. T. Oxadiazoles in medicinal chemistry. *J. Med. Chem.* **2012**, *55*, 1817-1830.

23. Bursch, W.; Ellinger, A.; Kienzl, H.; Torok, L.; Pandey, S.; Sikorska, M.; Walker, R.; Schulte-Hermann, R. Active cell death induced by the anti-estrogens tamoxifen and ICI 164 384 in human mammary carcinoma cells (MCF-7) in culture: the role of autophagy. *Carcinogenesis* **1996**, *17*, 1595-1607.

24. Zhang, J. F.; Liu, J. J.; Lu, M. Q.; Cai, C. J.; Yang, Y.; Li, H.; Xu, C.; Chen, G. H. Rapamycin inhibits cell growth by induction of apoptosis on hepatocellular carcinoma cells in vitro. *Transpl. Immunol.* **2007**, *17*, 162-168.

25. Wang, M.; Hossain, M. S.; Tan, W.; Coolman, B.; Zhou, J.; Liu, S.; Casey, P. J. Inhibition of isoprenylcysteine carboxylmethyltransferase induces autophagic-dependent apoptosis and impairs tumor growth. *Oncogene* **2010**, *29*, 4959-4970.

26. Zhao, D., Yuan, H., Yi, F., Meng, C., Zhu, Q. Autophagy prevents doxorubicin-induced apoptosis in osteosarcoma. *Mol. Med. Rep.* **2014**, *9*, 1975-1981.

27. Cohen, G. M. Caspases: the executioners of apoptosis. *Biochem. J.* **1997**, *326*, 1-16.

28. Bergo, M. O.; Leung, G. K.; Ambroziak, P.; Otto, J. C.; Casey, P. J.; Young, S. G. Targeted inactivation of the isoprenylcysteine carboxyl methyltransferase gene causes mislocalization of K-Ras in mammalian cells. *J. Biol. Chem.* **2000**, *275*, 17605-17610.

29. Michaelson, D.; Ali, W.; Chiu, V. K.; Bergo, M.; Silletti, J.; Wright, L.; Young, S. G.; Philips, M. R. Postprenylation CAAX processing is required for proper localization of Ras but not Rho GTPases. *Mol. Biol. Cell* **2005**, *16*, 1606-1616.

30. Kroth, H.; Hamel, C.; Benderitter, P.; Froestl, W.; Sreenivasachary, N.; Muhs, A. Novel compounds for the treatment of diseases associated with amyloid or amyloid-like proteins. PCT Int. Appl. WO2011128455 A1, **2011**.

31. Shields, C. J.; Falvey, D. E.; Schuster, G. B.; Buchardt, O.; Nielsen, P. E. Competitive singlet-singlet energy transfer and electron transfer activation of aryl azides: application to photo-cross-linking experiments. *J. Org. Chem.* **1988**, *53*, 3501-3507.

32. Sunada, Y.; Kawakami, H.; Imaoka, T.; Motoyama, Y.; Nagashima, H. Hydrosilane reduction of tertiary carboxamides by iron carbonyl catalysts. *Angew. Chem. Int. Ed.* **2009**, *48*, 9511-9514.

33. Eriksson, J.; Åberg, O.; Långström, B. Synthesis of [11C]/[13C]acrylamides by palladium-mediated carbonylation. *Eur. J. Org. Chem.* **2007**, *2007*, 455-461.

34. Honigberg, I.; Hartung, W. Notes- adducts with N-substituted acrylamides. *J. Org. Chem.* **1960**, *25*, 1822-1824.

35. Cvetovich, R. J.; DiMichele, L. Formation of acrylanilides, acrylamides, and amides directly from carboxylic ccids using thionyl chloride in dimethylacetamide in the absence of bases. *Org. Process Res. Dev.* **2006**, *10*, 944-946.

36. Kokosza, K.; Balzarini, J.; Piotrowska, D. G. Design, synthesis, antiviral and cytostatic evaluation of novel isoxazolidine nucleotide analogues with a carbamoyl linker. *Bioorg. Med. Chem.* **2013**, *21*, 1097-1108.

37. Prime, M. E.; Andersen, O. A.; Barker, J. J.; Brooks, M. A.; Cheng, R. K.; Toogood-Johnson, I.; Courtney, S. M.; Brookfield, F. A.; Yarnold, C. J.; Marston, R. W.; Johnson, P. D.; Johnsen, S. F.; Palfrey, J. J.; Vaidya, D.; Erfan, S.; Ichihara, O.; Felicetti, B.; Palan, S.; Pedret-Dunn, A.; Schaertl, S.; Sternberger, I.; Ebneth, A.; Scheel, A.; Winkler, D.; Toledo-Sherman, L.; Beconi, M.; Macdonald, D.; Munoz-Sanjuan, I.; Dominguez, C.; Wityak, J. Discovery and structure-activity relationship of potent and selective covalent inhibitors of transglutaminase 2 for Huntington's disease. *J. Med. Chem.* **2012**, *55*, 1021-1046.

38. Kuhnert, N.; Le-Gresley, A. Synthesis and capsule formation of upper rim substituted tetra-acrylamido calix[4]arenes. *Org. Biomol. Chem.* **2005**, *3*, 2175-2182.

39. Ali, A. A. M.; El-Sawy, N. M.; Al Sagheer, F. A. Radiation polymerization of 4-N-acryloylamidobenzonitrile: amidoximation, complexation and biological activity. *Int. J. Polym. Mater.* **2005**, *54*, 359-373.

40. Nishio, T.; Tabata, M.; Koyama, H.; Sakamoto, M. Photochemistry of N-(2-acylphenyl)-2-methylprop-2-enamides: competition between photocyclization and long-range hydrogen abstraction. *Helv. Chim. Acta* **2005**, *88*, 78-86.

41. Allen, C. E.; Curran, P. R.; Brearley, A. S.; Boissel, V.; Sviridenko, L.; Press, N. J.; Stonehouse, J. P.; Armstrong, A. Efficient and facile synthesis of acrylamide libraries for protein-guided tethering. *Org. Lett.* **2015**, *17*, 458-460.

42. Zhu, M.; Zhang, C.; Nwachukwu, J. C.; Srinivasan, S.; Cavett, V.; Zheng, Y.; Carlson, K. E.; Dong, C.; Katzenellenbogen, J. A.; Nettles, K. W.; Zhou, H.-B. Bicyclic core estrogens as full antagonists: synthesis, biological evaluation and structure-activity relationships of estrogen receptor ligands based on bridged oxabicyclic core arylsulfonamides. *Org. Biomol. Chem.* **2012**, *10*, 8692-8700.

43. Choe, H.; Kim, J.; Hong, S. Structure-based design of flavone-based inhibitors of wild-type and T315I mutant of ABL. *Bioorg. Med. Chem. Lett.* **2013**, *23*, 4324-4327.

44. Pasquinucci, L.; Prezzavento, O.; Marrazzo, A.; Amata, E.; Ronsisvalle, S.; Georgoussi, Z.; Fourla, D. D.; Scoto, G. M.; Parenti, C.; Arico, G.; Ronsisvalle, G. Evaluation of N-substitution in 6,7-benzomorphan compounds. *Bioorg. Med. Chem.* **2010**, *18*, 4975-4982.

45. Hutchins, R. O.; Adams, J.; Rutledge, M. C. Stereoselective hydride reductions of cyclic N-diphenylphosphinyl imines. Highly diastereoselective syntheses of protected primary amines. *J. Org. Chem.* **1995**, *60*, 7396-7405.

46. Fujioka, H.; Yamamoto, H.; Miyazaki, M.; Yamanaka, T.; Takuma, K.; Kita, Y. Reductive Beckmann fragmentation of α-alkoxycycloalkanone oxime acetates. *Tetrahedron Lett.* **1991**, *32*, 5367-5368.

47. Jadhav, G. P.; Chhabra, S. R.; Telford, G.; Hooi, D. S. W.; Righetti, K.; Williams, P.; Kellam, B.; Pritchard, D. I.; Fischer, P. M. Immunosuppressive but non-LasR-inducing analogues of the pseudomonas aeruginosa quorum-sensing molecule N-(3-oxododecanoyl)-l-homoserine lactone. *J. Med. Chem.* **2011**, *54*, 3348-3359.

48. de Greef, T. F. A.; Nieuwenhuizen, M. M. L.; Sijbesma, R. P.; Meijer, E. W. Competitive intramolecular hydrogen bonding in oligo(ethylene oxide) substituted quadruple hydrogen bonded systems. *J. Org. Chem.* **2010**, *75*, 598-610.

49. Baron, R. A.; Casey, P. J. Analysis of the kinetic mechanism of recombinant human isoprenylcysteine carboxylmethyltransferase (Icmt). *BMC Biochem.* **2004**, *5*, 1-12.

50. Tsai, F. D.; Lopes, M. S.; Zhou, M.; Court, H.; Ponce, O.; Fiordalisi, J. J.; Gierut, J. J.; Cox, A. D.; Haigis, K. M.; Philips, M. R. K-Ras4A splice variant is widely expressed in cancer and uses a hybrid membrane-targeting motif. *Proc. Natl. Acad. Sci. U.S.A.* **2015**, *112*, 779-784.

51. Sung, P. J.; Tsai, F. D.; Vais, H.; Court, H.; Yang, J.; Fehrenbacher, N.; Foskett, J. K.; Philips, M. R. Phosphorylated K-Ras limits cell survival by blocking Bcl-xL sensitization of inositol trisphosphate receptors. *Proc. Natl. Acad. Sci. U.S.A.* **2013**, *110*, 20593-20598.